

**Structure and Tectonic Geomorphology**  
**of the Lowry Peaks Range-Waikari Valley District,**  
**North Canterbury**

---

A thesis  
submitted in partial fulfilment  
of the requirements for the Degree  
of  
Master of Science in Geology  
in the  
University of Canterbury  
by  
**Nicola Jane Litchfield**

---

University of Canterbury

1995

**Frontispeice** An oblique aerial view towards the west, of the Waikari Flat area. In the foreground are the plunging Mt Alexander and Waikari Anticline structures. In the centre is the Waikari Flat region, bound to the west by Hawarden Anticline (traversing the photo) and the north by the Trig C Structures. The Southern Alps in the background are bound on their eastern side by N-S and NW-SE trending structures of the Mt Mason to Island Hills Region.

QE  
637.5  
.C3  
.L776  
1995

## ABSTRACT

Structures of the Lowry Peaks Range - Waikari Valley district are complex. The majority comprise three members of a predominantly WSW-ENE striking major northwards-directed, leading edge imbricate thrust system, with associated angular, asymmetric fault-propagation folds. This system forms anomalously within a large NE-SW trending belt of structures characterising the entire east coast of north Canterbury, both onshore and offshore and terminates westwards against N-S striking, east facing fold-fault zone. The objectives of this study address the origin, geometry and kinematics of the interaction between these diversely trending systems.

Stratigraphy and small-scale structures denote three periods of deformation, namely: i) Middle Cretaceous deformation of the basement rocks, ii) weak Middle Oligocene deformation associated with the inception of the plate boundary through the South Island, and iii) major Pliocene - Recent deformation that formed the majority of the above-mentioned structures.

Stress tensor analyses within competent basement and limestone cover rocks suggest two sets of sub-horizontal compression, NE-SW and NW-SE, the former likely to relate to a localised earlier period of deformation, now overprinted by the latter. NW-SE oriented sub-horizontal compression correlates well with results from other parts of north Canterbury. The result of NW-SE compression on the W-E to WSW-ENE striking structures is a large component of oblique motion, which is manifest in four ways: i) movement on two, differently oriented splays rather than a single fault strand, ii) the development of a sinuous trace for a number of the major folds, whereby the ends are oriented normal to the compression direction, the centres parallel to the strike of the faults, iii) the development of a number of cross-folds, striking NNE-SSW and iv) the apparently recent development of a strike-slip component on at least one of the major thrust faults.

The origin of the W-E, or WSW-ENE striking structures may be reactivation of Late Cretaceous faults, stratigraphic evidence for the existence of a "structural high" (the Hurunui High) over the majority of the area in the Late Cretaceous to Early Eocene times suggests the formation of a W-E trending horst structure, with a corresponding asymmetric graben to the south.

The junction of WSW-ENE trending structures with N-S trending structures to the west centres on an alluvial-filled depression, Waikari Flat, into which the structures of the WSW-ENE trending imbricate thrust system plunge, locally curling to the SW at their ends to link with N-S trending structures to the south. Roof thrusting on two orientations, W-E and N-S, towards to SE is currently occurring above these structures.

Currently the area is not highly seismically active, although a magnitude ~6.4 Ms earthquake in historic times has been recorded. The effects of tectonics on the drainage of the area does suggest that the majority of the systems, are still potentially active, albeit moving at a comparatively slow rate. The majority of the recent motion appears to be concentrated on the roof-thrusting occurring in Waikari Flat, and uplift along the Lowry Peaks Fault System. Increasing amounts of secondary movement on back-thrusts and cross fractures is also implied for western ends of the major imbricate thrust system. In contrast, the southern-most fault system appears to be largely sustaining dextral strike-slip motion, with some local folding in central portions.

# TABLE OF CONTENTS

<b>TITLE PAGE</b> .....	i
<b>FRONTISPIECE</b> .....	ii
<b>ABSTRACT</b> .....	iii
<b>TABLE OF CONTENTS</b> .....	iv
<b>LIST OF FIGURES</b> .....	ix
<b>LIST OF TABLES</b> .....	x
<b>CONTENTS OF VOLUME TWO</b> .....	xi
chapter one: <b>INTRODUCTION</b> .....	1
<b>1.1 BACKGROUND</b> .....	1
<b>1.2 REGIONAL SETTING</b> .....	1
<b>1.3 THESIS AIMS</b> .....	7
<b>1.4 THESIS ORGANISATION</b> .....	8
<b>1.5 DESCRIPTION OF THE STUDY AREA</b> .....	8
<b>1.6 PREVIOUS WORK</b> .....	10
chapter two: <b>STRATIGRAPHY</b> .....	14
<b>2.1 INTRODUCTION</b> .....	14
<b>2.2 BASEMENT ROCKS</b> .....	16
<b>2.2.1 Torlesse Supergroup</b> .....	16
<b>2.3 COVER ROCKS</b> .....	17
<b>2.3.1 Eyre Group</b> .....	17
<b>2.3.1.1 Conway Formation</b> .....	17
<b>2.3.1.2 Waipara Greensand Formation</b> .....	18
<b>2.3.1.3 Ashley Mudstone Formation</b> .....	19
<b>2.3.1.4 Homebush Sandstone Formation</b> .....	20
<b>2.3.2 Amuri Limestone</b> .....	21
<b>2.3.3 Motunau Group</b> .....	23
<b>2.3.3.1 Omihi Formation</b> .....	23
<i>Weka Pass Stone Member</i> .....	23
<i>Gorries Creek Greensand Member</i> .....	26
<b>2.3.3.2 Waikari Formation</b> .....	27
<b>2.3.3.3 Mt Brown Formation</b> .....	28
<b>2.3.3.4 Greta Formation</b> .....	29
<b>2.3.3.5 Kowai Formation</b> .....	29
<b>2.3.4 Late Quaternary deposits</b> .....	30
<b>2.4 DISCUSSION AND SUMMARY</b> .....	31
<b>2.4.1 Basement-cover rock unconformity</b> .....	31
<b>2.4.1.1 The Hurunui High</b> .....	31
<b>2.4.1.2 Lateral extent</b> .....	32
<b>2.4.1.3 Structural significance</b> .....	32
<b>2.4.2 Deformation recorded within the cover rocks</b> .....	34
<b>2.4.2.1 Middle to Late Oligocene deformation</b> .....	34



2.4.2.2 Deformation events synchronous with Motunau Group deposition.....	35
2.4.2.3 Motunau Group - Late Quaternary deposits unconformity.....	35
chapter three: <b>MACROSCOPIC DEFORMATION</b> .....	37
3.1 <b>INTRODUCTION</b> .....	37
3.2 <b>THE KAIWARA FAULT SYSTEM AND ASSOCIATED STRUCTURES</b> .....	37
3.2.1 Major range-bounding faults.....	42
3.2.2 Major folding.....	43
3.2.2.1 Waikari Anticline.....	44
3.2.2.2 Moores Hill Anticline.....	45
3.2.2.3 Moores Hill Syncline.....	47
3.2.2.4 Folding in Waikari Valley.....	47
3.2.2.5 Folding associated with Greta Peaks Fault.....	47
3.2.3 Summary and Conclusions.....	49
3.3 <b>THE MT ALEXANDER-MAXWELTON FAULT SYSTEM AND ASSOCIATED STRUCTURES</b> .....	50
3.3.1 Major range-bounding faults.....	50
3.3.2 Scargill Hills Outlier.....	51
3.3.2.1 Foxdown Anticline and Syncline.....	52
3.3.2.2 The transfer fault.....	55
3.3.2.3 Scargill Creek Fault.....	55
3.3.2.4 Smaller-scale faulting.....	57
3.3.3 Discussion of the link between structures in Scargill Hills Outlier and Mt Alexander and Maxwelton Faults.....	57
3.3.3.1 Model One.....	59
3.3.3.1 Model Two.....	59
3.3.4 Major folding.....	60
3.3.4.1 Mt Alexander Anticline.....	60
3.3.4.2 Karaka Syncline.....	61
3.3.4.3 Scargill Anticline.....	62
3.3.5 Summary.....	63
3.4 <b>THE LOWRY PEAKS FAULT SYSTEM AND ASSOCIATED STRUCTURES</b> .....	63
3.4.1 Lowry Peaks Fault System.....	64
3.4.2 Folding associated with Hurunui Bluff Fault.....	65
3.4.2.1 Ben Lomond Syncline.....	65
3.4.2.2 Lowry Peaks Anticline.....	66
3.4.3 Summary.....	67
3.5 <b>STRUCTURES AT THE WESTERN END OF THE STUDY AREA</b> .....	67
3.5.1 Trig. C Ridge Structures.....	67
3.5.2 Hawarden Anticline and Pyramid Valley Anticline.....	68
3.6 <b>SUMMARY</b> .....	69

chapter four: MESOSCOPIC DEFORMATION.....	71
<b>4.1 INTRODUCTION.....</b>	71
<b>4.2 MESOSCOPIC BASEMENT DEFORMATION.....</b>	71
<b>4.2.1 Pseudo-folding of the basement.....</b>	71
<b>4.2.2 Stress tensor analysis.....</b>	72
<b>4.2.2.1 Methodology.....</b>	73
<i>Data Collection.....</i>	73
<i>Computation of the stress tensor.....</i>	75
<b>4.2.2.2 Results.....</b>	75
<i>Lowry Peaks Fault System.....</i>	77
<i>Mt Alexander - Maxwellton Fault System .....</i>	77
<i>Kaiwara Fault System.....</i>	81
<b>4.2.2.3 Conclusions.....</b>	81
<b>4.3 MESOSCOPIC COVER ROCK DEFORMATION.....</b>	82
<b>4.3.1 Strain analysis.....</b>	83
<b>4.3.1.1 Methodology.....</b>	84
<i>Data collection and sample preparation.....</i>	84
<i>Computation of the strain ellipse.....</i>	84
<b>4.3.1.2 Results.....</b>	88
<b>4.3.1.3 Conclusions.....</b>	88
<b>4.3.2 Small-scale structures.....</b>	92
<b>4.3.2.1 Joints.....</b>	92
<i>Subvertical orthogonal joints.....</i>	93
<i>Low angle joints.....</i>	94
<i>Summary.....</i>	94
<b>4.3.2.2 Pressure solution seams.....</b>	94
<b>4.3.2.3 Small-scale faults.....</b>	96
<b>4.3.3 Stress tensor analysis.....</b>	96
<b>4.3.3.1 Results.....</b>	98
<b>4.3.3.2 Conclusions.....</b>	98
<b>4.4 CONCLUSIONS.....</b>	100
 chapter five: STRUCTURAL MODEL.....	 102
<b>5.1 INTRODUCTION.....</b>	102
<b>5.2 IMBRICATE THRUST SYSTEM MODEL.....</b>	102
<b>5.2.1 Thrust faults.....</b>	102
<b>5.2.1.1 Cross-sectional shape.....</b>	102
<b>5.2.1.2 Cross-sectional spacing.....</b>	104
<b>5.2.1.3 Spatial geometry and mechanisms of displacement transfer.....</b>	105
<b>5.2.1.4 Basal decollement.....</b>	107
<b>5.2.1.4 Displacement.....</b>	108
<b>5.2.2 Fault-related folds.....</b>	108
<b>5.2.2.1 Cross-sectional shape.....</b>	112
<b>5.2.2.2 Amplitude.....</b>	113
<b>5.2.2.3 Wavelength.....</b>	115
<b>5.2.2.4 Plan-view geometry.....</b>	117
<b>5.2.2.5 Interference folding.....</b>	119

<b>5.3 THE JUNCTION WITH STRUCTURES AT THE WESTERN END OF THE STUDY AREA</b>	120
<b>5.3.1 Introduction</b>	120
<b>5.3.2 Western end of Kaiwara Fault System and associated structures</b>	120
<b>5.3.3 Western end of Mt Alexander - Maxwellton Fault System and associated structures</b>	122
<b>5.3.4 Western end of Lowry Peaks Fault System and associated structures</b>	124
<b>5.4 CONCLUSIONS</b>	124
 chapter six: <b>GEOMORPHOLOGY AND ACTIVE TECTONICS</b>	126
<b>6.1 INTRODUCTION</b>	126
<b>6.2 GEOMORPHOLOGICAL MAP</b>	128
<b>6.3 DRAINAGE PATTERN ANALYSIS</b>	129
<b>6.3.1 Introduction</b>	129
<b>6.3.2 Drainage patterns of the major trunk streams</b>	129
<b>6.3.3 Drainage patterns of the smaller streams</b>	139
<b>6.3.3.1 Drainage patterns related to lithology</b>	139
<b>6.3.3.2 Drainage patterns related to faulting</b>	141
<b>6.3.4 Conclusions</b>	144
<b>6.4 GRADIENT INDEX ANALYSIS</b>	144
<b>6.4.1 Introduction</b>	144
<b>6.4.2 Longitudinal valley floor profile</b>	145
<b>6.4.3 Gradient index</b>	147
<b>6.4.4 Methodology</b>	147
<b>6.4.5 Results</b>	149
<b>6.4.5.1 Isolating the effects of bedrock</b>	154
<b>6.4.5.2 The effects of faulting</b>	155
<i>Moore's Hill - Greta Peaks Range</i>	155
<i>Mt Alexander Range</i>	155
<i>Lowry Peaks Range</i>	156
<b>6.4.6 Conclusions</b>	157
<b>6.5 SINUOSITY INDEX ANALYSIS</b>	157
<b>6.5.1 Introduction</b>	157
<b>6.5.2 Methodology</b>	158
<b>6.5.3 Results</b>	160
<b>6.5.4 Conclusions</b>	163
<b>6.6 TIMING OF EVENTS</b>	164
<b>6.7 HISTORICAL SEISMICITY</b>	165
<b>6.8 CONCLUSIONS AND NEOTECTONIC GEOMORPHIC MAP</b>	172
 chapter seven: <b>CONCLUSIONS</b>	173
<b>7.1 SYNTHESIS</b>	173
<b>7.2 REGIONAL CORRELATION</b>	176
<b>7.3 FUTURE WORK</b>	178

	viii
<b>ACKNOWLEDGMENTS</b> .....	180
<b>REFERENCES</b> .....	181
<b>APPENDICES</b> .....	193
appendix one: <b>STRESS TENSOR ANALYSIS</b> .....	193
appendix two: <b>STRAIN ANALYSIS</b> .....	201
appendix three: <b>GRADIENT INDEX ANALYSIS</b> .....	204

# LIST OF FIGURES

Figure 1.1	Elements of the Australia-Pacific plate boundary zone.....	2
Figure 1.2	Landsat Image of the north Canterbury region.....	3
Figure 1.3	Major structures characterising the north Canterbury region.....	4
Figure 1.4	Principal horizontal compression direction acting upon the northern portion of the South Island.....	6
Figure 1.5	Major topographic, drainage and cultural features of the study area....	9
Figure 2.1	Schematic stratigraphic column of the major rock units in the study area.....	15
Figure 2.2	Stratigraphic features and relationships at "the gap".....	22
Figure 2.3	Jointing in the tuffaceous bands of the Weka Pass Stone Member.....	25
Figure 2.4	Clasts of Waikari Formation within the base of the Mt Brown Fm.....	25
Figure 2.5	Lateral extent of the Hurunui High.....	33
Figure 3.1	Summary diagram of the major fault systems.....	38
Figure 3.2	Summary diagram of the macroscopic structures.....	39
Figure 3.3	Angular cross-sectional shape of Moores Hill Anticline.....	46
Figure 3.4	Schematic diagram of the folding relationships in Waikari Valley.....	48
Figure 3.5	Conical fold characteristics and stereoplots.....	53
Figure 3.6	The geometry of conical folds in terms of fold tightness of interference sets.....	54
Figure 3.7	The scarp preserved along the northern side of Scargill Anticline.....	56
Figure 3.8	Three models for the arrangement of structures in Scargill Hills Outlier.....	58
Figure 4.1	Location map and fault plane data for the basement stress tensor analysis sites.....	74
Figure 4.2	Full set of basement stress tensor analysis results.....	76
Figure 4.3	Interpreted $\sigma_1$ plots with respect to their locations.....	78
Figure 4.4	Location map for samples used in the strain analysis.....	85
Figure 4.5	"Best" strain analysis results.....	89
Figure 4.6	"Worst" strain analysis results.....	90
Figure 4.7	Strain analysis plots that contain a large ellipse.....	91
Figure 4.8	Low angle joints in the Weka Pass Stone Member.....	95
Figure 4.9	Summary diagram showing the relationship of joints to folding.....	95
Figure 4.10	Location map, fault plane data and interpreted $\sigma_1$ results of the Waikari Quarry stress tensor analysis.....	97
Figure 4.11	Full set of Waikari Quarry stress tensor analysis results.....	99
Figure 5.1	Block diagram showing the 3-d geometry of the structures in the area.	103
Figure 5.2	Summary diagram of the mechanisms of displacement transfer.....	106
Figure 5.3	Measurement of fault-related fold amplitude and total structural elevation difference.....	110
Figure 5.4	The end-member types of folding associated with thrust faults.....	111
Figure 5.5	The development of fault-propagation folds by kink band migration....	111
Figure 5.6	Graphical relationship of vertical fault displacement and fold amplitude	114
Figure 5.7	Structural features of Pleistocene sedimentary basins in north Canterbury.....	116
Figure 5.8	Bow-shaped trace of thrust faults and their progressive relationship to fault-propagation folding.....	118
Figure 5.9	Sigmoidal fold trace as the result of oblique compression.....	118
Figure 5.10	Model of continuation of major structures beneath Waikari Flat.....	121
Figure 5.11	Structure contouring on the basement-cover rock unconformity of the Doctors Dome.....	123

Figure 6.1	Classification of basic drainage patterns.....	130
Figure 6.2	Classification of modified basic drainage patterns.....	132
Figure 6.3	Drainage of the study area divided into major catchments.....	133
Figure 6.4	Major catchments of the study area compared to structure.....	134
Figure 6.5	Drainage of the study area classified according to stream order.....	135
Figure 6.6	Anomalous drainage patterns due to a lithological control.....	140
Figure 6.7	Anomalous drainage patterns of the study area due to a structural control.....	142
Figure 6.8	Classification of “knick points” that appear on longitudinal valley profiles.....	146
Figure 6.9	Definition of the symbols used for calculating stream gradient index....	148
Figure 6.10	Results of the stream gradient index study for the major streams.....	150
Figure 6.11	The effects on a braided river crossing a growing anticlinal structure...	159
Figure 6.12	The results of the sinuosity index study in relation to mapped structures.....	161
Figure 6.13	Station locations of the National Digital Seismograph Unit.....	166
Figure 6.14	Seismicity in New Zealand for the periods 1965-1975 and 1964-1987..	167
Figure 6.15	Seismicity in New Zealand for the period 1990-1993.....	168
Figure 6.16	Seismicity in north Canterbury for a 10 week period in 1990.....	169
Figure 6.17	Isoseismal maps of the 25th December 1922 earthquake.....	171
Figure 8.1a-f	Results of the tests of stress tensor analysis with different variables.....	197
Figure 8.2	Comparison of STEREO contouring methods.....	200
Figure 8.3	The Fry method.....	202
Figure 8.4	Test plots for the size and number of points needed for the strain analysis.....	202

## LIST OF TABLES

Table 3.1	Summary of the major faults.....	40
Table 3.2	Summary of the major folds.....	41
Table 4.1	Summary of strain analysis results.....	87
Table 5.1	Relative amounts of throw on the major faults.....	109
Table 6.1	Descriptions of the basic types of drainage patterns.....	131
Table 8.1	Results of the tests of stress tensor analysis with different variables.....	196

## CONTENTS OF VOLUME TWO

- Map 1      Geology of the Lowry Peaks Range-Waikari Valley area, north Canterbury
- Map 2      Structure contour map on the surface of the basement rocks area, north Canterbury
- Map 3      Geomorphology of the Lowry Peaks Range-Waikari Valley area, north Canterbury
- Map 4A     Locality map of streams used for the gradient index analysis
- Map 4B     Results of the stream gradient index analysis
- Map 4C     Results of the stream gradient index analysis compared to major lithologies and structure
- Map 5      Results of the sinuosity index analysis
- Map 6      Neotectonic Geomorphic map of the Lowry Peaks Range-Waikari Valley area, north Canterbury

### Geological Cross Sections

## INTRODUCTION

### 1.1 BACKGROUND

The north Canterbury region comprises the southern-most portion of the plate boundary transfer zone between the west-facing Hikurangi Margin subduction zone lying offshore of the east coast of New Zealand to the NNE-SSW trending, oblique-dextral Alpine Fault along the west side of the South Island (figure 1.1). The actively widening transfer zone has been the target of a number of recent studies under the "North Canterbury Active Tectonics Programme" of the University of Canterbury (Cowan, 1989, Nicol, 1991, Syme, 1991, McMorran, 1991, Garlick, 1992, Mould, 1992, Cowan, 1992, Pope, 1994), which has lead to the recognition of the very complex nature of active thin-skinned tectonics characterising the region. Studies have thus far targeted areas on the western, southern and northern boundaries of the region, but have not studied in detail the kinematics of much of the structures in central and eastern portions. The purpose of this study is to detail the geometry and kinematics of motion of WSW-ENE trending structures forming the south-western end of the large belts of structures of central and eastern portions of north Canterbury, and to determine the transition between these and N-S trending structures mapped to the west by Nicol (1991) and Mould (1992).

### 1.2 REGIONAL SETTING

Topographically, the actively evolving and widening plate boundary zone in north Canterbury is characterised by low relief basin and range topography. To the north and west, high relief areas occur adjacent to the Hope and Alpine Faults. In contrast, the area south of the Porters Pass-Amberley Fault Zone is characterised by large alluvial plains, the Canterbury Plains (figure 1.2).

The topographic contrasts between these three areas can be related directly to geology; the relatively mountainous areas consist almost exclusively of Torlesse Supergroup "basement rocks", whereas the basin and range area is characterised by basement cored-



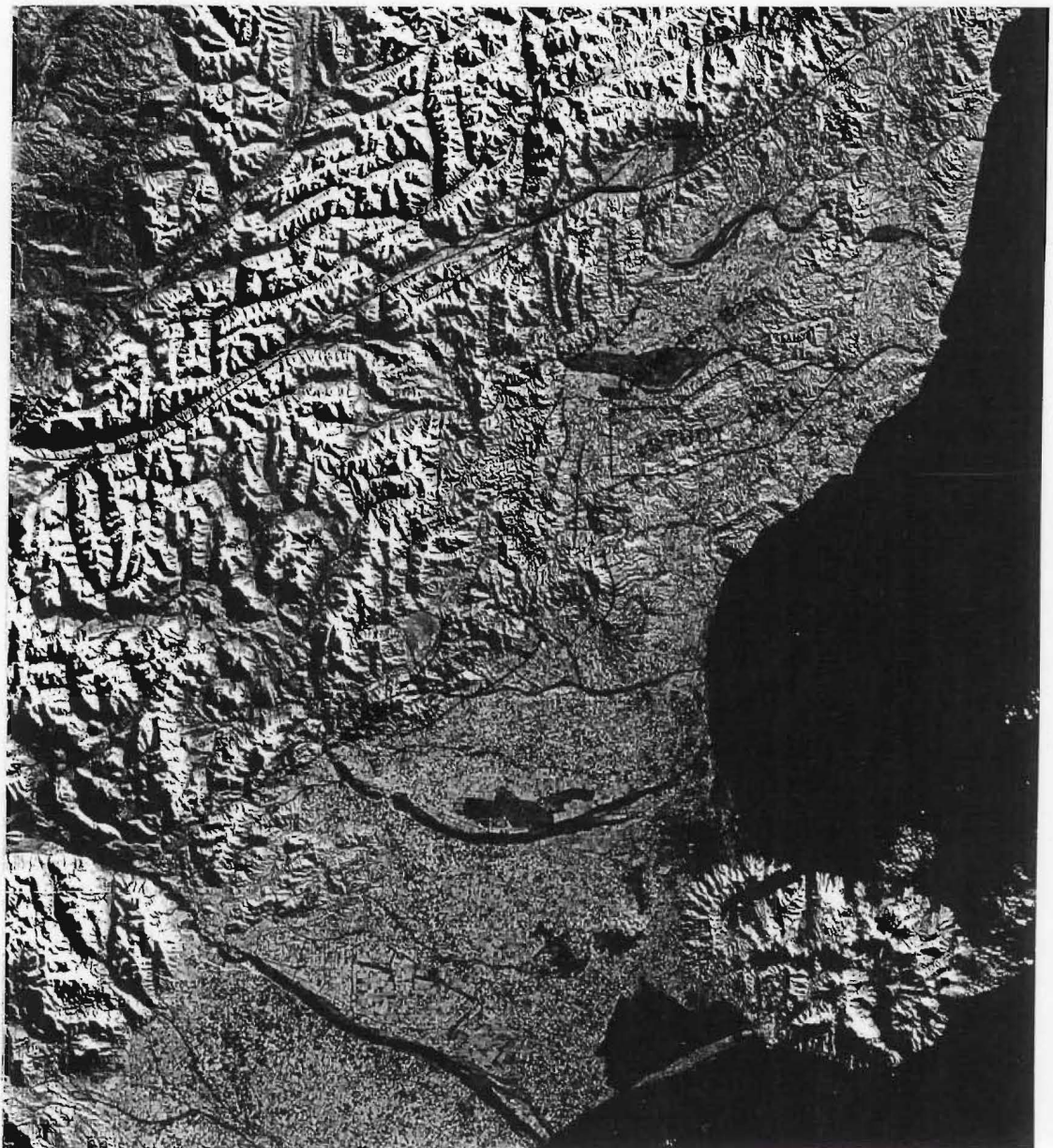


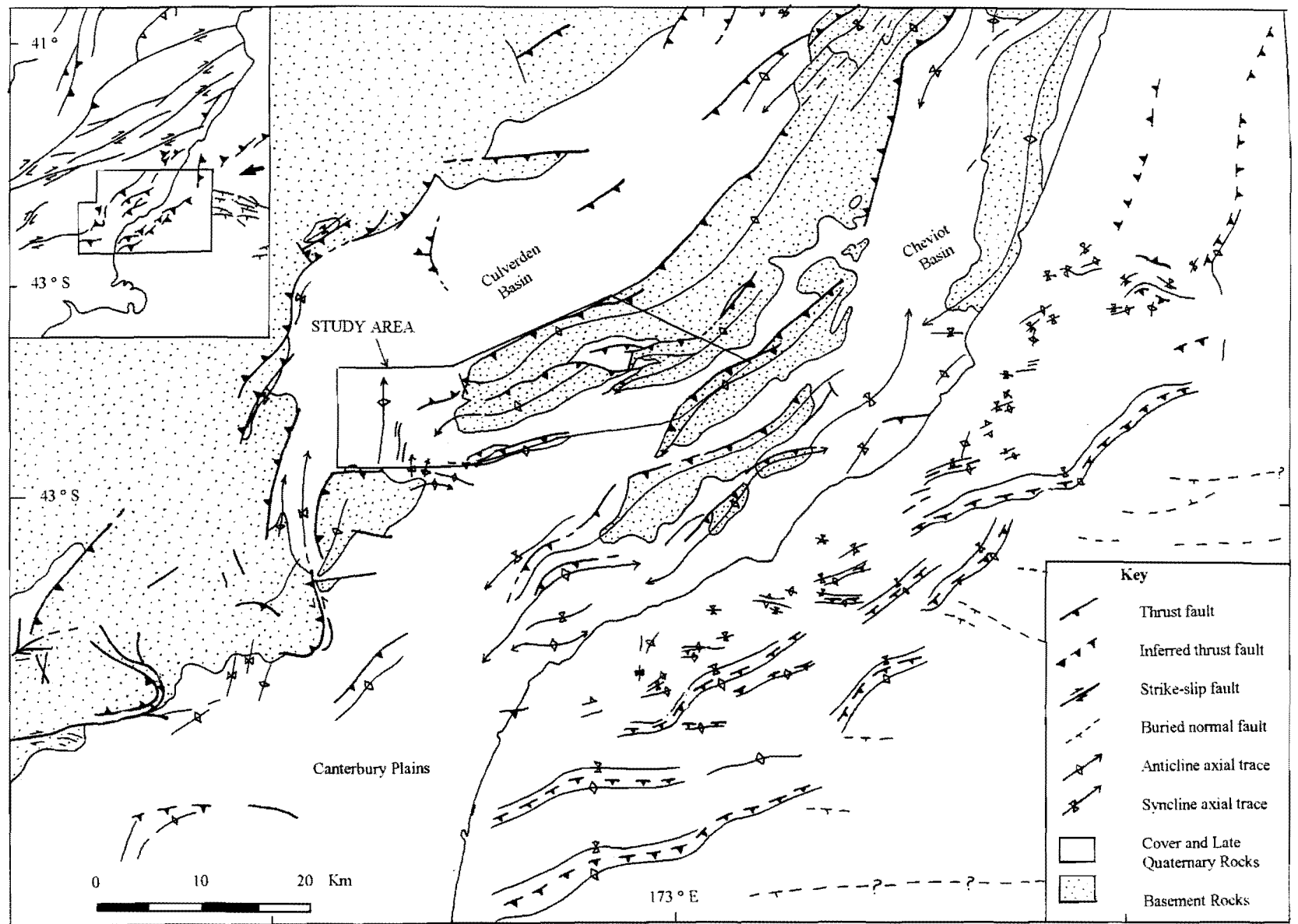
**Figure 1.2** Landsat image of the Canterbury Region, showing the major topographic contrasts between: i) the mountainous areas north of the Hope Fault and the Southern Alps region, ii) the flat alluvial plains south of the Porters Pass Amberley Fault Zone and iii) the structurally controlled basin and range topography of the north Canterbury region.

ranges with the less resistant "cover rocks" preserved in various-sized basins and as aprons around the ranges. Therefore, it is clear that more uplift has occurred in the southern Alpine Fault and Marlborough regions and, since all areas are currently tectonically active, deformation clearly commenced earlier in these regions. Recent studies in the north Canterbury region have supported this hypothesis, the only evidence for significant syn-depositional deformation being restricted to the uppermost units such as the Kowai Formation (Pliocene to Lower Pleistocene) (eg. Nicol, 1991, Cowan, 1992).

Structurally, the basin and range topographic domain is bound by a series of thrust faults on the western margin (eg. Mould, 1992) and by the Hope Fault and Porters Pass - Amberley Fault Zone (Cowan, 1992) in the north and south respectively (figure 1.2). The area is characterised by a set of very young, often very complex, faults (predominantly thrust faults) and fault-related folds (eg. Nicol, 1991, Mould, 1992), giving rise to the basin and range - style of topography (compare figures 1.2 and 1.3). Barnes (1993) was able to recognise similar structures in the area immediately offshore (figure 1.3).

Many of the faults in the north Canterbury area, however, depart dramatically from a simple NE-SW trend predicted by plate motion vectors (de Mets et al, 1990) and principal horizontal compression directions for the entire northern South Island (Arabasz and Robinson, 1976, Rynn and Scholz, 1978, Bibby, 1975, 1970, 1981, Walcott, 1978, Nicol and Campbell, 1990, Nicol and Wise, 1992, Pettinga and Wise, 1994) (figure 1.4). The south-western edge of the range and basin region is characterised by a distinct set of N-S trending faults and folds, having their origins in the Porters Pass-Amberley Fault Zone (figure 1.3). These structures bound the western side of the Culverden Basin, considered a contractional basin by Mould (1992) (figure 1.3). Immediately to the east of the N-S trending structures are a set of W-E trending faults and folds in the Waipara-Weka Pass region, apparently synchronous in their development with the N-S set (Nicol, 1991 and 1992). Barnes (1993) has described W-E trending, north-facing normal faults on the north slope of the Chatham Rise that appear to have undergone continued episodes of extension from the Cretaceous to the present (dashed faults in figure 1.3). He suggested that these extended onshore in the Cretaceous and are now overprinted by the Late Cainozoic deformation. Nicol (1991 and 1992) found evidence for reactivation on at least two W-E trending faults in the Waipara to Weka Pass region and proposed

**Figure 1.3** Major structures characterising the north Canterbury region, both onshore and offshore. (Adapted from Barnes, 1993).



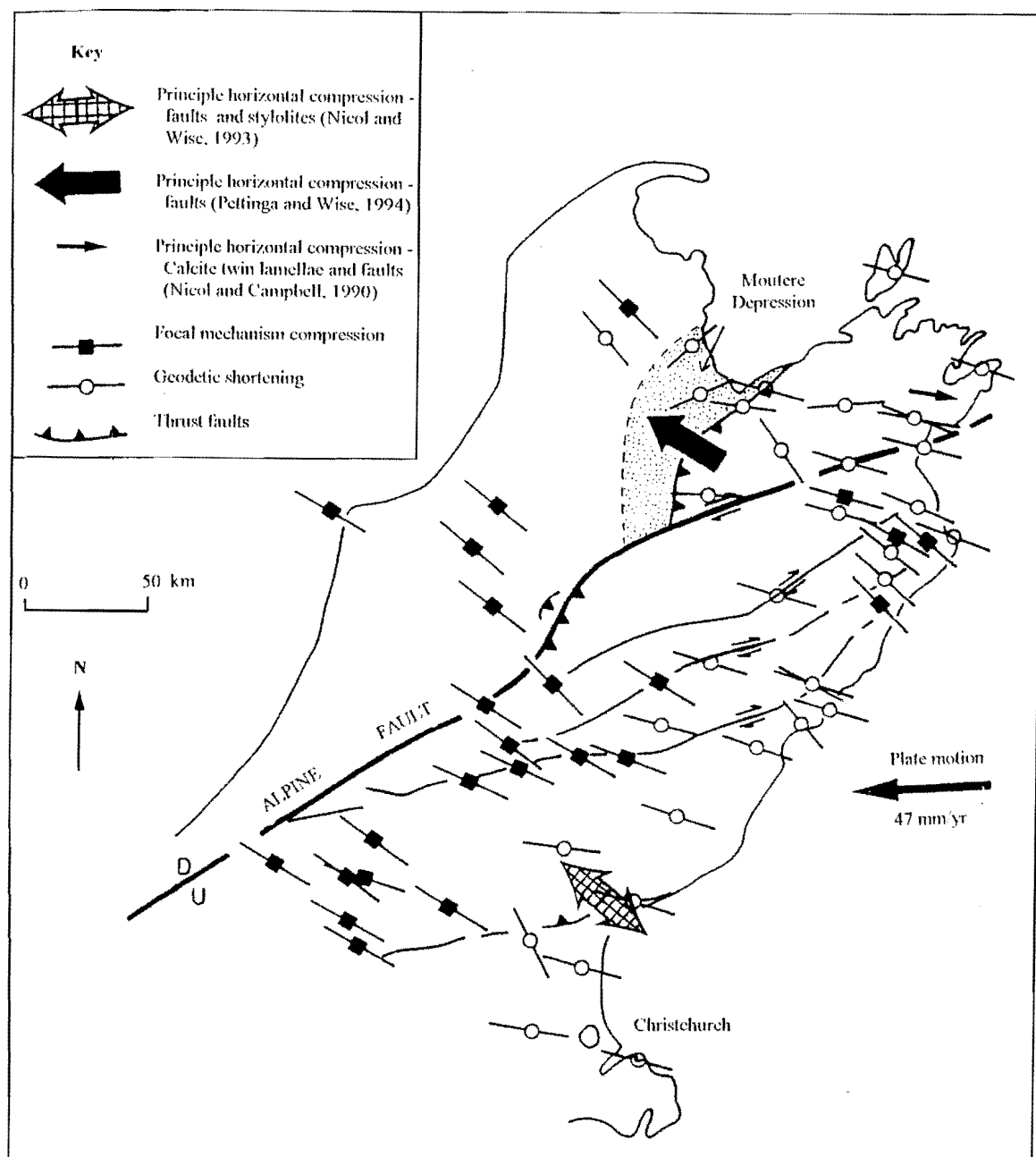


**Figure 1.4** A compilation of the available focal mechanism (Arabasz and Robinson, 1976, Rynn and Scholz, 1978), geological principal horizontal compression (see figure), and geodetic triangulation (Bibby, 1975, 1976 and 1981, Walcott, 1978) principal shortening data for the northern South Island. The orientation of the principal horizontal compression and shortening is marked by the long axis of the symbols. (Redrafted from Nicol and Wise, 1992, Pettinga and Wise, 1994).

that at least in that area, presence of pre-existing structures has caused a partitioning of the NW-directed stress into two components, one N-S and one W-E (Nicol, 1991).

The remainder of north Canterbury is made up of a very large (80-100 km long) belt of predominantly NE-SW trending thrust faults and folds that locally comprise the eastern margin of the Culverden Basin. These can also be traced to continue some distance offshore (figure 1.3) (Barnes, 1993). A major characteristic of this belt is a number of unexplained localised departures from the typical NE-SW trend, to a more W-E or WSW-ENE trend (figure 1.3). Barnes (1993) suggested that offshore, reactivation of Cretaceous normal faults were dominating the trend of these structures. Onshore however, these structures have not been studied in detail.

One set of anomalously W-E to WNW-ENE trending structures is located at the southern end of the Culverden Basin, where the NE-SW trending belt meets the orthogonal structures described above of the Waipara-Weka Pass region. These structures are generally WSW-ENE trending, but locally form W-E, N-S and NE-SW trends, suggesting a complex geometry and history of deformation. They include the southwestern end of the Kaiwara Fault and the Lowry Peaks Fault (eg. Gregg, 1964), two major range-bounding structures that have been mapped to bound the eastern and western sides of the Culverden and Cheviot Basins respectively, to which clear response of drainage to their trends suggest likely recent activity. This region, the Lowry Peaks Range - Waikari Valley district, forms the subject of this thesis.

### **1.3 THESIS AIMS**

The aims of this thesis are:

- i) to map in detail the geometric relationships between the major structures of the Lowry Peaks Range - Waikari Valley district
- ii) to characterise the kinematics and internal strains of the component structures mapped
- iii) to propose models linking structures of WSW-ENE and N-S trends
- iv) to document Quaternary activity, particularly focusing on the response of drainage to recent activity.



## **1.4 THESIS ORGANISATION**

A relatively detailed study of stratigraphy was found to be valuable in terms of highlighting inherited tectonic controls and therefore a whole chapter (Chapter 2) is devoted to it. The major (or macroscopic) structures mapped (map 1) are described in detail in Chapter 3, with an examination at the internal strains and stresses of the component fault blocks presented in terms of mesoscopic deformation in Chapter 4. Chapter 5 contains a description of the resulting three-dimensional model based on the results of Chapters 3 and 4 and discusses the junction with structures mapped by Nicol (1991) to the SW. Chapter 6 investigates in more detail suggestions of the presence or absence of active tectonic activity proposed in Chapters 4 and 5, by describing the geomorphology (map 3) of the area in more detail, both qualitatively and quantitatively, and investigates possible evidence for the effects of these tectonic activities on the major drainage systems of the area.

## **1.5 DESCRIPTION OF THE STUDY AREA**

The study area is situated just to the north of Weka Pass, 72 km from Christchurch along State Highway 7 (see inset of figure 1.5) and encompasses a 41x17 km area bound to the north and east by the Hurunui River, to the west by the valley occupied by the north branch of the Waipara River and to the south by an arbitrary line through the Moores Hill and Greta Peaks Ranges (named for the purposes of this thesis, as shown on figure 1.5 and map 1).

The area is centered upon the southwestern portion of the Lowry Peaks Range (which has been subdivided into the northern, Lowry Peaks Range and the southern, Mt Alexander Range for the purposes of this thesis, as shown in figure 1.5), which forms the south-eastern boundary of the Culverden Basin.

The broad Waikari Valley is situated between Mt Alexander and Moores Hill Range, occupied by Waikari River, which is fed by a number of similar-sized streams such as Scargill Creek, Eastcott Stream (informal name) and Tipapa Stream (see figure 1.5).

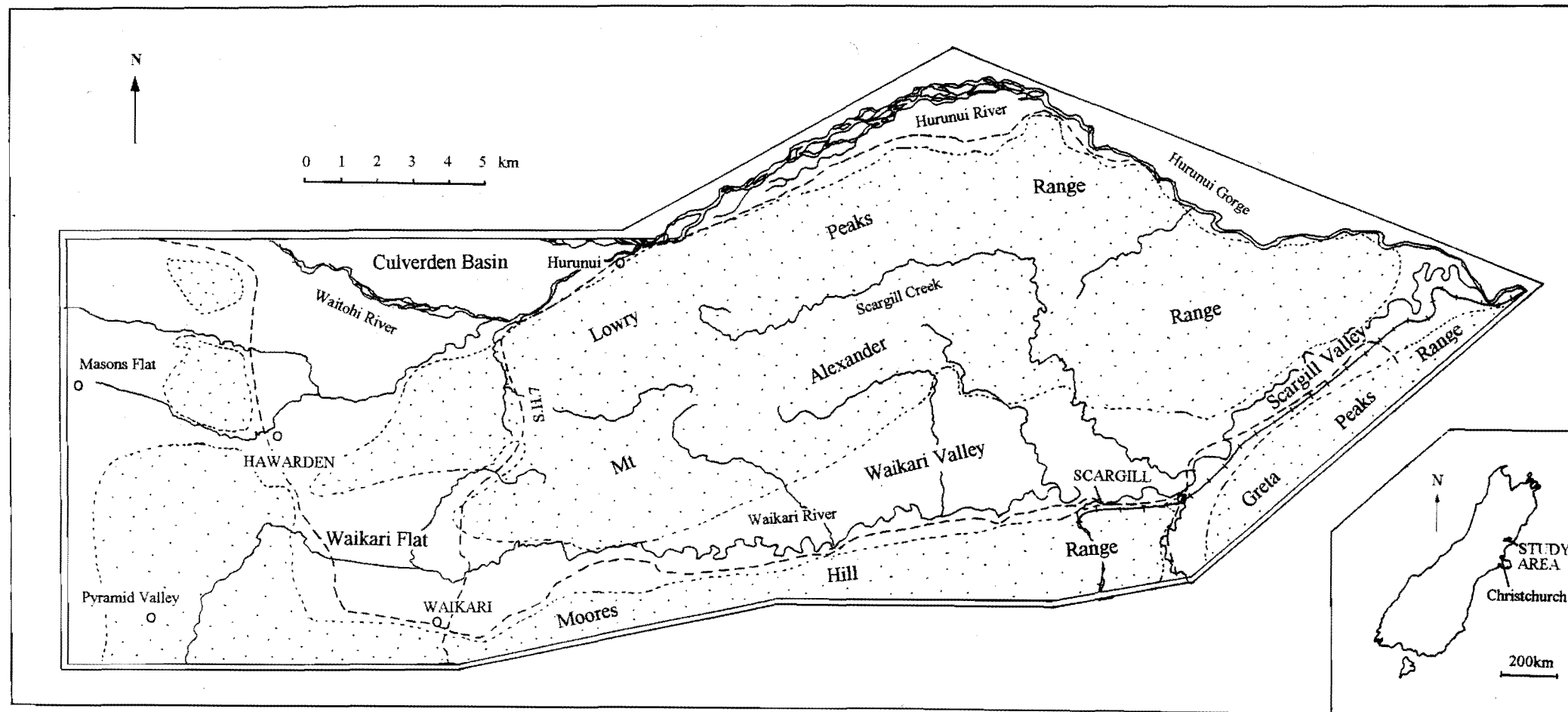


**Figure 1.5** Major topographic, drainage and cultural features of the Lowry Peaks Range - Waikari Valley area. Dotted pattern represents areas of high relief.

The valley is bound to the west by a number of low hills, both west and south of Hawarden, which define the upper catchment area.

The area is not heavily populated, although there are a number of small townships, the largest being Hawarden and then Waikari, with smaller settlements of Scargill, Hurunui, Pyramid Valley, Masons Flat and Horsley Down (figure 1.5). However, due to the relatively low topography, the area is extensively farmed (eg. see the major properties shown on map 1), with only a low scrub (generally Matagouri) cover over the higher peaks. Access to the area is readily available, namely through Pyramid Valley or Masons Flat area in the west (including Lake Sumner Road), Weka Pass (state highway 7) in the south, Greta Valley and Ethelton Roads in the SE and state highway 7 to the north.

Outcrops of cover rocks are largely confined to a number of key creeks, but some such as the Hurunui River give near complete stratigraphic sections. The more resistant rocks such as the coarse sandstone members of the basement rocks (also locally some conglomerates, volcanics and cherts), and limestones of the cover rocks form strike ridges on the hill slopes that proved to be very useful in terms of the detailing of much of the structure.

## **1.6 PREVIOUS WORK**

Early workers in the Lowry Peaks Range - Waikari Valley district concentrated primarily on aspects of stratigraphy, but discussions are brief, mainly conducted in conjunction with the Waipara-Weka Pass Region to the southwest or the Motunau region to the south (eg. Buchanan, 1868, Haast, 1871a, Hutton, 1874, Hutton, 1885 and Speight, 1915a).

The above works concentrated primarily on stratigraphy at the western end of the study area and lead to the proposal that the ranges of basement rocks originally formed islands in a "Mesozoic Bay" (Haast, 1871), the younger sediments deposited in an apron-like fashion in the straits around them. The current basin-and-range topography was then thought to represent the results of vertical uplift whereby the straits in between the



islands have been reduced to river valleys and eroded downwards in accordance with the uplift.

Not long after the turn of the century a new model of uplift and downcutting was being proposed due to the recognition of a number of important structures in the region. Cotton (1913) was the first to suggest that the basement-composed ranges in the area were in fact anticlinal cores, supported by Thomson (1920) who considered that where the Late Cretaceous to Cenozoic rocks were stripped off the Moores Hill Range the fossil Cretaceous Peneplain on the basement rocks was exposed.

Speight (1915a), recognised a number of "intermontaine basins" in the Canterbury region, and suggested that both the "Waiau-Hurunui" (Culverden Basin) and the "Waikari Creek" Basin (Waikari Valley) (considered to represent separate portions of the same basin) were formed by a combination of both faulting and folding. Faults were proposed for the southern margins of each of these basins and were considered to grade into folds at their western ends. Later, Speight (1918) classified his "Waikari-Kaiwara" Basin (Waikari Valley) as a "tilted-strip basin", in which the cover rocks had been down-faulted to form a valley that had been subsequently enlarged by erosion.

Speight and Wild (1918) described rocks in an "upper-basin", now referred to as Scargill Hills Outlier. A number of W-E trending faults were noted in the upper-basin, but not mapped in detail, considered to contribute to the repetitions of the limestones observed there.

The new patterns of uplift suggested by the structures of the region lead to the hypothesis that the major rivers in the region established their courses before the major anticlines were uplifted (and hence were antecedent) (eg. Cotton, 1913, Speight, 1915b and 1918, Thomson, 1920 and Cotton, 1938). A coastal plain created during the first few increments of uplift was proposed on which the rivers took consequent paths to the sea. While this coastal plain was in existence, it was suggested that many of the major rivers underwent enough downcutting to allow them to maintain their courses when major anticlines were uplifted across their path, hence were considered to represent antecedent drainage. This theory could then explain the anomalous paths of the Hurunui and Waiau Rivers across Basement Rocks of the Lowry Peaks-Mt Alexander Range, instead of utilizing "structural lows" containing softer, cover rocks, such as Weka Pass

(Thomson, 1920). Powers (1962) adhered to the above "superimposition hypothesis", when he studied the terraces along the entire Hurunui River.

A series of Masters Theses studying portions of north Canterbury were completed from 1949 to 1964 which presented the first detailed stratigraphy of much of the study area. (Schofield, 1949, Hamilton, 1950, Falloon, 1954 and Maxwell, 1964).

Schofield (1949) essentially studied the western parts of the Lowry Peaks Range - Waikari Valley area, particularly west of State Highway 7. However, emphasis was placed on the well-exposed MacDonald Downs-Doctors Hill Area and consequently the structure and stratigraphy of the northern part of Schofield's study area was largely ignored, with the exception of the observation of a set of river terraces 100 feet above the basin floor, just south of Trig C.

Hamilton's (1950) study area was very similar to the present one. Structurally, the area was considered to be divided into a number of tilted blocks, bound on the north side by steeply-dipping, range-bounding faults. However, except for the major structural observations, the structure was not studied in detail. Hamilton's structures were largely adopted by Gregg (1964) on the 1:250 000 scale Geological Survey map, with the exception that Gregg considered Hamilton's Moores Hill Fault to be the southern extension of the Kaiwara Fault mapped by Maxwell (1964) to the NE.

Hamilton's (1950) most significant contribution was his detailed descriptions of stratigraphy, although most of the units have since been renamed (Browne and Field, 1985). In particular, Hamilton noted a number of unconformities in the region, the most important being the widespread continuation of an unconformity noted in the west of the area by Thomson (1920), in which the Cretaceous to Paleocene units present in other portions of north Canterbury, are largely missing. The complete absence of the Amuri Limestone was also documented (although a very small portion has been found since, Lewis, 1992), and evidence for an unconformity between the Scargill Siltstone (now Waikari Formation) and Mt Brown Formations was noted in the east of the area. The Weka Pass Stone was noted to undergo several facies change across the area, including the incorporation of some volcanic material in northern portions.

Falloon (1954) studied the entire Culverden Basin, but largely drew on Hamilton's then recently completed study. His study is important in that it renames much of Hamilton's stratigraphy to correlate the various units across the Culverden Basin. Furthermore, Falloon considered the range-bounding faults of the Lowry Peaks and Moores Hill Ranges to be complex fault-zones (the Lowry Peaks and Waikari Faults Zones) rather than simple faults.

Maxwell (1964) primarily concentrated on the Kaiwara region to the NE of the study area but his southern boundary was the Hurunui River. He again renamed many of Hamilton's (1950) units and mapped the Kaiwara Syncline in the Hurunui Gorge. Maxwell (1964) named the Kaiwara Fault and proposed that it continued as a single fault into this study area. Maxwell also named the Ethelton Conglomerate, a conglomerate in the Torlesse Supergroup that straddles the Hurunui River which Hamilton had considered to represent the boundary between two sub formations of the Torlesse Supergroup. The Ethelton Conglomerate has since been included in two studies of Torlesse Supergroup conglomerates, in an attempt to define a possible source-terrane for the Torlesse Supergroup (Smale, 1978 and Dean, 1993).

Since the above theses, there has been essentially no study of the area, except for the description of a number of key stratigraphic sections preserved in the small creeks, in an attempt to produce a lithostratigraphy for the north Canterbury Region as a whole (Andrews, 1960, 1963 and 1968, Browne and Field, 1985 and 1988, Field and Browne, 1989). Dibble's unpublished gravity data of the Culverden Basin also covers a small part of the study area, particularly the northern side of Lowry Peaks Range and Waikari Flat area.

## STRATIGRAPHY

### 2.1 INTRODUCTION

Structural controls on the distribution of the rocks in the Lowry Peaks Range - Waikari Valley area make stratigraphic correlations across the area difficult. Conversely, abrupt lithological changes of units can reflect the degree and age of structural control. The units in the study area have been found to be highly sensitive to tectonic activity, particularly since Middle Cretaceous times, and hence are described in some detail. The stratigraphy from the area mapped by Nicol (1991) occurring in the SW portions of map 1 (see insert on map 1) are excluded from this discussion.

The amount of exposure in the study area is highly variable, the more resistant rocks can be found in abundance throughout the region, exposed as a number of strike-ridges on the hillsides, whereas exposures of softer, Cretaceous to Cenozoic cover rocks are largely restricted to the major drainage systems; good outcrops can be found in Scargill Creek, Eastcott and Tipapa Streams and the eastern portions of Waikari River, with excellent exposures in the high terrace scarps along the Hurunui River. Outcrops on the Moores Hill Range are abundant in general, most creeks and a number of slips contain exposures and Waipara Greensand Formation can be found in abundance as a thin capping over much of Moores Hill Anticline and the eastern end of Waikari Anticline (map 1).

As mentioned in Chapter 1, the stratigraphic sequence can be divided into two: i) Mesozoic "basement rocks"; consisting entirely of the Torlesse Supergroup, which dominates the area as the cores of the large fault-bound anticlines, and ii) Late Cretaceous to Cenozoic "cover rocks", preserved as an apron around the anticlines and in any other "structural lows" that occur. A further subdivision is also made in the upper units of the cover rocks between the Kowai Formation (?Late Miocene - Early Pleistocene) and the "modern" alluvial fan gravels that lie unconformably above them, which are referred to here as Late Quaternary deposits. The general stratigraphic succession is shown in figure 2.1. All of the unit names follow Browne and Field (1985).

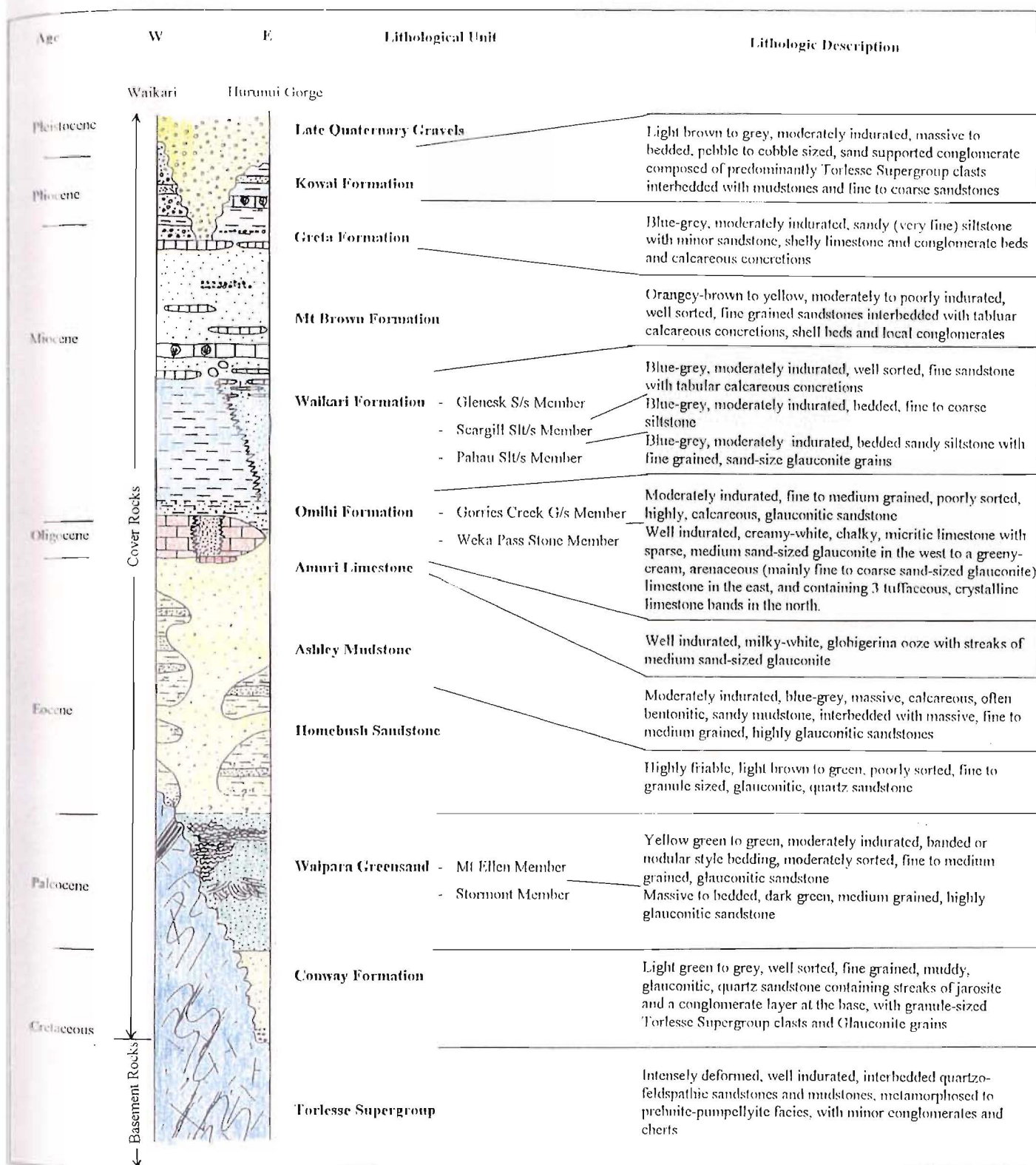


**Figure 2.1** Schematic stratigraphic column (not drawn to scale) summarising the distributions and nature of the contacts between the major units in the study area, following a generalised transect from a position immediately east of Waikari, through to the Hurunui Gorge.

## 2.2 BASEMENT ROCKS

### 2.2.1 Torlesse Supergroup (Warren, 1967): *Late Jurassic - Middle Cretaceous*

The study area lies in the Pahau Subterrane of the Torlesse Terrane, which contains the younger rocks of the Torlesse Supergroup, deposited in an accretionary prism setting during Late Jurassic to Middle Cretaceous times (Bishop, et al, 1985).

The Torlesse Supergroup was not mapped in detail but the presence of resistant, near-vertical sandstone strike-ridges, particularly in the ranges on the north side of the valley, allowed the detailing of the gross structure by means of "form lines", as drawn from aerial photographs (map 3). The distribution of these form lines suggest that bedding generally trends WSW-ENE and has been folded into a number of large-scale folds with approximately N-S trending axes.

Exposures that were visited were found, in general, to be moderately to relatively unweathered and structurally complex on a mesoscopic scale. Lithologically, the Supergroup is dominated by well indurated, interbedded (bedding on a variety of scales from a few centimetres to tens of metres), quartzofeldspathic, sandstones and mudstones, regionally metamorphosed to prehnite-pumpellyite facies with minor conglomerates, volcanics and cherts. Numerous shear zones were evident, commonly confined to the argillite beds and many disrupted, minor folds.

A characteristic of the Torlesse Supergroup in this region is the presence of topographically smooth, low gradient surfaces in a number of areas (map 3). These surfaces are often clearly punctuated by the sandstone strike-ridges and found predominantly to occur near the faults and/or where the cover sequence has clearly been recently stripped off (although in some places this is accentuated by pastoral cultivation). This surface is interpreted to represent the "fossil Cretaceous Peneplain" of Thomson (1920), which can be identified in a number of other places in north Canterbury (eg. along the north Canterbury foothills, Cowan, 1992). One of the features of the surface in this study area however, is the lack of a very deep weathered zone beneath this surface. The deep weathering is usually attributed to exposure before marine transgression deposited the first units of the cover rocks (although the added presence of coal measures may enhance this effect). The lack of such a surface here

suggests either that the area was still beneath sea level and undergoing no deposition during the Late Cretaceous, or that a great deal of erosion took place before the cover rocks were deposited. The latter is the most likely given the nature of the unconformity in the cover rocks above the basement as discussed below.

## 2.3 COVER ROCKS

The Late Cretaceous to Cenozoic cover rock sequence in this area is relatively thin (approximately 500 m), by comparison with the thick, well studied equivalent sequence in the Waipara-Weka Pass Region (up to 1 km), due to at least two major unconformities. The first involves the complete absence of any Late Cretaceous to Early Paleocene rocks over extensive parts of the region, the second is the apparently widespread removal of the Amuri Limestone (except for the very thin occurrences in Scargill Hills Outlier mentioned previously).

### 2.3.1 Eyre Group (Mcpherson, 1947): *Late Cretaceous - Middle Oligocene*

The Eyre Group consists of predominantly sandy rocks deposited unconformably on the Torlesse Supergroup as a transgressive shelf unit (Browne and Field, 1985). It consists of seventeen formations, six of which occur in the map area, but only four have been mapped by this author (the other two are in the area mapped by Nicol, 1991) and the discussion is limited to them.

#### 2.3.1.1 Conway Formation (Warren and Speden, 1978): *Late Cretaceous*

The Conway Formation is restricted to the very east of the area, clearly exposed in the Hurunui Gorge and the eastern reaches of the Waikari River. There it unconformably overlies relatively un-weathered Torlesse Supergroup where it contains a number of small pebbles of Torlesse Supergroup sandstone to form a conglomerate in its lower 20 cm. Maxwell (1964) described the conglomerate as containing a number of rounded, to

subrounded, boulders of Torlesse Supergroup sandstone but these were not observed, however the contact is not well exposed at present.

Apart from Torlesse Supergroup pebbles, the basal conglomerate also contains a number of granule-sized glauconite grains which decrease in concentration upwards in a very irregular fashion (several "pods" of glauconite-rich sandstone occur throughout the lower metre of the unit). The Torlesse Supergroup clasts and glauconite grains are supported by a greeny-brown, highly friable, poorly sorted, fine to medium grained, muddy, glauconitic, quartz sandstone. Numerous streaks of jarosite also occur and there is a large amount of limonite staining, especially in the lower 20 cm.

Above the conglomeratic basal unit is a rather uniform, massive, highly friable, light green to grey, well sorted, fine grained, glauconitic quartz sandstone. This appears to grade conformably into the overlying Waipara Greensand Formation, with a relatively rapid increase in glauconite content upwards. No concretions have been noted.

A barred submarine depression was suggested by Warren and Speden (1978) for the Conway Formation, in which gentle bottom currents allowed sedimentation from suspension. The occurrence in the very east of the study area and to the west in the Weka Pass region has lead to the proposal that a topographic high occurred between the two regions, the Hurunui High, to be discussed in detail later.

#### 2.3.1.2 Waipara Greensand Formation (Thomson, 1920): *Paleocene*

Waipara Greensand Formation has been observed in several localities in the study area, particularly in eastern and central portions. Varying thicknesses of the outcrops on the hill slopes of central portions of the Moores Hill Range area, and the localised outcrops in Scargill Creek (immediately north of "the gap", an airgap through one of the strike-ridges of limestone in Scargill Hills Outlier, grid reference 972 134) and along the Lowry Peaks range-front suggest that the basement-cover rock contact was not completely flat, but contains a number of hollows in which Waipara Greensand Formation was deposited (however, the relief is not considered to be enough that the surface of the basement cannot be used as a regular surface for structure contouring at the scale used in later chapters).



Typically it forms a dark green (to almost black in the Hurunui River), moderately indurated, moderately well sorted, fine to medium grained, slightly calcareous, sulphurous in places, glauconitic sandstone. Both the Mt Ellen and Stormont Members can be recognised in the study area, the banded or nodular Mt Ellen Member is predominant in the Moores Hill Area and in Scargill Hills Outlier, while the massive, dark green Stormont Member prevails in the Hurunui Gorge. (The Stormont Member can also be recognised in the many portions of the Moores Hill area though).

Northern parts of the area, where the Waipara Greensand Formation clearly is not present, are suggested to have still been largely undergoing erosion during the Paleocene, forming part of the of the slowly-subsiding Hurunui High.

The Waipara Greensand Formation is interpreted as a shallow marine deposit that accumulated under conditions of very slow sedimentation interrupted by bursts of high energy during the early stages of the Stormont Member deposition (Browne and Field, 1985), which fits with the environment suggested here.

#### 2.3.1.3 Ashley Mudstone Formation (Mason, 1941): *Eocene*

Ashley Mudstone Formation can be observed to rest unconformably on basement rocks in the remaining parts of Scargill Creek and in Ben Lomond Syncline. The contact with the Torlesse Supergroup in Scargill Creek, on the down-thrown side of the Mt Benger Fault is particularly well exposed, and is marked by a thin band of extremely glauconitic sandy mudstone. The rocks immediately above are characterised by a sharp decrease in glauconite content and a corresponding, but sporadic increase in mud content. In the other sections it has a gradational contact with the underlying Waipara Greensand Formation.

The formation is dominated by typically blue-grey, massive, calcareous mudstones, often bentonitic and nearly always containing a small, irregularly distributed content of sand to granule - sized glauconite (these have been aptly described as forming clumps or nests by Mason, 1941). Interbedded with the mudstones are a number of variously thick, friable to moderately indurated, fine to medium grained, highly glauconitic sandstones.

Browne and Field's (1985) Gower and the Hurunui Members (the former containing a greater proportion of, and thicker, sandstone beds), can be recognised throughout the area, nearly always occurring together, but any boundaries between them cannot be clearly defined (particularly due to the additional presence of Homebush Sandstone Formation as described below).

The onlapping of Ashley Mudstone Formation onto the basement signifies the beginning of transgressive deposition over the entire region, the Hurunui High now being completely covered.

#### 2.3.1.4 Homebush Sandstone Formation (Carlson et al, 1980): *Eocene*

A highly friable, light brown to green, poorly sorted, fine to granule sized, glauconitic, quartzose sandstone can be recognised beneath the Weka Pass Stone in many parts of the study area, outcrops in small slips being common. This unit is considered here to be part of the Homebush Sandstone Formation first described by Carlson et al, (1980) in the Coalgate area, Mid Canterbury (formerly known as the unnamed sandstone, Browne and Field, 1985).

In the Hurunui Gorge, Scargill Creek and Eastcott Stream however, an unusual and complex relationship with the Ashley Mudstone Formation can be observed. In some areas the relationship appears to represent a simple interfingering (eg. the middle portions of Scargill Creek, where a thin bed of Ashley Mudstone Formation can be observed, apparently concordant with bedding in the other units, in the Homebush Sandstone Formation), however, in others, randomly oriented contacts (some apparently vertical) suggest another mechanism, such as sandstone diapirism.

Homebush Sandstone Formation diapirism has been recognised in several other localities in north Canterbury; Browne and Field (1985) suggested that these were restricted to a zone north of Waikari, but recently Barrell (1989) described some from the Motunau River mouth region so they may be more widespread than originally thought. Lewis, Smale and van der Lingen (1979) found evidence to suggest diapirism occurred before or during the development of the unconformity between the Amuri Limestone and the

overlying Omihi Formation and proposed a tectonic initiation rather than localised excessive loading or a slump origin.

The fact that Homebush Sandstone Formation has never been observed in direct contact with the basement rocks (ie. originally underlying the Ashley Mudstone Formation) may be a function of the poor exposures in many localities, but may also indicate almost complete depletion of the source body (Lewis, pers. comm. 1995). Furthermore, Nicol (1991) does map Homebush Sandstone Formation beneath Ashley Mudstone Formation in his area to the SW.

The type locality for the Homebush Sandstone Formation indicated a fluvial, perhaps deltaic or tidal channel environment (Carlson, Grant-Mackie and Rodgers, 1980), but Browne (1985) suggested a shallow marine setting for the formation further north, which was thought to account for the apparent restriction of the diapiric mobilisation to this area (ie. marine sands possess a higher water content, allowing mobilisation).

### **2.3.2 Amuri Limestone (Hutton, 1874): *Late Cretaceous to Middle Oligocene***

The Amuri Limestone is the most widespread formation in Canterbury and because of its diachronous nature it is considered to be a separate unit from any other group (Browne and Field, 1985). In this study area it is Middle Oligocene in age.

The Amuri Limestone can be traced northwards into the region near Hawarden from that mapped by Nicol (1991), but then disappears completely over the entire study area with the exception of the small outcrops immediately east of "the gap" in Scargill Hills Outlier (figure 2.2). The Amuri Limestone was described here as having an unconformable relationship to the overlying Weka Pass Stone by Lewis (1992). The outcrops are very small (only approximately 30 cm thick) but stand out due to a difference in the degree of erosion (figure 2.2).

The limestone in "the gap" is a chalky white, micritic, globigerina ooze containing streaks of fine to medium grain sized glauconite. It possesses the orthogonally-jointed appearance described by Nicol (1991) and most of the joints contain greensand leached

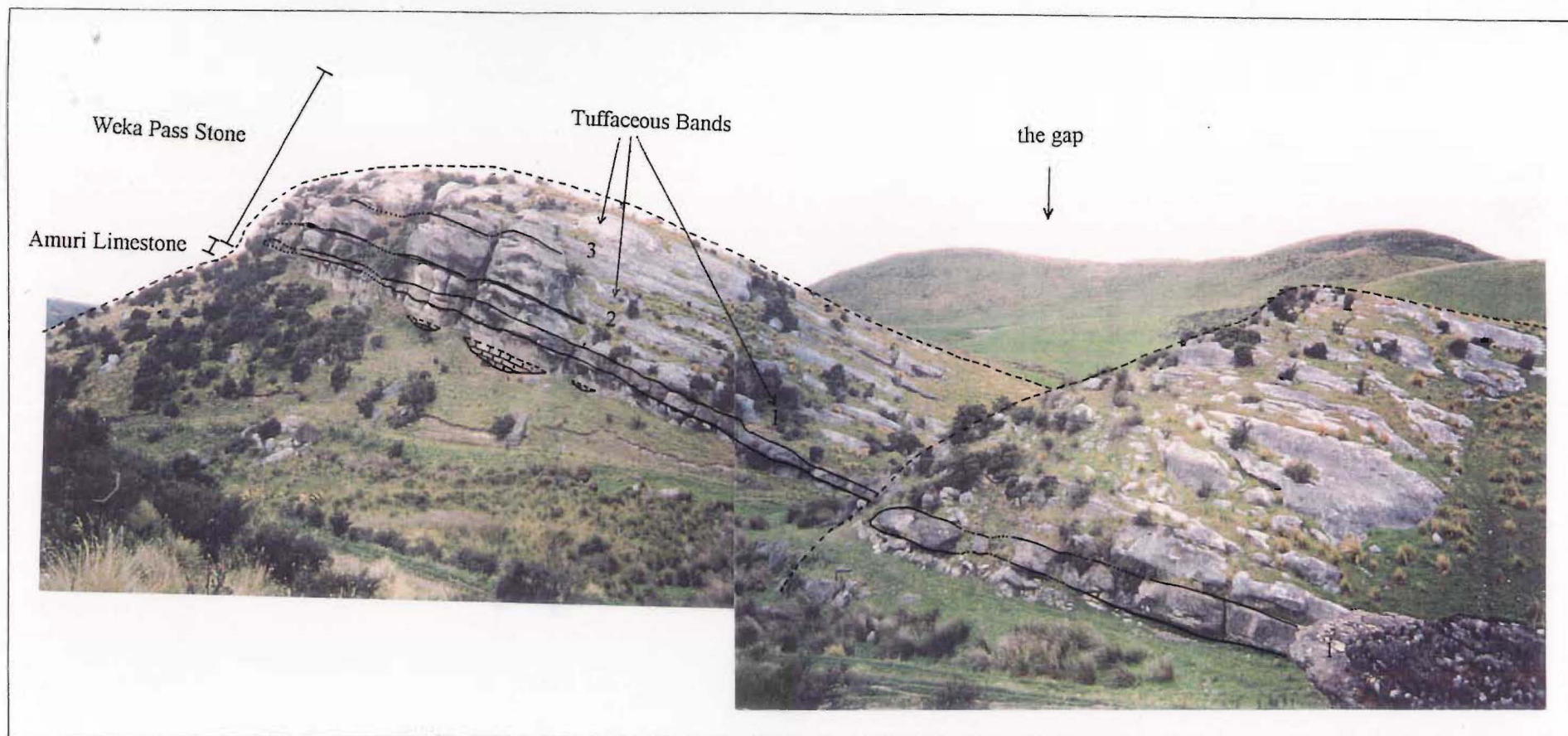


**Figure 2.2** Features of the Weka Pass Stone Member of the Omihi Formation and the Amuri Limestone at “the gap” (grid reference 972 134), view to the ESE.

down from the overlying Weka Pass Stone Member. The contact is represented by a highly bored zone, many of the borings also infilled with greensand.

The Amuri Limestone is thought to represent a pelagic limestone, ie. deposited some distance offshore where soft bottom conditions such as an ooze prevailed (Browne and Field, 1985).

### **2.3.3 Motunau Group (Browne and Field, 1985): *Late Oligocene - Pleistocene***

The Motunau Group contains a highly varied range of lithologies that lie unconformably on the Amuri Limestone and parts of the Eyre Group and conformably on the Cookson Volcanics Group and remaining portions of the Eyre Group. The Motunau Group is considered to represent "a period of largely shallow marine sedimentation that culminated in Late Miocene to Pleistocene regression" (Browne and Field, 1985).

#### **2.3.3.1 Omihi Formation (Andrews, 1963): *Oligocene- Early Miocene***

Browne and Field (1985) recognise six members of the Omihi Formation, two of which occur in the study area. The most predominant is the Weka Pass Stone which forms the abundant strike-ridges preserved in many places throughout the area. The second member is the Gorries Creek Greensand which occurs in central portions of the study area, which is thought to represent the near-shore facies equivalent of the Weka Pass Stone. The Omihi Formation is absent in the east of the region.

#### ***Weka Pass Stone Member***

Andrews (1963) describes the Weka Pass Stone as a typically "thoroughly cemented, cream to light grey, massive, sandy limestone with fine disseminated glauconite". In the study area however there are a number of facies changes that can be recognised across the area. Two in particular warrant further discussion.

The first is a change from a very pure, creamy-white, chalky, micritic limestone in the SW, to a greeny-cream, relatively highly glauconitic, highly bored, coarser grained, arenaceous limestone in the east. In outcrop they are very similar in appearance, with the exception that the former is characterised by numerous, well developed, subvertical joints developed perpendicular to strike, and the latter by a more rounded, "ribbed" appearance. Common to both is a "honeycombed" weathering pattern, created by preferential erosion of the material surrounding the now-flattened numerous borings that parallel bedding. This facies change was attributed by Hamilton (1950) to shallowing eastwards. The absence of the Omihi Formation in the Hurunui Gorge may attest to the presence of a topographic high there.

The second change occurs due to the appearance of three beds of a pinkish-grey, well bedded, coarse-grained, highly fossiliferous, crystalline limestone containing sparse basaltic rock fragments, in northern parts of the area. They first appear in outcrops above the Waitohi River and occur extensively in Scargill Hills Outlier.

All three beds (here loosely called tuffaceous bands) are well exposed in "the gap" (figure 2.2). There it is clear that the bands decrease in thickness and become spaced further apart in an upwards direction. A close examination reveals that they possess a sharp lower contact, while the upper contact is clearly gradational. They also are characteristically "platy" to "blocky" in outcrop, the platy nature created by stylolites parallel to and in some cases perpendicular bedding (figure 2.3).

Thin sections reveal the tuffaceous bands to contain abundant broken fossil fragments, particularly crinoid ossicles, with only a minor arenaceous content (mainly glauconite). The grain size and abundances of fossil and basaltic fragments have been found to vary considerably between outcrops, while the arenite content generally remains uniform, suggesting continued background deposition. In the lower, thicker band at least, there also appears to be a fining upwards and a decrease in the abundance of basaltic fragments.

The basaltic tuffaceous fragments suggest that the bands are related to a series of volcanic events, the abundant fossil material then possibly representing "organic blooms" in the warmer water conditions. Hamilton (1950) correlated these with the numerous Oligocene volcanic deposits found around north Canterbury (now known as the



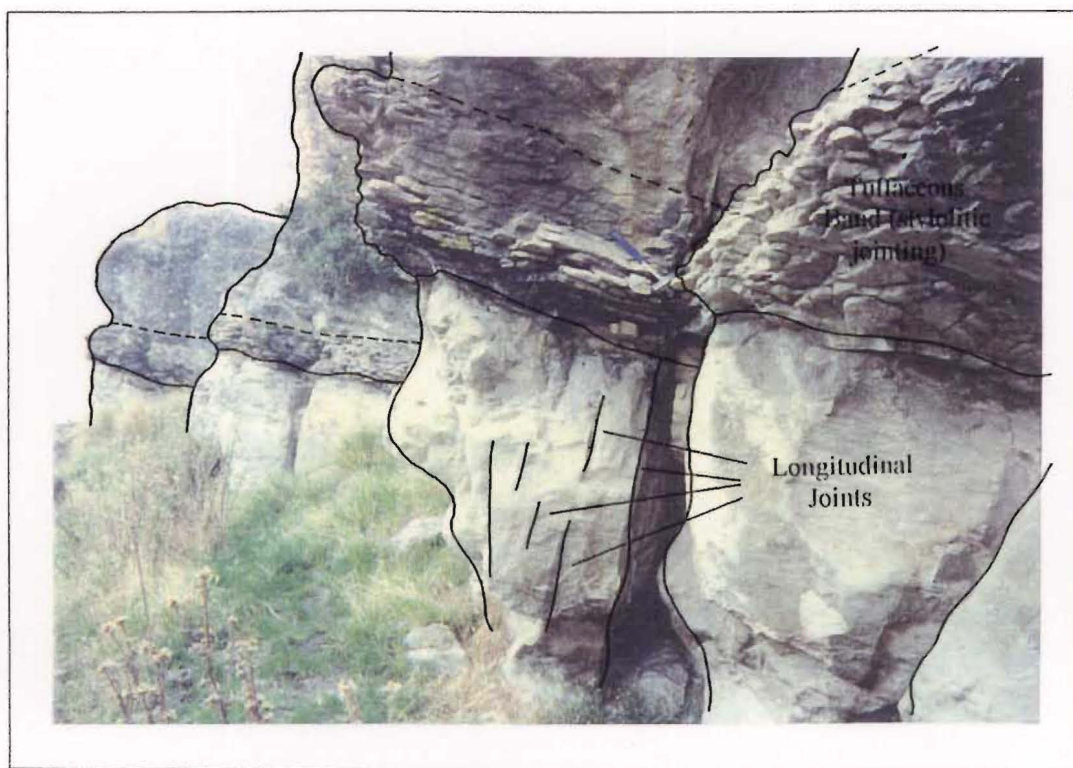


**Figure 2.3** Stylolitic and longitudinal jointing (chapter four) characterising the “tuffaceous bands” in the Weka Pass Stone Member of the Omihi Formation, approximately 100m east of “the gap” (grid reference 974 135), view to the east.

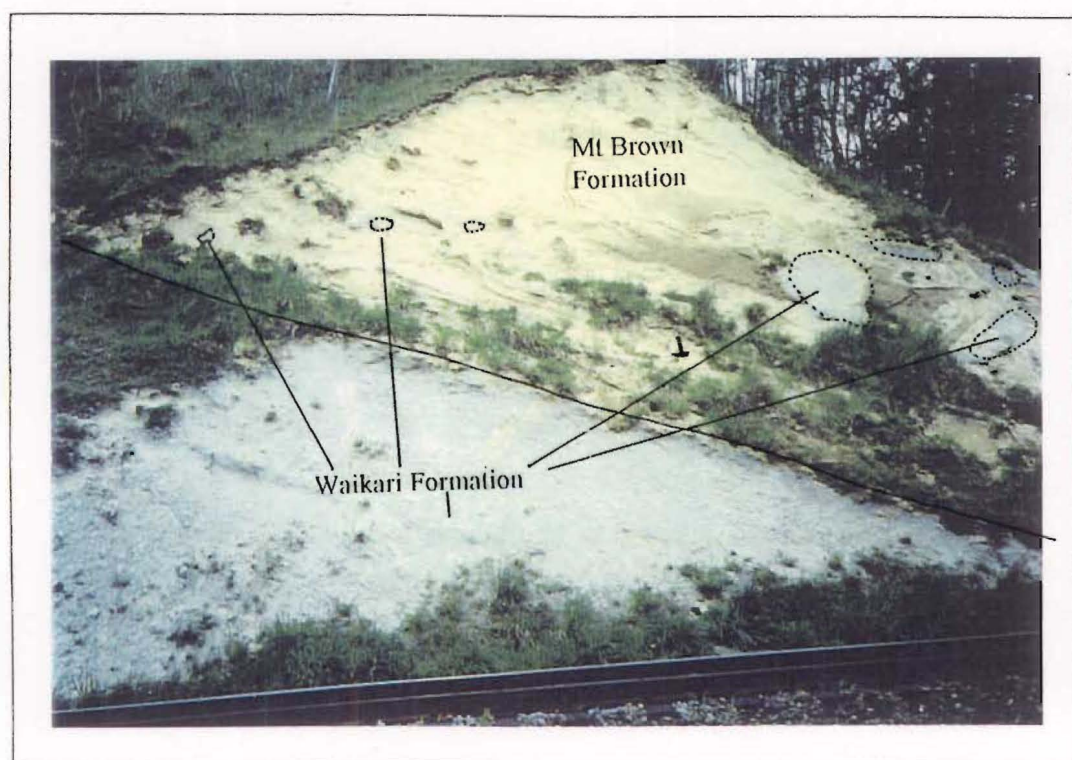


**Figure 2.4** Boulder sized clasts of the Scargill Siltstone Member of the Waikari Formation incorporated in the base of the Mt Brown Formation in the Railway Cuttings through Moores Hill Range (grid reference 036 065), view to the east.

Cookson Volcanics, Browne and Field, 1985), and if this is the case there may be clear evidence here for the number and timing of events.

### *Gorries Creek Greensand Member*

In outcrop the greensand is very similar in appearance to the Weka Pass Stone but is characterised by a significant decrease in induration, higher degree of weathering, and a medium to dark green colour. In thin section it appears simply to represent a highly glauconitic Weka Pass Stone.

The change from the well indurated Weka Pass Stone to the moderately indurated Gorries Creek Greensand is reflected by a sudden disappearance of the strike-ridges. This is particularly evident in Waikari Valley, where the very well developed hog-back ridges in western parts, although slightly faulted at their eastern end, reduce rapidly in thickness and become more glauconitic before disappearing from sight completely at Laverock. An intermediate lithology occurs in Laverock Stream where the moderate degree of induration preserves a short, two metre thick "ridge" of limestone before outcrops are reduced to 1-2m long, rounded outcrops in Eastcott and Foxdown Streams and Scargill Creek. The Greensand can also be traced through into Scargill Hills Outlier where it is exposed in Scargill Creek near Maxwellton homestead.

The lithological changes in the Omihi Formation can generally be treated in a W-E fashion across the area. However, abrupt variations can also be detected in a N-S direction, that can be directly related to structure. In the Moores Hill Region, well indurated Weka Pass Stone predominates. In the Waikari Valley, well indurated Weka Pass Stone grades rapidly into Gorries Creek Greensand (locally extended into Scargill Hills Outlier) before disappearing entirely to the east. At the western end of the Lowry Peaks Range, and in Scargill Hills Outlier, well indurated Weka Pass Stone containing tuffaceous bands occurs across the region before disappearing to the east. The distinct changes appear to be very abrupt and correspond with a number of the structures mapped in the area (map 1), therefore it is proposed that the major control is structural, serving to accentuate N-S facies changes.



### 2.3.3.2 Waikari Formation (Andrews, 1963): *Early Miocene*

Browne and Field (1985) recognise seven members of the Waikari Formation, three of which occur in the study area.

The Scargill Siltstone Member is the most predominant unit in the central and western portions of the area, lower portions of Scargill Creek being the type-locality for the member. The Scargill Siltstone Member is uniform throughout the region, bedding occurring in only the largest outcrops as a faint, rhythmic coarsening, often forming distinct bands in the stream beds.

The more glauconitic, thin Pahau Siltstone Member has only been noted in lower Scargill Creek but due to the fact that the base of the Scargill Siltstone Member has not been observed anywhere else it is inferred to underlie the Scargill Siltstone Member in most areas. The boundary between it and the Scargill Siltstone Member is not well defined, generally marked by a gradual decrease in glauconite content.

In the very east of the region the Waikari Formation is represented by the Glenesk Sandstone Member, which is often difficult to distinguish from the Mt Brown Formation, due to the presence of tabular concretionary bands often characteristic to the Mt Brown Formation.

The underlying contact with the Gorries Creek Greensand Member of the Omihi Formation is relatively well defined in Scargill Creek, characterised by a sudden change in weathering and grain size.

Andrews (1968) proposed a simple NE-SW trending basin existed in the Early Otaian in which Pahau Siltstone was accumulating on the edges where the sedimentation rates were low, with Scargill Siltstone being deposited in the middle. At some point in the upper Otaian sedimentation patterns were inferred to have changed, with an increase of both sediment supply and the rate of production, inhibiting the formation of glauconite and hence deposition of the Pahau Siltstone. Basin morphology is inferred to have remained the same, deposition of Scargill Siltstone continuing in most of the study area, with Glenesk Sandstone deposition as a linear body in the NE of the study area.

### 2.3.3.3 Mt Brown Formation (Haast, 1871b): *Miocene*

Resistant beds in the Mount Brown Formation crop out as strike-ridges of relatively continuous shelly limestones, conglomerates and tabular concretions in many parts of the study area, particularly notable in the Moores Hill Range area and eastern portions of Waikari River.

The contact with the underlying Waikari Formation can be clearly observed in many places, often highlighted by a distinct colour change from the blue-grey Scargill Siltstone Member of the Waikari Formation to the orangey-brown Mt Brown sandstone. However, in the eastern regions, the absence of shelly limestone beds and the facies change of the Waikari Formation to a fine grained sandstone obscures the contact somewhat. Furthermore, the presence of blue-grey siltstone beds in the upper part of the Mt Brown Formation makes the contact with the overlying Greta Formation difficult to define in a number of places.

In several small creeks in north-eastern Waikari Valley and along the Railway Cuttings (grid reference 036 065), a number "clasts" of Scargill Siltstone Member of the Waikari Formation can be found in the overlying Mt Brown Formation, some up to a metre in diameter (figure 2.4). These were considered by Hamilton (1950) to be evidence for an unconformity between the two units in the NE of the area, the "clasts" of Waikari Formation inferred to have undergone considerable rolling due to their well rounded shape.

Browne and Field (1985) proposed that the Mt Brown Formation was deposited in a rapidly subsiding basin in which the sandstones were deposited as mass flows against the background hemipelagic sediment (siltstones). The finer grained facies that followed was inferred to indicate deep water conditions, culminating in the deposition of the Greta Formation. Depositional depths were inferred to be similar to the Omihi and Waikari Formations. Local abundances of conglomerate were suggested to indicate increases in tectonic tempo. The Mt Brown Formation is considered to be a tongue of sandstone that separated the siltstone basins of the Greta Formation and the Tokama Formation.

#### 2.3.3.4 Greta Formation (Hutton, 1888): *Late Miocene - Early Pleistocene*

The Greta Formation is restricted to the eastern third of the area, where it forms a very thick unit of blue-grey, moderately indurated, calcareous, very fine sandy siltstone with minor sandstone, shelly limestone and conglomeratic beds. Also present are calcareous concretions. In many places, such as Tipapa Stream and the southern Hurunui Gorge however, the formation has been clearly folded into an asymmetric syncline, hence the thickness is over- exaggerated.

The most complete section is the southern Hurunui Gorge, where it is composed largely of a siltstone containing light and dark bands, clearly denoting bedding. In many places along the Waikari River tabular concretions, shelly limestone and conglomerates occur in both siltstone and sandstone, prompting Hamilton (1950) to call these beds a separate formation (the Ethelton Formation) but Browne and Field (1985) considered them a part of the clearly very diverse Greta Formation.

The Greta Formation is restricted to the eastern and northern parts of north Canterbury. It is contemporaneous with the upper part of the Tokama Siltstone of the Waipara-Grey River area and the lower part of the Kowai Formation of SW north Canterbury. The contact with the Kowai Formation must occur in central portions of the study area, but in stream sections such as Eastcott Stream and Lower Scargill Creek, no outcrops of either Greta or Kowai Formations were observed, they were overlain instead by modern alluvial fan gravels (this is discussed further later).

The Greta Formation is considered to have been deposited in a slowly subsiding continental shelf or slope environment where quiet waters prevailed, at upper bathyal depths (Browne and Field, 1985 - after Maxwell, 1964).

#### 2.3.3.5 Kowai Formation (Speight, 1919): *?Late Miocene - Early Pleistocene*

The Kowai Formation is restricted to the western third of the area, where it forms the terrestrial stratigraphic equivalent to the Greta Formation in its position overlying the Mt Brown Formation. In general it is poorly exposed, but appears to consist predominantly of bedded gravels in a mud to medium sand sized matrix, with minor

amounts of mudstone and sandstone. The gravels very closely resemble Lower Quaternary river gravels, and are generally only distinguished from the latter by possessing a dip of  $>5^\circ$  in accordance with the underlying units.

The Kowai Formation was deposited in a shallow marine to non-marine environment and represents the last unit in the marine regression sequence. In many localities in north Canterbury the upper part of the sequence was deposited contemporaneously with deformation, uplift of the Southern Alps to the west providing the large amounts of basement-rock gravel material.

#### **2.3.4 Late Quaternary deposits: *Middle Pleistocene to Recent***

The only previously differentiated Late Quaternary deposits in the area are a set of aggradational terraces preserved along the Hurunui and Waitohi Rivers, in the NW corner. However, in this area the distinctions are not clear between the units, and therefore they have been mapped together as undifferentiated aggradation gravels. The majority of alluvial terraces along the rest of the Hurunui River have been uplifted by faulting and therefore cannot be correlated in terms of height with any of the terraces in the Culverden Basin. Only the very lowest are considered to represent degradational terraces associated with the present river system, and are assumed to be Holocene in age. Terraces along the Hurunui Gorge have been largely degraded down to bedrock, containing only small pockets of gravels on their surface.

Late Quaternary deposits throughout the rest of the area consist predominantly of alluvial fan deposits, with minor amounts of alluvial gravels. No glacial-related aggradational terraces can be recognised in Waikari Valley; the narrow zone of alluvial deposits along Waikari River and Scargill Creek largely represent degradational terraces, with a small active bedload. Alluvial fans are associated with nearly every stream coming off the ranges. In Waikari Valley, the large streams such as Laverock Stream, Eastcott Stream and Scargill Creek, have formed correspondingly large fans, which, along with the asymmetry of the underlying bedrocks, largely account for the position of the Waikari River close to the southern side of the valley. None of the fans have been dated, but the majority appear to be Late Pleistocene (P. Tonkin, pers. comm., 1995) in age, with some of the more active, Holocene in age. Well logs held by the Christchurch

District Council for the Waikari Flat to Waikari Valley area, suggest that the gravels are interbedded with clay materials and are in excess of 30 m thick in places.

## **2.4 DISCUSSION AND SUMMARY**

Stratigraphically, this area has yielded more detail than surrounding areas in north Canterbury, despite the fact that the majority of the units are lithologically identical. In particular, a number of unconformities, evidence for sandstone diapirism and some volcanic deposits suggest that tectonics have had an important role during deposition of many of the units and are summarised and discussed below.

### **2.4.1 Basement-cover rock unconformity**

Rocks within the study area were readily divided into two, namely: i) basement and ii) cover rocks, due to the presence of a regional unconformity between them. In most parts of north Canterbury the unconformity spans the Middle Cretaceous, and represents deformation and uplift of basement rocks during the Rangitata II deformation event (Bradshaw, 1989). The extensional, marine transgression event that followed deposited rocks of the Eyre Group, of which the basal units, Broken River and Conway Formations, were largely deposited in a number of fault-controlled asymmetric basins.

Over most of this study area, lower units of the cover rocks sequence such as the Conway Formation are not present, younger units such as the Waipara Greensand Formation and the Ashley Mudstone Formation form the basal units. Therefore, the length of time represented by the basal unconformity is locally extended for much of this region, as is discussed below.

#### **2.4.1.1 The Hurunui High**

The lack of a deeply weathered surface to the basement rocks and the presence of conglomeratic basal units in the Conway, Waipara Greensand and Ashley Mudstone

Formations provides evidence that this area was undergoing widespread erosion during the Late Cretaceous and Paleocene, hence, a topographic high over the majority of the region, the Hurunui High has been proposed by Browne and Field (1988) (figure 2.5). Furthermore, a small amount of topographic relief can be recognised on the surface of the high, with pockets of Waipara Greensand Formation being preserved.

#### 2.4.1.2 Lateral extent

The unconformity produced by the Hurunui High can be traced in the west through the area from Mt Mason to the Green Hills (and probably to the southern slopes of Mt Culverden) (Mould, 1992), and to the Hurunui River mouth far to the east (figure 2.5). (Note that in the above mentioned localities Waipara Greensand Formation rests directly on basement rocks; it appears that this study area contains the only localities of Ashley Mudstone Formation resting on basement.) Therefore, as seen in figure 2.5, the general trend of the high appears to be W-E, although a notable sharp bend to a N-S trend does occur before it finally trends NW-SE in western portions, but, as noted with the detailed study of the Omihi Formation present structure needs to be taken into account before the exact shape and extent of the high can be resolved.

#### 2.4.1.3 Structural significance

In the Weka Pass - Waipara Region (Nicol, 1993a), and in seismic sections offshore (Barnes, 1993), clear thickening of the Cretaceous units (particularly the Broken River Formation) against some presently active, W-E trending faults provides evidence that at least some of these faults operating in the present NW-SE directed compressional regime are reactivated Cretaceous normal faults.

The widespread removal of Cretaceous units denies the use of similar lines of evidence in the central portions of this area, apart from the general observation that the Hurunui High has a W-E trend. However, the Broken River Formation is thickest at Boundary Stream, immediately south of the proposed high, a thickening to the NE from the South Branch of the Waipara River was noted by Browne and Field (1985), before a rapid thinning to complete absence in the Hurunui River. The thickening and the apparently

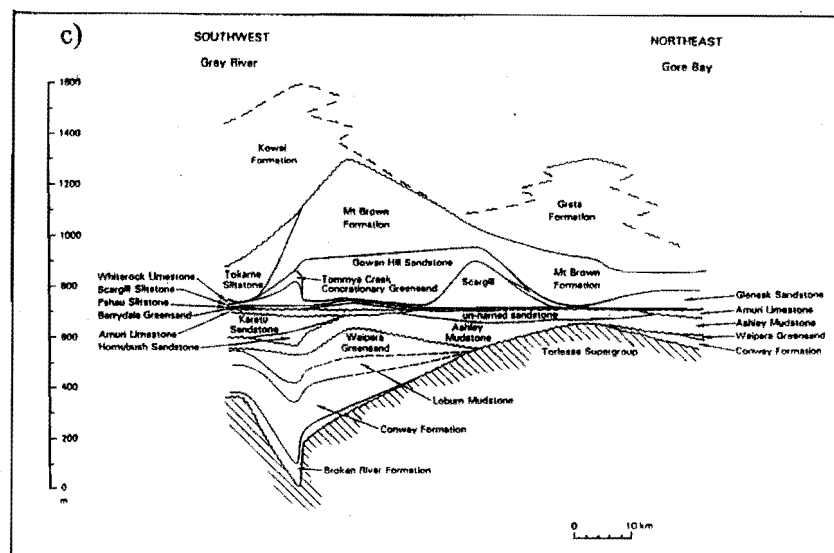
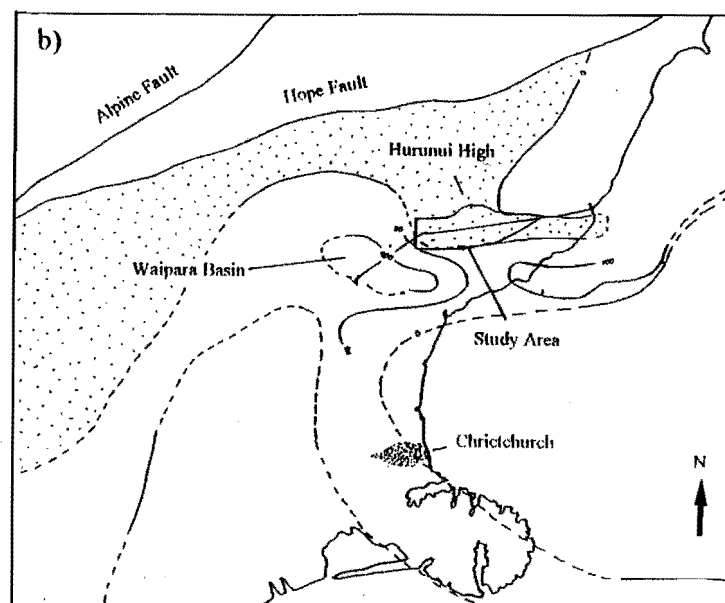
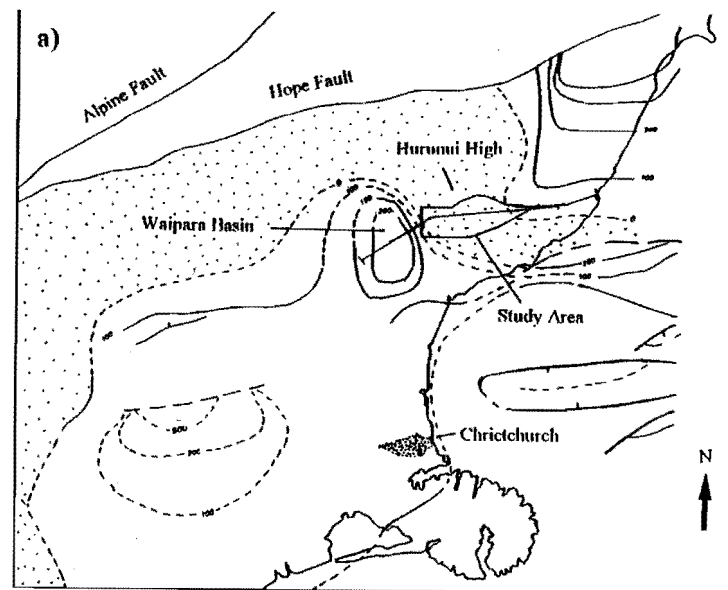


**Figure 2.5** Lateral extent of the Hurunui High in terms of: a) and b) isopach maps of thickness (m) of sediments in north Canterbury during the Late Cretaceous (a) and Paleocene (b), and c) cross sectional view. (Adapted from Field and Browne, 1989).

relatively straight edge to the high may indicate that at least the southern boundary was fault controlled, the fault providing the steep, northern boundary to a very large asymmetric basin. Furthermore, the small amounts of relief noted on the surface of the Torlesse Supergroup may attest to the presence of internal structures. Again however, the present structures must be taken into account before any detailed observations can be made.

#### **2.4.2 Deformation recorded within the cover rocks**

Relative to the scale of the Rangitata deformation event, the sequence of cover rocks deposited on top of the basement appears to have been comparatively undisturbed until the Late Pliocene to Pleistocene, when the Kaikoura deformation event produced the majority of structures mapped in this thesis. However, a number of lesser events have clearly been preserved within the cover rock sequence that are either localised within this area, or have had only minor effects on the deposition of the cover rock sequence.

##### **2.4.2.1 Middle to Late Oligocene deformation**

Throughout most of north Canterbury, variously thick to non-existent Amuri Limestone "separates" the Eyre and Motunau Groups, the contact between the top of the Amuri Limestone and the base of the Motunau Group being everywhere unconformable (Browne and Field, 1985. Lewis (1992) proposed that the unconformity was produced by a major change in plate motions during the Middle to Late Oligocene, namely the initiation of the plate boundary zone through southern New Zealand. The manifestations of this event in north Canterbury was proposed to be large scale warping, on which erosion of the crests of the anticlines had preferentially occurred.

In this study area the Amuri Limestone has largely been removed. Therefore, by correlation with Lewis's model, this study area is likely to have been characterised by a broad anticlinal structure consisting of the Eyre Group and Amuri Limestone sequence. The poor exposures and hence bedding of the underlying units, enhanced by the diapirism effects, means that evidence for any angular unconformity between the Eyre Group and the Omihi Formation cannot be evaluated.



The contraction placed on the Amuri Limestone and the Eyre Group is likely to have also been the major cause for the sandstone diapirism inferred for the emplacement of the majority of the Homebush Sandstone Formation (Lewis, pers. comm. 1995). No diapirism can be observed into the Omihi Formation and the evidence for intrusion into the Amuri Limestone in other locations dates the intrusion as occurring between the deposition of the two units. The lack of Amuri Limestone in this area means that this theory cannot be tested here.

#### **2.4.2.2 Deformation events synchronous with Motunau Group deposition**

Two events have been recorded by rocks of the Motunau Group:

Tuffaceous bands in northern exposures of the Weka Pass Stone Member of the Omihi Formation can be correlated with the widespread volcanism (in particular the Cookson Volcanics) that was occurring in northern parts of north Canterbury during the Late Oligocene.

A small unconformity was noted between the Waikari and Mt Brown Formations in eastern portions of the study area, but these have not been studied in detail and so no conclusions can be drawn to possible reasons for its existence.

#### **2.4.2.3 Motunau Group - Late Quaternary deposits unconformity**

Kowai Formation has only been mapped in western portions of the study area and is assumed to be the onshore, lateral equivalents of the Greta Formation mapped in the east. Upper parts of the Kowai Formation have been found lying above Greta Formation in the Kaiwara Region to the NE however, suggesting that in the Later Pliocene to Early Pleistocene, as the marine regression culminated, Kowai Formation should have been laid down over the entire area.

The absence of Kowai Formation in central and eastern portions of the study area may therefore indicate either: i) that this part of the north Canterbury was already undergoing uplift, while other areas remained at least partly submerged, and Kowai Formation was

never deposited there, ii) that Kowai Formation has been preferentially eroded off in those areas, or iii) some combination of the two. The lack of dates for the alluvial fan deposits that apparently now sit in the stratigraphic position where the Kowai Formation is expected, does not allow further interpretation.

## MACROSCOPIC DEFORMATION

### 3.1 INTRODUCTION

Previously, the major structures in the Lowry Peaks - Waikari Valley area have been mapped as a series of steeply-dipping normal faults that have served to uplift the ranges as a series of tilted-blocks (Hamilton, 1950, Gregg, 1964). It is proposed here that the majority of the region comprises a southward-dipping imbricate thrust system, composed of three major thrust-fault sets, the Lowry Peaks, the Mt Alexander - Maxwellton and the Kaiwara Fault Systems, from north to south respectively (figure 3.1). Furthermore, it is proposed that the basement-cored structural blocks uplifted on the south side of the major fault systems originate from one or more fault-propagation folds, produced in association with movement on the thrust fault systems.

The proposed structures can be viewed in detail on map 1 and are summarised in figure 3.2 and tables 3.1 and 3.2. The evidence for the thrust-nature of the faults and for the major ranges being considered as fault-propagation folds is outlined below. Each is described in relation to the major fault system, generally comprising a structural unit composed of an anticline-syncline pair truncated through their inflection point by a thrust fault.

### 3.2 THE KAIWARA FAULT SYSTEM AND ASSOCIATED STRUCTURES

Traditionally, the entire range system on the south side of Waikari and Scargill Valleys has been considered to be bound on its northern side by a single range-bounding fault, the Kaiwara Fault (eg. Maxwell, 1964, Gregg, 1964, Nicol, 1991). The Kaiwara Fault has been mapped by Gregg (1964) as a single, continuous fault extending from Waikari in the south as a southeast-dipping fault to bound the southern sides of the Waikari, Scargill and Kaiwara Valleys, to reverse in face in northeastern portions, to bound the western margins of the Cheviot Basin. The mapping for this thesis suggests that the Kaiwara Fault, at least in this area, is actually made up of a number of overlapping

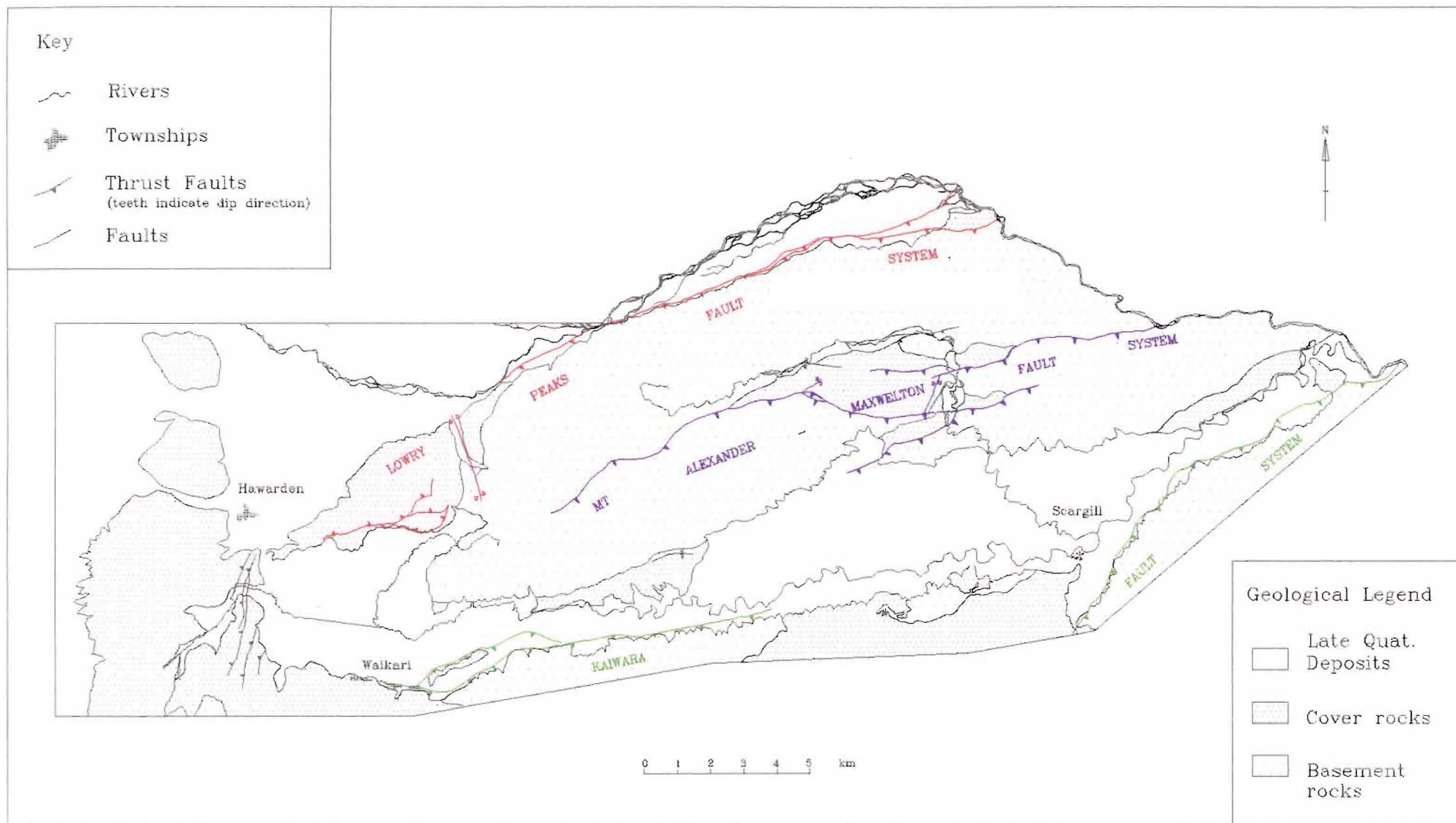


**Figure 3.1** Summary diagram of the three major fault systems of the Lowry Peaks Range - Waikari Valley area.

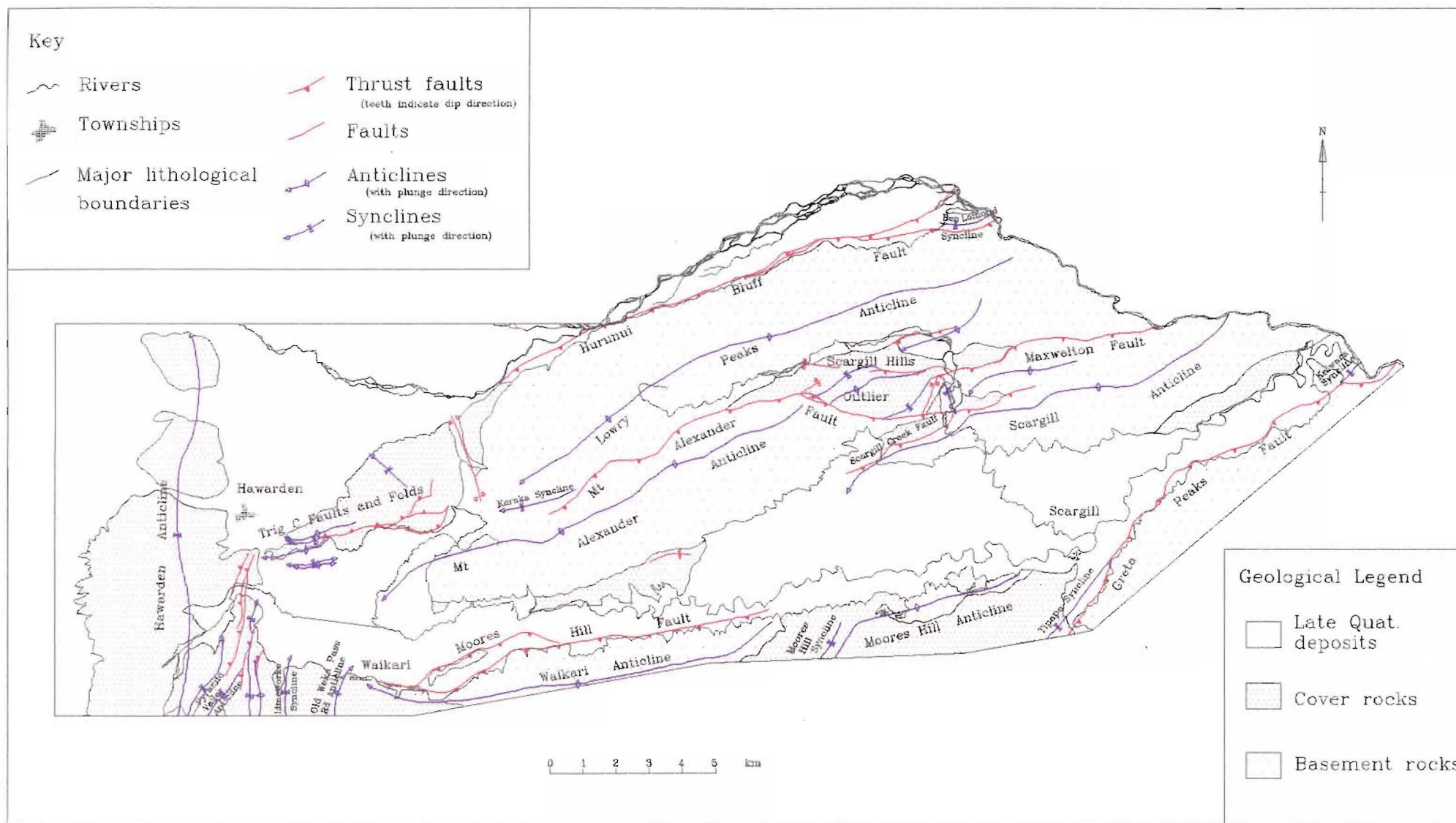


**Figure 3.2** Summary diagram of the macroscopic structures of the Lowry Peaks Range - Waikari Valley area

Name	Fault System	Location	Best Exposure	Orientation	Lateral extent	Type	Comments
<b>Hurunui Bluff Fault</b>	Lowry Peaks	N side of Lowry Peaks Range	Gulley west of Mt Bengier Homestead. Hurunui River south of Ben Lomond Syncline	WSW-ENE, moderate (?) dip to S	16 km +	Thrust	Largely bounds SE side of Culverden Basin, uplifts a number of terraces along the Hurunui River. A single splay occurs at the eastern end, Hurunui Gorge Fault.
<b>Trig C Faults</b>	Lowry Peaks	W of Lowry Peaks Range	Trig C Ridge	W-E, shallow to moderate dip to N	4km	Thrust	Opposite facing to all other faults. Possesses active fault scarps.
<b>Mt Alexander Fault</b>	Mt Alexander	N side of W portion of Mt Alexander Range	Mt Alexander Road	Varies, overall trends W-E., moderate - shallow (?) dip to S	16 km +	Oblique thrust	Large bend in eastern portions to trend anomalously W-E
<b>Maxwelton Fault</b>	Mt Alexander	N side of E portion of Mt Alexander Range	-	W-E, moderate (?) dip to S	10 km +	Thrust	Anomalous W-E trend
<b>Transverse Fault</b>	Mt Alexander	Scargill Hills Outlier	-	SSW-NNE, moderate to steep (?) dip to ESE	1.25 km	Lateral ramp	Transfers motion from Mt Alexander to Maxwelton Faults, creates coaptation syncline on western side
<b>Scargill Creek Fault</b>	Mt Alexander	S of Scargill Hills Outlier	Scargill Creek	WSW-ENE, moderate (?) dip to SSE	3.5 km +	Thrust	Splay off Mt Alexander Fault. Possible active trace at eastern end
<b>Moore's Hill Fault</b>	Kaiwara	N side of Moore's Hill Range	-	WSW-ENE, moderate (?) dip to S	12 km +	Oblique thrust	Trends more W-E than structures to the north
<b>Greta Peaks Fault</b>	Kaiwara	N side of Greta Peaks Range	Tipapa Stream Hurunui River	SW-NE, moderate to shallow (?) dip to SE	13.5 km +	Thrust	Bow-shaped trace, large overlap with Moore's Hill Fault

**Table 3.1** Description of the macroscopic faults in the study area

Name	Location	Trend	Axial Trace Length	Shape	Amplitude	Comments
<b>Lowry Peaks Anticlines</b>	Lowry Peaks Range	WSW-ENE	18km +	Asymmetric, vergence to NW, open	~600m	Closely associated with Hurunui Bluff Fault
<b>Ben Lomond Syncline</b>	Near entrance to Hurunui Gorge	W-E to SW-NE	2 km +	Asymmetric, vergence to S-SE, open	~300m	Closely associated with Hurunui Bluff Fault
<b>Mt Alexander Anticline</b>	W portions of Mt Alexander Range	WSW-ENE	15 km	Asymmetric, vergence to NNW, open	~600m	Closely associated with Mt Alexander Fault at W end, sigmoidal
<b>Scargill Anticline</b>	E portions of Mt Alexander Range	W-E to WSW-ENE	13 km +	Asymmetric, vergence to NNW, open	~500m	Closely associated with Scargill Creek and Maxwellton Faults, bifurcates
<b>Foxdown Anticline - Syncline pair</b>	Scargill Hills Outlier	WSW-ENE to W-E	2.5 km	Asymmetric, vergence to NNW, open	~100m	Closely associated with Maxwellton fault at E end
<b>Waikari Anticline</b>	W portions of Moores Hill Range	WSW-ENE	13 km	Asymmetric, vergence to NNW, open	~400m	Closely associated with Moores Hill Fault, sigmoidal
<b>Moores Hill Anticline-Syncline pair</b>	E portions of Moores Hill Range	WSW-ENE	7 km + (Anticline)	Asymmetric, vergence to NNW, open	~400m	Sigmoidal shapes
<b>Tipapa Syncline</b>	Tipapa Stream Area	SW-NE	3 km + ?	Asymmetric, vergence to SE	~250m	Closely associated with and cut by Greta Peaks Fault
<b>Kaiwara Syncline</b>	Scargill Valley -Hurunui River Area	SW-NE	?	Asymmetric, vergence to SE	?	Closely associated with and cut by Greta Peaks Fault

**Table 3.2** Description of the macroscopic folds in the study area

faults, and furthermore, in some localities it has not yet propagated the surface, as originally mapped. Therefore, the “Kaiwara Fault” is now suggested to be more correctly termed the Kaiwara Fault System.

The Moores Hill and Greta Peaks Ranges trend at slightly different orientation to each other and also to the ranges on the northern side of the valley. Moores Hill Range trends WSE-ENE, oblique to the SW-NE trending Mt Alexander Range on the northern side of Waikari Valley, causing the valley to widen considerably to its maximum at approximately Eastcott Stream. Greta Peaks Range actually starts forming behind eastern portions of Moores Hill Range to parallel the southern side of the eastern portion of Mt Alexander Range in a more SW-NE orientation. The large overlap between the two ranges is directly related to structure, caused by a large overlap between two range-bounding fault sets.

### **3.2.1 Major range-bounding faults**

At the very western end of Moores Hill Range the presence of an anomalous strike-ridge of Mt Brown Limestone, now largely covered by alluvial fan gravels, constrains the position of a major range-bounding fault on its southern side. Further, the position of the ridge does not appear to align with stratigraphically equivalent beds dipping off the basement cored-range on the northern side of the valley, so it is proposed that the ridge contains faults on either side, indicating splaying of the range-front fault in that position. The fault is inferred to continue westwards for some distance towards Waikari before being truncated by the N-S trending structures mapped by Nicol (1991) (discussed in more detail in Chapter 5). East of the strike-ridge no surface trace of the fault can be observed, but the absence of any cover rocks and the very straight range-front characterised by large truncated spurs, separated by alluvial fans suggests that it continues as a major range-bounding fault to at least a position immediately north of Roto-iti homestead (map 1).

The remaining Moores Hill Range-front does not possess any characteristics of being fault-bound. The range-front is highly sinuous, does not possess a distinct break in slope with the valley at its base and the presence of Waipara Greensand Formation dipping northwards off the flanks of the range containing Moores Hill North (map 1), suggest



that folding rather than faulting is important there, and is discussed further in section 3.2.2.

The Greta Peaks Range however, is again very clearly fault-bound. In the Hurunui Gorge, an asymmetric syncline containing nearly all of the cover rock units on both limbs (Kaiwara Syncline, Maxwell, 1964) has been faulted against basement rocks. A corresponding syncline can be observed in Tipapa Stream, although it only contains Greta Formation preserved on the steep limb. The syncline is likely once to have been continuous between the two areas, the steep limb to have been over-thrust by the adjacent anticline in central portions.

Although no surface trace exists, Greta Peaks Fault is correlated with the break in slope at the range-front and assumed to be largely buried by alluvial fan gravels. The fault is assumed to continue some distance along the south-eastern side of the Kaiwara Valley to form at least part of the fault mapped there as the "true" Kaiwara Fault, but the above observations of the variations in magnitudes of movement suggests that the point of maximum displacement is in fact roughly in the centre of the trace mapped here, (giving the fault a correspondingly bow-shaped trace, characteristic of thrust faults). Therefore it is likely that yet another splay of the major range-bounding fault has been formed there.

The fan gravels along the Moores Hill and Greta Peaks Range-fronts bury any cross-sectional exposures of the faults in the streams cutting across them (other than the two rivers already mentioned for the Greta Peaks Fault, and even there, the fault can only be constrained to within a few metres), hence the actual dip of the faults cannot be measured. The evidence to suggest that these are thrust faults therefore, are the typical thrust fault-fold relationships, overlapping nature of the system and the highly bow-shaped trace and sense of movement for the Greta Peaks Fault.

### **3.2.2 Major folding**

Folding appears to have formed an integral part of the deformation associated with the range-bounding faults. In western and eastern portions of the range-front system, folds

have formed in association with displacement on the major faults, but in central portions folding represents the only surface expression of deformation.

### 3.2.2.1 Waikari Anticline

The cover rocks at the western end of the Moores Hill Range clearly denote the westward-plunging end of an anticline (Waikari Anticline, Nicol, 1991), truncated by the Moores Hill Fault on its northern side. Mapping in this thesis has concentrated on the eastern end of the anticline, but it is clear that apart from some minor faulting, cover rocks continue relatively uninterrupted on the shallow, southern limb of the anticline between the two areas mapped (eg. Gregg, 1964), while none occur on the northern side due to the presence of Moores Hill Fault. The eastern end is poorly defined, with some evidence for slumping of the upper units, but the distribution of Mt Brown Formation suggests the anticline plunges generally north-eastward.

Structure contouring on portions of the now-exposed unconformity contact between the basement and the cover rocks was found to be very instructive as to the shape and orientation of the folding (portions of which are shown on map 2). A generally asymmetric profile was suggested (sense of vergence to the NNW), and the close relationship in trend (particularly in central portions) with the Moores Hill Fault. However, at the eastern end of the fold, a noticeable swing to the NE occurs (accentuated by some faulting just off the map area), giving the anticline a sigmoidal axial trace.

Structure contouring also reveals that Waikari Anticline is not highest in elevation in its central portions, as would be expected by the observed double-plunge, but in fact has two "structural highs", separated in the centre by a "structural low" (map 2). These warps are attributed to cross-folding at high angles, with an approximately NNW-SSE trend and is discussed further in Chapter 5.

### 3.2.2.2 Moores Hill Anticline

Accommodating deformation in central portions of the Moores Hill - Greta Peaks Range is Moores Hill Anticline. The anticline differs from the majority of the others in the area due to its smaller size, presence of cover rocks over most of its surface, and the lack of an associated thrust fault on its northern side.

The western end of the fold is clearly defined by a capping of Weka Pass Stone Member. There the fold is clearly asymmetric, with sense of vergence to the NW, and possesses a somewhat angular shape (figure 3.3), which is likely to be mainly a function of the competence of the limestone units, discussed further in Chapter 5. Characteristic of the angular shape is the removal of the intermediate limb between the shallow back limb and the steep forelimb by selective erosion.

In central portions, Waipara Greensand Formation is preserved on both limbs of the anticline, where generally shallow dips are recorded, suggesting a generally symmetrical shape, but can only be measured near the crest. The remaining units appear to have been removed by erosion caused by trimming of the range-front by Waikari, clear evidence for which exists at the eastern end. The original possible extent of this and the other structures beneath Waikari Valley are investigated in Chapter 6.

Due to the small area of the fold over which the basement is exposed, it has not been structure contoured in the same manner as Waikari Anticline. Some structure contouring was performed on the surface of the Weka Pass Stone Member, particularly at the western end, where the fold appears to possess an asymmetric profile (compared to central portions) and a highly sigmoidal axial trace, ie. the western end undergoes a significant swing in strike to the SW. Terminated eastern portions as mentioned above, is not well defined, but the exposed sections do suggest another slight swing to a NW-SE trend, like that described above for the western portions, thus giving the overall fold a sigmoidal trace. This will be discussed further in Chapter 6.

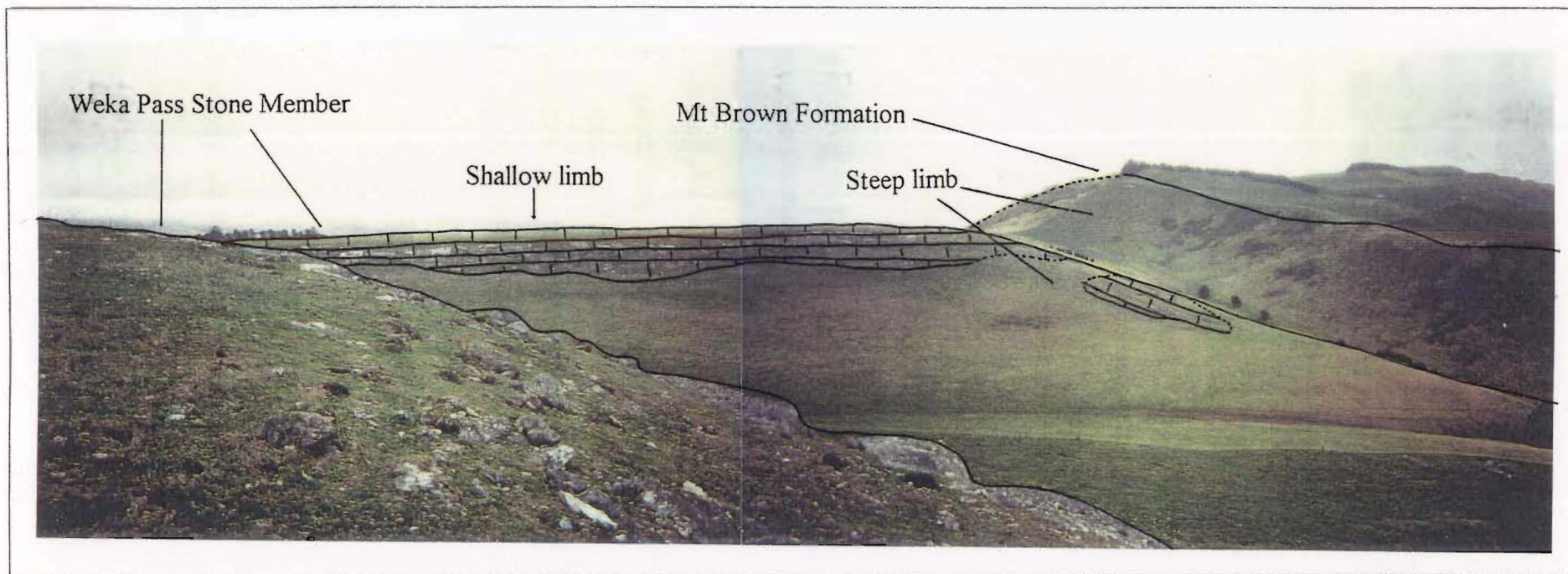


**Figure 3.3** Angular cross-sectional shape of Moores Hill Anticline (grid reference 991 061), view to the SW.

### 3.2.2.3 Moores Hill Syncline

Moores Hill Syncline has been created to accommodate geometric space problems associated with the transfer of motion between the Moores Hill Fault-Waikari Anticline structure and Moores Hill Anticline. The opposite senses of plunge between the two structures (and the significant difference in scale) gives the fold a complicated form, forming a secondary, W-E trending cross-warp in central portions.

Dip measurements made in the Weka Pass Stone Member show that in correspondence with the anticlines either side, the syncline is highly asymmetric with a steep limb on the SE side and that overall the fold possesses a sigmoidal form, swinging from a SW-NE trend in the north to a more WSW-ENE trend in the south.

### 3.2.2.4 Folding in Waikari Valley

Exposure of cover rocks within Waikari Valley is largely restricted to the northern side, where they form the shallow limb of a number of anticlines mapped in the Mt Alexander Range area. Although the majority of units in the cover rocks are not exposed (as described above), the lack of evidence for a fault along the northern side of Moores Hill Anticline suggests that the cover rocks should be dipping steeply to the north there. The result is that the cover rocks between the two areas form a very broad syncline (Waikari Valley Syncline), likely to be very flat in its central portions (this has not been shown on map 1 due to the lack of constraint as to its position). The same syncline is likely to continue westwards, past Moores Hill Syncline, which must open up rather than close (mostly due to the effects of W-E cross-warping as described above), until truncated by Moores Hill Fault as shown in figure 3.4.

### 3.2.2.5 Folding associated with Greta Peaks Fault

Any evidence from cover rocks for a major anticline associated with Greta Peaks Fault lies well to the south of the study area. Indirect evidence that the fold is likely to exist is provided by the presence of folding on the down-thrown side of Greta Peaks Fault ie.

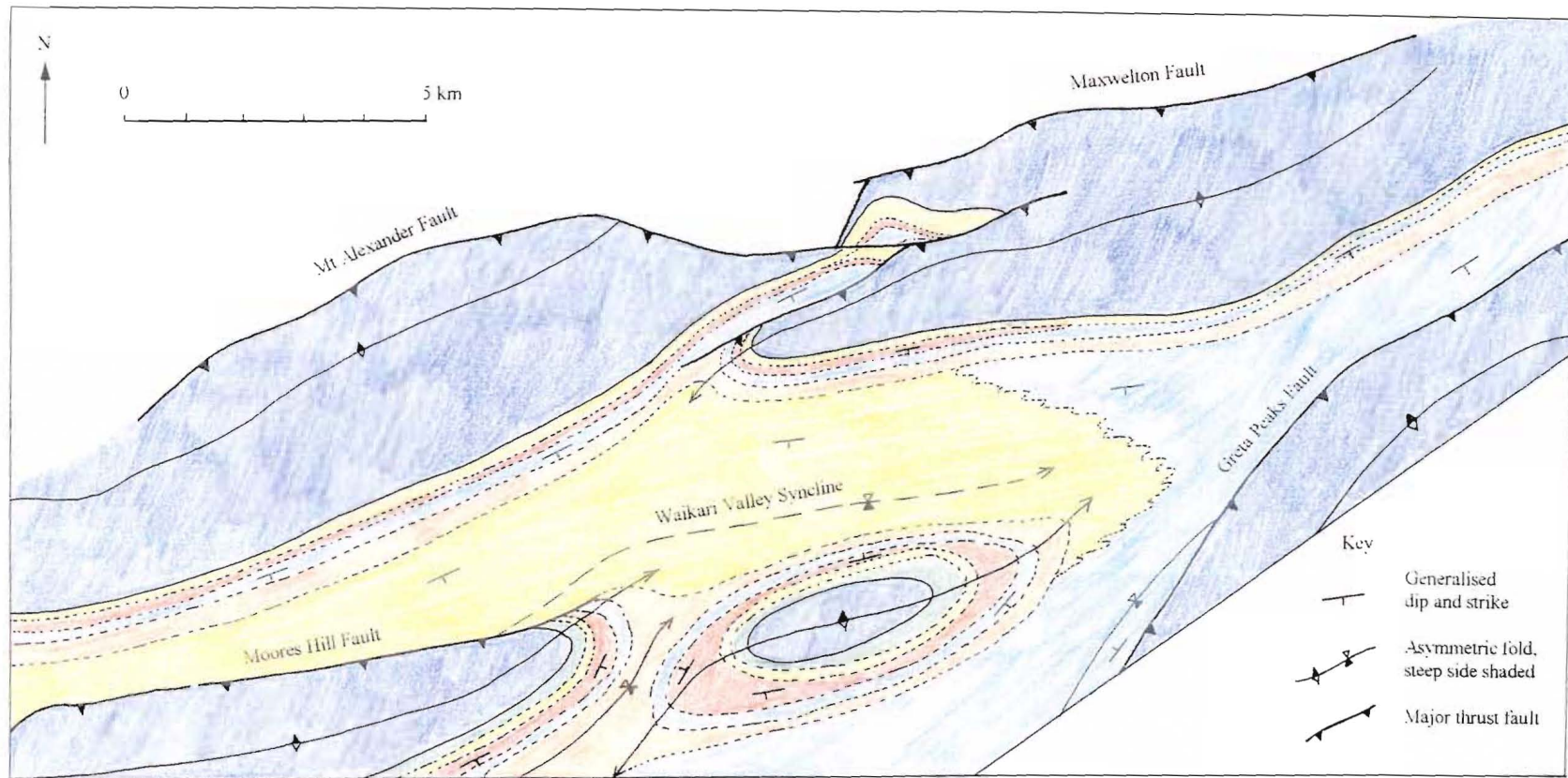


**Figure 3.4** Schematic diagram of the folding relationships in Waikari Valley. Colour of the individual units follows Map 1.



Scargill Valley, as discussed in section 3.2.1. The majority of the proposed anticlinal fold does not occur within the study area however, so no further discussion is undertaken.

The partially-preserved synclines on the down-thrown side of Greta Peaks Fault have had their steep limb created by movement on Greta Peaks Fault and the shallow limb by folding of the next set of structures to the north, Scargill Anticline (described in section 3.3.2.3) and partly Moores Hill Anticline. The obscured relationship between the syncline representing the majority of Scargill Valley (considered to be the south-western portions of the Kaiwara Syncline of Maxwell, 1964) and the Waikari Valley Syncline must be complex. It is likely that the structures bifurcate from Scargill Valley Syncline near Scargill, with Moores Hill Anticline between the two resulting axial traces.

### **3.2.3 Summary and Conclusions: *Kaiwara Fault System and associated structures***

Structures associated with the Kaiwara Fault System are complex, consisting of en-echelon sets of asymmetric folds and thrust faults. The overall trend varies from WSW-ENE in western portions to SW-NE in eastern portions. This swing in strike may account for the large overstep between Moores Hill Anticline and Greta Peaks Fault.

Structures of the Moores Hill Range have been studied in some detail, consisting of two sigmoidal, asymmetric anticlines separated by a correspondingly asymmetric and sigmoidal syncline. Possible reasons for the sigmoidal trace are discussed in Chapter 5. Waikari Valley represents a very broad syncline formed on the northern side of Moores Hill Range, the axial trace of which is somewhat oblique to the range-front, causing the southern limb to be over-ridden by Moores Hill Fault in western portions.

Folding also occurs in relation to Greta Peaks Fault, two asymmetric synclines with south-eastward sense of vergence are preserved on the down-thrown side, suggesting the likelihood of a major fault-related anticline makes up the Greta Peaks Range. The synclines are likely to have once formed part of a continuous structure, now overridden by the typically bow-shaped Greta Peaks Fault, bifurcating in central portions, one branch forms a syncline continuous with that along Waikari Valley, and the other Tipapa Stream branch through Greta Valley.

No active deformation can be observed along Moores Hill and Greta Peaks Faults, any fault scarps corresponding to the last faulting event now lie completely buried beneath alluvial fan gravels, although the truncated spurs, accompanied by well-developed alluvial fans characterising western portions of Moores Hill Range-front do suggest faulting there is relatively young.

### **3.3 THE MT ALEXANDER - MAXWELTON FAULT SYSTEM AND ASSOCIATED STRUCTURES**

The Mt Alexander - Maxwellton system of structures are the most complex of the entire area. Like the ranges on the southern side of Waikari Valley, two discrete segments of Mt Alexander Range can be described; the western segment trends SW-NE and containing Castle Hill and Mt Alexander (before being apparently "truncated" by Mt Alexander Fault), the eastern segment being somewhat more triangular in shape, with a southern boundary trending SW-NE, and a northern boundary trending more W-E (map 1). In the centre, a structural depression has preserved a set of cover rocks, here-named Scargill Hills Outlier (from the predominant property on which it occurs). The entire structures of the Mt Alexander-Maxwelton Fault System are currently riding "piggy-back" on structures of the Lowry Peaks Range, hence their relatively high elevation.

#### **3.3.1 Major range-bounding faults**

Mt Alexander Fault can clearly be traced out to show thrusting of basement rocks over cover rocks as the south-western boundary to Scargill Hills Outlier. As it is traced westward, it is defined by a series of intense shear zones along Mt Alexander Road where basement rocks thrust over basement, before passing into folding of Mt Alexander Anticline (discussed below). Rock exposures on either side of the fault are highly shattered, characterising a very wide shear zone containing a variety of small-scale faults, ranging from thrusts, reverse faults and back-thrusts to normal faults. The strike of the fault varies considerably, but overall is WSW-ENE. No modern fault scarps have been observed along this fault, but generally it corresponds to large breaks in slope between the Mt Alexander and Lowry Peaks Block, the width of the broad break in



slope corresponding well to the size of the observed fault zone. The fault is interpreted as a thrust fault due to its fault-fold relationships, bow-shaped nature, highly sinuous trace, and sense of throw relative to the moderate southward dip indicated by the intersection of the trace with topography.

Maxwelton Fault clearly thrusts basement rocks over cover rocks NE of Maxwelton homestead and continues as the northern, W-E trending boundary of the range to the east, accounting for much of the W-E trend of the Hurunui River there. For most of its length, Maxwelton Fault can again only be located by a break in slope, but in the Hurunui Gorge a rather narrow shear zone in basement rocks can be recognised against which there appears to be some uplift of the terraces on the south side. Although the fault has only been mapped to the edge of the map area there is a possibility that it links up with Limestone Glens Fault mapped in the Kaiwara Region by Maxwell (1964), particularly given the fundamental break in the range morphology that can be observed from Landsat images (see figure 1.2) on both sides of the Hurunui Gorge.

In the central part of Scargill Hills Outlier, the continuation of each of the faults is poorly defined. For example, the continuation of Mt Alexander Fault across Scargill Creek is very difficult to trace due to the similarity of non-glaucconitic parts of the Ashley Mudstone Formation and the Scargill Siltstone Member of the Waikari Formation there. Because there is good stratigraphic evidence for the continuation of a single major fault system between the Mt Alexander and Maxwelton Faults (section 2.3.3.1.1), some effort has gone into the proposition of possible alternative models as to how this might be achieved. Two models appear the most likely, each possible under the present regional stress configuration and involving various combinations of structures mapped in Scargill Hills Outlier, and are discussed in section 3.3.3, together with possible configurations proposed by Hamilton (1950).

### **3.3.2 Scargill Hills Outlier**

Scargill Hills Outlier has been formed by a combination of down-faulting along the various faults making up the Mt Alexander - Maxwelton Fault System and large-scale cross warping about approximately NNW-SSE axes which serves to up-warp basement rocks on either side ( map 2). A number of important macroscopic scale faults and folds

occur within Scargill Hills Outlier to accommodate deformation transfer between the two large faults described above. It is important to note there that the term “Outlier” is only used loosely to describe the set of cover rocks largely, but not wholly, surrounded by basement rocks in the centre of the Mt Alexander Range.

### 3.3.2.1 Foxdown Anticline and Syncline

The most important macroscopic structure in Scargill Hills Outlier is the Foxdown Anticline-Syncline pair, faulted through their inflection point at their eastern end, together producing much of the repetition of lithologies in Scargill Hills Outlier. The faulted-fold pair forms a smaller scale version of some of the major structures already discussed, but its nearly complete preservation by resistant cover rocks provides detailed information on fold morphology and possible mechanisms.

Foxdown Anticline is well defined by a capping of Weka Pass Stone Member and in cross section is clearly asymmetric with the steep limb on the north side. It possesses a rather angular shape, much like Moores Hill Anticline. Foxdown Syncline is slightly less well defined, but in western portions a core of Mt Brown Formation and Weka Pass Stone (dragged up from deeper levels by to a splay of the Mt Alexander Fault) is preserved. Both the anticline and the syncline abut into Mt Alexander Fault at their western end, due to a major swing in strike of the fault there; the only effects of Mt Alexander Fault being a small amount of drag folding. Reasons for the anomalous apparent obliquity between the folds and Mt Alexander Fault are discussed in Chapter 4.

Stereoplots of the poles to bedding for both the anticline and syncline define small circle distributions, hence representing conical rather than cylindrical-shaped folds (Ramsay, 1967 and Nicol, 1993b) (figure 3.5). Conical folds have been noted in other localities in North Canterbury, particularly immediately to the west and southwest (Nicol, 1991 and Mould, 1992) and have been attributed to cross-folding at high orientations by Nicol (1993b) (figure 3.6). The cross-folding is clearly detectable in the field, both the anticline and the syncline plunge down to the west at their western ends and the anticline may be seen to plunge down to the east at the eastern end. Hence cross-folding has now been detected on at least two scales.

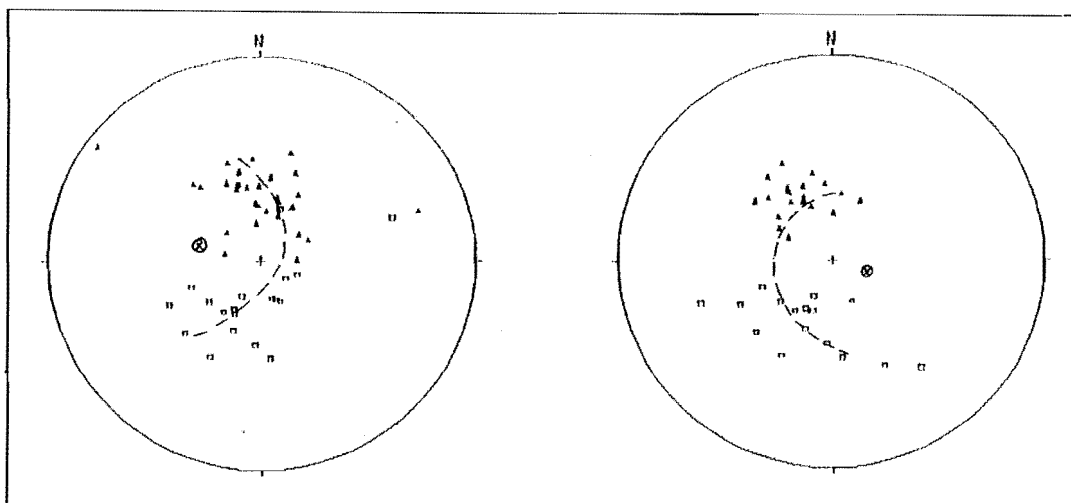


**Figure 3.5a** Stereoplots of poles to bedding for a) Foxdown Anticline and b) Foxdown Syncline. Filled triangles represent one limb, while hollow squares represent the other.

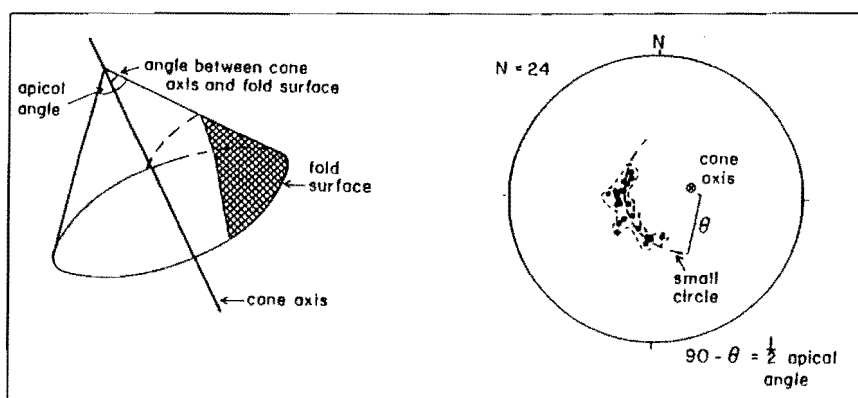


**Figure 3.5b** Comparison of a) geometric fold surface of conical folds, to b) their representation on an equal area stereonet, the example shown is for Weka Pass Anticline. (From Nicol, 1993b).

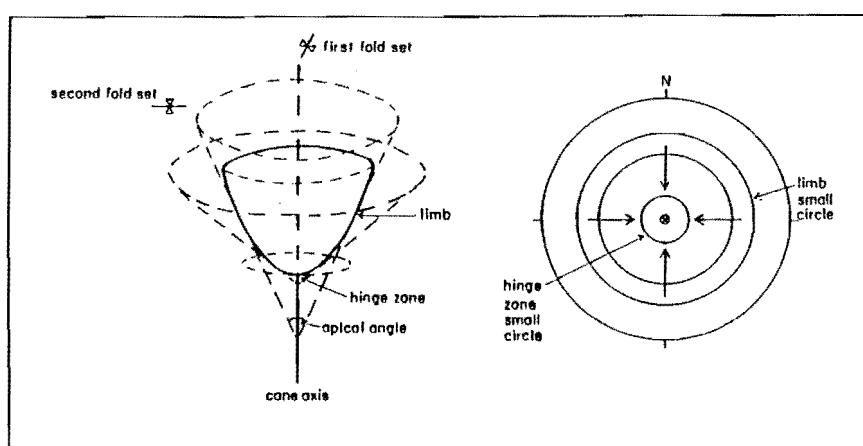


**Figure 3.5c** Schematic representation of a) the changes in fold geometry towards a fold basin interference structure and b) the corresponding decrease in small circle size of poles to bedding. (From Nicol, 1993b).

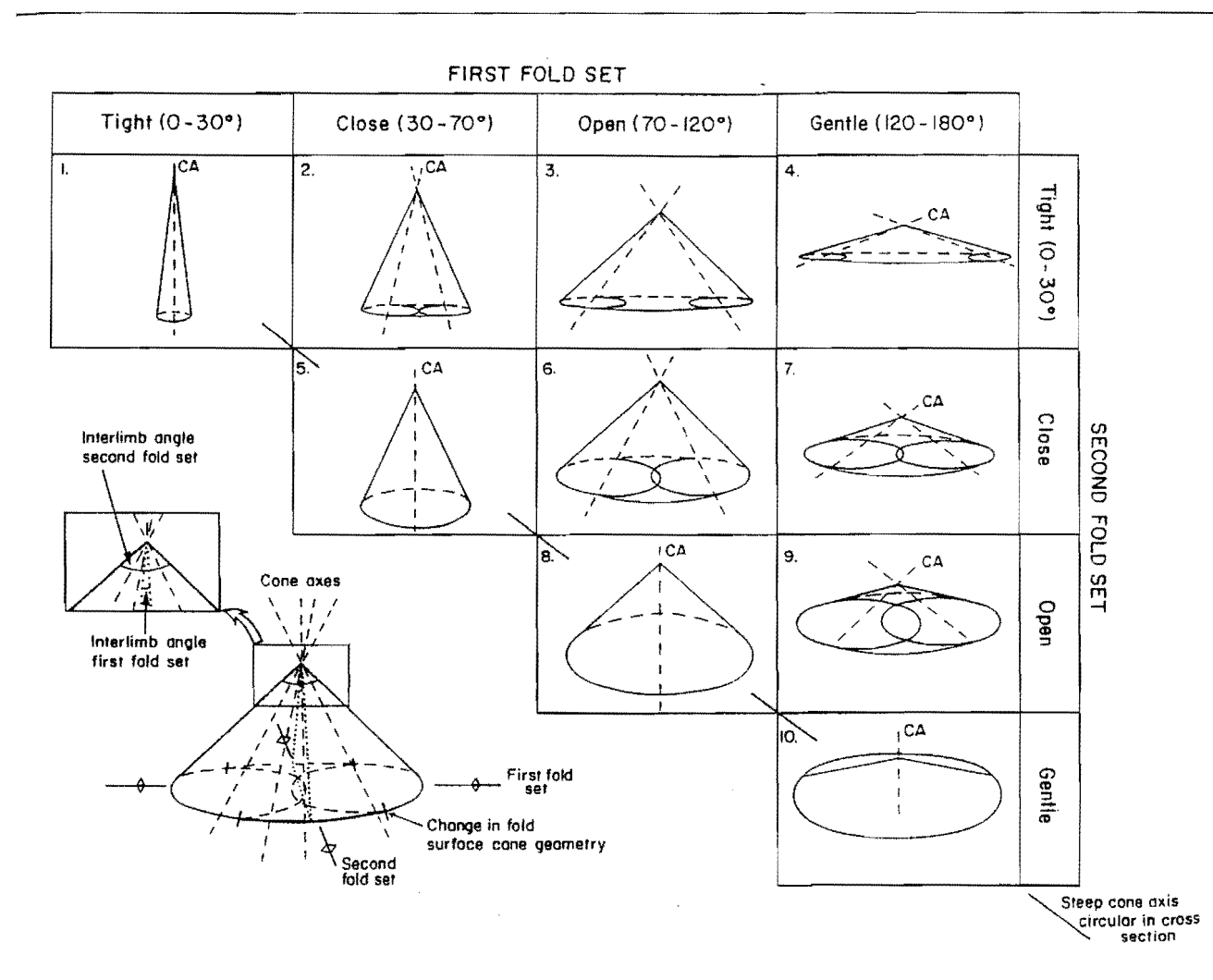


**Figure 3.6** Predicted changes in the geometry of conical folds produced by changes in the tightness of interfering fold sets, for upright interfering fold sets. (From Nicol, 1993b).

### 3.3.2.2 The transfer fault

Another important structure is the transfer fault, a fault at an anomalously high angle to any other fault in Scargill Hills Outlier. Hamilton (1950) mapped the fault to extend some distance further to the north than has been mapped here. In particular, he did not recognise the presence of the fault intersecting the Foxdown Anticline - Syncline pair, a splay of which appears to truncate the transfer fault. The westward-verging folding associated with movement on the transfer fault has created a very open syncline mainly represented by poorly-exposed Mt Brown Formation beneath the airstrip (grid reference 010,127), formed by a secondary "pleating", or coaxial folding (Stauffer, 1988) to overcome the space problems associated with the interference folding of two anticlines at high angles (Nicol, 1991). This set of folding represents another example of cross-folding on a smaller scale.

### 3.3.2.3 Scargill Creek Fault

Another important fault that contributes to the structures making up Scargill Hills Outlier is Scargill Creek Fault. Scargill Creek Fault is notable in that it is one of the few faults in the study area to possess a possibly active fault scarp. A 1-2 m high scarp, formed in the lowest matched river terrace surface of Scargill Creek, can be traced from the approximate position of the fault trace in Scargill Creek, to the W-E trending strike-ridge of Mt Brown Formation, along the front of the basement cored range uplifted by the fault there (figure 3.7). The surface does not appear to have a correlative across Scargill Creek. On the downstream side, the terrace is basement-cored; on the upstream side aggradation river gravels sit on a bedrock strath of greensands, approximately 0.5 m above the stream level, which are in turn capped by a Late Holocene soil profile (P. Tonkin, pers. comm., 1995).

If the scarp height represents real magnitude of ruptures by a single Late Holocene event, then the short apparent length of the scarp presents similar problems to other North Canterbury examples (Campbell et al, 1994). The scarp is almost certainly accentuated by erosion however, a small stream channel presently flows along the scarp, and during any faulting events, uplift of the downstream side is likely to have created temporary damming effects and hence scouring of the scarp-face. Furthermore,

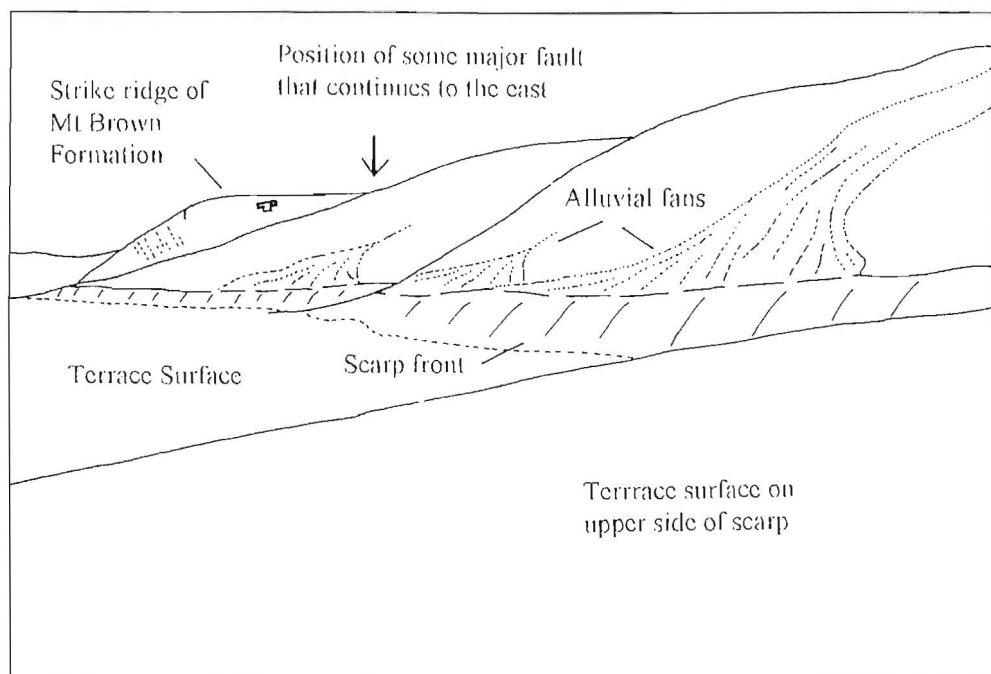


**Figure 3.7** The ?fault scarp preserved along the front of Scargill Anticline. The photograph is taken from a position immediately above the junction of the scarp with Scargill Creek, facing east, towards the dip-slope of the W-E trending ridge of Mt Brown Limestone that coincides with the eastern termination of the scarp (grid reference 119 019).

degradation by the river have modified stream exposures so that genuine over-thrusting of gravels by basement rocks cannot be observed. Therefore, the scarp is considered to remain a “suspect fault scarp”, and is not studied in any further detail. Furthermore, any attempts to undertake a detailed site investigation would be hampered by the abundant fan material that is sourcing from the slopes above (figure 3.7).

#### **3.3.2.4 Smaller-scale faulting**

There are a number of other small faults in Scargill Hills Outlier, but most serve to displace the cover rocks by only a few metres and hence prove only to be of minor importance to the overall arrangement of cover rocks there. One exception is Mt Bengier Fault, similar in style to the other thrust faults in the region, with important consequences for the eastern end of Foxdown Syncline. Mt Bengier Fault thrusts a small anticline of basement rocks over cover rocks exposed in north-eastern reaches of Scargill Creek. The unusual feature of this fault however, is its locality directly along strike from the shallow limb of Foxdown Syncline. The consequence of movement along Mt Bengier Fault is to ramp the syncline over the end of the anticline in a somewhat peculiar fashion, pinching it, before it takes a swing back in strike to parallel Maxwellton Fault. The anticline uplifted by Mt Bengier Fault (unnamed) is thought to grade into southern portions of Lowry Peaks Anticline at its eastern end.

### **3.3.3 Discussion of the link between structures in Scargill Hills Outlier and Mt Alexander and Maxwellton Faults**

As mentioned above, the structures described in Scargill Hills Outlier can be linked with Mt Alexander and Maxwellton Faults in at least two ways, each of which is compatible with movement under the present contractional regime. These are shown in figure 3.8 and discussed below.

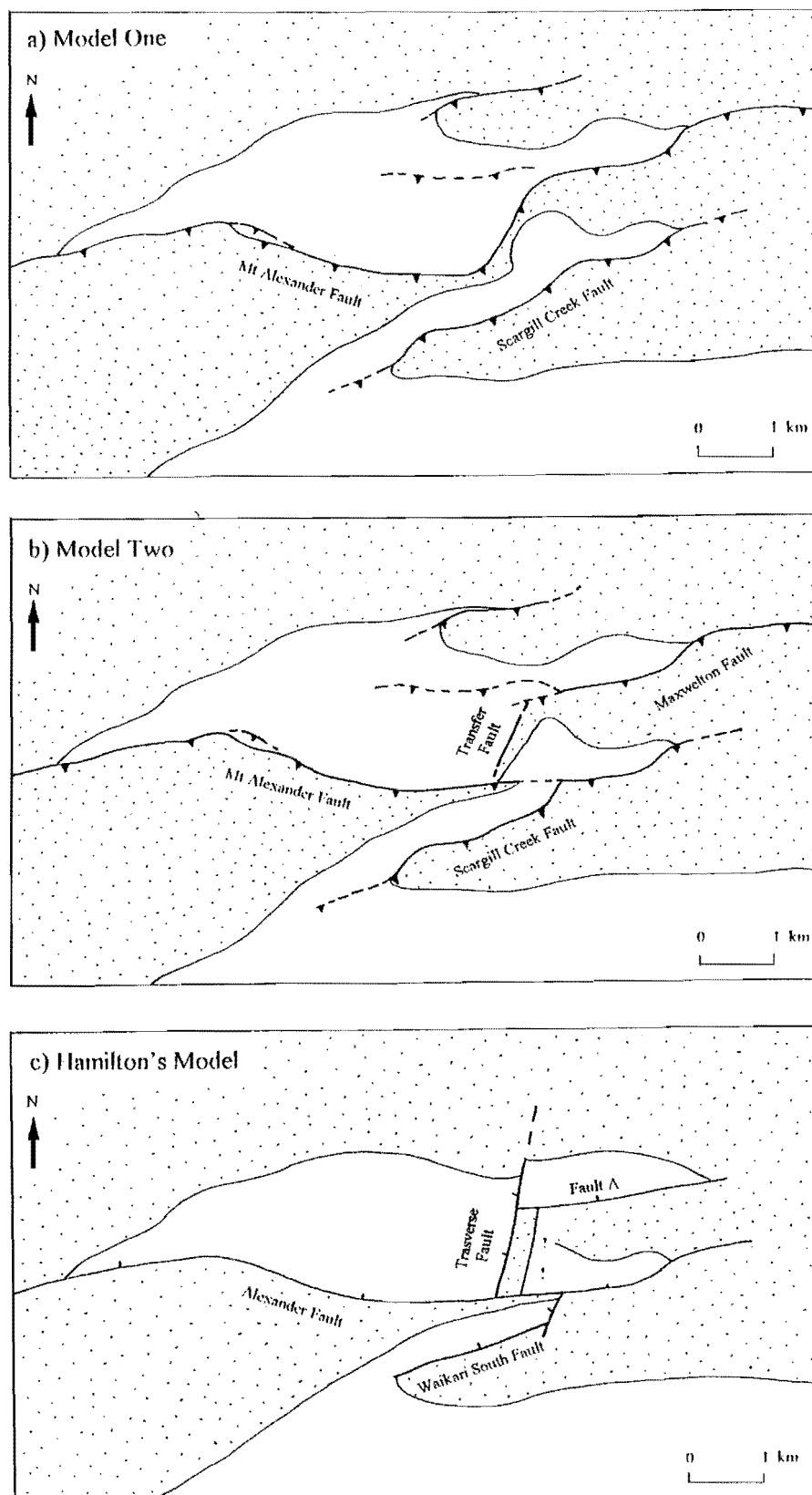


**Figure 3.8** Three different models for the arrangement of faults in Scargill Hills Outlier. Models one and two are proposed here, and consist of a combination of thrust faults (with teeth indicating dip direction) and steep reverse faults. Model two is that shown on Map 1. Hamilton's model largely consists of normal faults ("tic" shows direction of dip). Coloured area represents basement rocks, remaining is cover rocks.



### 3.3.3.1 Model One

Model one is the simplest and proposes two thrust faults, highly sinuous in nature, but generally parallel and containing at least a partly formed anticline on their upthrown side (figure 3.8a). The proposed swing in strike of Scargill Creek and Maxwellton Faults in this model, appears to mirror the swing of Mt Alexander Fault mapped immediately west of Foxdown Syncline and could be attributed to the effects of large NNW-SSE trending cross-folding, although a simple swing in strike for Mt Alexander Fault does not fit all the evidence described above and in Chapter 4.

In this model, the increased length of Scargill Creek Fault would be more appropriate for the amount of displacement recorded by the possible active fault scarp. However, as noted, there is the possibility that the height of the scarp has been exaggerated somewhat by the effects of fluvial action and furthermore, commonly observed relationships between fault length and displacement may not necessarily be applicable in north Canterbury (Campbell et al, 1994). Another problem is the sharp bend that the fault must undergo before continuing in a W-E orientation. The difference in height between the scarp on the terraces of Scargill Creek and the constraints on the position of the fault between basement rocks and the strike ridge of Mt Brown Formation is such that as well as bending, the fault would have to steepen dramatically over a very short space (partly shown on figure 3.7).

### 3.3.3.2 Model Two

In model two, Mt Alexander and Maxwellton Faults have been designated as two separate major range-bounding faults that strike W-E in central and eastern portions of Scargill Hills Outlier (figure 3.8b). In model one, the W-E striking fault that appears in the inflection point of the Foxdown Anticline-Syncline pair, would have to die rapidly at its eastern end, here it is considered to form the western extension of Maxwellton Fault. Likewise, the fault mapped between basement rocks and the strike-ridge of Mt Brown Formation is considered here to be the eastern continuation of Mt Alexander Fault, mainly due to the similarity in orientation and geometric problems associated with the connection to Scargill Creek Fault as outlined in the discussion of model one. Therefore the arrangement of faults appears to be more internally consistent.

In this model it is proposed that the transfer fault would act as a lateral ramp to "transfer" the major range-bounding motion from Mt Alexander to Maxwellton Fault. An alternative interpretation, suggested by Hamilton (1950), is that the transfer fault is in fact the northward continuation of Scargill Creek Fault, representing an earlier, NNE-SSW trending structure, now offset across Mt Alexander Fault (figure 3.8c). However, there are several problems with this suggestion in view of the mapping completed here:

- i) the transfer fault is now recognised to be "cut" by Maxwellton Fault, across which there is no possible corresponding fault.
- ii) the northward-directed thrusting suggested here for Mt Alexander Fault should produce an apparent right-lateral offset of the faults after thrusting and subsequent erosion, rather than the apparent left-lateral motion preserved here.
- iii) the transfer fault thrusts only a very small sliver of basement rocks over cover rocks, whereas Scargill Creek Fault thrusts a sizable anticline of basement rocks (Scargill Anticline) over a somewhat different set of cover rocks.

From the above arguments it would appear that the transfer fault and Scargill Creek Fault are in fact separate faults, and the preferred interpretation is that the transfer fault represents a lateral ramp and the overall arrangement of faults follows model two. Consequently, Scargill Creek Fault would simply represent a diverging splay, and the major range-bounding motion is taken up on the W-E trending eastern portions of Mt Alexander Fault and Maxwellton Fault.

### **3.4.3 Major folding**

#### **3.4.3.1 Mt Alexander Anticline**

The range of rocks behind Mt Alexander Fault is interpreted as having been folded into a fault-related anticline, Mt Alexander Anticline. There are very few cover rocks exposed around the western end where the fold plunges beneath a veneer of river gravels, but this is not surprising given the complex structures mapped to the west and obvious fluvial erosion that has led to the creation of Waikari Flat. Cover rocks are abundant on the shallow-dipping southern limb. If it is assumed that the ridge crests on basement rocks

are lowered little below the stripped basement-cover rock unconformity, the contouring of the base of the cover rocks and the smoothed residual topography upon basement indicates a distinctly anticlinal shape (map 2). A number of small perturbations do exist within the generalised structure contours however, tentatively interpreted to represent back-thrusts, now exploited by a number of the larger streams in the area and hence are represented as deep gorges. Further evidence is discussed in Chapter 6.

The anticline proves to be highly asymmetrical (with a north-westward sense of vergence), slightly sigmoidal, and doubly plunging, but is notable in that the double plunge is quite asymmetric (steeper in the east). Furthermore, it is clear that the overall trend of the fold is SW-NE, and does not mirror the swing in strike of Mt Alexander Fault at its eastern end, nor do structures in Scargill Hills Outlier. Instead the fold appears to have been cut-off by the fault, hence its rapid termination there. Reasons for the departure of folding from the influences of Mt Alexander Fault are discussed in Chapter 4.

The structure contouring also highlights a series of cross-folds across the anticline although the magnitudes of these may be slightly accentuated by movement on the back-thrusts. The largest "up-warp" is represented by Mt Alexander and the corresponding large "down-warp" to the east creating Scargill Hills Outlier is likely to account for some, but not all, of the asymmetry mentioned above. Two more structural "up-warps" can be observed west of Mt Alexander, but appear to occur on a shorter wavelength than that of Mt Alexander, suggesting that the intensity of NNW-SSE trending cross-folding may be increasing in a westward direction.

#### 3.4.3.2 Karaka Syncline

Immediately north of the western portions of Mt Alexander Anticline is a topographically low, triangle-shaped area of basement rocks. The relatively smooth topography suggests that the surface is likely to be close to the basement-cover rock unconformity surface, now largely devoid of cover rocks due to a combination of preferential erosion by Karaka Stream and its tributaries, and faulting along a NNW-SSE trending tear fault. The shape of the surface of the basement rocks is clearly indicative of a syncline, Karaka Syncline. It is possible that the northern side is

influenced by back-thrusting however, due to the fact that Karaka Stream flows hard against a very steep portion of basement rocks. Again, these effects are discussed in detail in Chapter 6.

The trace of the syncline further west is complicated by faulting along the Trig C Faults and associated tear fault, largely causing the fold to be overridden at an oblique angle, and is described fully in Chapter 5.

The presence of a complete anticline-syncline pair at western ends of the Lowry Peaks and Mt Alexander Blocks is the main reason to suggest the eventual disappearance of Mt Alexander Fault there.

### 3.4.3.3 Scargill Anticline

Scargill Creek Fault thrusts basement rocks over cover rocks for its entire length before characteristically disappearing into the core of a westward-plunging anticline-syncline pair at its western end, creating the complicated succession found in Eastcott Stream. The range of basement rocks behind the fault is therefore interpreted to be a fault-related anticline, the so-called Scargill Anticline.

Scargill Anticline appears to grow in size eastwards, past the dying-out ends of Mt Alexander Fault, and surpasses a small anticline associated with Maxwellton Fault to become the major anticline of the eastern portion of the Mt Alexander Block. Between the two is likely to be a small syncline, faulted on its southern side by the eastern continuation of Mt Alexander Fault. If Maxwellton Fault does join up with Limestone Glens Fault then it is likely that Scargill Anticline continues across the Hurunui Gorge and up the western side of the Kaiwara Valley for some distance. The morphology of the range from Landsat images again suggests this is likely.

Structure contouring on the surface of the basement rocks highlights typical characteristics such as asymmetry and a general parallelism to the major faults.

### **3.5.3 Summary: *Mt Alexander - Maxwellton Fault System and associated structures***

The Mt Alexander Block is divided into two distinct portions, characterised by two major sigmoidal anticlines, Mt Alexander Anticline and Scargill Anticline, that essentially overlap en-echelon, with a complex transfer zone in between. The transfer is accommodated by a number of smaller-scale structures preserved in the cover rocks of Scargill Hills Outlier, which has been created as both the consequence of the down-plunge of the major structures associated with the transfer zone and NNW-SSE trending cross-folding. The presence of cross-folding can be traced to the west of Scargill Hills Outlier, by structure contouring on the unconformity between the basement and the cover rocks, where it appears to be decreasing in wavelength.

Maxwelton Fault and the majority of Mt Alexander Fault are unique in the study area in that they trend approximately W-E. Mt Alexander Anticline does not appear to relate as closely to its northern bounding fault as most others in the study area, particularly at its eastern end. Scargill Anticline appears to strike W-E in relation to the Maxwelton Fault for much of its length, although it trends more SSW-NNE in its western portions, due to the influence of a diverging splay, Scargill Creek Fault.

Scargill Creek Fault is notable in that it is the only range-bounding fault in the study area to possess a possible active fault scarp. However, evidence that the scarp was at least partly created by erosion cannot be dismissed.

## **3.4 THE LOWRY PEAKS FAULT SYSTEM AND ASSOCIATED STRUCTURES**

Structures of the Lowry Peaks Fault System are the most continuous of all three major sets of structures, characterised by a single range, the Lowry Peaks Range, which continues across the north-eastern side of the Hurunui River to form the entire eastern boundary to the Culverden Basin. The northern boundary of the study area is the Hurunui River, so only the very southern portions of any structures formed on the down-thrown side of the fault systems (ie. in the Culverden Basin) are discussed.

### 3.4.1 Lowry Peaks Fault System

The Lowry Peaks range-front is characterised by a series of river terraces, preserved at a variety of elevations along its length. Most terraces are composed of basement rocks overlain by river gravels and are capped by a sequence of alluvial fan gravels sourced from the range above. The majority of the terraces have been clearly uplifted as they are currently situated at a height far above any likely to be created by downcutting of the Hurunui River alone and cannot be correlated with any other terraces preserved in the Culverden Basin. The lack of clear evidence for faulting along the range-front (apart from some possible back-tilting of the terraces) means that the evidence for faulting verses folding as a mechanism to have created the uplift needs to be considered carefully.

Any direct evidence for faulting has largely been either removed by the Hurunui River or buried by terrace deposits and alluvial fans. If any terrace has been differentially uplifted by individual strands of the fault, the corresponding fault scarp has been extensively trimmed. However, at the very western end of the area there is some evidence for internal cross-faulting of the terraces, provided by anomalous drainage patterns, combined with some back-tilting effects that extends along the majority of the range-front. Clear evidence for faulting does exist at the eastern end as described below.

A number of cover-rock localities along the range-front suggest that folding has had an important effect on the uplift of the range. Many of these localities possess a steep northward-dip and a corresponding lack of shearing of both the basement and the cover rocks in these localities means that it is possible that the contacts in fact represent unconformable sedimentary contacts. It is possible that uplift of the terraces could be achieved by folding alone in these localities; slight back-tilting of many terraces (ie. in the wrong sense for the steep limb of the anticline) suggests that some effects of faulting exist, even if it is only late stage after the greater part of the folding has ceased.

Clear evidence for major faulting does exist in the Hurunui Gorge. Large shear zones, many relatively shallow-dipping, with clear reverse sense of movement, and some apparently representing back-thrusts, occur in basement rocks at the entrance of the gorge. Cover rocks preserved immediately west of this locality lie adjacent to intensely sheared basement rocks, but dip anomalously moderately SE. The possibility exists that

they are overturned, again, the similarity between the Ashley Mudstone Formation and the Scargill Siltstone Member of the Waikari Formation making interpretations difficult. If they are overturned, they provide clear evidence for the existence of faulting, and that the faults represent thrust-faults, if not, the possibility of some strike-slip faulting there. The southern boundary of a small syncline of cover rocks (Ben Lomond Syncline) in the Hurunui Gorge is also clearly faulted, with an intensely sheared zone of basement rocks immediately adjacent to the cover rocks.

In conclusion, the relative effects of faulting verses folding appears to be variable, but can be observed in a general sense to increase in an eastward direction, folding preceding faulting in all portions. Therefore, it is proposed that the range-front is currently characterised by two southward-dipping listric thrust faults: i) the WSW-ENE trending Hurunui Bluff Fault, provisionally shown to bound the entire range-front until reaching the eastern end, where it veers into the range bounding the southern side of Ben Lomond Syncline (discussed below), and ii) Hurunui Gorge Fault, which takes up the range-bounding position across the mouth of the Hurunui Gorge and trends more SW-NE. The change in strike of the overall fault system is likely to account for the splaying of the faults at this point.

### **3.4.2 Folding associated with Hurunui Bluff Fault**

Folding on the down-thrown side of the Hurunui Bluff Fault has largely been eroded by the Hurunui River and for this reason, combined with the very small part of the Culverden Basin mapped here, no firm conclusions are drawn concerning the bedrock beneath the gravels on this side of Culverden Basin. Instead, emphasis has been placed on the folding on the up-thrown side of the fault.

#### **3.4.2.1 Ben Lomond Syncline**

Cover rocks preserved in the Hurunui Gorge are clearly folded into an asymmetric, southward-verging syncline, Ben Lomond Syncline (Hamilton, 1950). Outcrops in small gullies cut into the high terrace to the west suggest that the syncline continues westwards some distance where the presence of anomalously thick river gravels in the

terrace scarps north of Mt Benger and Hitchin Hills homesteads (map 1) suggests that the river may have once been preferentially scouring out the softer cover rocks. The syncline does continue some distance to the east of the Hurunui River, although poorly preserved its location is defined by a large landslide that has occurred preferentially on the softer, cover rocks there (M. Armstrong, pers comm. 1994).

Despite the fact that the syncline appears to possess a smaller wavelength than many others in the area (which may be just a function of the level of erosion), it is proposed that the folding has formed in association with the major faulting observed on the southern side and that an anticline is formed in association with the faulting along Hurunui Gorge Fault.

#### **3.4.2.2 Lowry Peaks Anticline**

Hurunui Bluff Fault bounds a large range of basement rocks overlain by cover rocks at its western end that apparently define the western, plunging end of an anticline (Lowry Peaks Anticline). Notable here is that the shape of the plunging end of the anticline is very square, a feature directly attributed to faulting along a proposed NNW-SSE trending tear fault, that serves to transfer motion between the Hurunui Bluff Fault and the Trig C Faults (discussed in section 3.5.1) and the swing in strike to the W-E caused by the effects of folding in the Mt Alexander Block.

Structure contouring on the surface of basement rocks denotes the shape and trend of the anticline, the shape being slightly sigmoidal, the trend closely paralleling Hurunui Bluff Fault (map 2). Notable also is the largely symmetrical profile, which is partly a function of the presence of at least one small imbricate splay of the major fault indicated by the structure contouring (map 2), but is also probably indicative of the very young age of the faulting along the range-front (as discussed in Chapter 5).

Structure contouring also highlights NNW-SSE oriented cross-folding. Three structural highs occur along the length of the Lowry Peaks Anticline, two of which bound the structural down-warp in which Scargill Hills Outlier is preserved, the other some distance west. The distance between the crests is greater between the eastern than the western pair, similar to that observed along Mt Alexander Anticline, suggesting the



wavelength is decreasing in a westerly direction. Like the structure contours for Mt Alexander Anticline, there also appears to be some evidence for back-thrusting on the southern limb of Lowry Peaks Anticline (map 2), which may have accentuated the magnitudes of these effects.

### **3.4.3 Summary: *Lowry Peaks Fault System and associated structures***

The Lowry Peaks Fault System structures are dominated by one large WSW-ENE trending, asymmetric anticline, Lowry Peaks Anticline, formed in close association with faulting along Hurunui Bluff Fault. At its eastern end Hurunui Bluff Fault splays into two strands, the southern strand creating the Ben Lomond Syncline on its down-thrown side, the northern continuing across the Hurunui River to bound at least part of the range-front to the NE as the Hurunui Gorge Fault.

Lowry Peaks Anticline is well defined by cover rocks at its western end, where it plunges steeply before being complicated by a number of secondary structures, serving to give the plunging end of the fold a rather square shape. Structure contouring on the surface of the basement rocks highlights NNW-SSE trending cross-folding, which appears to tighten in a westward direction.

## **3.5 STRUCTURES AT THE WESTERN END OF THE STUDY AREA**

### **3.5.1 Trig C Ridge Structures**

Immediately west of Lowry Peaks Anticline, a series of active thrust faults with southward sense of vergence thrust Kowai Formation over the Omihi, Waikari and Mt Brown Formations lying on the north-western limb of Lowry Peaks Anticline (see cross sections). The result is a hybrid, well developed, but poorly exposed ridge of predominantly Kowai Formation, with isolated outcrops of Mt Brown Formation and Weka Pass Stone Member. The fact that Kowai Formation has been thrust across lower units suggests that the faults are very superficial and shallow-dipping (see cross sections).

The sense of vergence of these faults is opposite to that of Hurunui Bluff Fault, the change of facing direction apparently largely achieved by movement along the NNW-SSE trending tear fault that has been mapped to offset cover rocks at the end of Lowry Peaks Anticline. However, a mechanism for the faulting is lacking and therefore, on the cross sections it has been proposed that the faults have formed by out-of-sequence thrusting (Jadoon et al, 1994) off the plunging trace of the Lowry Peaks Fault. This is likely to be facilitated by movement on the tear fault, which may in fact be accommodating some thrust-type motion towards the east, and the result being the shallow faulting of the Waikari Flat area above the plunging ends of the major structures described above. These aspects are discussed further in Chapter 5.

The faults are characterised by a single fault trace in central portions, that is well marked by a break in slope approximately halfway up the hybrid ridge described. The fault then appears to decrease in throw westwards to eventually disappear from sight beneath a southward-verging, asymmetric anticline, trending W-E, and plunging gently westwards to disappear beneath the flood plain east of Gemmels Road. Immediately south of the last traces of the fault a series of river gravels have apparently been ramped-up northwards, folded into an anticline at their western end with northward sense of vergence, suggesting another complete change in facing direction. South of this structure again, another W-E trending small fold has been formed in the valley-floor gravels.

At its eastern end the fault breaks up into three splays, serving to repeat the ridge of Kowai Formation three times, the lower being thrust over the Weka Pass Stone Member. Each fault appears to curve around into a more N-S trend at their eastern end, suggesting a component of oblique strike-slip motion there before motion is absorbed into the soft cover rocks.

### **3.5.2 Hawarden Anticline and Pyramid Valley Anticline**

The very west of the study area is characterised by a set of anomalously N-S trending structures, two of which (Hawarden Anticline and Pyramid Valley Anticline) have been mapped here. Both structures plunge northwards, appear to be very symmetrical and are likely to represent very young, deformation restricted to cover sequence only. Hawarden

Anticline shows evidence at the northern end at least, of having some uplifted river terraces preserved on it. Active deformation associated with these structures are discussed in Chapter 6.

Immediately west of Hawarden Anticline is a set of SW-NE trending structures mapped by Mould (1992). He attributed the N-S trend of the range-front to a weak zone in the basement, apparently not associated with the trend of the recent structures preserved there, but further south, the structures are very clearly N-S trending (e.g., MacDonald Syncline, Karetu Thrust, Nicol, 1991) due to the partitioning of strain into two directions at right angles due to the presence of pre-existing (L.Cret.) structures, trending W-E in the basement rocks. By association then, if the folds are associated with faults at depth, these faults are likely to dip westwards and belong to part of the Mt Grey to Island Hills System (the smaller thrust faults that disrupt the Pyramid Valley Anticline also dip westwards) locally trending N-S here as motion is partitioned between these structures and W-E trending structures such as Pyramid Valley Fault and the Trig C Faults as described in Chapter 5.

### **3.6 SUMMARY**

Macroscopic structures in the study area can be divided into four groups, three of which are interpreted as the three local members of a major imbricate thrust system that bounds the south-eastern side of the Culverden Basin. The fourth group comprises an anomalous set of N-S trending structures proposed to have close affinities with structures mapped on the south and western margin of the Culverden Basin by Nicol (1991) and Mould (1992) respectively.

The Kaiwara Fault system and associated structures is a hybrid group of en-echelon faults and folds that vary in strike between WSW-ENE and SW-NE in association with the anomalous WSW-ENE strike of Moores Hill Fault. The result is a major step-over in the system between structures of Moores Hill Range to those of Greta Peaks Range. A component of NNW-SSE trending cross-folding is also apparent, down-warpage occurs in the Moores Hill Anticline area and central portions of Waikari Anticline. This set of

structures form the southernmost member of the portion of the imbricate thrust system found in this area.

The middle member of the imbricate thrust system, the Mt Alexander - Maxwellton Fault System and associated structures are also affected by a number of anomalously-trending faults in central portions, namely Maxwellton Fault, the transfer fault and the eastern end of Mt Alexander Fault. These form a complex set of transfer structures between two major en-echelon fault-fold systems (the Mt Alexander Fault - Mt Alexander Anticline System and the Maxwellton Fault - Scargill Anticline System, the latter still anomalously W-E trending). The complex transfer zone is preserved in Scargill Hills Outlier, a structural depression formed as a combination of the plunge of structures associated with the transfer and NNW-SSE trending cross-folding. The cross-folding can also be traced in a westward direction, where the wavelength appears to be decreasing.

The Lowry Peaks Fault System and associated structures are the simplest of the three systems, forming a single, but apparently very young fault system for most of its length, that uplifts a very large anticline of predominantly basement rocks on its southern side. At the eastern end a single splay creates an intermediate syncline-anticline pair in front of the southern splay. A set of secondary structures complicates the western end of this system, causing a change in facing direction to the south and the apparent over-riding of structures of the Mt Alexander - Maxwellton System. NNW-SSE trending cross-folding is very clearly preserved in this system with two major down-warps corresponding to northern portions of Scargill Hills Outlier and the area behind Fire Lookout (map 1) respectively.

Structures at the western end of the study have largely been mapped by Nicol (1991), but the northern part of Hawarden Anticline and the highly faulted Pyramid Valley Anticline were included in the mapping for this thesis. The structures are clearly northward-plunging and appear to form very young structures associated with the north and eastward propagation of the structures mapped on the western margin of the Culverden Basin. The junction of these with the Trig C Structures is described in Chapter 5.

## MESOSCOPIC DEFORMATION

### 4.1 INTRODUCTION

The lack of good cross-sectional exposure of the major faults described in Chapter 3 has meant that general conclusions regarding their thrust fault nature have been largely based on the association with features such as fault-related folding, the overlapping nature of the faults and a generally bow-shaped trace. However, each of these features are not exclusively sure thrust fault features. Oblique-slip motion is characteristic of faulting in the north Canterbury region and good kinematic indicators of the sense of slip on the poorly exposed faults are difficult to find. The widespread indication of both fault-parallel folding and cross-folding and the relay system connecting overlapping faults all indicate a high degree of internal strain within the fault bound blocks. This chapter discusses directions of internal strains and small-scale structures used to explore the deformation kinematics.

### 4.2 MESOSCOPIC BASEMENT DEFORMATION

#### 4.2.1 Pseudo-folding of the basement

In section 2.2.1 it was noted that on a large scale, bedding in the Torlesse Supergroup possesses a near-vertical attitude, with an overall WSW-ENE trend. Form lines were drawn on discontinuous sandstone marker beds from aerial photographs, denoting gentle warping about N-S axial traces, in contrast to the apparently intense and complex deformation noted on an outcrop scale (map 3). Similar types of deformation have been noted throughout the Torlesse Supergroup in north Canterbury (eg. Bradshaw, 1972). The deformation primarily consists of bedding-parallel shearing and folding, the former often confined to the mudstone (or argillite) beds, disrupting beds along strike, while still allowing larger-scale trends (such as the gentle warping noted here) to be traced. This style of deformation is completely truncated by bedding in the cover rocks, leading to the conclusion that the majority of these structures were formed during the Late

Cretaceous Rangitata deformation event (Bradshaw et al, 1980) and therefore are not discussed any further here.

However, the consistent WSW-ENE trend of the basement rocks, and the fact that the gentle warping does not appear to correspond with the NNW-SSE trending cross-folding noted for the major structures, suggests that there has been no systematic rotation of these earlier structures in accordance with the obvious large-scale folding recorded by the overlying cover rocks. There is no evidence for detachment between basement and cover rocks (so that great use has been made of structure contouring the surface of the basement rocks, clearly delineating the folding of this contact), therefore a type of deformation is needed to produce a fold shape without rotating any of the beds.

Using similar evidence, and the relatively abundant small-scale fractures in the Doctors Dome region (to the SW) by comparison with structurally deeper basement rocks to the NW, Nicol et al (1990) proposed a style of deformation analogous to the type of motion of a bean-bag, triboplastic deformation, in which the top 1-3 km of basement rocks have deformed brittly along numerous pre-existing small-scale fractures in accord with the changing shape of the overlying cover rocks. Furthermore, the intensity of the strain showed a marked increase towards the major faults and the hinge zones of the major folds.

It is proposed that the basement rocks in this study area have also been deformed into a folded shape by triboplastic deformation. It is therefore important to note here the difference between faulting of a rigid basement block over which the cover rocks are passively forced or drape folded (ie. typical Rocky Mountain Foreland style eg. Stearns, 1978, Reches, 1978, Reches and Johnson, 1978, Cook, 1988) and the type of deformation described here where the two sets of rocks are deforming in response to the same regionally imposed strain, but are accommodating that strain internally in two very different ways.

#### **4.2.2 Stress tensor analysis**

A useful property of deformation of the basement rocks by triboplastic deformation is that, as described above, the intensity of small-scale faulting increases towards the faults.

Therefore, sampling of the internal fractures near the major faults should provide good kinematic indicators of the motion on the major faults (particularly useful where no exposures of the actual fault planes exist and/or where the faults are represented by a large fault zone).

An extension of the above is to calculate the average stress tensor configuration operating in an area, by inverting slip orientations to principle stress orientations for a number of localities. The basic assumption is that movement indicators on a given fault plane will parallel the maximum shear stress, regardless of the orientation of that plane (Wallace, 1951, Bott, 1959). Recently, Dupin et al (1993) showed that in most cases this assumption appears valid, Pollard et al (1993) suggesting that possible exceptions being if: i) more than one deformation event is recorded, ii) the stress tensor orientation has changed throughout deformation, iii) different parts of a highly curved fault plane are sampled or iv) another fault with a different stress configuration interferes. Nevertheless many of the methods suggest ways of separating data resulting from the above situations. Methods range from the purely graphical (eg. Arthaud, 1969, Angelier and Mechler, 1977, Aleksandrowski, 1985 and Ritz, 1994), to the numerical (eg. Carey and Brunier, 1974, Angelier, 1979, 1984, 1989, Armijo and Cisternas, 1978, Etchecopar et al, 1981, Angelier et al, 1982, Michael, 1984, Gephart and Forsyth, 1984, Reches, 1987, Celerier, 1988, Will and Powell, 1991 and Fry, 1992), many of the latter involving the aid of computer programs.

#### 4.2.2.1 Methodology

##### *Data Collection*

Although small-scale fracturing in basement is widespread, the method requires both slip direction and slip sense to be determined and localities at which enough such data could be obtained restricted to a number of sample sites. Five sites suitable for stress tensor analysis in the basement rocks were located in the study area, the localities of which (accompanied by the raw fault plane data) are shown in figure 4.1. Three of the sites occur along the Mt Alexander Fault which allowed a somewhat more detailed study to be performed on that fault, but restricted interpretations of the area as a whole.

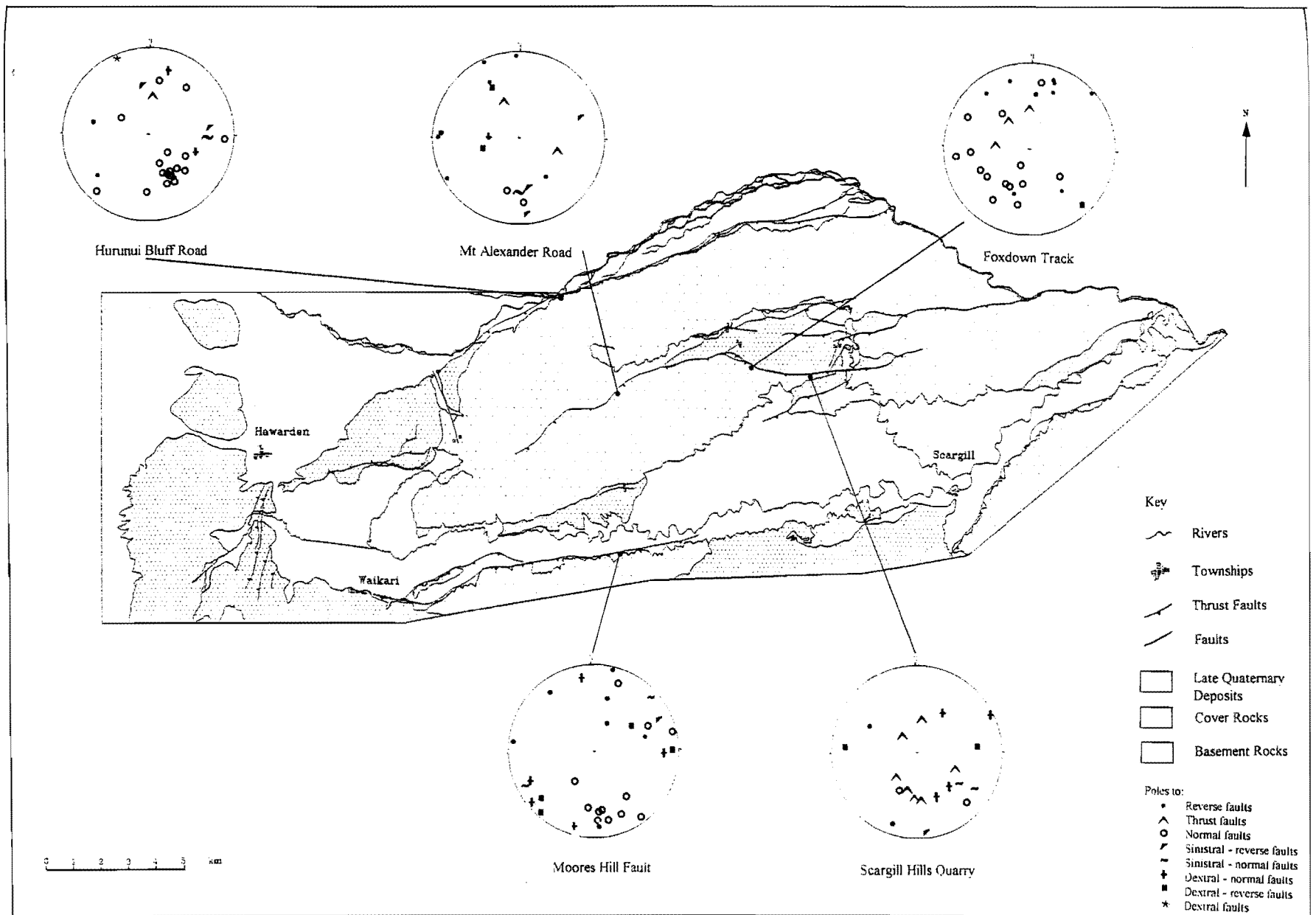


**Figure 4.1** Location map and fault plane data for the five basement rock stress tensor analysis sites.



Data collection involved measuring the dip and strike of the fault plane, the rake to the horizontal that any motion sense indicators made on that plane, the motion sense of the indicators and a reliability weighting of the motion sense indicators (1 = good, 3 = poor, 4 = no indication of motion direction, 5 = no motion indicators can be measured). Motion sense indicators were of two types; slickenside striations and calcite fibre lineations, the steps on the latter often providing the clearest indication of the relative motion of the missing fault block to the plane. 218 faults were measured in total, 135 contained good motion sense indicators

### *Computation of the stress tensor*

The method used here involves the computation of a partial stress tensor (defined in Appendix 1) by the computer program BRUTE10 written by Hardcastle and Hills (1991), based on philosophies developed by Gephart and Forsyth (1984). Briefly, the method involves a grid search of all possible tensor configurations for each measured fault plane to designate possible configurations for which movement could occur on that plane and a calculation of what that movement is likely to be, which is then compared to the movements measured in the field. A full discussion of the method, including variations according to the user-defined parameters follows in Appendix 1. The method has advantages over other numerical iterative methods in that it takes into account coefficients of friction and fluid pressure for the material being faulted and the rapidity of calculation (2-3 minutes on a 486 computer) makes it far superior to any of the graphical methods.

BRUTE10 produces ascii-files containing the possible orientations of  $\sigma_1$ ,  $\sigma_2$  and  $\sigma_3$ , the positions of which, when displayed as contoured or density stereoplots, will surround the areas in which the stress axes are predicted to lie. A brief discussion concerning appropriate contouring methods is also included in Appendix 1.

#### **4.2.2.2 Results**

Following the discussion in Appendix 1, the plots shown in figure 4.2 are considered to be the most reliable. The raw fault plane data, as mentioned, is shown in figure 4.1. The

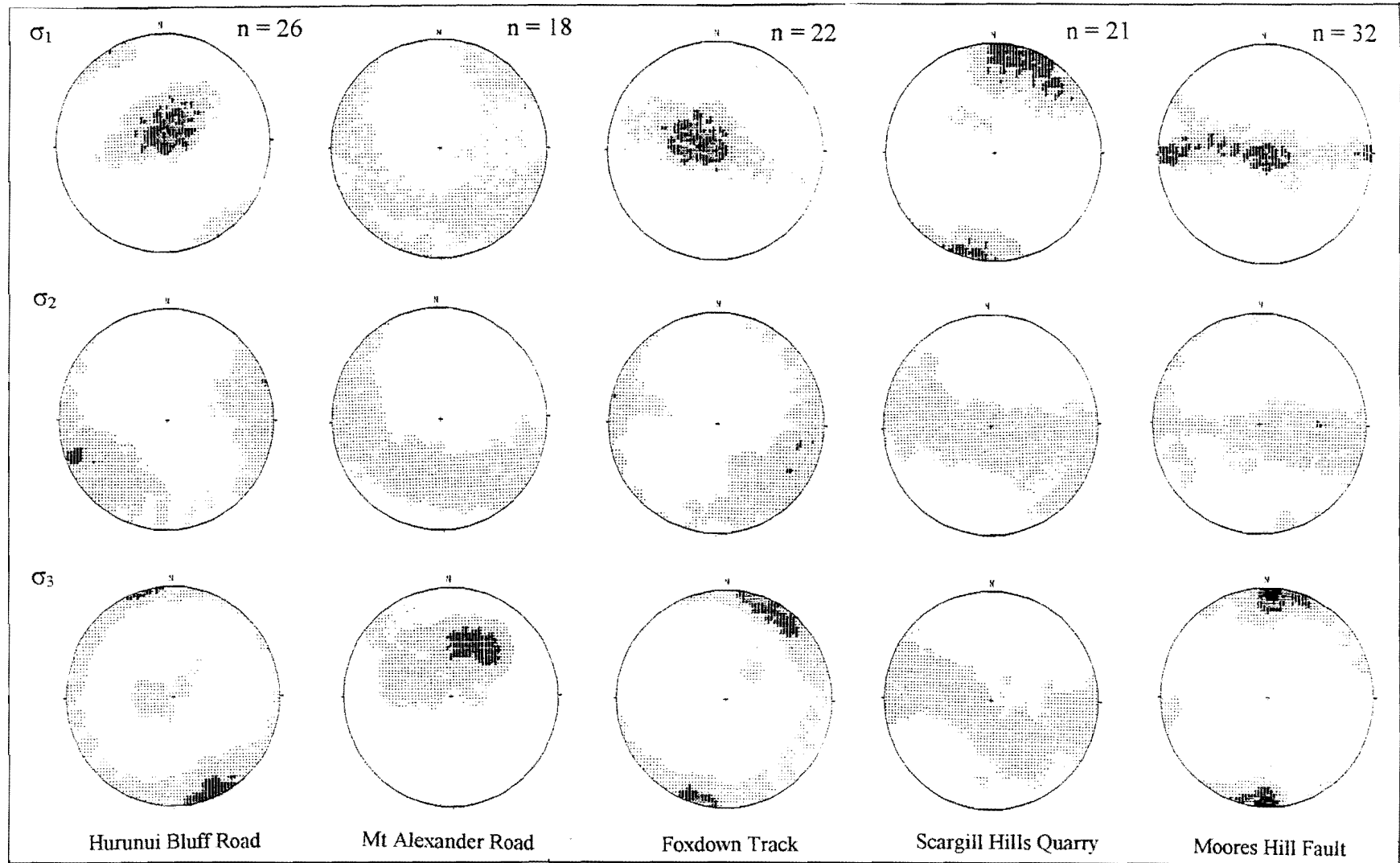


**Figure 4.2** Full set of stress tensor analysis results for the basement rock localities, displayed as density stereoplots of  $\sigma_1$ ,  $\sigma_2$  and  $\sigma_3$ , and following the discussions in Appendix 1.

plots for each locality are described below in terms of the major fault systems, from north to south. The interpreted results are summarised in figure 4.3, where the  $\sigma_1$  plots are contoured at an interval more appropriate to the individual site and placed in their respective locations.

### *Lowry Peaks Fault System*

The stress tensor configuration plots for the Hurunui Bluff Fault show a predominance of normal faulting, with a secondary configuration indicative of reverse faulting, but both apparently possessing the same orientation, normal to the strike of the fault. These are well reflected by the plots of the raw fault data, which clearly show two sets of faulting, normal and reverse (or thrust) with approximately the same orientation, accompanied by only a small number of faults accommodating oblique motion.

An interpretation that the Hurunui Bluff Fault is currently accommodating normal faulting is in direct conflict with the interpretations made in Chapter 3. However, it is possible that at least some of the faulting either represents: i) Cretaceous normal faulting, or even more likely, ii) localised collapse of the hanging-wall, particularly given the fact that the fault is interpreted to be very close to the range-front at that locality, and the clear observations of collapse at present due to undercutting by the Hurunui River. Even if the above effects do not dismiss entirely the possibility of more fundamental normal faulting at that particular locality, they are likely to diminish their significance to the point where they do not predominate over the population of faults indicating clear effects of compression.

It is therefore interpreted that the Hurunui Bluff Fault is largely accommodating reverse or thrust faulting, with a principal compression direction of NW-SE, overprinted by gravitational collapse of the leading edge of the hanging-wall.

### *Mt Alexander-Maxwelton Fault System*

The most obvious initial observation to be made concerning the three sites measured along the Mt Alexander Fault is that each displays a significantly different tensor

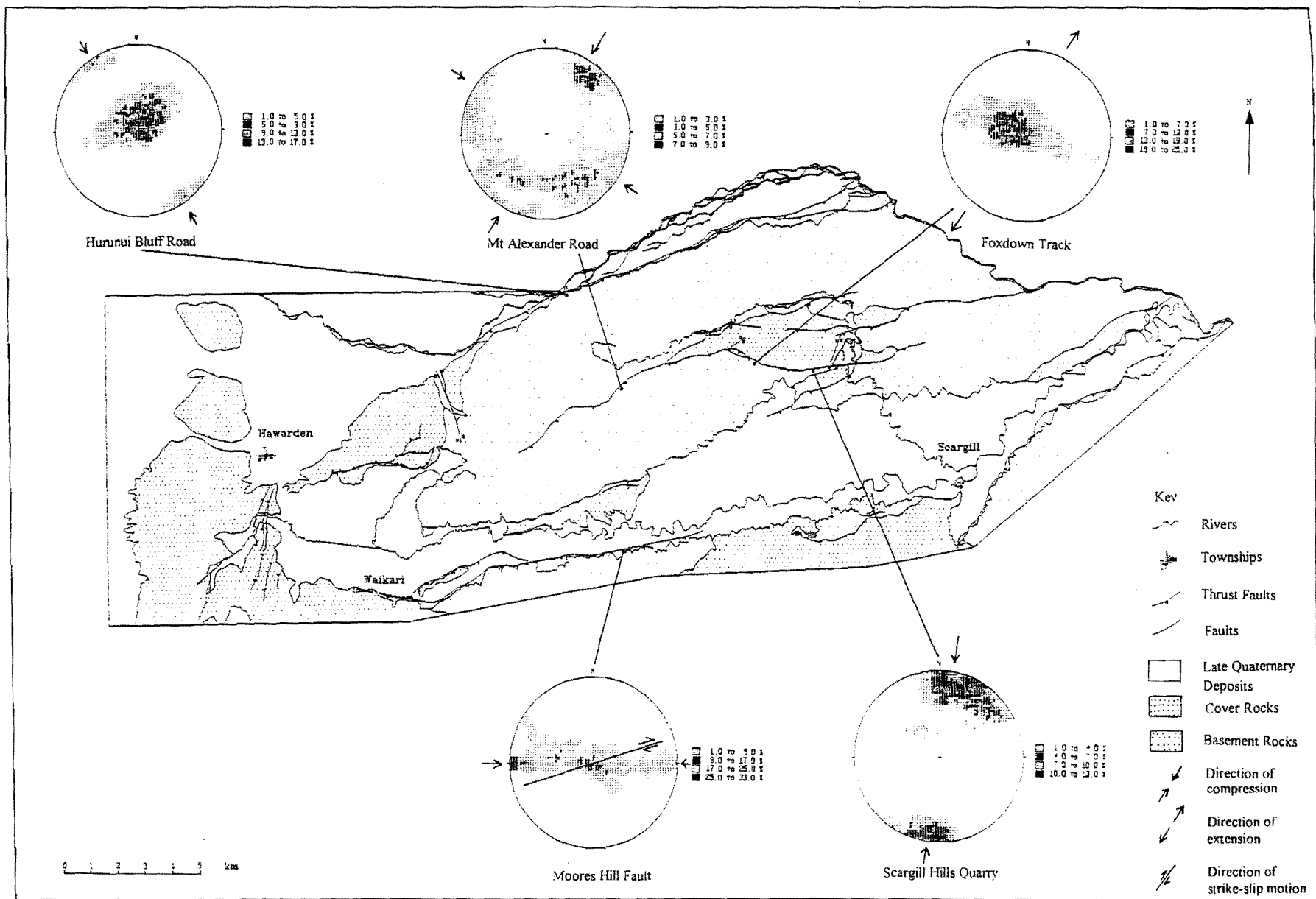


**Figure 4.3** Interpreted  $\sigma_1$  stress tensor analysis plots with respect

configuration (the only exception being the near coincidence of  $\sigma_2$  for the Mt Alexander Road and Scargill Hills Quarry localities, with some overlap to the pattern of the Foxdown Track locality), suggesting a more complex set of deformation for the fault than that of simple uniform over-thrusting as proposed in Chapter 3. The Mt Alexander Road and Scargill Hills Quarry localities do show a predominance of compression over extension (although here oriented NE-SW), but the Foxdown Track locality shows a predominance of extension, presenting something of an anomaly, particularly due to its position between the former two. Furthermore, the extension direction is apparently significantly different for each site.

The three localities straddle the area of Mt Alexander Fault where the fault undergoes a major bend from a SW-NE trend in the west to one of NW-SE and then finally W-E in the east (figure 4.1 and map 1). As noted in Chapter 3, the bend in the fault is not accompanied by a corresponding swing of the fold structures formed in the hanging-wall and footwall. Therefore, if the bend was formed by the cross-folding effects inferred to have down-warped Scargill Hills Outlier alone, a corresponding cross-folding effect should be reflected by at least the structures formed in the hanging-wall, which clearly does not appear to be the case. Instead it is proposed that the bend in the fault represents a thrusting event towards the NE, obliquely overriding structures formed in Scargill Hills Outlier, the bend likely to represent a type of lateral ramp structure, similar, but much larger (and likely to be dipping at a lower angle) than that inferred for the transverse fault.

The somewhat oblique trend of the fault trace at the Scargill Hills Quarry locality (W-E) to the NE-SW component of compression has accordingly resulted in a slightly oblique, sinistral component of motion on many of the faults there (figure 4.1). This is unusual for W-E trending faults in north Canterbury, a number show late stage effects of a dextral sense of motion (due to the NW-SE oriented compression regime) (eg. Boby's Creek Fault, Pyramid Valley Fault, Nicol, 1991), which may indicate that this localised NE-SW orientated compression represents an early stage of deformation.

The recognition of true lateral ramp faults and accompanying folds (ie. those that parallel the thrust transport direction) has been recently discussed by De Lamotte and Guezou (1995). They noted that folding associated with movement over a lateral ramp often leads to gravitational instability and collapse, which may directly account for the

extension inferred for the Foxdown Track locality. Motion there may be spread over a variety of orientations due to the geometric problems associated with faulting around a bend, and if the ramp structure has now largely been by-passed, then widespread gravitational spreading and collapse, facilitated by the significant topographic differences between Mt Alexander Anticline and Scargill Hills Outlier (ie. the area represented by Mt Alexander itself) may be occurring. It is important to note here the similarities between  $\sigma_1$  concentrations between the Foxdown Track locality and the Hurunui Bluff Road locality, the major difference being a slight difference in orientation, which can be directly related to the trend of the major thrust fault, upon which the collapse is occurring in these localities.

A NE-SW oriented principle compression direction for the Mt Alexander Road locality is somewhat more difficult to resolve however, particularly given its position near the centre of clearly WSW-ENE trending portions of Mt Alexander Fault. A number of possibilities exist to reconcile such motion, namely: i) overprinting of earlier NE-SW oriented compression by later NW-SE oriented compression, ii) the influence of back-thrusting, some of those suggested by the structure contouring possess a W-E to WNW-ESE trend, which may partly represent the NE-SW compression, iii) the eastern end of Mt Alexander Fault may be “locked” and continued movement at the western end may in fact be causing the stress tensor vector to be passively rotated with time. The fact that the Scargill Hills Quarry locality does not show any signs of overprinting either suggests that the fault is truly locked there, or that the overprinting effects at the western end are truly localised. Further evidence to resolve these results are discussed in the following chapters.

The final observation to be made from the stress tensor plots along Mt Alexander Fault is, as mentioned above, the near coincidence of  $\sigma_2$ . Apart from the fact that they signify a similar orientation of deformation on these faults, their distribution suggests a great circle-type girdle distribution. Two populations of data have been suggested as a possibility for the Mt Alexander Road locality, and therefore, the same may be expected from  $\sigma_2$ , but they may also indicate an axial compression. Such a compression may be directly indicating the internal along-strike shortening of the component fault blocks by cross-folding effects noted in Chapter 3.

The plots from Moores Hill Fault appear to again contain two populations of stress tensor configurations. The first indicates extension, with  $\sigma_3$  oriented N-S, similar, but rotated slightly in a clockwise direction from, the extension implied for Hurunui Bluff Fault (the rotation likely to be a direct reflection of the difference in orientation between the two). The second is a distinct component of oblique dextral strike-slip motion.

It is again possible that that some of the normal faults may be the result of either i) Cretaceous extension and/or ii) localised collapse of the hanging-wall, but it is notable that many of the normal faults shown on the raw fault data plots contain a distinct component of oblique motion in a dextral sense (as do a number of the reverse faults).

It is therefore interpreted that the major motion occurring on Moores Hill Fault at present is oblique strike-slip, with a small component of extension. The strike-slip motion is likely to be a very late stage effect, caused primarily by the near W-E orientation of the fault, similar to the observations of recent movement on other W-E trending faults in north Canterbury, as mentioned in the discussion of the Scargill Hills locality.

Again, the girdle-type distribution of  $\sigma_2$  may indicate a component of axial compression, which is likely to reflect the internal W-E shortening of the component fault block by cross-folding.

#### **4.2.2.3 Conclusions**

The stress tensor analyses highlight the complex internal deformation of the component fault blocks. The girdle-type distributions of  $\sigma_2$  indicate the likely internal shortening of the component blocks in a W-E direction, as well as the major NW-SE or NE-SW compression effects measured.

A number of the faults may also be showing two periods of deformation. Secondary collapse effects utilising fractures initially generated by thrusting are suggested for the

Hurunui Bluff Fault and the interpreted lateral ramp portion of the Mt Alexander Fault, the latter also likely to be undergoing gravitational spreading effects due to the geometry of the bend of the fault in that region. Overprinting of original NE-SW oriented compression by later NW-SE compression has also been suggested as a possibility for the motion on Mt Alexander Fault, particularly at the Mt Alexander Road locality. In contrast, motion on Moores Hill Fault appears to be currently of an oblique-dextral type, which is common to a number of W-E trending faults in north Canterbury as the late-stage effects of rotation of the plate motion vector.

Finally, when the stress tensor results ( $\sigma_1$ ) for each locality are compared between sites (figure 4.3) it is clear that there are major problems reconciling the stress tensor orientations between areas. In particular, the tensor configuration for Mt Alexander Fault is rotated  $90^\circ$  from that of Hurunui Bluff Fault and that implied by the geometry of the major fault systems. As mentioned above, it is possible that the NE-SW directed compression represents an earlier event, but other possibilities do exist, namely: the rotation of the stress tensor about the locked eastern end of the fault (particularly for the Mt Alexander Road locality), and the influence of W-E to WSW-ENE oriented back-thrusts. These will be discussed further in Chapters 5 and 6.

### **4.3 MESOSCOPIC COVER ROCK DEFORMATION**

Deformation of the cover rocks occurs in two ways. The first is the large scale folding of the cover rocks in which the limbs of the folds have clearly been rotated to their present position. The mechanisms of folding are not clear, bed-over-bed slip has been suggested for folding in other parts of north Canterbury where distinct bedding planes can be observed in the more resistant units such as the Amuri Limestone (eg. Nicol, 1991, Mould, 1992) but it is likely that the softer units have responded in a more ductile fashion, the poor outcrops here restricting evidence to prove such a conjecture. A “strain analysis” was undertaken here to determine how much of the deformation was accommodated within the fault blocks as folding, compared with the movement on the faults, and then, if possible, to determine the likely distribution of that strain.



The second type of deformation of the cover rocks is a widespread brittle fracturing of many of the units, particularly evident in the more resistant units such as the Amuri Limestone and Weka Pass Stone. A variety of mechanisms can be implied for their formation; most, but not all, can be related to the current deformation events and a detailed study of the fractures at Waikari Quarry provides correlations with the deformations described for the basement rocks.

#### **4.3.1 Strain analysis**

It was intended that one of the focuses of this study would be to determine the distribution of the internal strains throughout the major folds of the area, utilizing the distribution of glauconite grains in the widespread Weka Pass Stone Member of the Omihi Formation. However, ambiguous results were obtained, apparently suggesting only low amounts of strain (somewhat anomalous with respect to the structural mapping described in Chapter 3), leading to the abandonment of this aspect of the study. Nevertheless, a discussion of likely reasons as to why the method did not work, is given because the method has not been used previously in north Canterbury and because the method is relatively easy to apply and might have greater success in areas of higher strain.

The Weka Pass Stone Member possesses a high arenite content which means that in hand specimen the green-black glauconite grains clearly stand out against the creamy-white quartz, feldspar and calcite. If the grains were originally randomly distributed, specimens should now possess a distribution that reflects the orientation and magnitude of any imposed strain. The assumption that the grains were originally randomly distributed appears at first glance to be rather uncertain, particularly given the obvious bedding picked out by glauconite-rich layers surrounding bedding-parallel borings. However, sections purposely cut perpendicular to bedding also produced random plots, therefore it was thought that the possibility also exists that the abundant bioturbation has had a positive randomising influence, and removed any primary fabric effects of bedding created during deposition.

#### 4.3.1.1 Methodology

##### *Data collection and sample preparation*

Orientated specimens were collected at regularly spaced intervals along strike-ridges of Weka Pass Stone Member in the study area, initially concentrating on Scargill Hills Outlier (see figure 4.4 for locations). Many of the samples were oriented relative to bedding, others relative to a weathered surface (generally close to bedding anyway), as shown in table 4.1. In the laboratory, the specimens were cut and polished in three directions at right angles, generally parallel and perpendicular to the orientation mark respectively. The pattern of grains displayed on each face were then transferred to paper by means of a standard photocopier, enlarged to A4 or A3 size (table 4.1), depending on their size and shape. Control tests performed on a strained ironstone oolite and then on some of these samples to determine the optimum size of the face measured and the number of grains necessary to produce a clearly interpretable strain ellipse are described in Appendix 2.

##### *Computation of the strain ellipse*

The major problem with attempting a strain analysis lies in how best to measure the distribution of grains. If the original distribution was truly random, then the spacing between the grains is merely a function of the grain size. (ie. no two grains can be closer than the sum of their radii). Many methods have been proposed for the particular case where all the grains are touching (ie. an aggregate). These so-called centre-to-centre methods measure the spacing between the centres of the grains to see if it is greater in one direction than another, over and above any distributions due to original grain shape alone (eg. Ramsay, 1967, Lisle, 1979, Ramsay and Huber, 1987a). Clearly in these methods, the quality of the strain ellipse is highly dependent on the degree of sorting alone and therefore, because here the grains are not actually touching, the distribution can be likened to a very poorly sorted aggregate (ie. the grains will have a greater range of distances between their centres). Bearing this in mind, and the lack of any other known studies to deal with widely-distributed grains it was hoped that the clearly relatively highly strained rocks might produce some indications of strain, using a centre-to-centre method.

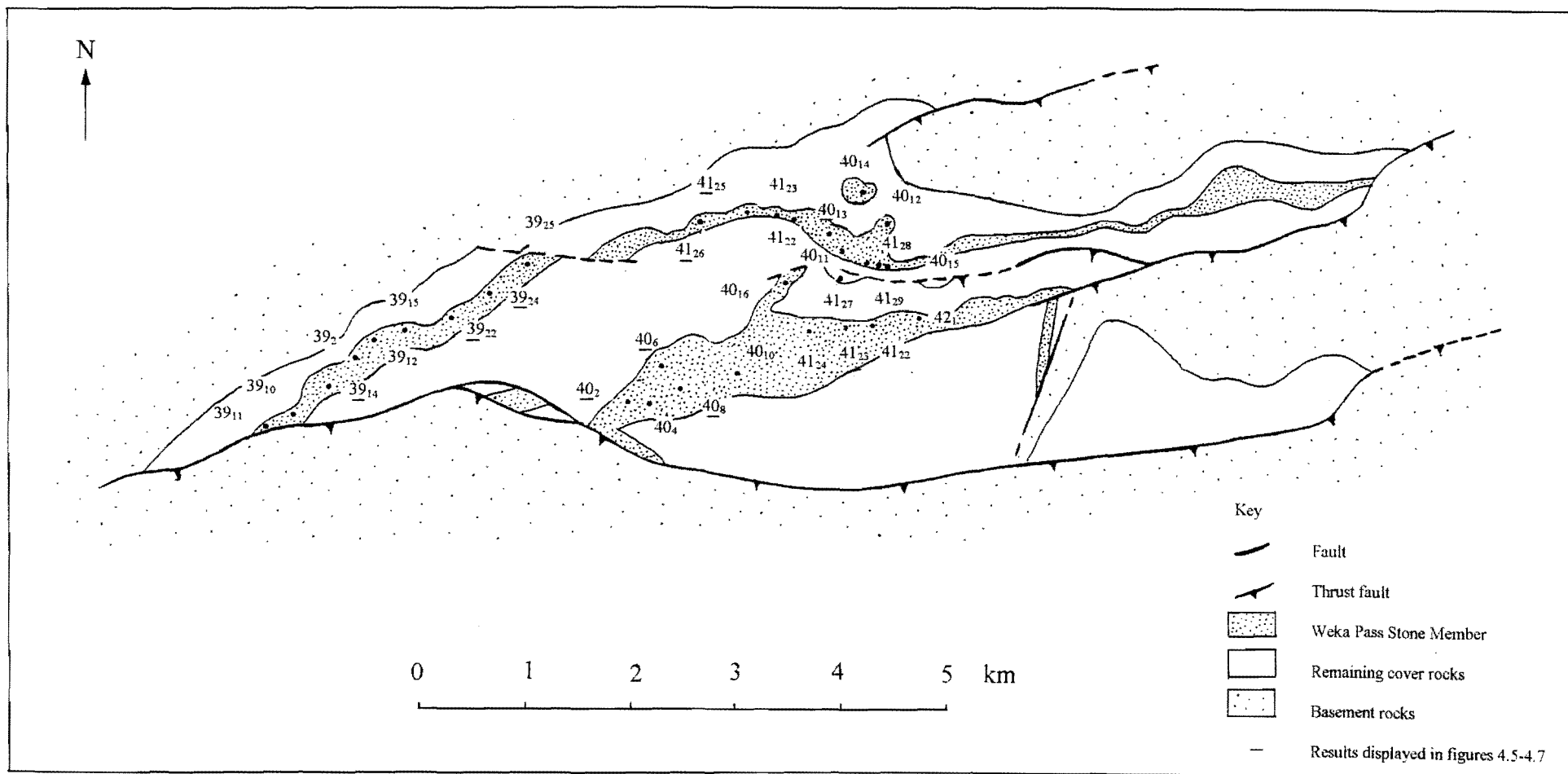


**Figure 4.4** Location map of samples used for the strain analysis from Scargill Hills Outlier.

Number	Orientation	Surface	n	Results:			
				Small gap in centre	Quality rating	Large ellipse	Quality rating
39 <sub>11a</sub>	242/49 N	weathered	100	*	3	*	3
39 <sub>11b</sub>			90	*	3		
39 <sub>11c</sub>			93				
39 <sub>10a</sub>	189/32 S	~ bedding	94	*	1		
39 <sub>10b</sub>			100	*	3		
39 <sub>10c</sub>			100				
39 <sub>14a</sub>	?		100	*	1		
39 <sub>14b</sub>			90	*	3		
39 <sub>14c</sub>			100				
39 <sub>2a</sub>	220/86 NW	weathered	96			*	3
39 <sub>2b</sub>			96				
39 <sub>2c</sub>			94				
39 <sub>15a</sub>	068/25 S	bedding	95				
39 <sub>15b</sub>			77				
39 <sub>22a</sub>	039/46 N	bedding	92	*	3		
39 <sub>22b</sub>			90	*	3	*	3
39 <sub>22c</sub>			93	*	3		
39 <sub>24a</sub>	069/61 N	weathered	99	*	3		
39 <sub>24b</sub>			95	*	3		
39 <sub>24c</sub>			95	*	3	*	3
39 <sub>25a</sub>	035/10 S	~ bedding	101	*	3		
39 <sub>25b</sub>			91				
39 <sub>25c</sub>			93			*	3
41 <sub>26a</sub>	273/22 N	bedding	100				
41 <sub>26b</sub>			100				
41 <sub>26c</sub>			95				
41 <sub>25a</sub>	054/11 S	weathered	100	*	2		
41 <sub>25b</sub>			100	*	2		
41 <sub>25c</sub>			101	*	2		
41 <sub>23a</sub>	112/40 W	weathered	95	*	3		
41 <sub>23b</sub>			95				
41 <sub>23c</sub>			96				
41 <sub>22a</sub>	219/85 N	weathered	97				
41 <sub>22b</sub>			101	*	3		
41 <sub>22c</sub>			100				
40 <sub>13a</sub>	030/38 E	weathered	95				
40 <sub>13b</sub>			98				
40 <sub>13c</sub>			92				
40 <sub>14a</sub>	146/26 NW	weathered	99	*	1	*	3
40 <sub>14b</sub>			101				
40 <sub>14c</sub>			100				
40 <sub>11a</sub>	246/74 N	weathered	96				
40 <sub>11b</sub>			98				
40 <sub>11c</sub>			96				

**Table 4.1** Summary of the strain analysis results, showing sample number, datum surface orientation and type, number of grains measured, type and quality of the results obtained.

40 <sub>12a</sub> b c	086/10 N	weathered	100 100 101	*	2		
40 <sub>15a</sub> b c	012/60 N	weathered	74 90 104				
41 <sub>28a</sub> b c	002/47 W	~ bedding	97 96 99	* * *	3 3 3		
40 <sub>2a</sub> b c	066/18 N	~ bedding	100 101 100	*	2		
40 <sub>6a</sub> b c	255/59 NE	~ bedding	95 97 100				
40 <sub>8a</sub> b c	038/59 SE	weathered	95 100 97			*	2
40 <sub>10a</sub> b c	092/45 N	weathered	93 97 95				
40 <sub>16a</sub> b c	056/09 N	weathered	100 99 87	* *	2 2		
41 <sub>27a</sub> b c	140/26 NE	bedding?	99 95 92	* *	3 3		
33 <sub>14a</sub>	083/29 S	bedding	92 (199)	*	3		
33 <sub>18a</sub>	087/22 S	bedding	100 + h	*	3		
33 <sub>48a</sub> b	084/25 S	bedding	100 (263) 91 (196)	*	2		
28 <sub>8a</sub>	109/34 S	bedding	88 (A3) 90 (A4)+h	* *	3 3		
28 <sub>6a</sub>	093/16 S	bedding	114 (157) 100 h				

**Table 4.1 cntd** (see previous caption)

The centre-to-centre method used here was the Fry Method (Fry, 1979), mainly due to its rapid and relatively easy application (made even quicker with the aid of the computer program INSTRAIN 2.5), particularly given the speculative and uncertain outcome of the method as outlined above. The method is described fully in Appendix 2, along with a brief discussion of the other features of the program INSTRAIN 2.5.

#### 4.3.1.2 Results

The results are summarised in table 4.1. The table, and selected plots showing the range of patterns produced (figures 4.5, 4.6, 4.7), clearly show that none of the plots prove totally unambiguous. Even the best plots may only show a pattern in one section and apparently do not record any strain in the other two sections. Furthermore, there does not appear to be a strict correlation between the patterns produced and areas of expected high strain verses low strain. For example, in Scargill Hills Outlier it can be noted that although some of the samples producing the best ellipses do occur close to Mt Alexander and Maxwellton Faults, but other samples from these localities show very little or no strain (compare table 4.1 and figure 4.5). Therefore, the lack of good results from the clearly highly strained rocks of Scargill Hills Outlier (and partly from Moores Hill Anticline) lead to the abandonment of further measurements from other localities in the study area.

#### 4.3.1.3 Conclusions

Due to the above anomalous results, it is concluded that the Fry Method alone can not be applied to rocks in which the grains do not form a packed aggregate, regardless of the magnitude of strain. Some quantification may be possible if the very best plots obtained could be compared to results obtained from other strain indicators such as deformed fossils if these could be found, and the relationship between twinning and the c-axis in calcite crystals (here not being able to be evaluated due to the high arenite content and a relatively small grain size).

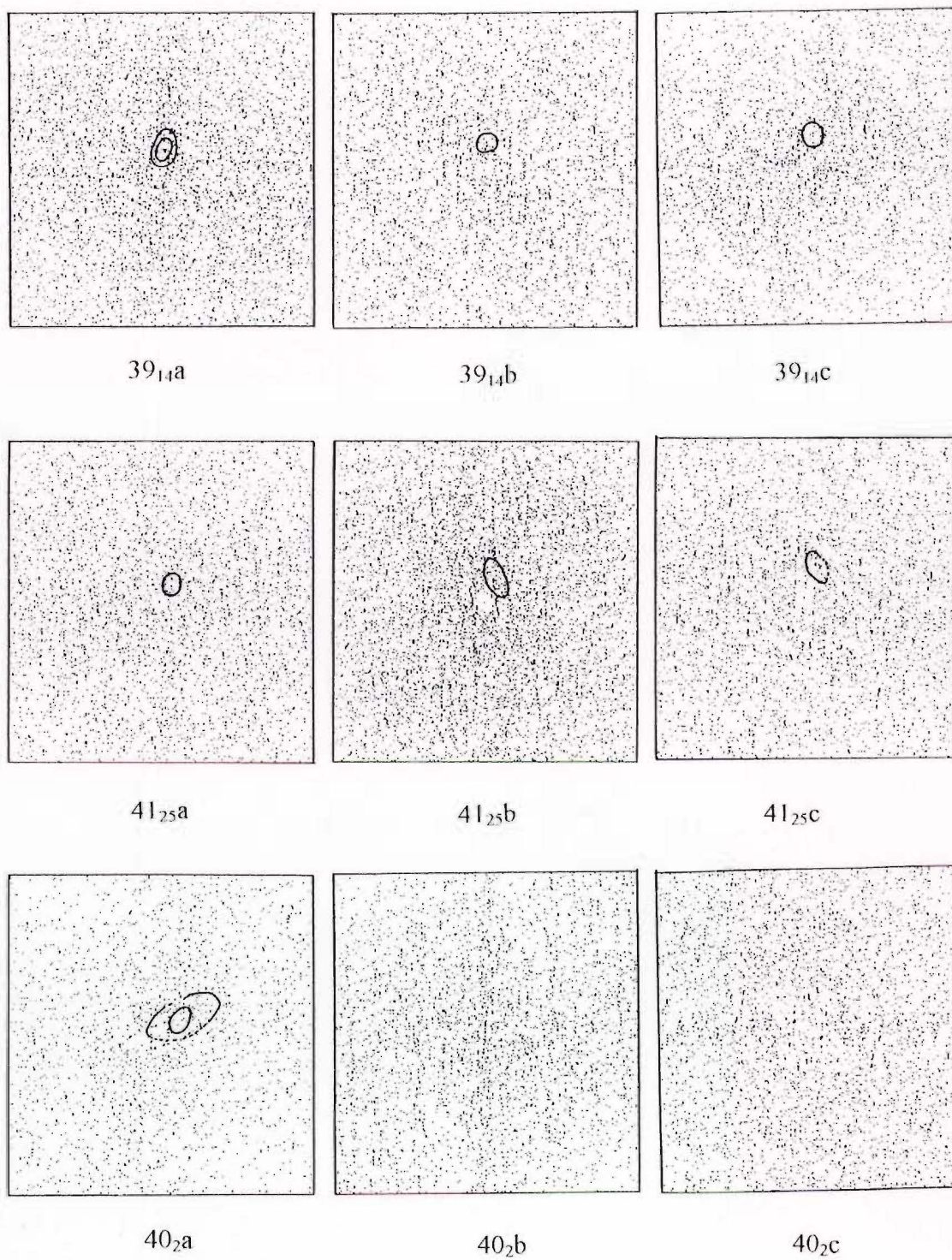


**Figure 4.5** The “best” strain analysis results from Scargill Hills Outlier (see figure 4.4 for locations).



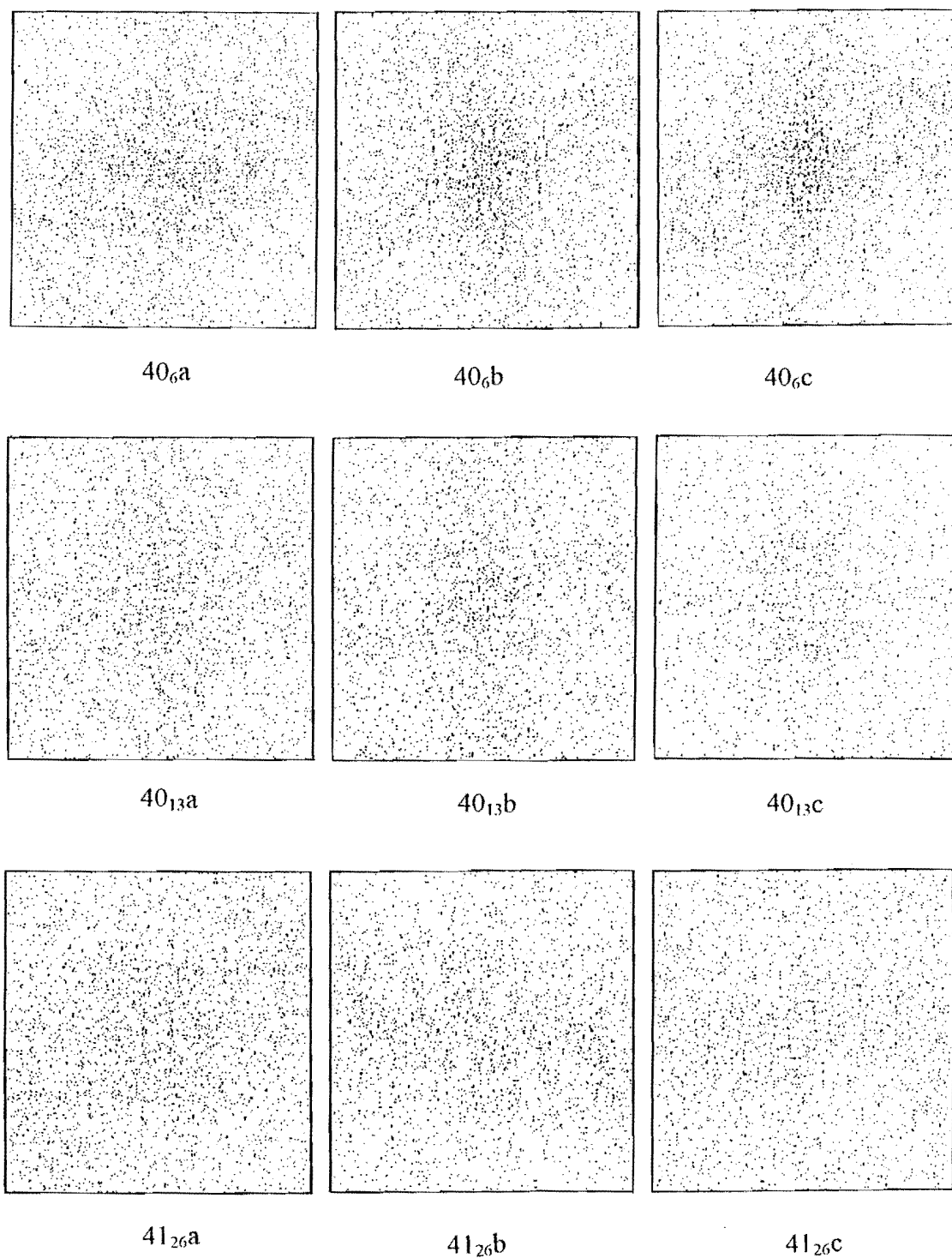


**Figure 4.6** The “worst” strain analysis results from Scargill Hills Outlier (see figure 4.4 for locations).



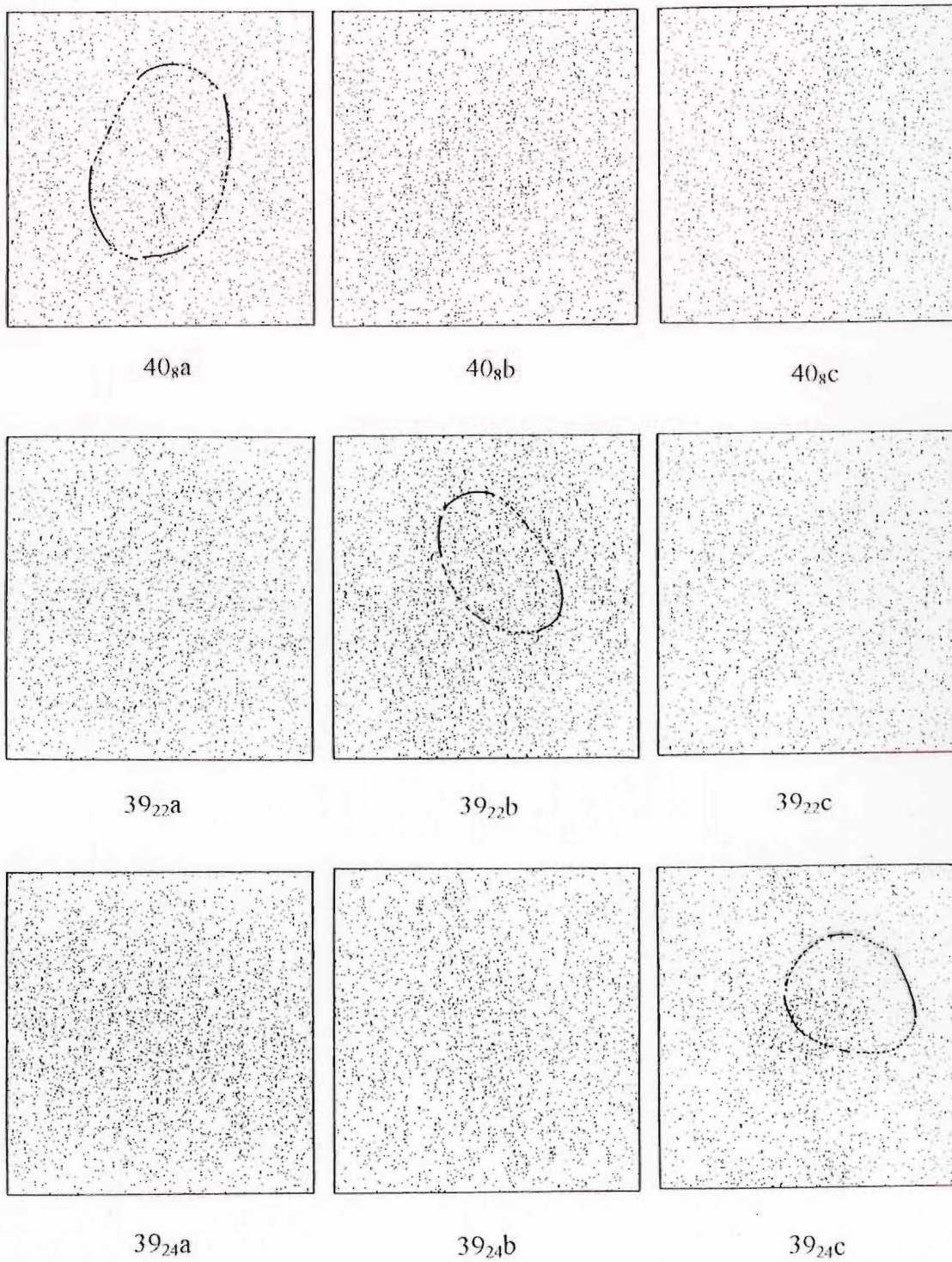


**Figure 4.7** Strain analysis results that contain large ellipses from Scargill Hills Outlier (see figure 4.4 for locations).

Potentially, rocks containing aggregates of objects with a known and easily measured shape, can have their strain characteristics relatively easily and rapidly evaluated using the computer program INSTRAIN2.5 and a standard digitiser.

#### **4.3.2 Small-scale structures**

Small, or meso-scale brittle or semi-brittle structures such as faults, veins, stylolites and joints have been found to be useful indicators of the timing and kinematics of deformation in mildly deformed rocks (eg. Engelder and Geiser, 1980, Buchner, 1981, Segal and Pollard, 1983, Nicol and Campbell, 1990, Zhao and Johnson, 1992). Such studies of stratigraphically equivalent units to those in this study have been described previously in north Canterbury (Syme, 1991, Nicol, 1992 and Mould, 1992).

Small-scale structures in the cover rocks are not abundant, largely confined to the more resistant units such as the Weka Pass Stone Member of the Omihi Formation and the Amuri Limestone. However, the very sandy nature of the Weka Pass Stone Member in this area means that it has not fractured to the degree that it has in other regions, and although the more micritic Amuri Limestone is clearly fractured to a higher degree, is absent for large parts of this area. For this reason, and because of the very small and widely dispersed outcrops of cover rocks in the area, the small-scale structures have only been noted in a qualitative sense, with only one locality (a quarry into Amuri Limestone, grid reference 812 042) treated in the same quantitative manner as the basement rocks. This locality was first described by Nicol (1991) and revisited during integration of the boundaries of adjacent mapping.

Cover rock small-scale structures tend to fall into one of three categories: variously oriented joints (the most abundant), stylolitic pressure solution seams, and small-scale faults.

##### **4.3.2.1 Joints**

The definition of the term “joint” used here is that of Hancock (1985). That is, a joint is a field term for a barren, closed fracture on which there is no measurable slip or dilation

at the scale of observation; if any mineral infilling occurs it is termed a vein, if any measurable motion occurs it is termed a fault. Joints form the most abundant fracturing of the Weka Pass Stone Member, and form two distinct groups:

#### *Subvertical orthogonal joints*

Two sets of systematic, subvertical joints can clearly be recognised in the strike-ridges of Weka Pass Stone Member in the study area, striking perpendicular to each other.

The first set strikes parallel to the strike of the bedding (see figure 2.3). The generally two-dimensional exposure of the strike ridges often means that these are under-sampled relative to other sets of fractures, most measurements only possible from gullies cut orthogonally through the strike ridges. These largely extensional joints subparallel the axial plane of the major folds in the study area and therefore can be considered longitudinal joints (Ramsay and Huber, 1987b).

The second set strikes orthogonal to both the above joints and to bedding. The spacing of these largely extensional fractures appears to be highly dependent on lithology; they are very closely spaced in the micritic, Amuri Limestone (5-10 cm) and much further apart in the slightly less resistant, sandy Weka Pass Stone Member (1-5 m). As a result of their wide spacing in the Weka Pass Stone Member, many of the joints have been exploited by drainage from the higher ranges, contributing to the regular spacing of the gullies cut through a number of the strike ridges (eg. along the southern side of Mt Alexander Anticline and the western end of Lowry Peaks Anticline).

These joints have formed largely perpendicular to the axial planes of the major folds, thus forming cross-joints (Ramsay and Huber, 1987b), but there could be some overprinting due to the NNW-SSE trending cross-folding (and therefore some could have actually formed as longitudinal joints). Likewise, the set formed perpendicular to bedding at the western end of the Mt Alexander and Lowry Peaks Anticlines, where, due to secondary deformation effects the beds themselves largely strike normal to the major structures, the joints are most likely to actually represent longitudinal joints, which is perhaps evidenced by their greater abundance there.

### *Low angle joints*

Another set of joints can be observed at low angles to bedding (figure 4.8). These again can be divided into two sets but appear to have formed symmetrically about the bedding plane rather than having formed strictly orthogonal to each other. Both joints in the pair appear to have developed geologically synchronously; cross-cutting relationships are highly variable within and between localities, and locally open to form orthogonal sets. These joints occur in both the Amuri Limestone and the overlying Weka Pass Stone Member and are cut by the subvertical joints described above.

Nicol (1992) described a similar set of joints from the Waipara-Weka Pass region. Evidence such as the consistent angular relationship to bedding, a somewhat uniform orientation (when the effects of bedding were removed), and observations of the relative age of the joints to the Middle to Late Oligocene unconformity, were used to suggest formation during the Middle Oligocene deformation event described in Chapter 2.

### *Summary*

A diagram showing the relationship of the above two groups of joints to the major structures in the area is shown in figure 4.9.

#### **4.3.2.2 Pressure Solution seams**

Pressure solution seams represent fractures subjected to pressure solution, the directions of the resulting stylolitic “teeth” considered to parallel the shortening direction (Hancock, 1985). Solution seams are abundant in the tuffaceous bands of the Weka Pass Stone Member of the Omihi Formation (see figure 2.3). Seams developed parallel to bedding are the most abundant and serve to give the tuffaceous bands a rather platy appearance. A large seam apparently formed at the upper contact between the rather crystalline tuffaceous bands and the less resistant, sandy Weka Pass Stone giving the bands a very flat upper surface. Less abundant are vertical seams, but where they do occur they serve to give the tuffaceous bands a rather blocky appearance, similar to the





**Figure 4.8** Low angle joints developed in the Weka Pass Stone Member of the Omihi Formation (including the tuffaceous bands).

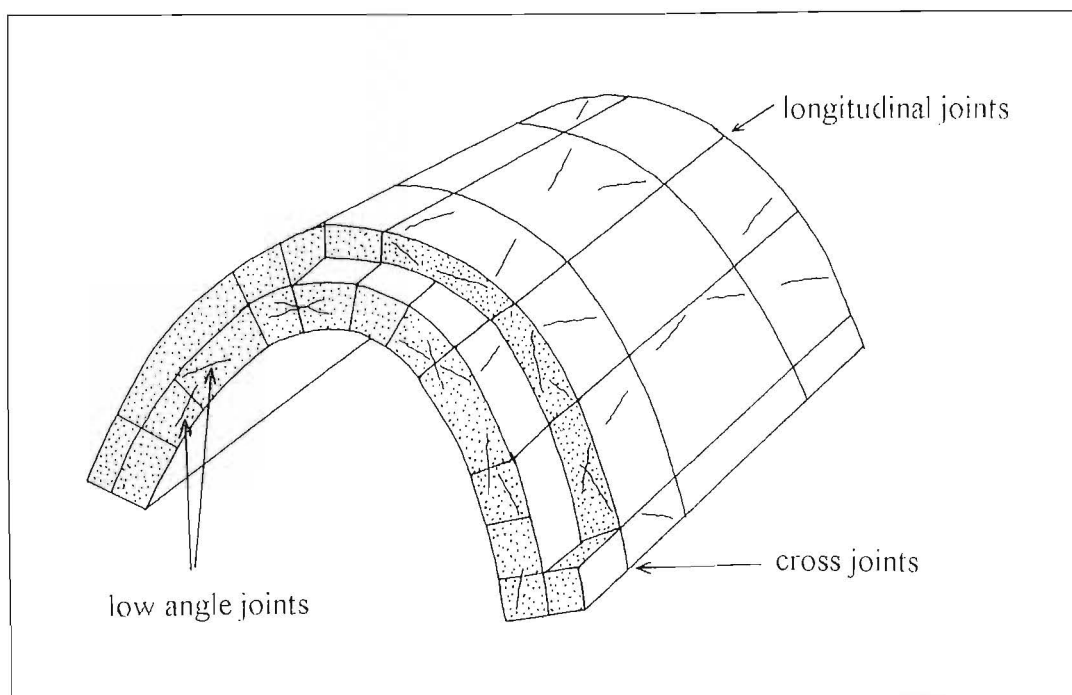


**Figure 4.9** Summary diagram of the relationships of joints to fold geometry. Joint surfaces are stippled, bedding planes are not.

typical fracturing of the Amuri Limestone. The restriction of the pressure solution seams to the tuffaceous bands in the Omihi Formation and their largely parallel attitude to bedding suggests they are likely to have formed due to loading by the overlying sediments, prior to the major uplift events described here.

#### **4.3.2.3 Small-scale faults**

Small-scale faults can be observed in a number of the units, particularly offsetting competent units such as the Weka Pass Stone Member of the Omihi Formation, the Amuri Limestone and limestone beds in the Mt Brown Formation, but can also be found in the less competent Homebush Sandstone Formation, where a leaching of calcite and/or limonite formed on the surface of the faults often causes their selective preservation. Faults in this category range from small scale offset of beds at an outcrop scale to the smaller of the major faults shown on map 1 (including the N-S trending structures mapped at the western end of the field area) and are thought to largely represent secondary faulting reflecting the movement on the larger structures. With the exception of faulting of the Amuri Limestone at Waikari Quarry (discussed below), no attempt has been made to study these in detail due to their general scarcity, except to note in a qualitative sense these faults tend to increase in abundance towards the major faults.

#### **4.3.3 Stress tensor analysis**

A stress tensor analysis was performed on the abundant fracturing noted in a recently-excavated part of Waikari Quarry, an along-strike pit cut into the Amuri Limestone forming the western limb of Limeworks Syncline (figure 4.10). This study was conducted as a comparison to the tensor configurations produced by the basement rocks and the only site at the western end of the study area. The methods were identical to those applied to the basement rocks, and with the exception of the coefficient of friction (here 0.532 from available experimental data), used the same parameters.

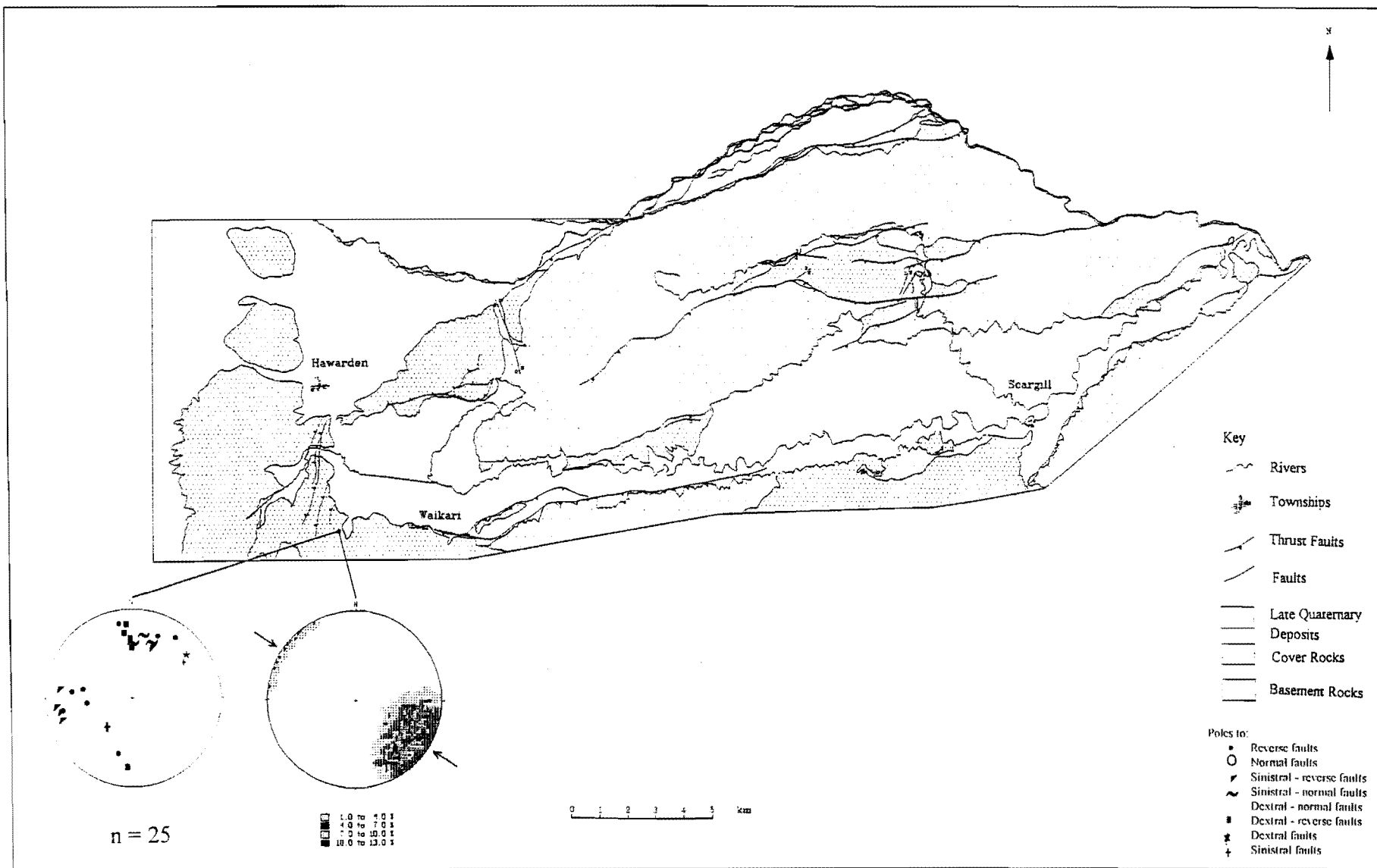


**Figure 4.10** Location map, fault plane data, interpreted  $\sigma_1$  results (density stereoplot) for the Waikari Quarry stress analysis site

#### 4.3.3.1 Results

The stress tensor configurations are shown on density stereoplots in figure 4.10, with the raw data and the interpreted  $\sigma_1$  plot displayed on figure 4.11.

A clear NW-SE oriented compression is implied by the plots for  $\sigma_1$ , but  $\sigma_2$  and  $\sigma_3$  are nearly coincident, distributed around a common great circle girdle. When the raw data plots are examined it is clear that the majority of the faults measured at Waikari Quarry were in fact reverse faults, but occur in two distinct populations (N-S and W-E trending). A series of moderate to shallow-dipping thrust faults can be observed in the walls of the N-S trending along-strike pit, and are notable in that they have the same orientation as the Moores Hill Fault, which has apparently terminated east of there. Also abundant are a number of N-S fractures which are likely to have affinities to the N-S trending faults mapped immediately to the west.

Furthermore, those oriented N-S appear to be accommodating a large component of oblique, sinistral strike-slip motion, while reverse faults oriented W-E have accommodated a component of dextral strike-slip motion. The plots of  $\sigma_2$  and  $\sigma_3$  are therefore interpreted to be currently reflecting strain partitioning of a NW-SE oriented compression into two directions of oblique strike-slip motion at right angles. The vertical portions of  $\sigma_2$ , and the NE-SW trending, sub-horizontal portions of  $\sigma_3$  therefore reflecting the significant strike-slip component on two sets of structures that have formed in close affinity with larger-scale structures on either side.

#### 4.3.3.2 Conclusions

While the predominant faulting direction in the surrounding rocks is trending N-S, the small-scale faults noted in Waikari Quarry were trending in two orientations (N-S and W-E). The result of NW-SE oriented compression was oblique motion on the largely reverse faults, sinistral for the faults oriented N-S and dextral for those oriented W-E. It is therefore likely that the N-S and W-E trending faults were formed during earlier events associated with the eastward-verging structures to the west and the northward-verging Moores Hill Fault to the east.



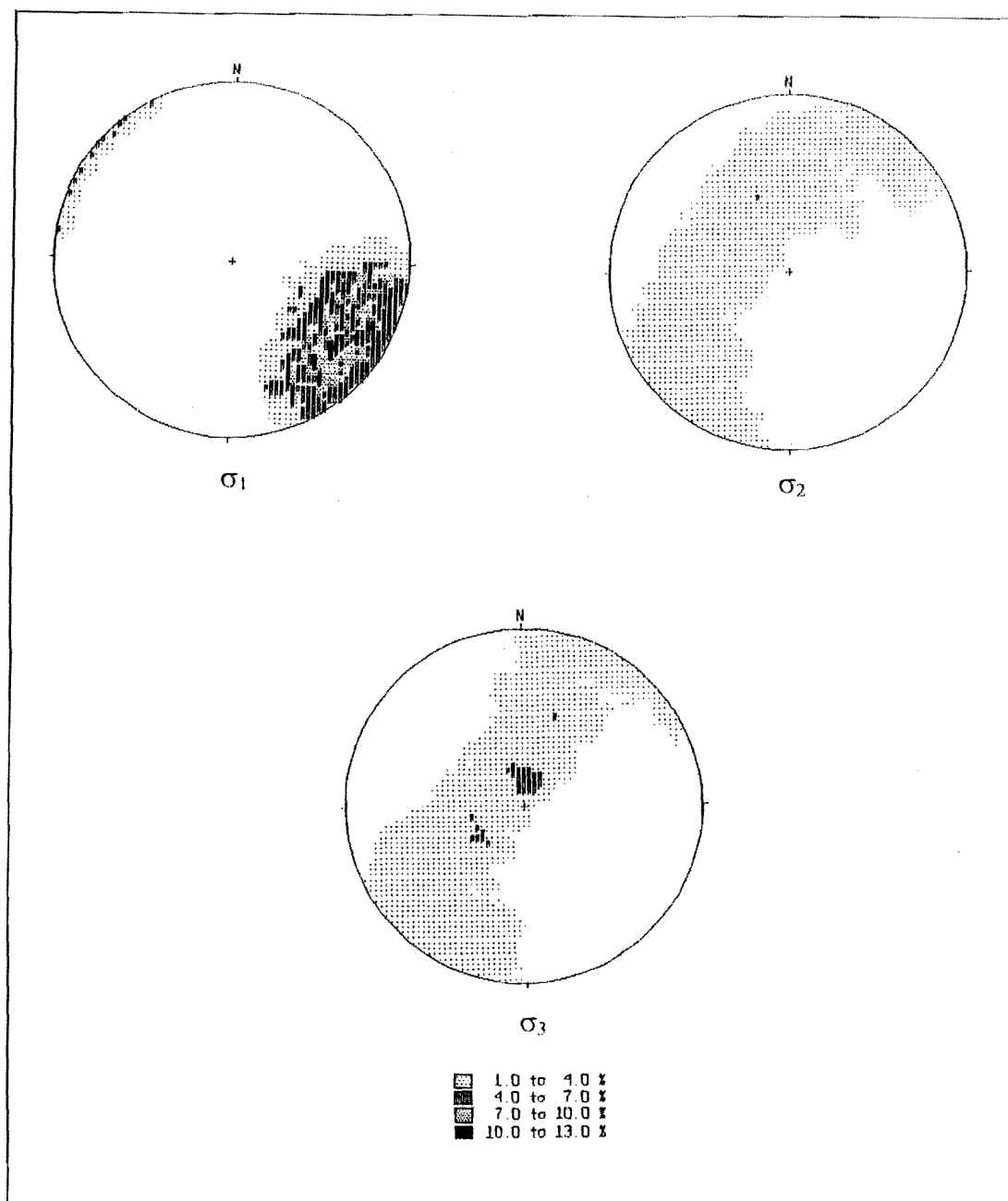


**Figure 4.11** Full set of stress tensor analysis results for the Waikari Quarry site, displayed as density stereoplots of  $\sigma_1$ ,  $\sigma_2$  and  $\sigma_3$ .

## 4.4 CONCLUSIONS

The results of the study of mesoscopic deformation within the basement and cover rocks were highly variable. The basement and the cover rocks have generally responded differently to the major folding effects; the former by triboplastic deformation, utilising the large number of pre-existing small-scale faults; the latter largely by ductile bending (possibly accompanied by bed-over-bed slip, both between and within the more resistant units), although the more resistant units also contain joints and small-scale faults that apparently reflect the folding motion. Both the basement and the cover rocks contain shear zones of faulting on small-scale faults of a variety of orientations as they approach the positions of the major faults.

A large component of internal deformation of the component fault blocks was inferred from both the description of the structures in Chapter 3 and the stress tensor analysis, the very poor sorting of the grains in the Weka Pass Stone Member meant that strain measurement using the Fry Method failed to provide a semi-quantitative measure of this.

The detailed study of the brittle structures in close proximity to the major faults however, was found to be useful in terms of kinematics indicators and prompted the following conclusions:

- i) Many of the faults in the study area appear to have been affected by localised range-front collapse, and gravitational spreading effects, a casualty of their thrust fault nature.
- ii) Faulting at a mesoscopic scale does not exclusively occur on faults oriented WSW- ENE to SW-NE, instead a wide variety of fault orientations appear to be accommodating a large component of oblique motion, thought to reflect the presence of pre-existing disconformities and defects of a wide variety of orientations.
- iii) The above also occurs on a macroscopic scale, the obliquity of faults such as the N-S trending faults in western portions of the area and Moores Hill Fault to the regional compression direction creating a large component of strike-slip motion, reflected in two populations of stress tensor orientations.
- iv) Axial compression appears to be characterising shortening on a number of fault blocks, reflecting W-E compression by cross-folding.

- v) Anomalous stress tensor configurations between localities cannot be easily resolved, in particular Mt Alexander Fault records a NE-SW oriented horizontal principal compression that is at right angles to that suggested by the Hurunui Bluff Road and Waikari Quarry localities and other localities in north Canterbury.

The latter conclusion is discussed further in following chapters.

## STRUCTURAL MODEL

### 5.1 INTRODUCTION

In Chapter 3 it was proposed that the major range-bounding faults in the Lowry Peaks Range - Waikari Valley district could be considered to form thrust faults belonging to one of three major fault members of an imbricate thrust system. Furthermore, the majority of the faults were considered to possess an associated major anticline on their upthrown side (corresponding to the major ranges, and predominantly composed of basement rocks) and at least a partially-developed syncline on their down-thrown side (generally corresponding to structural lows such as valleys or depressions in the major ranges, and containing the majority of the cover rocks).

The purpose of this discussion is to examine the typical imbricate thrust system features in three dimensions, particularly in terms of geometry, as proposed in figure 5.1 and the cross sections, (following map 1) and then to discuss possible fundamental reasons for the W-E trend of many of the structures, and the likely links of the structures mapped here to those mapped by Nicol (1991) to the SW. No relevant subsurface or geophysical data of the area exists (apart from the very generalised gravity data of Dibble, unpubl.) which can provide an aid in constraining the geometry of structures at depth, therefore, the model proposed here is based entirely on inferences from surface mapping.

### 5.2 IMBRICATE THRUST SYSTEM MODEL

#### 5.2.1 Thrust Faults

##### 5.2.1.1 Cross-sectional shape

At depth, the thrust faults are generally considered to possess a listric form, locally steepening to reverse faults near the surface. The possibility that the faults possess a ramp-flat geometry in their upper reaches cannot be ruled out, particularly where the

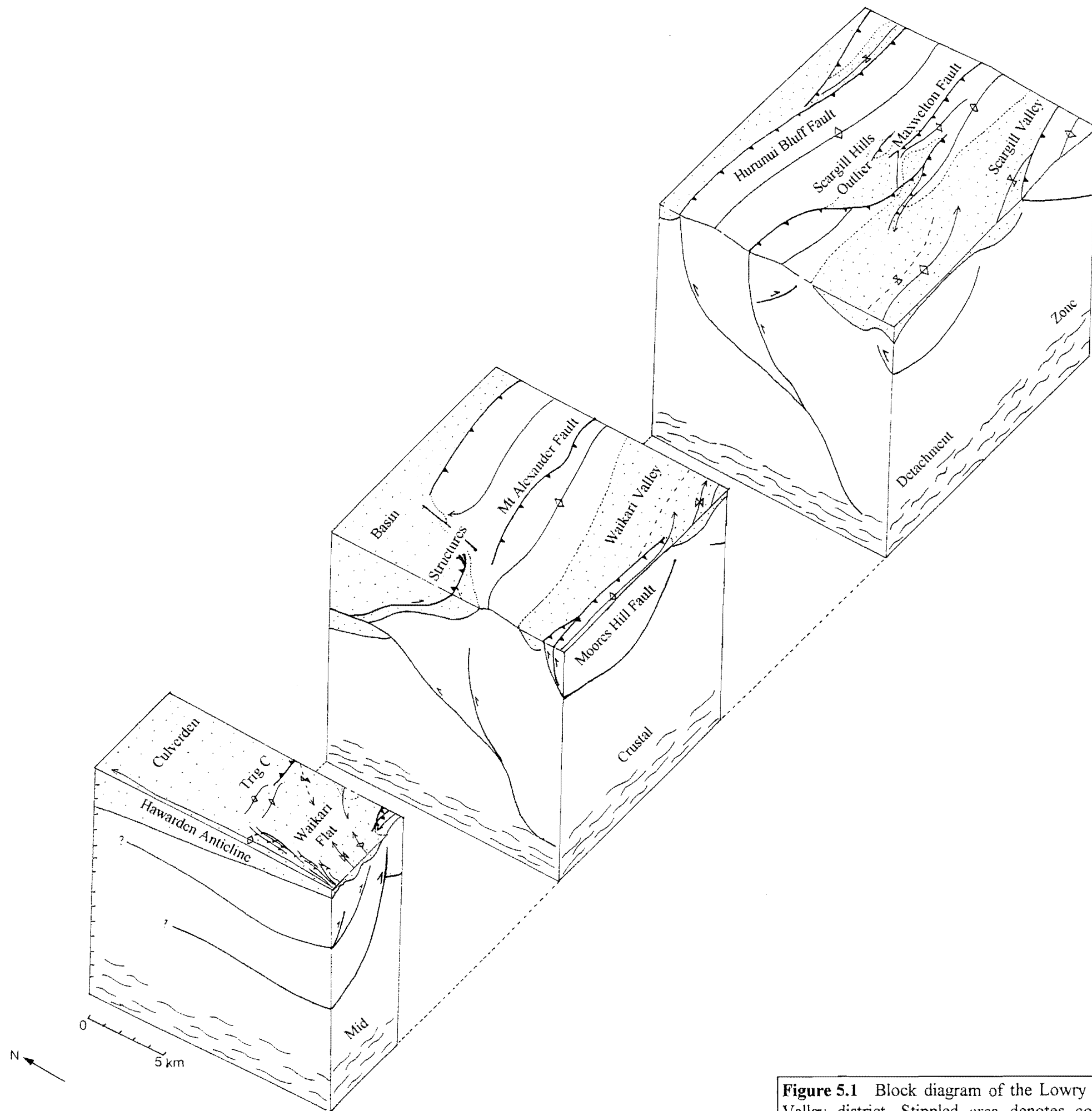


**Figure 5.1** Block diagram of the Lowry Peaks Range - Waikari Valley district. Stippled area denotes cover rocks, blank area, basement rocks.

faults pass from relatively resistant basement rocks to softer cover rocks, thought to be one of the major cause for a sudden shallowing of the fault plane in (eg. Rich, 1934, Douglas, 1950, Butler, 1982). However, the relatively thin cover rock sequence in this area (generally less than 500m), and the inclusion of a number of more resistant units within the sequence along which no evidence of detachment has been drawn, means that a listric form is preferred. Observations in other areas to the west and SW show that many faults are steep near the surface. This also has significant bearing on the likely folding style.

A feature of the cross sections is the presence of a number of back-thrusts. Evidence for back-thrusting was mainly given by major anomalies in the structure contouring of the basement-cover rock unconformity surface; but also, a significant number of mesoscopic-scale back-thrusts were noted during the data collection for the stress tensor analysis, and at least the Mt Alexander Road locality showed evidence from the stress tensor configurations produced for a late-stage overprinting by back-thrusting. The majority of mesoscopic scale back-thrusts were observed to be typically steep, but this is likely to be a function of a typically listric form, with some minor influence due to the generally sub-vertical bedding in basement, particularly where mudstones and the more resistant sandstones alternate. Above each of the major back-thrusts a secondary anticline has been formed, but are considered to be of minor importance in terms of overall kinematics.

#### 5.2.1.2 Cross-sectional spacing

In general, the spacing of the faults is rather regular, attributed to factors such as lithology, the magnitude of strain, probably depth to the original detachment and the presence of pre-existing disconformities.

The influence of pre-existing basement disconformities has been suggested for the Moores Hill Fault and eastern portions of Mt Alexander Fault, but it is possible that the latter may be attributed to an earlier phase of NE-SW to N-S horizontal compression (chapter 4). Nevertheless, the net result is an increase in cross-sectional spacing between the structures of the Kaiwara Fault System and the Mt Alexander - Maxwellton Fault

System, causing Waikari Valley to possess a rhomb-shape, with a maximum width at approximately Eastcott homestead.

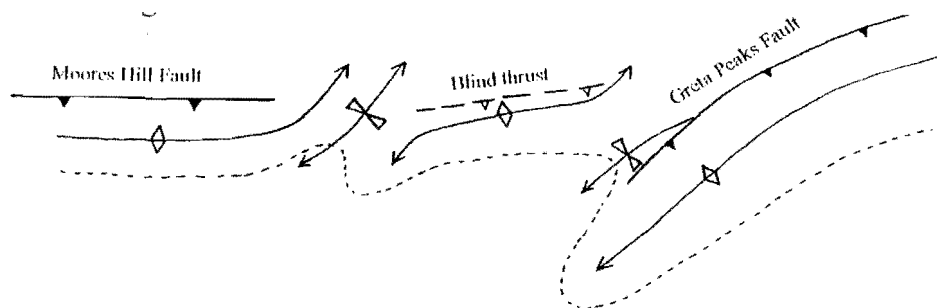
### 5.2.1.3 Spatial geometry and mechanisms of displacement transfer

It has been well documented in Chapter 3 that each of the major thrust systems are not characterised by a single continuous thrust fault, instead being comprised of a number of short, overlapping faults, the zone of “displacement transfer” (Dahlstrom, 1970) often proving to be rather complex. Similar observations made in large thrust belts such as the Wyoming-Idaho Thrust Belt have lead to the recognition of a number of characteristic mechanisms of displacement transfer, both from field studies (eg. Dahlstrom, 1970, Brown and Spang, 1978, O’Keefe and Stearns, 1982, House and Gray, 1982, Couzens and Dunne, 1994) and from laboratory experiments (eg. Gardner and Spang, 1973, House and Gray, 1982, Liu and Dixon, 1990 and 1991, Dixon and Tirrul, 1991, Dixon and Liu, 1992), namely:

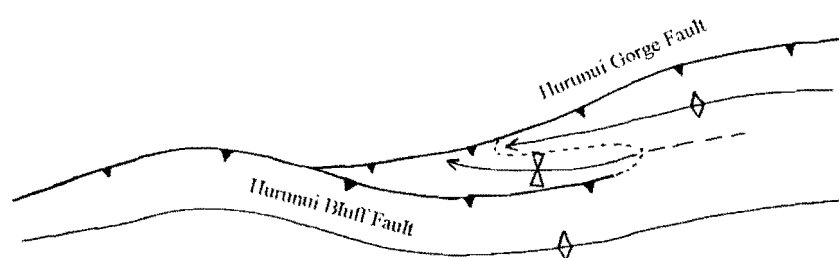
- i) the development of en-echelon folds
- ii) stepping of motion onto a splay
- iii) transfer of motion between two segments along a tear fault

In this area, displacement transfer is achieved by all of the above mechanisms, with a variation on mechanism ii) shown by transfer of motion from Mt Alexander to Maxwellton Faults on a lateral ramp structure, the Transfer Fault. Motion on the tear fault is also considered to contain a component of eastwards-directed thrusting, rather than true strike-slip motion on a sub-vertical fault. These are summarised in figure 5.2.

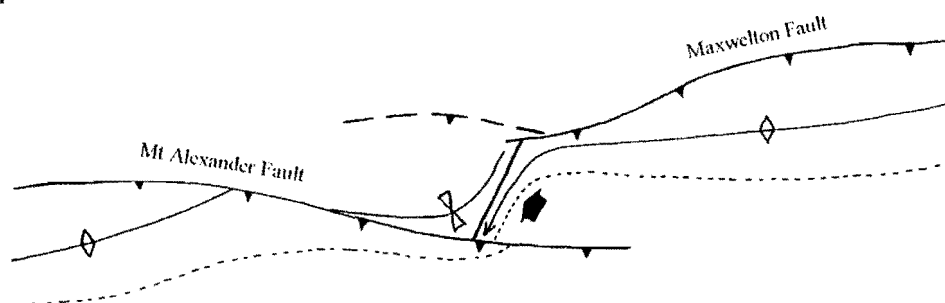
It is interesting to speculate as to the cause of displacement transfer in the localities mentioned above. It has already been mentioned on a number of occasions that a significant change in strike appears to accompany many of the step-overs, motion on which may then be the most easily achieved on two separate segments, rather than a single continuous fault (ie. particularly for mechanisms i and ii). Caution must be heeded here in that the observation of two distinct segments may be a factor of either: i) structural level and/or ii) time. That is, each of the segments in the fault system are considered to link into a single fault at depth, so that observation of either one or two segments may be merely a factor of erosional depth. The other factor influencing their segmented nature may be time ie. particularly important for cases where the fault is



### b) Splaying



### c) Ramp structure



### d) Tear faulting

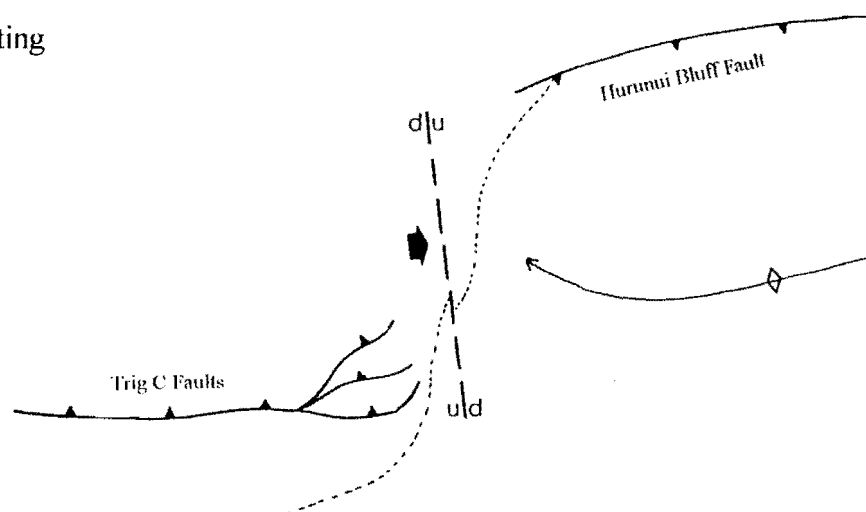


**Figure 5.2** Schematic summary diagram (not drawn to scale) of the mechanisms of displacement transfer between major thrust faults in the study area.



folded as may be the case for some faults here (that is, differently aged faults may be uplifted beside each other). Furthermore, it is likely that many faults are characteristically very segmented when they are geologically very “young” and that through time their step-overs and overlaps are smoothed out and a through-going fault developed. The smoothing may be either due to an increased component of motion transferring to faults more optimally oriented and/or continued faulting has meant that deeper levels of the fault are thrust up above the base level of erosion. Therefore, comparison between faults should consider relative age.

The reason for the transfer of motion by tear faulting between Hurunui Bluff Fault structures and the Trig C Fault structures (ie. mechanism iii), is clearly a function of the apparent change in facing direction between the two structures, suggested in Chapter 3 to be the result of out-of-sequence thrusting off the plunging western end of Hurunui Bluff Fault, the details and reasons for which are discussed in section 5.4.

#### 5.2.1.4 Basal decollement

The faults in figure 5.1 have been drawn to converge onto a single, sub-horizontal basal decollement at depth. Norris et al (1990) inferred a mid to lower crustal detachment zone beneath the Otago Region to the south from their study of wedge mechanics in relation to uplift along the Alpine Fault. Recently, such a detachment has also been proposed beneath north Canterbury (Nicol, 1991, Mould, 1992, Cowan, 1992, Nicol and Wise, 1992, Reyners and Cowan, 1993). Field evidence such as the limited lateral extent of the majority of faults in north Canterbury, combined with their apparent imbricate thrust nature (eg. Nicol, 1991, Mould, 1992, this study); paleomagnetic evidence for rotation of crustal blocks in the Marlborough Fault Zone Region (eg. Lamb, 1988); and the apparent presence of a ductile, or aseismic zone at 12-17 km depth from a microseismic study of the north Canterbury Region (Cowan, 1992, Reyners and Cowan, 1993) all suggest that a mid to lower crustal detachment is serving to transfer motion between the west-dipping Hikurangi Trench and the east-dipping Puysegur Trough (see figure 1.1). Reyners and Cowan (1993) consider that the lower crust consists of oceanic crust on which the Torlesse Supergroup was deposited, which is continuing to be subducted beneath southern parts of north Canterbury, while the upper plate is fixed as the eastern extension of the Chatham Rise.

Such a model allows faulting at a variety of orientations, as is suggested by a number of the fault orientations and the stress tensor analysis results presented in Chapter 4. It is probable that the consequence of thin skinned upper crustal imbricate thrusting onto a mid crustal decollement is accomplished on a more complex series of intermediate amalgamation of splays, ramps and detachments than is suggested in figure 5.1.

#### **5.2.1.5 Displacement**

The displacement on the majority of faults in the region has not been evaluated because of the lack of marker beds on both sides, as well as the poor definition of the fault trace in nearly all cases. Some indications of relative throw can be obtained (table 5.1), by comparing the relative amounts of faulting through the folds formed on the upper and lower plates (figure 5.3). These are discussed further in section 5.2.2.2.

#### **5.2.2 Fault-related folds**

With the possible exception of Moores Hill Syncline, all of the folds in the cover rocks appear to have been formed in association with movement on the major thrust faults. The importance of folding in thrust systems has long since been recognised (eg. Rogers and Rogers, 1894, Willis, 1894), but by the early to mid 1980's, most thrust-related folds were considered to belong to one of three types:

- i) Fault-bend folds - folds formed in the hanging wall as the result of movement over a footwall ramp ( Suppe, 1983) (also called ramp anticlines or trailing-edge folds)
- ii) Fault-propagation folds - folds formed at the tip of a propagating thrust fault (Suppe and Medwedeff, 1984) (also called ductile bead folds, leading edge folds, blind-thrust anticlines, decollement thrusts, tip anticlines or break-thrust folds).
- iii) Detachment Folds - folds formed above a bedding plane detachment (Jamison, 1987) (also called intraplate folds or lift-off folds)

and are shown in figure 5.4.

Relative amount of throw	Fault name	Fault System
Largest	Greta Peaks Fault	Kaiwara
	Moore's Hill Fault	Kaiwara
	Mt Alexander Fault	Mt Alexander - Maxwellton
	Maxwelton Fault	Mt Alexander - Maxwellton
	Scargill Creek Fault	Mt Alexander - Maxwellton
	Hurunui Gorge Fault	Lowry Peaks
Smallest	Hurunui Gorge Fault	Lowry Peaks

**Table 5.1** Relative amounts of throw on the major faults of the Lowry Peaks Range - Waikari Valley district, as estimated from the cross sections, and ignoring deformation by folding.

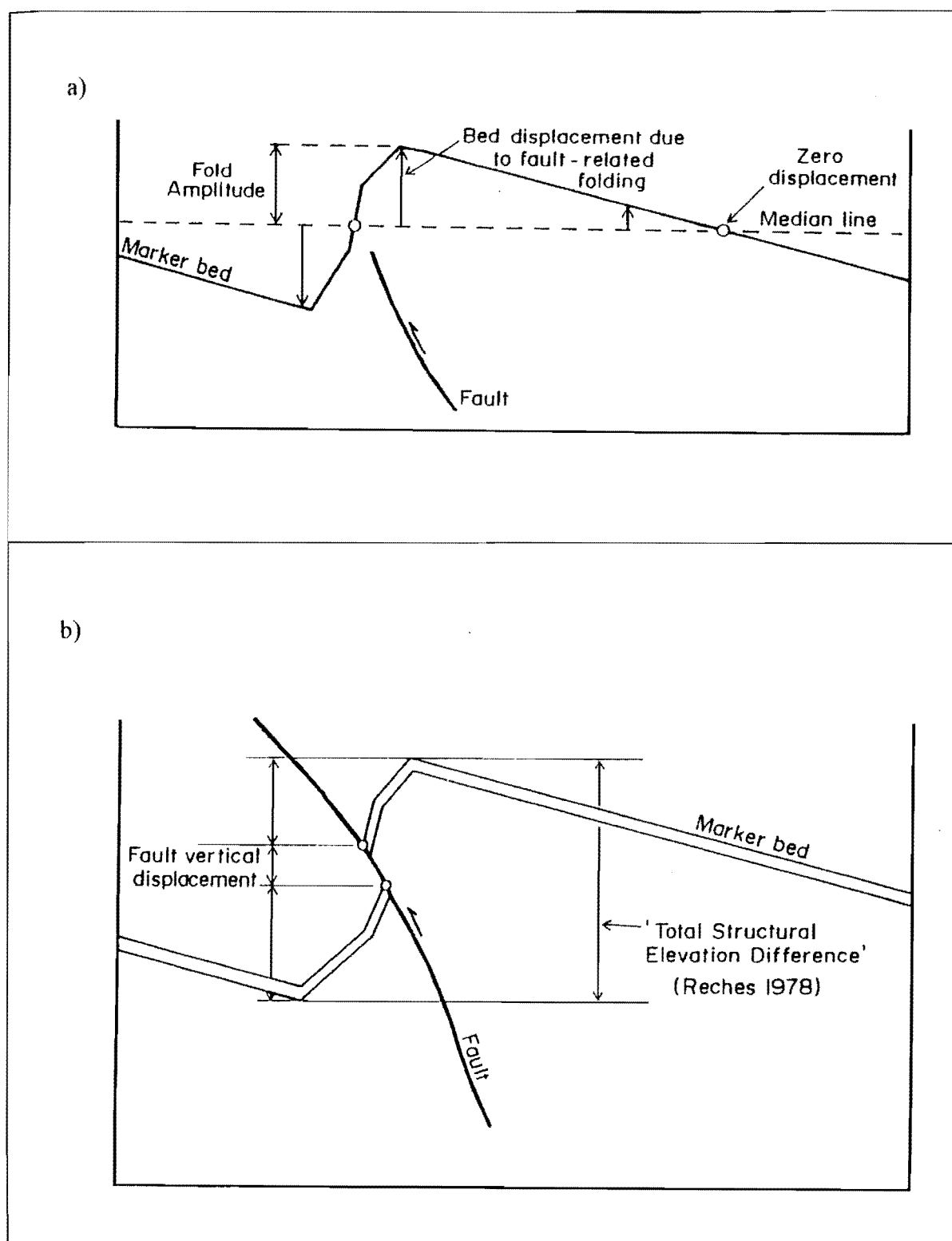


**Figure 5.3** Measurement of fault-related fold displacement by faulting and folding: a) the fault-related fold displacement can be measured as the fold amplitude from the median line and b) the total displacement after faulting (the total structural elevation difference) can be measured as  $2 \times$  fold amplitude (a) + the vertical fault displacement. (From Nicol, 1991).

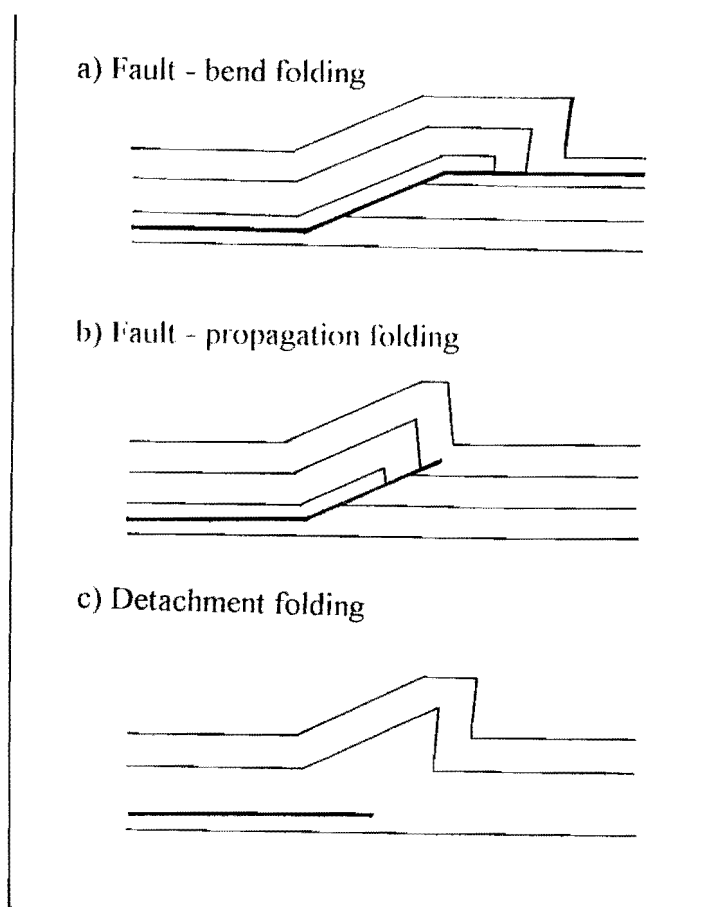


**Figure 5.4** The three end-member types of folding associated with thrust faults. (From Jamison, 1992).

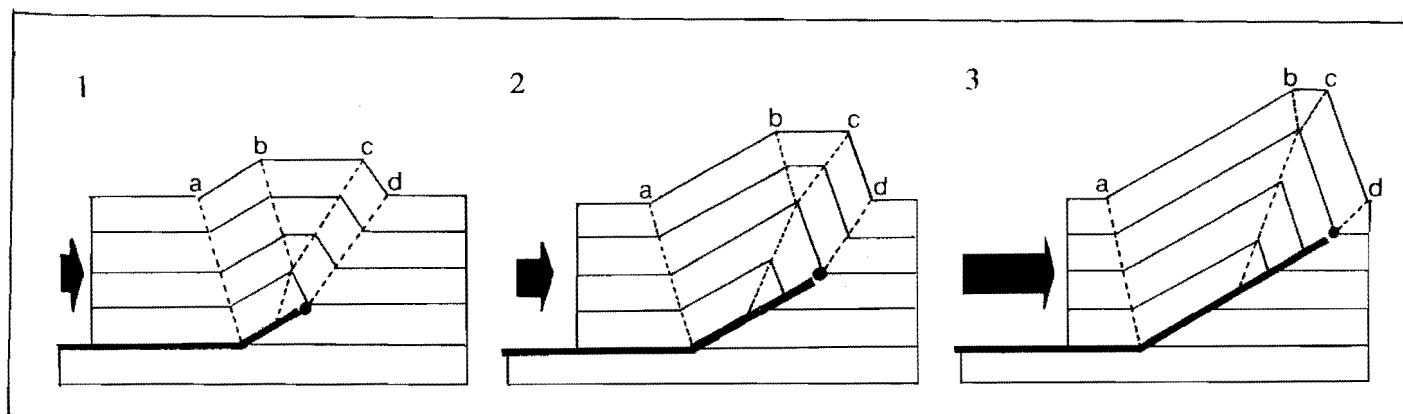


**Figure 5.5** The development of fault propagation folds by kink-band migration (simple step-up, constant thickness model). (From Mosar and Suppe, 1992).

The majority of the folds in this area have been truncated through their inflection point and therefore cannot be fault-bend folds (furthermore it has already been concluded that the faults are not likely to possess a fault ramp geometry), and the clear development of a syncline beneath the faults dismisses the possibility of detachment folding. Hence it is likely that all of the folds associated with faults in this study area have formed as fault-propagation folds, the characteristic features of which are discussed below.

#### 5.2.2.1 Cross-sectional shape

Folds that are well defined by a capping of Weka Pass Stone Member in this study area have been noted to possess a very angular cross-sectional shape, characterised by a very long, flat shallow limb and two very short, moderate to steep limbs, hence possessing a type of kink-band geometry. Although this is a typical feature of fault-propagation folds, (the original definition of the folds proposing that they formed by kink-band migration as the fault propagated into successively higher layers of a mullet-layered sequence, Suppe and Medwedeff, 1984, Suppe, 1985, Jamison, 1987, Suppe, Chou and Hook, 1992, figure 5.5), it is suggested that in this area, the cover rock portion of the sequence that is actually being folded is so thin that the effects of kink-band migration producing a kink-band shape are likely to be rather negligible. Instead, it is suggested that the angular shape is a function of the presence of resistant limestone beds (evidence for their rather brittle deformation was discussed in Chapter 4).

Furthermore, the kink-band migration model has been questioned recently by a number of workers, largely based on observations of a lack of evidence for strain throughout the entire sequence (which should be present if each layer is successively folded in turn in a caterpillar-type fashion). Instead some workers have proposed an episode of folding by buckling in a fixed position (still related to fault movement at depth however), until some point where the folds lock up, when strain is released by propagation of the fault through its inflection point (Mitra, 1990, Liu and Dixon, 1990, Dixon and Tirrul, 1991, Dixon and Liu, 1992, Fischer et al, 1992, Fisher and Anastasio, 1992).

One of the most convincing arguments for such a model is that in many folds, the degree of asymmetry can clearly be observed to increase with time (and therefore with the degree of faulting), to which the folds in this area appear to correlate well. Folds that are

not truncated by thrust faults (ie. Hawarden Anticline and Moores Hill Anticline) do tend to possess a highly symmetrical cross-sectional shape; Lowry Peaks Anticline, which is suggested to have only recently been faulted, is largely symmetrical (although there are complications due to secondary imbricate thrusting and back-thrusting, described further in Chapter 6); whereas Waikari Anticline and Mt Alexander Anticline are clearly asymmetrical, associated with the well developed Moores Hill and Mt Alexander Faults respectively. Therefore, the buckling model is preferred here, and by correlation with observations in the Amuri and Flaxdown Limestones by Nicol (1991) and Mould (1992), it is likely that this has been achieved by bed-over-bed slip.

#### 5.2.2.2 Amplitude

The majority of the folds in this study area do not possess distinctive marker beds preserved in the core of both the anticlines and the synclines, therefore, estimates of fold amplitude (see table 3.1b) have been based on twice the half amplitude of the basement-cover rock unconformity on the major anticlines. The likely modern degradation of this surface means that these estimates are at a minimum. Furthermore, by only measuring the amplitude of one half of the fold, the effects of faulting can be discounted (figure 5.3b).

The degree of faulting of the major folds has been noted in section 5.2.1.5 to provide a useful measure of the relative displacement on the faults, which lead to the conclusion that faults such as Greta Peaks, Moores Hill, Maxwellton and parts of Mt Alexander Fault have had a substantial amount of throw. When these results are compared with table 3.1b, it is clear that the folds associated with these possess some of the largest amplitudes of the area; those that are not affected by faulting as yet, but are likely to be responding to fault movement at depth (some of the evidence for which is discussed later in this chapter), such as Hawarden Anticline, Old Weka Pass Road Anticline and Moores Hill Anticline (although some effects of cross-folding have to be taken into account with the latter). There is an exception however in that the Lowry Peaks Anticline has a large amplitude, but is associated with very little fault movement.

Nicol (1991) was able to quantify such a relationship in his area, and showed that in accordance with the above observations, amplitude does increase with increasing fault displacement, but at an ever decreasing rate (figure 5.6). Therefore, it is clear that the

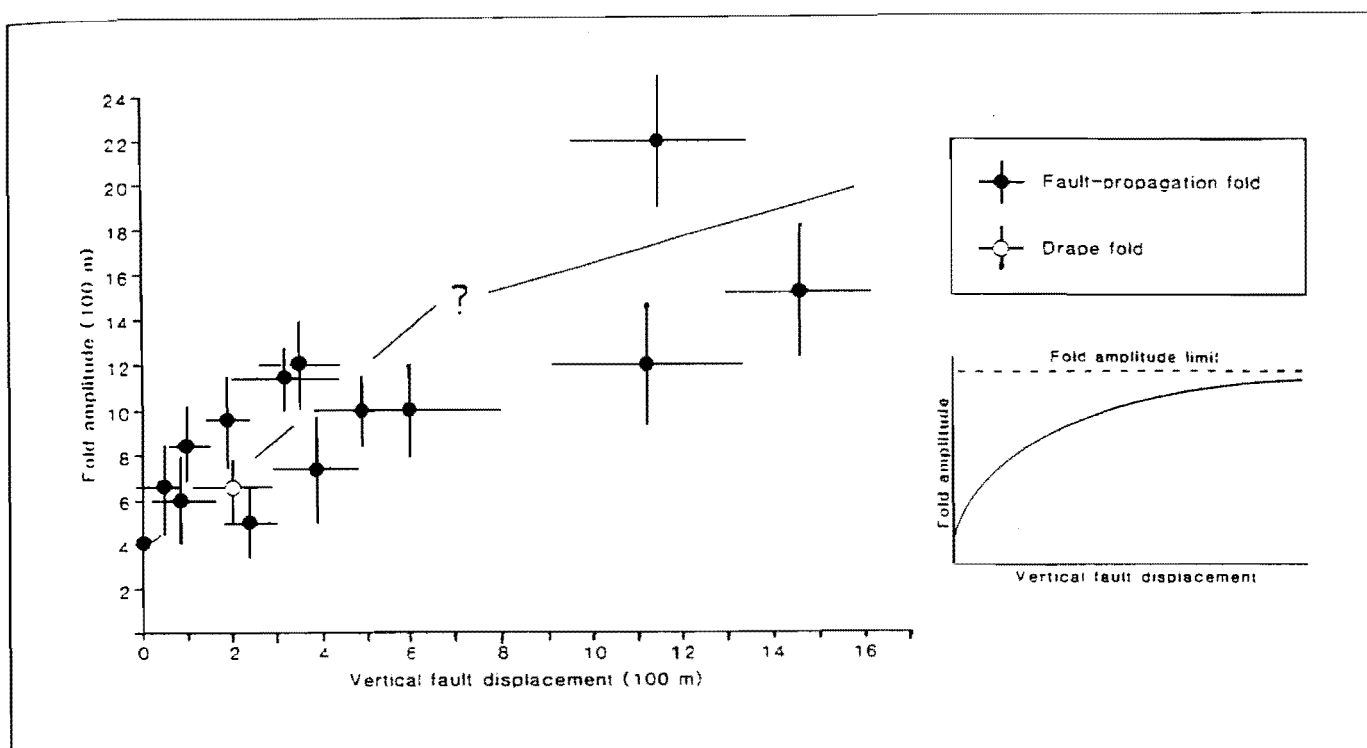


**Figure 5.6** The graphical relationship of vertical fault displacement and fold amplitude for 15 fault-related folds from north Canterbury (data from Nicol, 1991, Wilson, 1963, Maxwell, 1964, Yousif, 1987 and Barrel, 1989). The inset shows the predicted conceptual relationships for these variables. (From Nicol, 1991)



folds do lock up when they reach a particular amplitude, and hence Lowry Peaks Anticline is likely to have nearly reached the point of maximum amplitude, now being passively faulted over the syncline forming the eastern side of the Culverden Basin.

### 5.2.2.3 Wavelength

By definition, the wavelength of fault-propagation folds is directly proportional to the cross-sectional spacing between the thrust faults. Therefore, in accordance with the observations made in section 5.2.1.2, the wavelengths of the major folds in this study area are rather regular, obvious changes occurring where fault orientations are anomalous, such as Moores Hill Fault, which causes the half-wavelength of the “Waikari Valley Syncline” (approximately correlating to Waikari Valley) to vary from approximately 6 km near Eastcott Stream to only 4 km near Roto-iti homestead.

Nicol et al (1995) have shown that the formation of sedimentary basins in north Canterbury have an inherent link to wavelength of the major folds. If the cores of fault-related synclines (generally filled with soft cover rocks) are situated below the base level for sedimentation they will be filled with sediments according to the rate of sedimentation for the area. In this area the axis of the Waikari Valley Syncline and the syncline along Scargill Valley, as well as various complicated, down-plunged structures in the Waikari Flat area are clearly situated below such a base level, and collectively form a large sedimentary basin. By comparison, the broadly synclinal structure comprising Scargill Hills Outlier is largely well above the base level for sedimentation (due to the fact that it is being piggy-backed on the southern limb of Lowry Peaks Anticline) and hence is largely undergoing erosion.

Nicol et al (1995) also made some pertinent observations as to the relationships between basin width and wavelength, and between basin length and fold length (or fault length as was found often to be easier to measure) in north Canterbury, which included Waikari Valley and Waikari Flat, and these are shown in figure 5.7.

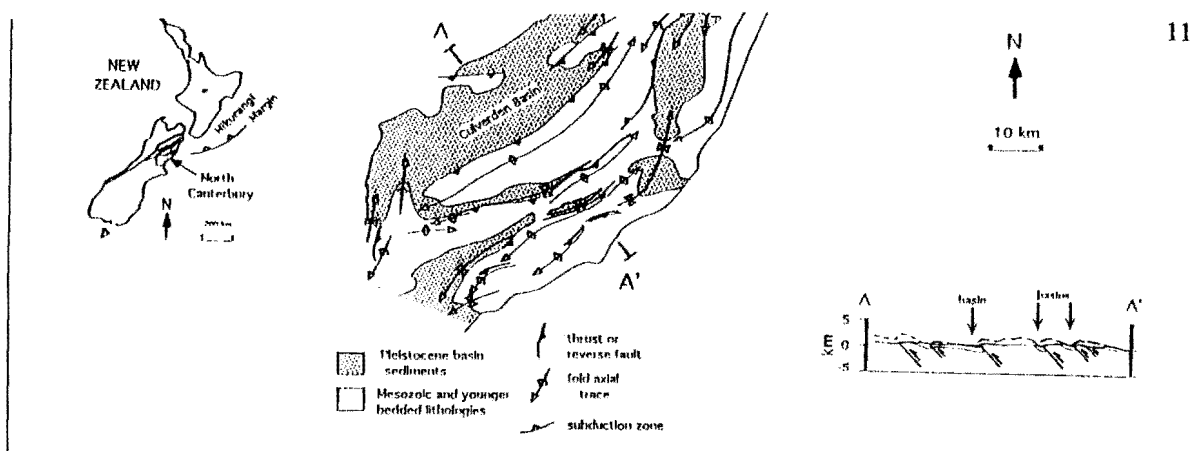


**Figure 5.7a** Pleistocene sedimentary basins of the north Canterbury region. (From Nicol et al, 1995)

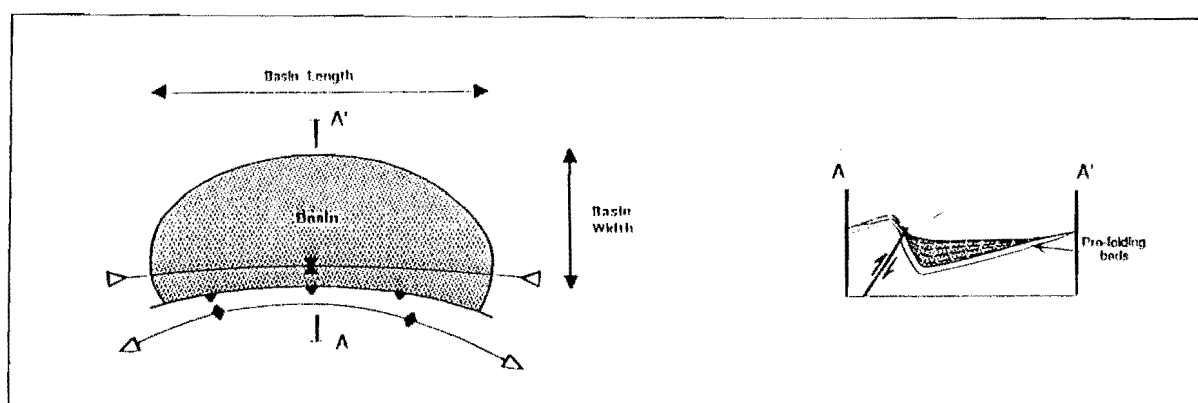


**Figure 5.7b** Schematic map and cross section showing the relationships between basin geometry, reverse (thrust) faulting and fault-related folding. (From Nicol et al, 1995)

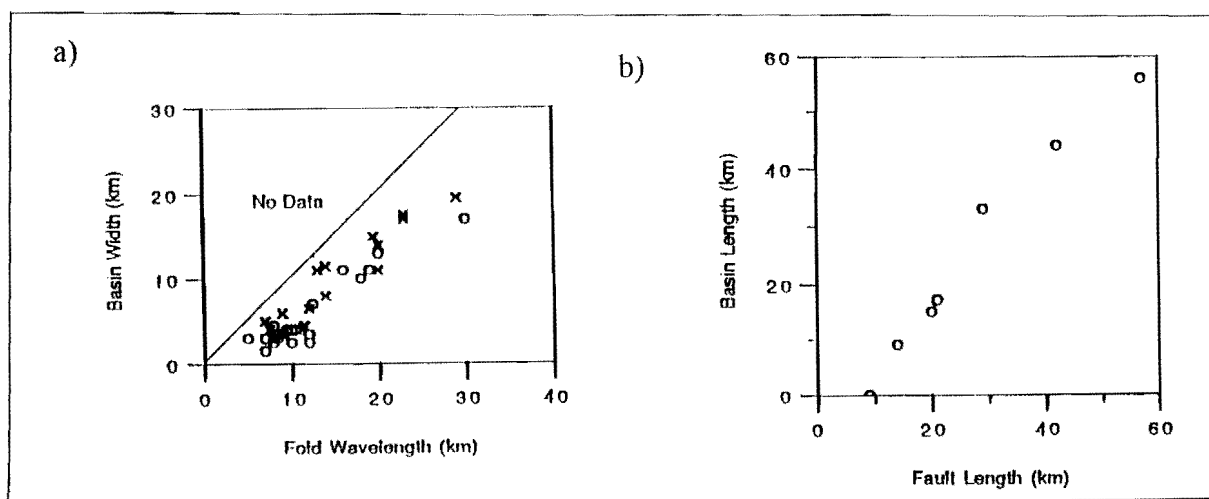


**Figure 5.7c** Graphical relationships between a) basin width and fold wavelength and b) basin length and fault length for  $n=20$  and  $n=7$  north Canterbury basins respectively. (From Nicol, et al, 1995)

#### 5.2.2.4 Plan-view geometry

As previously discussed, the trace of thrust faults is typically bow-shaped, with a displacement maximum in the centre (Elliot, 1976, Wilkerson, 1992). Therefore, at least until the point where the fault breaks through the inflection point of an associated anticline-syncline pair, the axial planes of the folds should also possess a typical bow-shaped trace, as shown in figure 5.8. When the fault does propagate through, as well as ceasing to fold, central portions of the folds will cease to rotate into the bow-shape, as the syncline is passively overridden by the anticline (figure 5.8).

Of the folds that can be seen in their entirety in this area (ie. that have not been affected by secondary structures), only the folds associated with Greta Peaks Fault appear to be behaving in such a fashion, (as described in Chapter 3, the likely anticline associated with Greta Peaks Fault is now overriding the floor of Scargill Valley Syncline, which is now exposed as two discrete portions, Kaiwara Syncline and Tipapa Syncline). Other structures, particularly in the Moores Hill Range, possess rather straight traces in their central portions, typically trending WSW-ENE, with an abrupt swing to trend NE-SW at both ends (particularly after the fault trace disappears), the result being an essentially sigmoidal shape, as shown in figure 5.9.

It is proposed here that these abrupt swings are a direct reflection of the oblique angle between the trend of a number of the major faults (generally WSW-ENE) and that proposed by the deformation associated with the principle horizontal compression (NW-SE) (figure 5.9). That is, in central portions, folding has occurred largely in response to the vertical component of motion on the faults (ie. normal to the fault trace), but at the ends, where faulting has not yet propagated into the cover rocks, folding has formed normal to the principal compression direction. This is particularly evident at the eastern end of Waikari Anticline, and probably the eastern end of Mt Alexander Anticline, but the best well preserved example of a sigmoidal shape is Moores Hill Anticline (figure 5.9), which therefore must have formed on a WSW-ENE trending blind thrust that is very close to the surface in central portions.

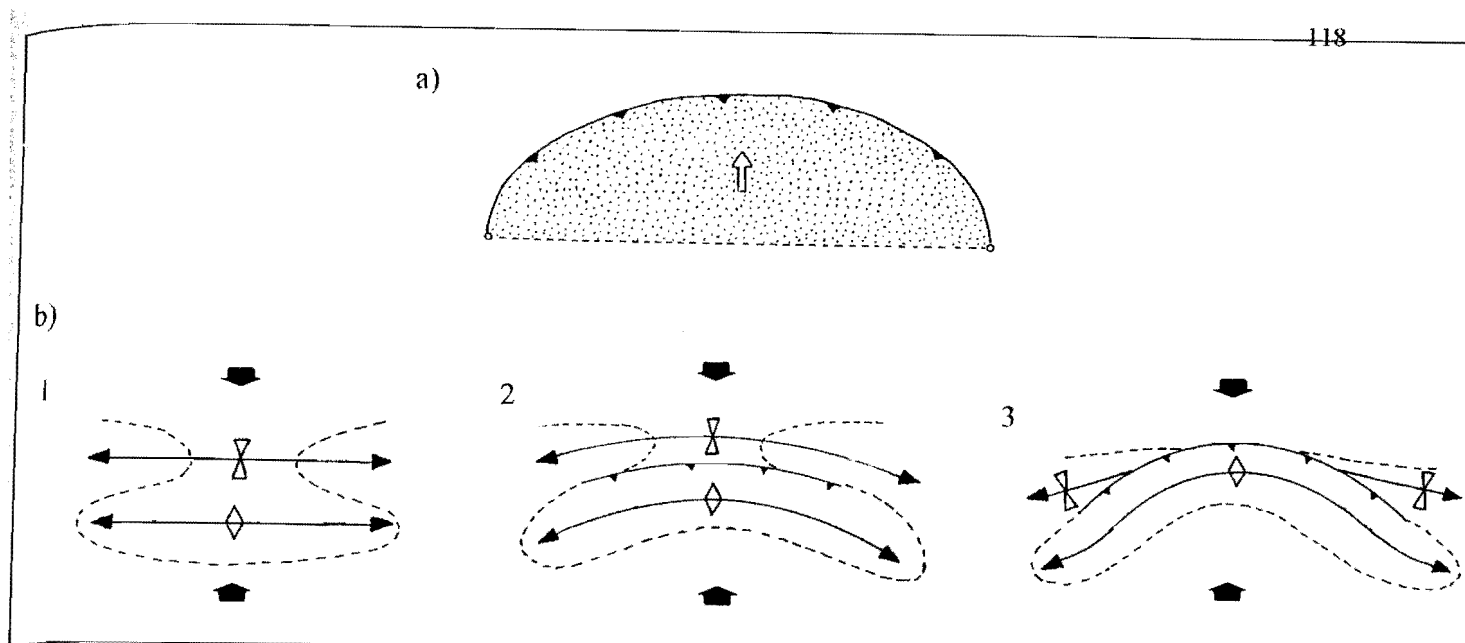


**Figure 5.8** a) The bow-shaped trace of thrust faults. b) fault-fold relationships as the degree of faulting increases and the syncline on the down-thrown side is progressively overridden.

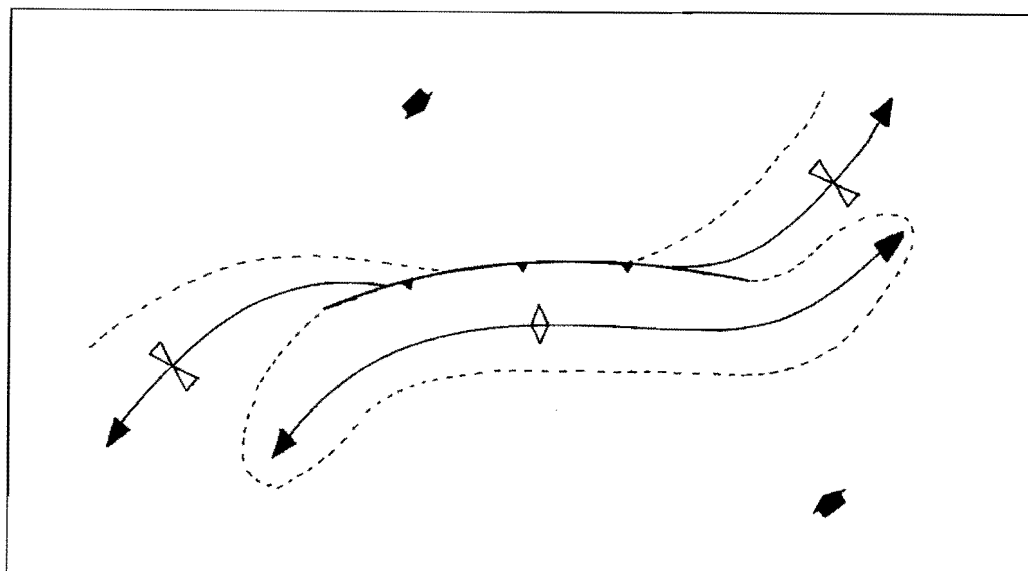


**Figure 5.9** Sigmoidal shape of folds in this study area as the result of oblique compression on the associated thrust faults.

### 5.2.2.5 Interference folding

It is proposed here that the general obliquity (or WSW-ENE trend) of the majority of the major faults to the principal horizontal compression direction is also the major cause of the development of the NNW-SSE trending cross-folds noted in Chapter 3 (map 2). It is important to note at this point however, the difference between structural lows associated with the displacement transfer between two major faults (eg. at the entrance and exit of Hurunui Gorge) and true folding effects. In some places these may be superimposed, such as in southern Scargill Hills Outlier, but the two effects are easily separated by comparing suspect folding effects with the adjacent structure, comparing the location of folding of Mt Alexander - Maxwelton Fault System with cross-warping of Lowry Peaks Anticline.

The most obvious, and most eastward effect of cross-folding is the production of a major synclinal structure in which cover rocks have now been preserved as Scargill Hills Outlier and structures of eastern Moores Hill Range (map 2). Cross-folding is on a rather broad scale and apparently along a NNW-SSE trending axis. Therefore, it is proposed that the effect of NW-SE oriented compression on W-E trending structures of southern Scargill Hills Outlier is to produce both WSW-ENE and the more subtle NNW-SSE trending folding. (Therefore, following the discussion in section 5.2.1.3, if the displacement transfer is also caused by differences in strike of the major structures, these effects are inherently linked, but neither causes the other.)

Further west, cross-folding can be noted to continue to form at high angles to the major fold structures (map 2), although in some cases their amplitudes may be accentuated by back-thrusting effects (discussed further in Chapter 6). As described in Chapter 3, the wavelengths of these cross-folds are not only a great deal shorter than that described above, but continue to decrease westwards, until they dominate the N-S trending folds, such as Old Weka Pass Road Anticline, Limeworks Syncline, and Pyramid Valley and Hawarden Anticlines, which are discussed below.

### **5.3 THE JUNCTION WITH STRUCTURES AT THE WESTERN END OF THE STUDY AREA**

#### **5.3.1 Introduction**

The major elements of the imbricate thrust model described above generally terminate in a zone trending approximately N-S from Waikari. Structures west of there trend N-S, while those to the north trend W-E, the two youngest members of which (the N-S trending Hawarden Anticline and the W-E trending Trig C Structures) having uplifted the uppermost units of the sequence and gravels of the floor of the Culverden Basin to enclose the rather square-shaped area of Waikari Flat, into which a number of the other structures plunge. The purpose of this section is to describe the junctions of these two sets of structures, both between the active members and between those now largely buried beneath Waikari Flat. The proposed model is shown in figure 5.10, although this model is likely represent an oversimplification, given the complexity of structures on either side and lack of exposure and subsurface information beneath Waikari Flat, it is described in terms of the three major thrust systems below.

#### **5.3.2 Western end of Kaiwara Fault System and associated structures**

The western end of Waikari Anticline is affected by the sudden predominance of N-S trending structures, in particular, Old Weka Pass Anticline which serves to fold the Weka Pass Stone Member and Amuri Limestone suddenly at right angles, and therefore defines the junction between the two sets of structures at that locality. These effects are in fact best displayed by the N-S trending cross-folding of the well preserved, W-E trending Timpendean Syncline (formed immediately south of Waikari Anticline), which has a remarkably straight, N-S trending, box-shaped, western end (Nicol, 1991).

Such an abrupt change in trend prompts the suggestion that a fundamental break occurs in that locality, for which the reasons are unclear. Although a pre-existing basement control may have existed, it is likely that now such a break is represented by a blind thrust beneath Old Weka Pass Road Anticline, verging to the east, if Old Weka Pass Road Anticline is assumed to be a fault-propagation fold. It is perhaps also important to note that Moores Hill Fault terminates at the approximate position of such a fault.

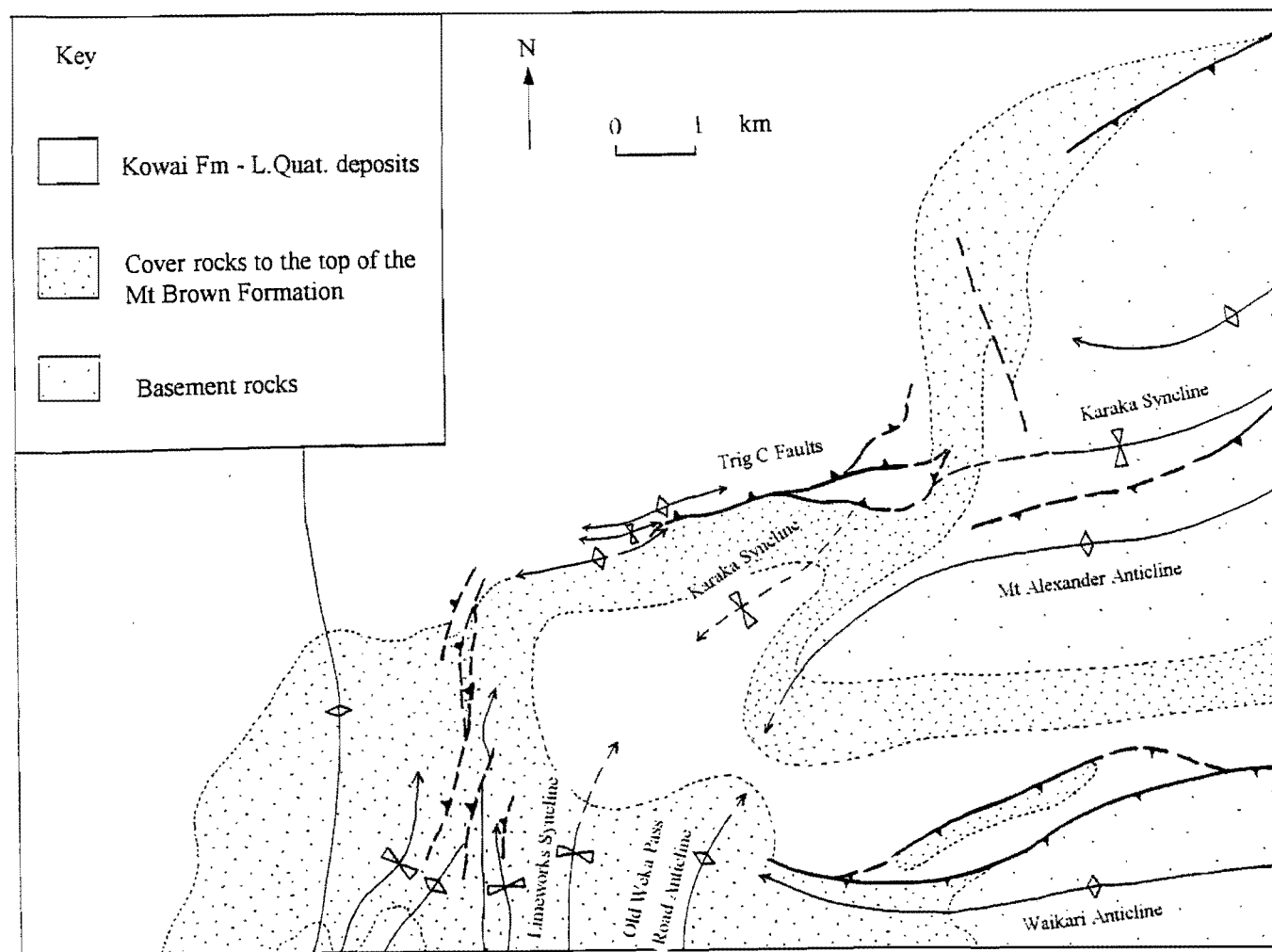


**Figure 5.10** Proposed model of the continuation of the major structures beneath Waikari Flat. The inferred position of Karaka Syncline in Waikari Flat is modified by uplift along the southern side of the Trig C Faults, rather than being a mere continuation of the syncline mapped north of Mt Alexander Anticline.

West of Old Weka Pass Road Anticline is a set of tight, N-S trending structures including Limeworks Syncline, Pyramid Valley Anticline and Hawarden Anticline, accompanied by a number of small, eastwards-verging thrust faults. The unusual relationship of these structures to the W-E trending Pyramid Valley Fault and the major anticline associated with it (figure 5.11) is not the subject of this thesis, but it is important to note that the current motion on the Pyramid Valley Fault is dextral strike-slip (Nicol, 1991), and therefore motion on these structures may be very closely related to that of the eastwards-verging structures mapped to the west (Mt Arden Fault, MacDonald Anticline and Syncline), and partly to the NW. That is, in a very simplified form, the structures may form part of an imbricate thrust system verging to the east from those structures, the majority of the current motion reflected as the very young folding, likely to be forming on blind thrusts at depth, and superficial folding.

### **5.3.3 Western end of Mt Alexander - Maxwellton Fault System and associated structures**

Mt Alexander Anticline is the only structure to plunge beneath the gravels of Waikari Flat without interference by any other structures, and as a consequence extends some distance further west than for example, the Lowry Peaks Anticline to the north. The trace of the Mt Alexander Fault is considered to terminate some distance east of Waikari Flat. Therefore the swing of Mt Alexander Anticline (described in section 5.2.2.4 to be reflecting the oblique component of compression acting on Mt Alexander Fault), is likely to be mirrored by a swing of Karaka Syncline. The small fragment of southward-dipping cover rocks preserved on the southern side of the Trig C Ridge is presently forming the northern side of the syncline, but has clearly been locally dragged up by folding at the western end of the Trig C Structures, rather than representing the original limb now overridden by the Trig C Faults.

The trend of these structures appears to be directly in line with the similarly-sized structures of Old Weka Pass Road Anticline and Limeworks Syncline, to which the cover rocks are therefore likely to link beneath Waikari Flat. These structures may largely close before they meet, given that the above discussion implies a distinctly different fault association and motion sense for each set (figure 5.10), but the traced connection implies a transfer connection for the linked folds.



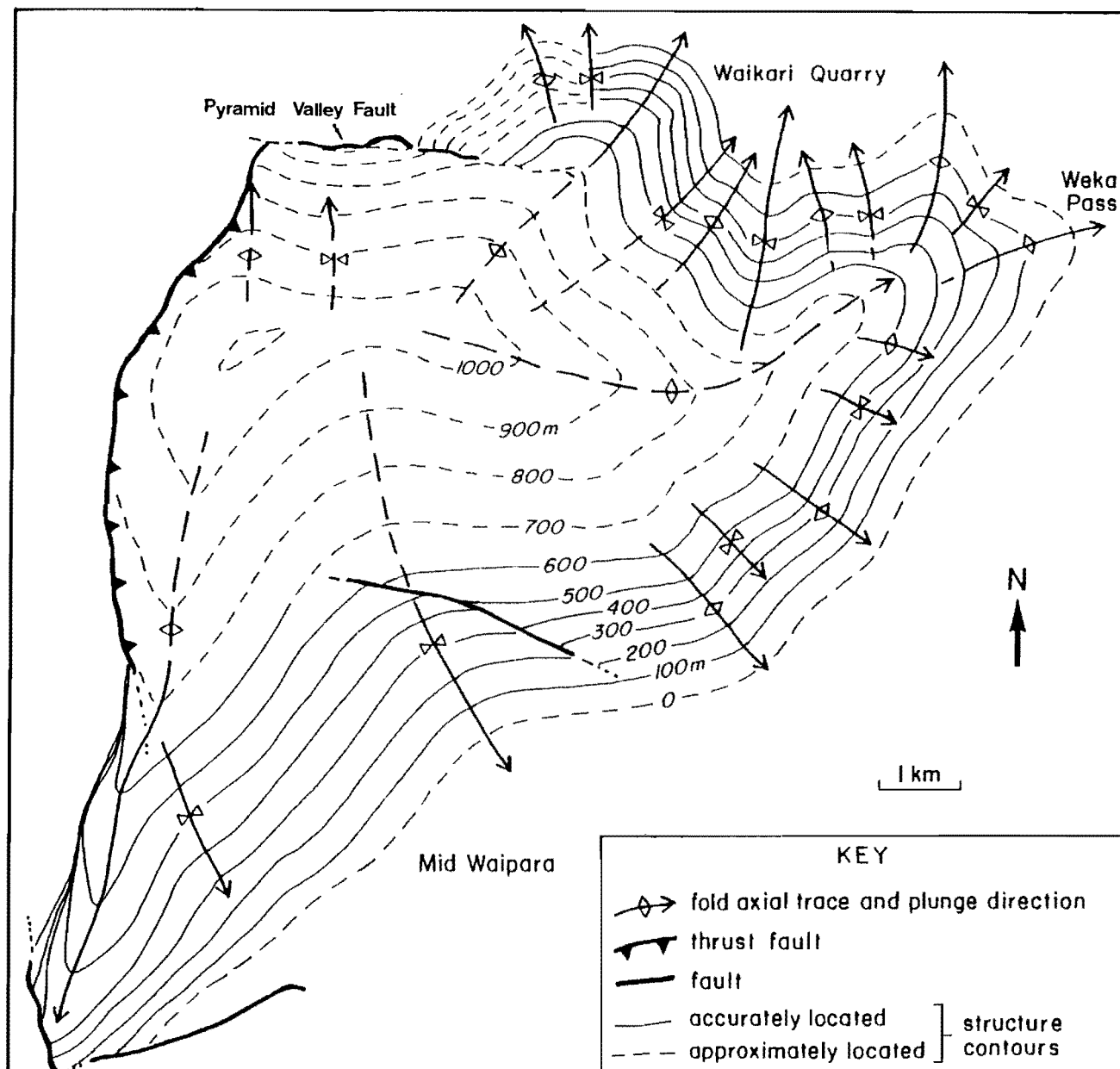


**Figure 5.11** Structure contour map on the basement - cover rock unconformity surface of the Doctors Dome, Waipara - Weka Pass region, north Canterbury. (From Nicol, 1991)

### 5.3.4 Western end of Lowry Peaks Fault System and associated structures

The western end of Lowry Peaks Anticline currently possess a distinct square-shape due to faulting along the NNW-SSE trending tear fault. The tear fault has formed to assist in the transport of motion from the south-facing Hurunui Bluff Fault to the south-facing Trig C Faults, the latter suggested to be forming as an out-of-sequence thrust upon the plunging end of the former (figure 5.1 and the cross sections).

The Trig C Structures possess a very W-E trend, the reasons for which are not clear, given that the Hurunui Bluff Fault and Lowry Peaks Anticline are likely to swing to the SW at depth. However, these structures are the youngest in the area, particularly younger than the majority of the movement on the eastward-verging N-S trending structures to the west, and therefore may have formed due to strain partitioning between the two sets of structures, in response to SW-directed compression. Furthermore, there is a possibility from the geomorphology on the gullies in which the faults appear to reside, that the N-S trending faults in the plunging end of Pyramid Valley Anticline in fact curl around to join the W-E trending structures. Therefore, the entire system of structures surrounding Waikari Flat is apparently over-thrusting the plunging ends of the major fault-fold systems of the WSW-ENE trending imbricate thrust belt.

The junction between the N-S and W-E trending sets clearly forms the most recent deformation in the whole area, represented by the gentle warping and uplift of the gravels of the floor of Waikari Flat. The northward “ramping” of gravels of Waikari Flat on the southern side of the western end of the Trig C Structures may represent the effects of interference between the two sets; their northward-vergence may represent the geometrical space problems associated with the convergence of two sets of structures at right angles.

## 5.4 CONCLUSIONS

Many of the features on the imbricate thrust model as drawn in figure 5.1 are typical of other major thrust belts. These include faulting on a number of listric thrust faults and associated back-thrusts, which merge at depth onto a mid. to lower crustal detachment.

Folding on associated angular-shaped fault-propagation folds has formed in association with thrust fault movement at depth until such time as folding locks up and faulting propagates through the inflection point of the anticline-syncline pair, to passively carry the anticline over the syncline.

However, there are a number of features that are somewhat unique, particularly to this part of north Canterbury and which have been mainly attributed oblique motion on W-E to WSW-ENE trending faults, namely:

- i) the development of a substantial number of often complex zones of displacement transfer
- ii) the development of a sigmoidal axial trace for a number of the folds
- iii) the development of cross-folds at high angles to the major thrust faults (and hence major folds).

The other effect of oblique compression is faulting on overlapping segments rather than a single fault trace, and the consequent production of complex displacement transfer zones.

The cross-folding mentioned above is thought to increase in intensity in a westwards direction to culminate in the full development of the set of N-S trending structures mapped by Nicol (1991). The major junction between these true N-S trending structures and the WSW-ENE trending Kaiwara Fault System may be expressing blind thrusting beneath Old Weka Pass Road Anticline.

Beneath Waikari Flat structures are proposed to assume a NE-SW trend, linking N-S trending, eastward-verging structures of the Weka Pass area and WSW-ENE trending, north-westward verging structures of the imbricate thrust system. Currently the whole system is being over-ridden by superficial faulting and folding by two systems at right angles, the N-S trending, eastwards-verging Hawarden and Pyramid Valley Anticlines and associated structures, and the W-E trending, southward-verging Trig C Structures. The latter appears to have formed as roof or out-of-sequence thrusting off the plunging end of the Lowry Peaks Fault System.

## GEOMORPHOLOGY AND ACTIVE TECTONICS

### 6.1 INTRODUCTION

The recognition of the tight link between geology and geomorphology dates well back into the last century. Early works particularly noted the influence of bedrock lithology and structure on drainage patterns (eg. Campbell, 1896, Hobbs, 1901 and 1911, Zernitz, 1932), but more recently the recognition of the link between geomorphological features and active tectonics has received a great deal of attention. These features include:

- i) Drainage patterns (eg. Harvey and Wells, 1987, Friederking, 1989, Deffontaines and Chorowicz, 1991, Deffontaines et al, 1992, Pubellier et al, 1994)
- ii) Stream gradient (eg. Burnett and Schumm, 1983, Seeber and Gornitz, 1983, Bull and Knuepfer, 1987, Wells et al, 1988, Merritts and Vincent, 1989, Rhea, 1993)
- iii) Stream sinuosity (eg. Adams, 1980, Burnett and Schumm, 1983, Ouchi, 1985, Campbell, and Yousif, 1985, Gomez and Marron, 1991, Howard and Hemberger, 1991)
- iv) Mountain-front sinuosity (eg. Wallace, 1978, Bull, 1984, Mayer, 1986, Wells et al, 1988)
- v) Fault-scarp morphology (eg. Wallace, 1977, Bucknam and Anderson, 1979, Nash, 1984, Mayer, 1984, Garlick, 1992, Avouac, 1993)
- vi) Direct evidence for active tectonics such as geomorphic features offset along faults, particularly strike-slip faults (eg. Allen et al, 1984, Cowan, 1989, McMorran, 1992, Pope, 1994)
- vii) A variety of other localised features such as ridge-venting, seismically-triggered landslides, surface-warping, dating of uplifted surfaces such as marine terraces (eg. Beck, 1968, Yousif, 1987, Mould, 1992),

which provide information that could potentially be used to construct a neotectonic map of a study area, which is one of the aims of this chapter.

An integral part of the description of the macroscopic structures in Chapter 3 was to note the evidence for active deformation using range-front characteristics and the

occurrences of active fault scarps. The major conclusions to be drawn from those observations and some of the conclusions made in Chapter 5 are summarised below:

- i) The majority of the current activity on the major fault systems appears to be concentrated at the western end, particularly evident as the uplift of the gravels of Waikari Flat by structures such as the Trig C Faults, Hawarden Anticline and the western end of Mt Alexander Anticline. This may support the suggestion that in the east structures such as Mt Alexander Fault are currently locked.
- ii) The motion there appears to be partitioned into two directions at right angles, between N-S trending structures such as Hawarden Anticline and Pyramid Valley Anticline (and associated faults), and the W-E trending Trig C Structures, which have formed as roof-thrusts off the western, plunging end of Hurunui Bluff Fault.
- iii) The majority of the recent motion appears to be associated with the Lowry Peaks Fault System; structures such as Greta Peaks Fault and Maxwellton Fault appear to have the least evidence of recent activity, suggesting that faulting may have been generally transferred from south to north as a leading-edge imbricate fan. A general decrease in throw also occurs from south to north (table 5.1).

Furthermore, the evidence from Chapter 4, in particular the stress tensor analysis, suggested that the latest set of deformation on at least two of the major fault systems is somewhat different to that suggested by the model of Chapter 5, namely:

- i) The major change in facing direction that appears to have accompanied motion at the western end of the Lowry Peaks Fault System may have had the secondary effect of producing a significant component of back-thrusting on both the Mt Alexander - Maxwellton and Lowry Peaks Fault Systems
- ii) Moores Hill Fault shows evidence that the majority of the latest set of motion to be accommodated by that fault is strike-slip

Small-scale faults in Waikari Quarry also appear to be currently sustaining NW-directed motion, originally forming on two sets striking N-S and W-E, verging eastwards and northwards respectively.

The purpose of this chapter is to assess the influences that active deformation may have had on the drainage of the area (particularly using features i, ii, and iii from the list of geomorphic features above), and therefore, in places where no evidence for active deformation can be mapped from outcrops, use the effects on drainage to detail evidence of young activity and to add to some of the above conclusions. A brief look at the seismicity of the area is also included in this chapter, and the final conclusions of the chapter are summarised on a neotectonic map.

## **6.2 GEOMORPHOLOGICAL MAP**

An integral part of studying the drainage of an area is to not only to examine the features of the actual streams themselves, but to also consider the features associated with fluvial systems, past and present, such as terrace risers, terrace surfaces, abandoned channels and alluvial fans. Therefore, these features have been included in the generalised geomorphological map of the study area (map 3), with the stream traces, as appears on the NZMS 270 series (1:25 000 scale) topographic maps.

Also shown on map 3, and forming an important part of the discussion of this chapter, are the resistant members of both the cover and the basement rocks, the latter having been determined from aerial photographs, as described in Chapter 2.

Finally the fault and fold traces of the major macroscopic structures have been superimposed, from map 1.

The above features are referred to in the discussions below.

## 6.3 DRAINAGE PATTERN ANALYSIS

### 6.3.1 Introduction

The study of drainage patterns, as mentioned, forms one of the oldest studies of geomorphology in relation to geology, and has consequently lead to the recognition of a number of standardised patterns with a direct link to features such as strata dip, lithology, structure and joint patterns etc. These are summarised (from Howard, 1967) in figure 6.1 and table 6.1, with the recognised standard modifications to these patterns shown in figure 6.2.

The study of drainage patterns is highly dependent on scale. On a very broad scale the drainage pattern of this area is of a trellis-type; when the drainage is divided into the major catchments (figure 6.3) it is clear that the main trunk streams follow closely the major faults and/or axes of the major synclines (including cross-folds), and that the tributaries join them at an angle close to  $90^\circ$  (figure 6.4). However, on a scale of the tributaries the drainage can be observed to possess a highly variable form, ranging from rectangular to nearly parallel. Both scales of patterns are described below.

### 6.3.2 Drainage patterns of the major trunk streams

The definition of the “major trunk streams”, as shown in figure 6.3, was based entirely on field observations of the “largest” streams in the area (generally corresponding to the streams that contain water all year around, and as a consequence tend to possess the best exposures). However, a more objective approach is to divide the streams according to an hierarchical system of stream order (Strahler, 1957), whereby two channels of  $n$ th order join to form a channel of order  $n+1$  (ie. every stream begins as a first order stream), as shown in figure 6.5. The application of this system also allows the drainage basin of streams of different size orders to be defined.

It is clear from figure 6.5 that the major streams, as defined in figure 6.3, roughly correspond to streams of order 4 or greater, and that the major catchments are utilising the synclinal axes of the down-thrown blocks of the Hurunui Bluff Fault, Mt Alexander Fault and the Kaiwara Fault System, namely the Hurunui (and Waitohi) River, northern

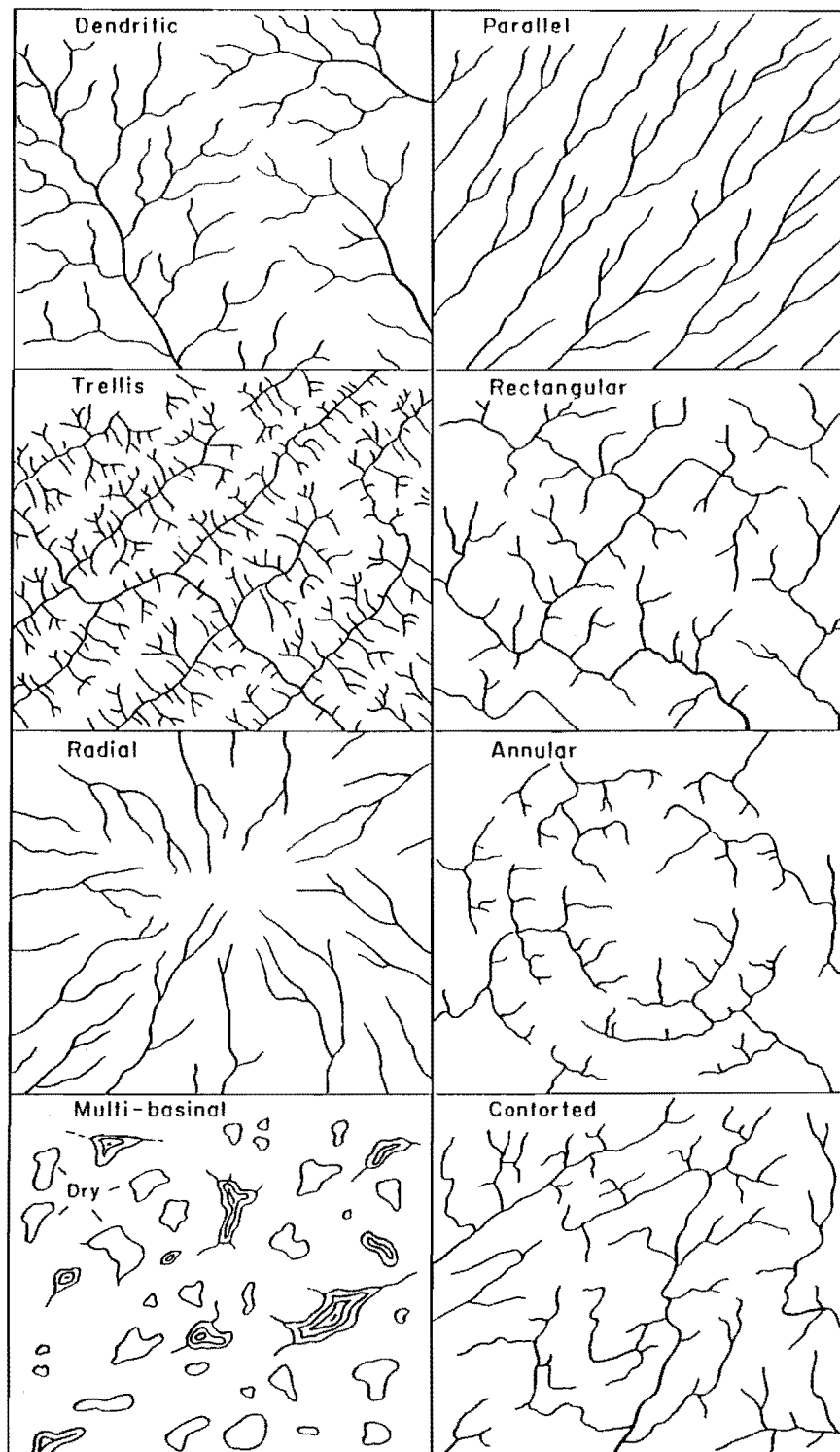


**Figure 6.1** Basic drainage patterns. The relation of these patterns to geology are summarised in table 6.1. (From Howard, 1967)



<i>Basic</i>	<i>Significance</i>	<i>Modified Basic</i>	<i>Added Significance or Locale</i>
Dendritic <sup>1</sup>	Horizontal sediments or beveled, uniformly resistant, crystalline rocks. Gentle regional slope at present or at time of drainage inception. Type pattern resembles spreading oak or chestnut tree.	Subdendritic	Minor secondary control, generally structural.
		Pinnate <sup>2</sup>	Fine-textured, easily erodable materials.
		Anastomotic <sup>10</sup>	Floodplains, deltas, and tidal marshes.
		Distributary (Dichotomic)	Alluvial fans and deltas.
Parallel <sup>2</sup>	Generally indicates moderate to steep slopes but also found in areas of parallel, elongate landforms. All transitions possible between this pattern and type dendritic and trellis.	Subparallel	Intermediate slopes or control by subparallel landforms.
		Colinear	Between linear loess and sand ridges.
Trellis <sup>3</sup>	Dipping or folded sedimentary, volcanic, or low-grade metasedimentary rocks; areas of parallel fractures; exposed lake or sea floors ribbed by beach ridges. All transitions to parallel pattern. Type pattern is regarded here as one in which small tributaries are essentially same size on opposite sides of long parallel subsequent streams.	Subtrellis	Parallel elongate landforms.
		Directional Trellis	Gentle homoclines. Gentle slopes with beach ridges.
		Recurved Trellis	Plunging folds.
		Fault Trellis	Branching, converging, diverging, roughly parallel faults.
Rectangular <sup>4</sup>	Joints and/or faults at right angles. Lacks orderly repetitive quality of trellis pattern; streams and divides lack regional continuity.	Angulate	Joints and/or faults at other than right angles. A compound rectangular-angulate pattern is common.
Radial <sup>5</sup>	Volcanoes, domes, and erosion residuals. A complex of radial patterns in a volcanic field might be called multi-radial.	Centripetal	Craters, calderas, and other depressions. A complex of centripetal patterns in area of multiple depressions might be called multi-centripetal.
Annular <sup>6</sup>	Structural domes and basins, diatremes, and possibly stocks.		Longer tributaries to annular subsequent streams generally indicate direction of dip and permit distinction between dome and basin.
Multibasinal <sup>7</sup>	Hummocky surficial deposits; differentially scoured or deflated bedrock; areas of recent volcanism, limestone solution, and permafrost. This descriptive term is suggested for all multiple-depression patterns whose exact origins are unknown.	Glacially Disturbed	Glacial erosion and/or deposition.
		Karst	Limestone.
		Thermokarst	Permafrost.
		Elongate Bay	Coastal plains and deltas.
Contorted <sup>8</sup>	Contorted, coarsely layered metamorphic rocks. Dikes, veins, and migmatized bands provide the resistant layers in some areas. Pattern differs from recurved trellis (Fig. 2, II) in lack of regional orderliness, discontinuity of ridges and valleys, and generally smaller scale.		The longer tributaries to curved subsequent streams generally indicate dip of metamorphic layers and permit distinction between plunging anticlines and synclines.

**Table 6.1** Geological significance and relationship between basic and modified basic drainage patterns.

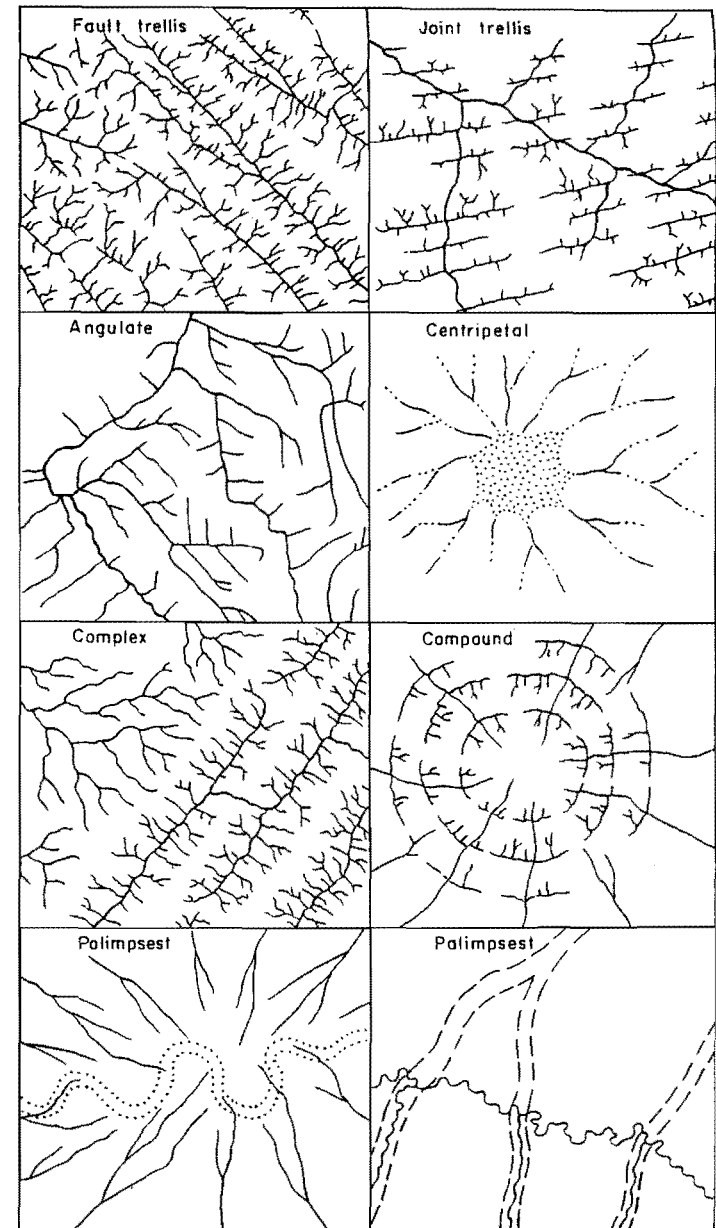
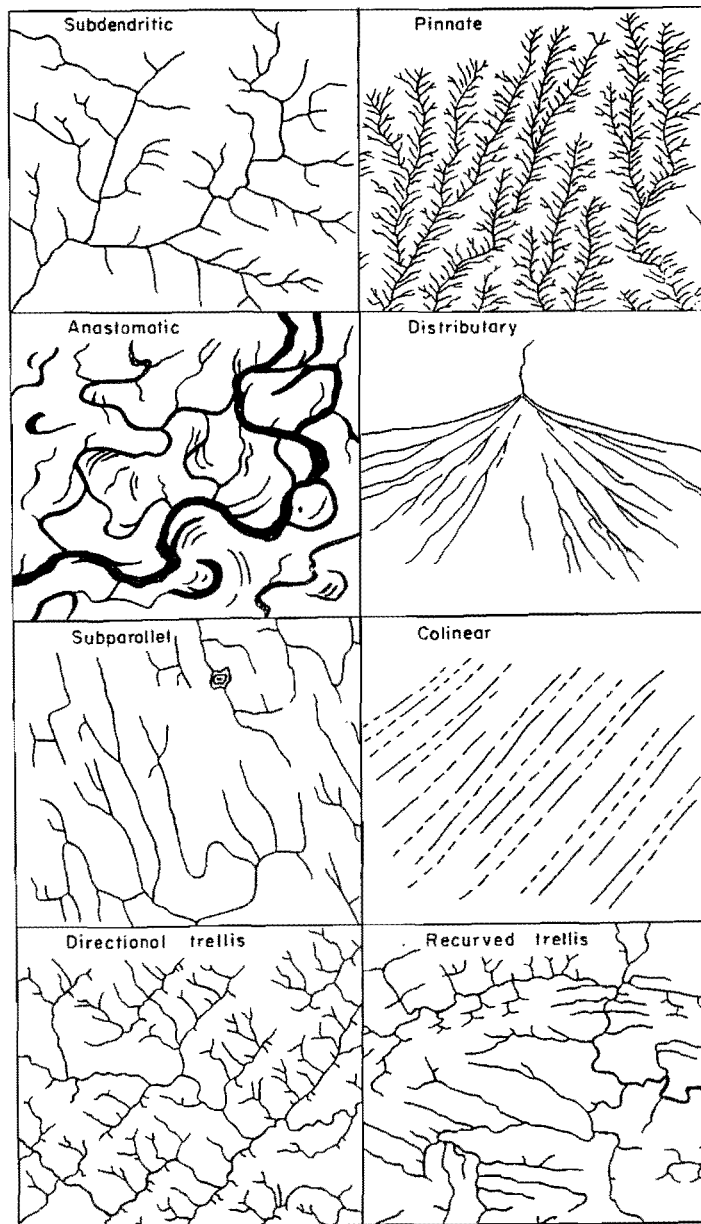


**Figure 6.2** Modified basic drainage patterns. The relationship of these patterns to the basic patterns, and hence geology are summarised in table 6.1. (From Howard, 1967)

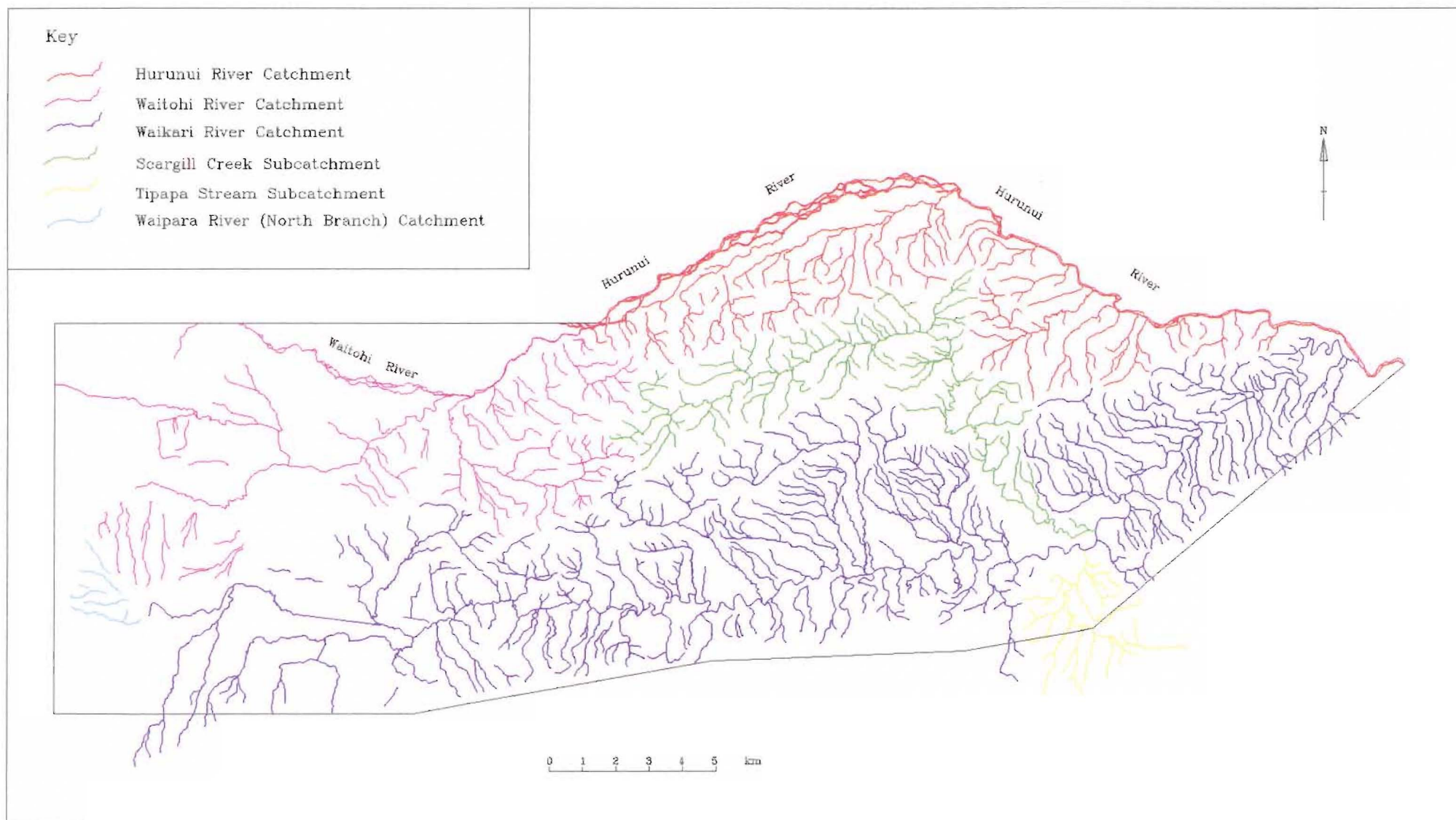


**Figure 6.3** Drainage of the study area divided into major catchments.

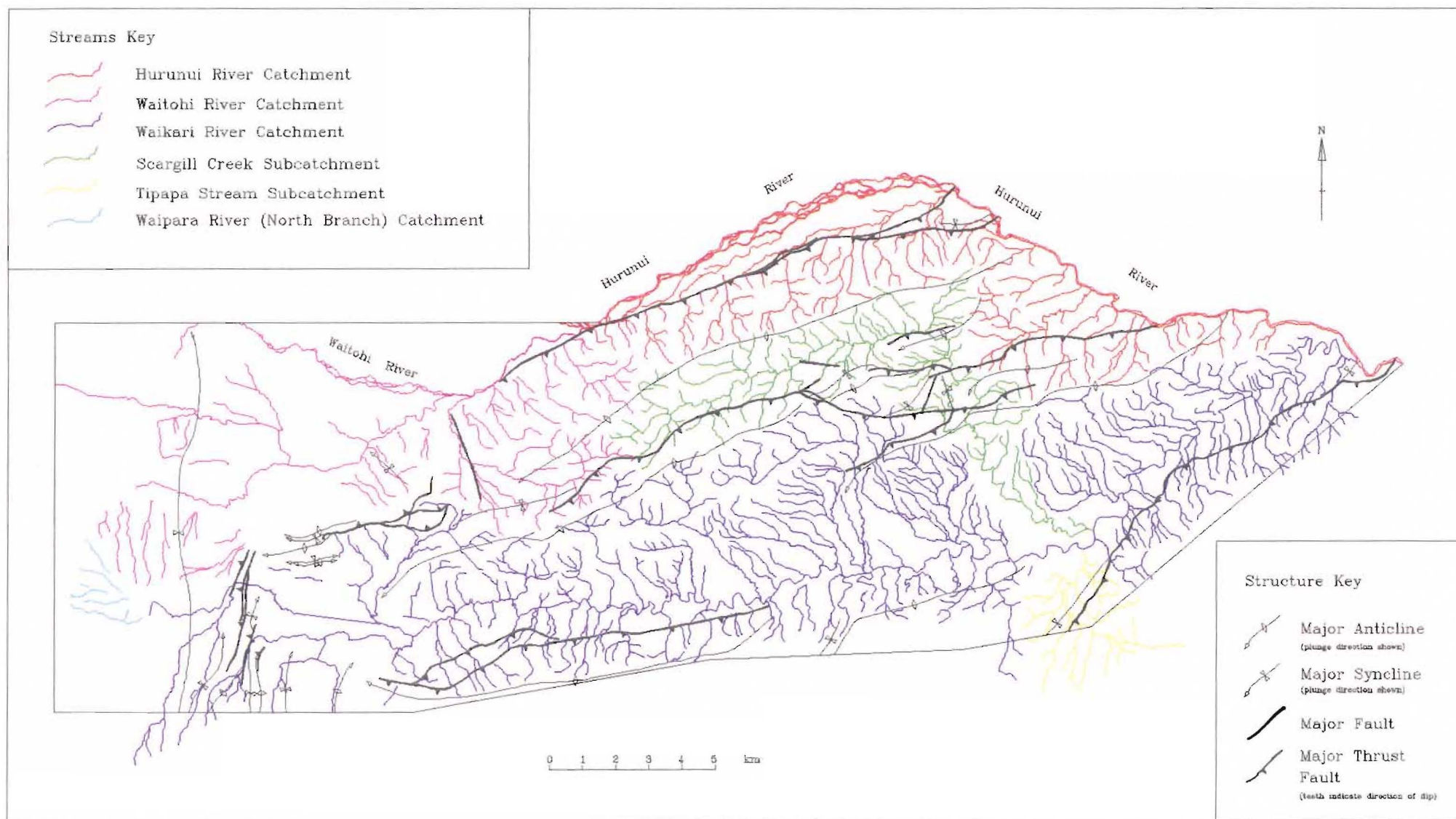


**Figure 6.4** Major catchments of the study area compared to structure.



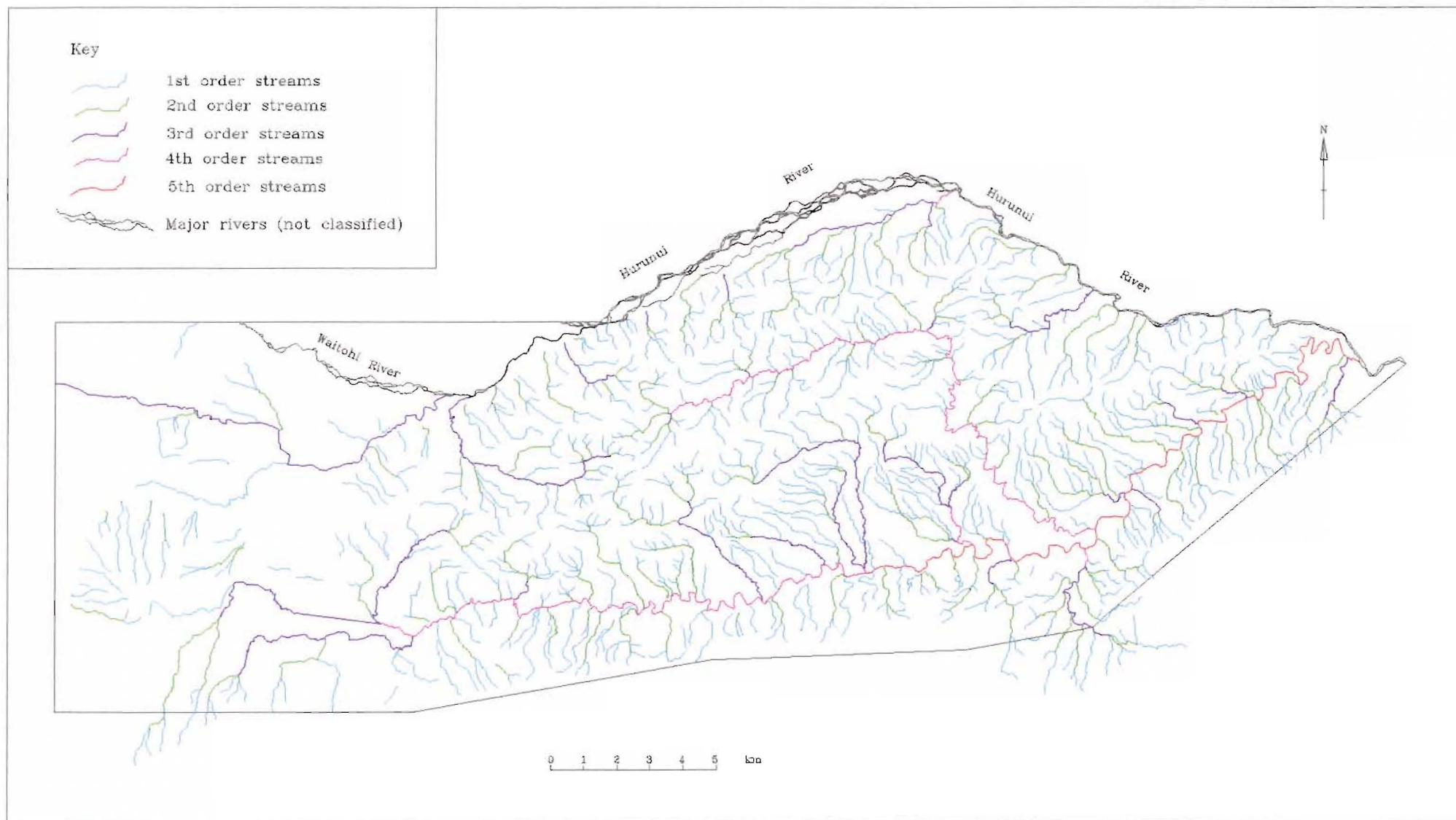


**Figure 6.5** Drainage of the study area classified according to stream order.

portions of Scargill Creek and Waikari River, and the structural low occupied by Scargill Hills Outlier and Moores Hill Anticline and Syncline.

The most important observation to be made from figure 6.5 however, is that the catchment for Waikari River is contained entirely within the study area, and consequently, the river only ever reaches fifth order, which is a great deal “smaller” than that of rivers to the north such as the Waitohi or Hurunui, despite the fact that it occupies a rather broad valley. However, it was noted above that the uplift of the structures on the northern and western side of Waikari Flat are very recent, and the similarity of the floor of Waikari Flat to the floor of Culverden Basin (as discussed in Chapter 2) suggests that they were once continuous and formed by the same process (ie. alluvial aggradation). Therefore it would seem likely that a relatively large size river occupied the Waikari Flat area in the Late Quaternary, which was then subsequently cut off by the uplift of the floor by the Trig C structures and Hawarden Anticline and the highly faulted Pyramid Valley Anticline.

Evidence that the Waitohi River may have actually flowed across the Waikari Flat area in the recent past, but now has been forced to the north, is suggested by the set of river terraces preserved along its southern side. A set of terraces trending WNW-ESE on the southern side of the river descend towards the north with a greater spacing than those on the northern side of the river, indicating the northward migration of the river there (partly shown on map 3). Furthermore, a distinct pattern of abandoned channels, and the apparently “trimmed” sides of the northernmost gap through Hawarden Anticline currently occupied by Washpen Stream are combined with the presence of an uplifted terrace along the south-western side of the northern-most portion to suggest that a river of a greater size than Washpen Stream once flowed through the gap (map 3). Following the channel patterns to the SE, it seems likely that the river would have exploited the structural low that currently represents the low saddle of the junction between the Trig C Structures and Hawarden Anticline. This was described in Chapter 5 to be the product of recent folding and up-warping of the floor of Waikari Flat as the two systems converge.

The next issue to address is that if a river did flow into Waikari Flat, where did it exit? Two possibilities exist. The first is that a major river once flowed down Waikari Valley, as was hinted above. This seems a likely option given factors such as the very broad size

of Waikari Valley, currently occupied by the seemingly underfit Waikari River. However, evidence such as large aggradational terraces, meanders of a scale too large to have been created by the Waikari River, or even an alluvial surface on which the alluvial fans of the valley sit, are lacking, as is evidence pointing towards a place of exit for the river. Furthermore, it was noted in Chapter 2 that the Kowai Formation is lacking in central and eastern portions of the area, the uppermost portions of which would form the likely deposit that any river would make (P. Tonkin, pers. comm., 1995).

The other possibility, and that preferred by the author, is that such a system drained out through Weka Pass, before structures such as the western end of Waikari Anticline, the Timpendean Syncline and Old Weka Pass Road Anticline were uplifted to their current height. Nicol (pers. comm. 1994) cited some evidence for drainage across Old Weka Pass Road Anticline, in that a sequence of recent river gravels preserved in Weka Pass contains deposits of reworked greensand that are derived from the Waipara Greensand Formation, and therefore must have been flushed there by drainage from the north. The most likely source would be the Waipara Greensand of the eastern limb of Old Weka Pass Road Anticline, the present course of drainage from Weka Pass does not expose the Waipara Greensand Formation. Some evidence for drainage in a generally southern direction (as compared to an eastern) is supplied from the abandoned channels on the floor of Waikari Flat (see map 3).

It is interesting then to speculate on the likely drainage patterns of the area one step back in time, when the majority of the major folds were just beginning to emerge above the base level for sedimentation, particularly focusing on the path of the Hurunui River. The current course of the river is somewhat anomalous, cutting straight across basement rocks of major structures of each of the three fault-fold systems. Previous workers, as mentioned in Chapter 1, debated this issue in some detail, the most recent conclusion being that the drainage was superimposed from a path inherited from flow on a large alluvial plain consisting of upper Kowai Formation gravels. The above discussion demonstrated the sensitivity of a river of approximately the size of the Waitohi River, to uplift of even moderately small structures such as Trig C Ridge, which is composed of relatively soft Kowai Formation gravels. More importantly, the discussions of stratigraphy in Chapter 2, and noted above, suggested that the Kowai Formation had not been uniformly distributed over the whole area, instead forming geologically synchronously and episodically with uplift of the major structures of the region.

When the entrance to Hurunui Gorge is examined, it is clear that the major control on the river's entrance at that particular point is structural. The Hurunui River flows along the Lowry Peaks Fault System to precisely the point where the system undergoes a displacement transfer from the southwestern Hurunui Bluff Fault to the northeastern Hurunui Gorge Fault, the latter being stepped out north-westwards from the former into the Culverden Basin. Early phases of faulting produced a syncline of soft cover rocks (Ben Lomond Syncline) over which the river has flowed, leaving a terrace on its surface on the south-eastern side of the valley (map 3) and downcutting against the adjacent anticlinal barrier of basement. Later phases have caused the river to scour-out the cover rocks forming the western end of Ben Lomond Syncline, while the river was trimming the scarp face to the major degradational terrace surface along the range-front and down Hurunui Gorge. This was finally apparently abruptly abandoned, with downcutting and movement of the river bed some distance out into Culverden Basin, close to its current position.

Therefore, the major control on the position of the river at that point was the presence of a structural low caused by the major displacement transfer of the fault members. The other possible structural low of which a major drainage system might have exploited, is that occupied by Scargill Hills Outlier and Moores Hill Syncline and Anticline. There is very little evidence preserved for the presence of a significant drainage system through that area, the only high level gravels preserved throughout Scargill Hills Outlier being the localised set constituting the high terrace on the western side of Scargill Creek. The possibility that this may have once been a braided river valley is suggested by the very smooth texture of the basement rocks forming the southern limb of Lowry Peaks Anticline, as if the cover rocks were stripped by a broad, flowing river system there, by comparison with the highly dissected topography on either side where erosion has been mainly caused by down-cutting of small streams. Alternatively, the smooth topography may be simply the product of stripping of the basement - cover rock unconformity surface, without much further dissection by localised drainage systems only. The fact that a single fault is considered to have uplifted Lowry Peaks Range as a continuous anticline, means that the structural low is not as clearly expressed on the northern side of Lowry Peaks Range and therefore was likely to have been abandoned in favour of the lower topography characterising the displacement transfer zone, at the current location of Hurunui Gorge.



### 6.3.3 Drainage patterns of the smaller streams

The drainage patterns of streams of order 3 or less was noted above to be highly variable. As discussed, these streams generally flow into the major trunk streams at right angles, and therefore, since the major streams are generally following the major faults and/or axes of the major synclines, the major control on their orientation is dip of the major fold limbs. From figure 6.1, it is clear that the characteristic pattern of flow on a dipping bed is dendritic, which does feature prominently in the drainage, however, there are a number of notable exceptions, which are attributed to two controls, namely lithology and structure. These are discussed in turn below:

#### 6.3.3.1 Drainage patterns related to lithology

The effects of lithology on the drainage patterns of the area can be divided into two types:

- i) effects due to the differences in lithology between the major units
- ii) effects due to the presence of resistant beds within some of the major units.

These effects can be compared on figure 6.6.

It is clear that the less dense and most “erratic” style of drainage pattern is confined to the small alluvial plains area of Waikari Flat and the Culverden Basin. There the drainage forms very short and discontinuous meandering streams, which directly reflects the lack of power of the majority of these streams as they flow over a horizontal surface (note that the very straight portion of the southern branch of the Waikari River there is due to the presence of an irrigation canal). The presence of a large number of abandoned channel patterns (map 3) attests to their highly ephemeral nature.

Conversely, some of the most dense drainage forms on the surface of the alluvial fans in the area, particularly in central portions of Waikari Valley where it possesses a typically sub-parallel form. Streams are both actively down-cutting and flowing down the dip of the older fans, and have also been noticeably diverted away from the active fans (compare the positions of triangular-shaped gaps and the active fans shown on map 3). Hence, the major control on their orientation is fan dip.

The drainage on the cover rocks is highly variable, forming short, often sparse, irregular-shaped drainage that has cut deep gullies, but are likely to be very ephemeral, due to the effects of the slumping characteristic to these rocks. Drainage patterns are largely dendritic and the major control is dip (as is particularly evidenced by the fanning effect on the central portions of Hawarden Anticline SW of Hawarden). In many cases the general effects of dip have been overprinted by the influence of resistant limestone beds. These beds deflect the drainage either directly (for example the drainage at the eastern end of the Weka Pass Stone Member ridge in western portions of Waikari Valley) or by causing tributaries to converge into single streams that cut through the ridges (eg. the sudden “pinching” of a stream and tributaries through the Mt Brown Limestone ridge at the eastern end of Scargill Valley). These are very localised effects.

The drainage on the basement rocks is slightly more ordered, often following a regular dendritic to rectangular-type pattern, but possesses a wide variety of orientations. The major control on the rectangular-type pattern is the presence of resistant sandstone beds, which have had a similar effect to that of the resistant beds in the cover rocks. Areas where bedding is proposed to have had the most influence are highlighted on figure 6.6.

The last set of lithologically-controlled drainage patterns are those that reflect the influence of the contrast in resistance between the major units. As described above, each unit is characterised by a different style of pattern, and often a different density, which has largely been attributed to bed resistance and bed dip. Similar observations then hold between the major units, particularly between units of markedly different resistance, such as basement and cover rocks and between units of different dips, ie. dipping basement and cover rocks and sub-horizontal Late Quaternary deposits.

#### 6.3.3.2 Drainage patterns related to faulting

Figure 6.7 shows the interpreted anomalies that could not be related to the above effects of lithology or bed dip and therefore are considered to reflect a fracture control. It is notable that these anomalies are often continuous between streams, forming trends that are longer than those suggested to be related to bedding. Four major groups can be identified:

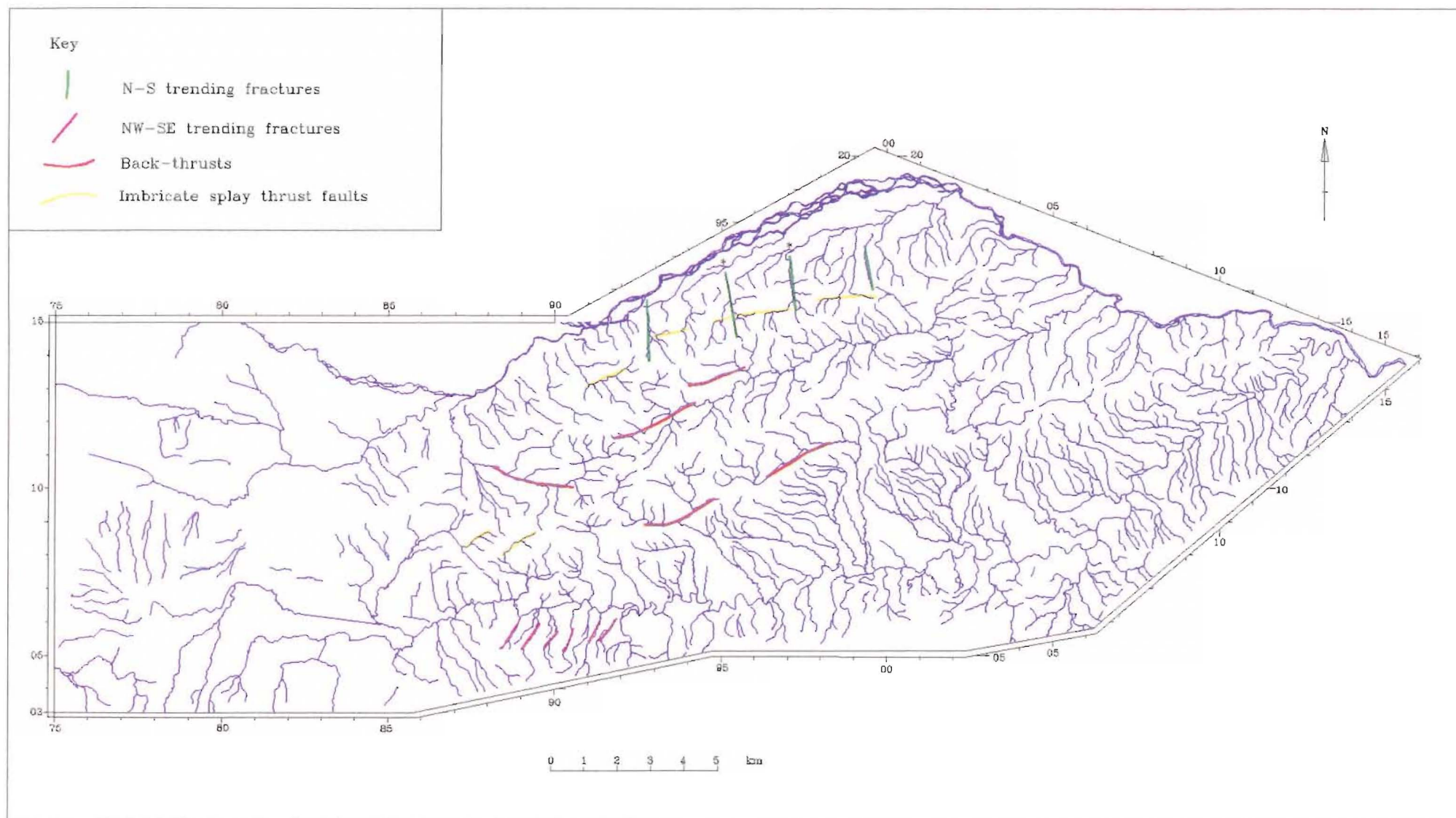


**Figure 6.7** Anomalous drainage patterns of the study area due to a structural control.

A set of drainage trending NE-SW east of Waikari is thought to indicate some sort of fracture control beneath the fan gravels of Waikari Valley. There, no well defined alluvial fans could be mapped (map 3), instead the area is a typified hummocky texture and characterised by the sets of anomalously straight, parallel gullies trending oblique to the dip of the range-front (NNE-SSE to N-S). The occurrence of the fractures at the eastern end of the splay of Moores Hill Fault may be an indication that they represent active deformation, and may have formed due to strain partitioning of motion on the WSW-ENE trending, northward verging splay.

Within the basement rocks on the northern side of Lowry Peaks Range are a set of anomalously straight, approximately N-S trending streams. These are also interpreted to represent a fracture control. Between two of the fractures (marked \* and \*), some possible evidence for down-faulting of a block was noted by a difference of intervening elevation between, and the sudden division into two sets, of the major terraces there. Therefore, it is proposed that these fractures are active and that they may represent a W-E trending component of compression, whereby the major fold structure (Lowry Peaks Anticline) is at present being “stacked” internally in a W-E direction.

The set of anomalies trending WSW-ENE on the northern side of Lowry Peaks Range are interpreted as imbricate splay thrust faults of Hurunui Bluff Fault. At least one set can be correlated with the splay proposed by the structure contouring of the basement-cover rock unconformity and the cross-sections. A similar fault at the western end of Mt Alexander Range may suggest that Mt Alexander Fault actually extends further west than where mapped, the fact that it is not highlighted by mapping and structure contouring may suggest that its trace there is very recent.

Finally, within the basement rocks at the western end and central portions of both the southern Lowry Peaks and Mt Alexander Ranges another set of anomalies can be identified, here trending WSW-ENE to W-E to WNW-ESE. These are interpreted to represent back-thrusts that splay off the major range-bounding fault systems. Some evidence has already been provided for back-thrusting by structure contouring and the stress tensor analysis of the Mt Alexander Road locality, and therefore it is proposed that these form the complement to the N-S trending fractures (in terms of vector addition of movement related to NW-SE compression), of which they clearly form the predominant set. It is also likely that the back-thrusts are a direct reflection of the recent

change in facing direction of the Lowry Peaks Fault System along the Trig C Faults. These may then be influencing the stress tensor analysis results for the Mt Alexander Road locality.

#### **6.3.4 Conclusions: *Drainage pattern analysis***

The effects of tectonics on the drainage patterns or orientations in this area are considerable, and occur on at least two different scales. Large scale effects are the apparent diversion of a major river, suggested to be the Waitohi River, out of the Waikari Flat area during the Late Quaternary, over which it may have been originally flowing to drain through Weka Pass. Waikari Valley appears to be anomalously wide for the current stream draining it (Waikari River), but evidence is lacking to conclude that a major stream once flowed along it. It is possible however, that the Hurunui River traversed the structural low of Scargill Hills Outlier and the Moores Hill Syncline and Anticline region, before establishing its course in its present position, entering the traverse across basement rocks at the point of displacement transfer between faults of the Lowry Peaks Fault System.

Smaller-scale faulting has been invoked to account for a number of relatively continuous anomalous lineations in: i) the Quaternary gravels at the western end of Waikari Valley, as a set of cross-faults associated with recent movement on Moores Hill Fault System, and ii) basement rocks of the major ranges in the area, as imbricate thrust faults and recent faulting on both N-S trending fractures and WSW-ENE to W-E trending, southward-verging back-thrusts.

### **6.4 GRADIENT INDEX ANALYSIS**

#### **6.4.1 Introduction**

The gradient of an individual stream bed is highly sensitive to the influences of a number of external factors including:

- i) climate

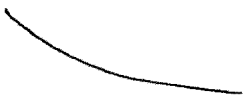
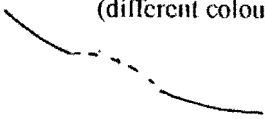
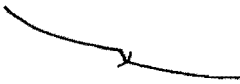


- ii) changes in sediment load
- iii) the entry of large tributaries
- iv) the presence of resistant lithologies
- v) tectonic uplift,

the relative magnitudes of these influences being largely dependent on the size of the stream. Therefore, if the former four factors can be taken into account and/or eliminated the influences and likely age of tectonic uplift effects can be readily evaluated. Climate (i) is not a factor considering that this study deals with an instant of time (ie. the present), and it was also hoped that: ii) changes in sediment load were also minimal, given that the majority of the streams flow follows short paths from the resistant ranges of basement rocks into larger streams at their ends; iii) only the Waikari River is affected by the entry of large tributaries; and iv) the effects of resistant lithologies could be easily taken into account by direct comparison with the geological map.

#### **6.4.2 Longitudinal valley floor profile**

The most visual way to study stream gradients is to construct the longitudinal valley floor profile, a plot easily constructed from topographic maps by plotting topographic contour heights of points along a stream profile against its length. A stream not showing the influences of the listed external factors (and hence said to be “at grade”, ie. the gradient is in equilibrium with both discharge and load) has generally been found to possess a concave form (due to the fact that discharge increases downstream). The influences of the above factors should therefore appear as distinct departures from the idealised concave form and can be defined along the stream length by the appearances of distinct knick-points relating to sudden increased concavity or the appearance of a convexity (figure 6.8). Attempts at mathematically idealising the graded stream profile form have been made using logarithmic, exponential or power functions (eg. Woodward, 1951, Hack, 1957, Shepherd, 1985, Snow and Singerland, 1987), although none have been found to be universally applicable in the field.

Visual estimates of sudden changes in slope are quick and can provide evidence for the type of influences on the valley floor profile (figure 6.8), but are subjective in nature, particularly being highly dependent on the scales of the plots (directly proportional to the length of the streams), and given that in practice it is easier to construct plots of the

Types of profile patterns produced (and symbol)	Classification	Gradient index relationship
	predicted concave profile	general and steady increase in GI values
 (different colour)	convex bulge	GI values steadily increase and then either decrease or increase at a slower rate, before eventually increasing again
	step-type knick point	sudden increase in GI, followed by a sudden decrease
	step-type knick point (2)	sudden decrease in GI
	cusp-type knick point	sudden increase in GI, which slowly returns to normal values

**Figure 6.8** Classification and interpretations of knick-points observed along longitudinal valley profiles in terms of physical appearance and gradient index values.

same length (particularly if plotted by computer), the plots will have varying amounts of vertical exaggeration. Therefore, a quantitative value for the gradients is required.

### 6.4.3 Gradient index

The gradient index (GI) of a segment of a stream profile can be defined as:

$$GI = \frac{\Delta H \times L}{\Delta L} \quad 1.$$

Hack (1973), where  $\Delta H$  and  $L$  are defined as in figure 6.9. Following the general concave form of the longitudinal valley floor profile, these values measured for every segment of the stream between successive topographic contours should show a general increase in value downstream, and therefore sudden large changes in these values should reflect departures from the overall concave form of the profile.

However, these numbers are still meaningless unless compared to an ideal set of values (ie. the level of significance of changes is difficult to establish). Hack (1973), by assuming a logarithmic form for the longitudinal valley floor profile proposed a comparison between the gradients of individual segments, GI (where GI is redefined as:

$$GI = \frac{\Delta H}{\text{Log}_e L_2 - \text{Log}_e L_1} \quad 2.$$

also shown on figure 6.9) and  $K$ , the gradient index of the entire profile, where:

$$K = \frac{H_j - H_i}{\text{Ln} L_j - \text{Ln} L_i} \quad 3.$$

(again defined on figure 6.9). Following the general increase in gradient index values downstream, the values of  $GI/K$  will slowly increase from values slightly less than one to slightly greater than one. Therefore, any sudden changes in the values will reflect corresponding changes in the profile and give some indications as to the relative significance of these changes.

### 6.4.4 Methodology

The division of the streams with respect to stream order (figure 6.5), allowed the delineation of a number of distinct zones of drainage (46 in total), many of which were



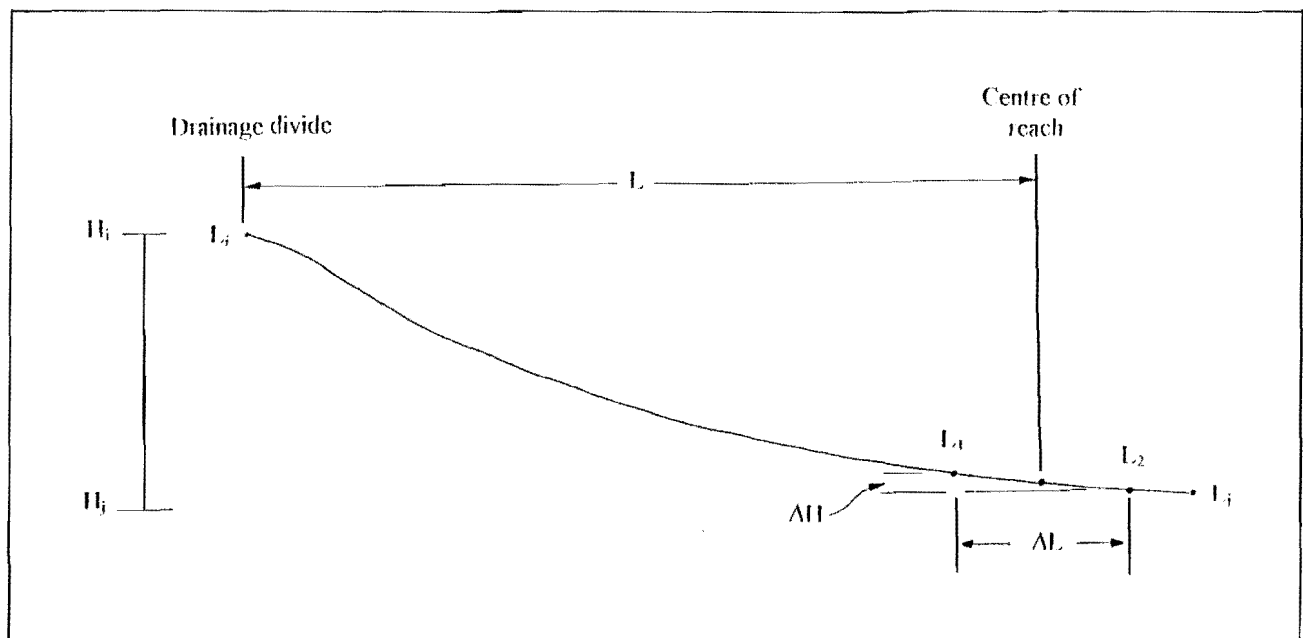


**Figure 6.9** Definition of the symbols used in equations 1., 2. and 3.. (Redrafted from Hack, 1973)

able to be defined as individual catchments (map 4A). A representative sample of streams from each zone were then chosen for the gradient index analysis (also map 4A), generally corresponding to the largest streams in each zone (a minimum of three topographic contours have to be crossed by an individual stream to provide a useful measure of gradient index).

Values for GI/K and the plotting of logarithmic valley floor profiles as defined above were relatively quickly achieved for the 236 streams chosen, using a computer program written by Yousif (1987) and a standard digitiser. The program very simply involves digitising the head of the stream and the relative positions of consecutive topographic contours along a stream length, once the values of the highest and lowest topographic contour have been entered. Then the computer calculates the values of GI, K and hence GI/K for each segment. The final output includes the values of GI, K, GI/K and a logarithmic valley floor profile with a fixed length, x-axis.

#### **6.4.5 Results**

“Knick-points” were identified for the selected streams for relatively large changes in the values of GI/K (generally  $> 0.5$ ), and were drawn on each of the profiles according to the classification shown in figure 6.8. A selection of the profiles (generally streams of order 3 or greater) are shown in figure 6.10. Interpreted knick-points and convex portions of the stream profile were then transferred back to the map using the symbols shown in figure 6.8, (map 4B). The major lithological units, resistant beds, faults and folds were then superimposed on the resulting plots to allow a direct comparison of their effects (map 4C).

The approach to interpreting the results of the gradient index analyses was the same as that for the drainage pattern analysis: first to isolate the effects of lithology, particularly in terms of resistance, and then to consider remaining anomalies in terms of structure. These are discussed in turn below.

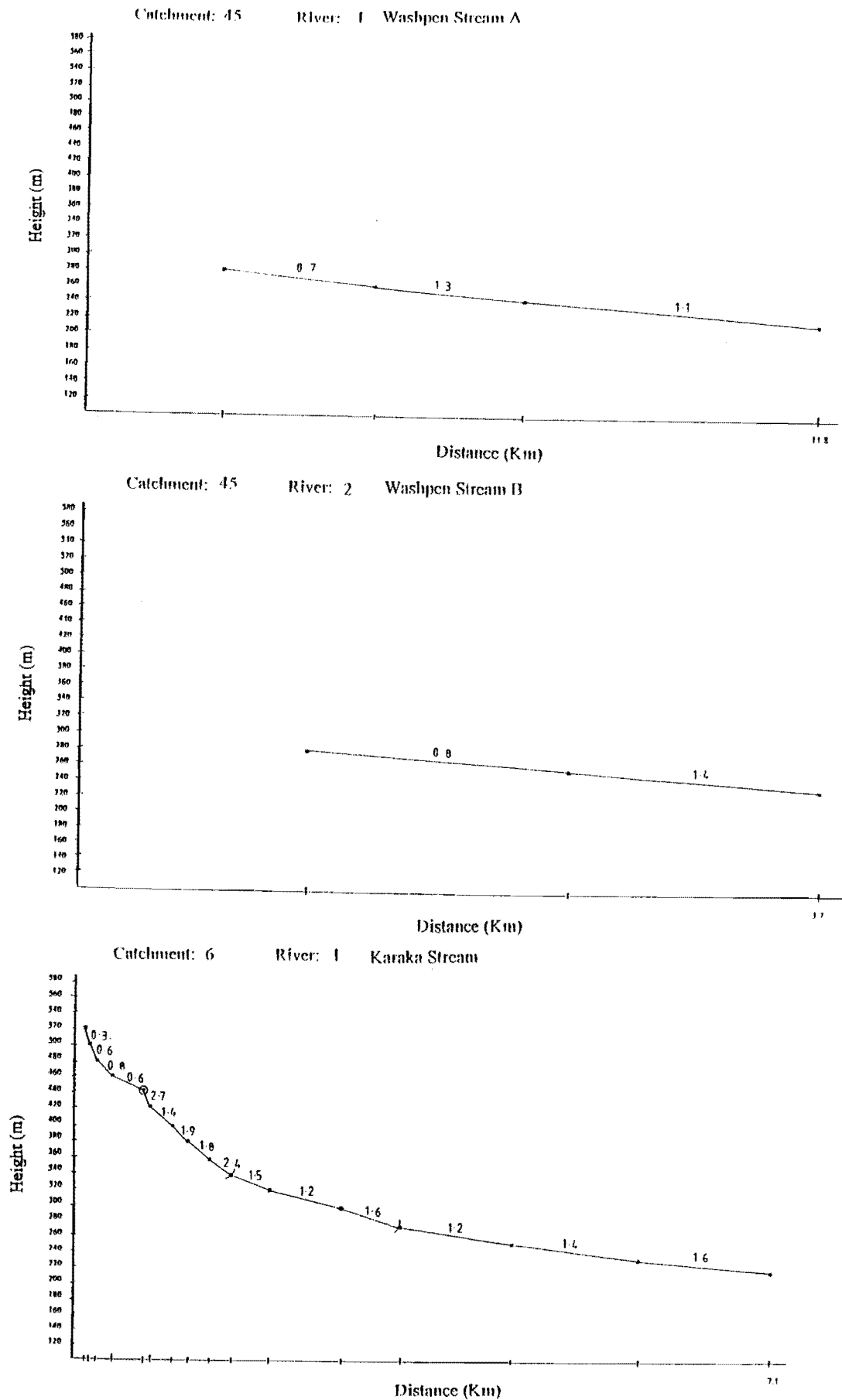
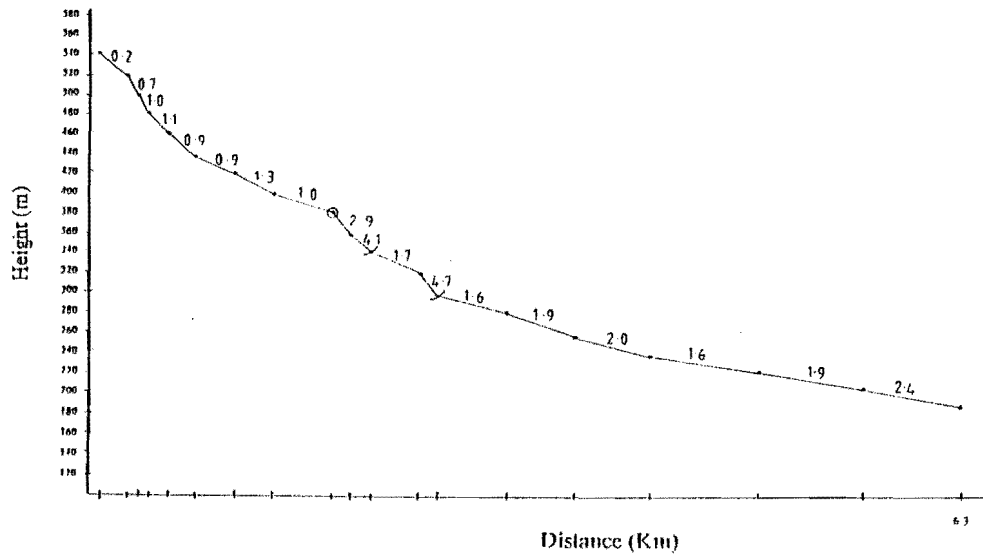
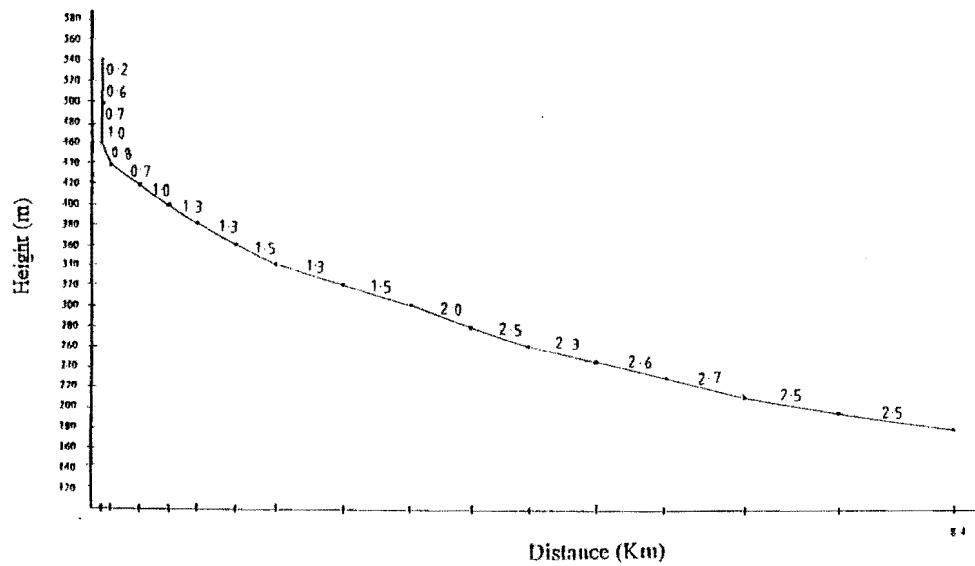


**Figure 6.10** Results of the stream gradient index analysis for streams of order 3 or greater. Shown as both longitudinal valley profiles and gradient index values.

Catchment: 4 River: 1 Laverock Stream



Catchment: 2 River: 1 Eastcott Stream



Catchment: 3 River: 1 Foxdown Stream

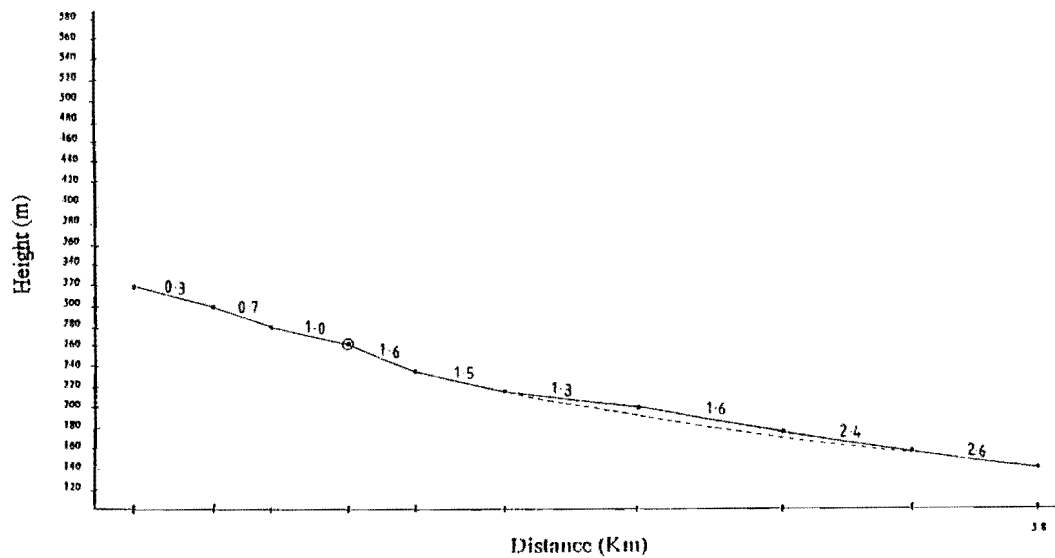
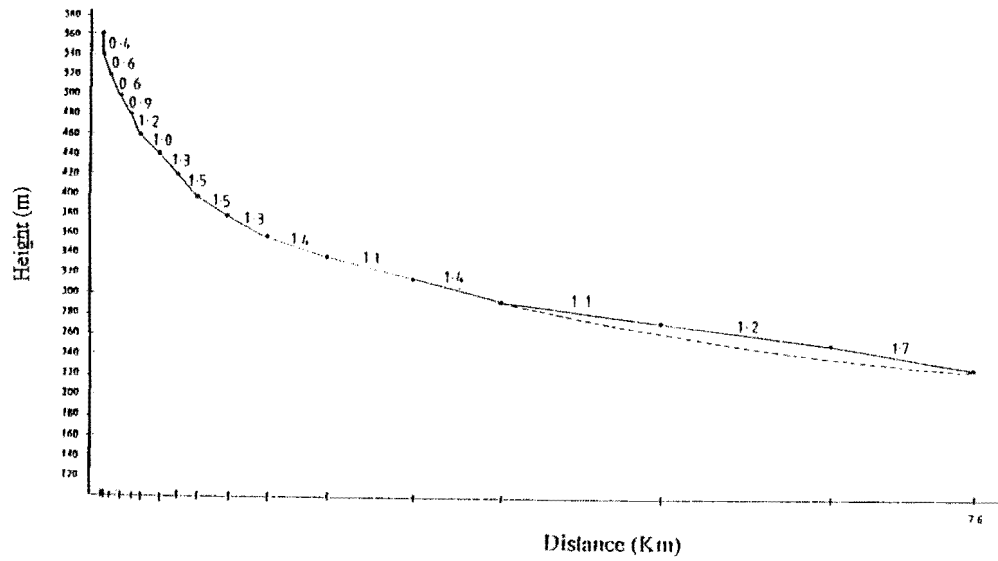
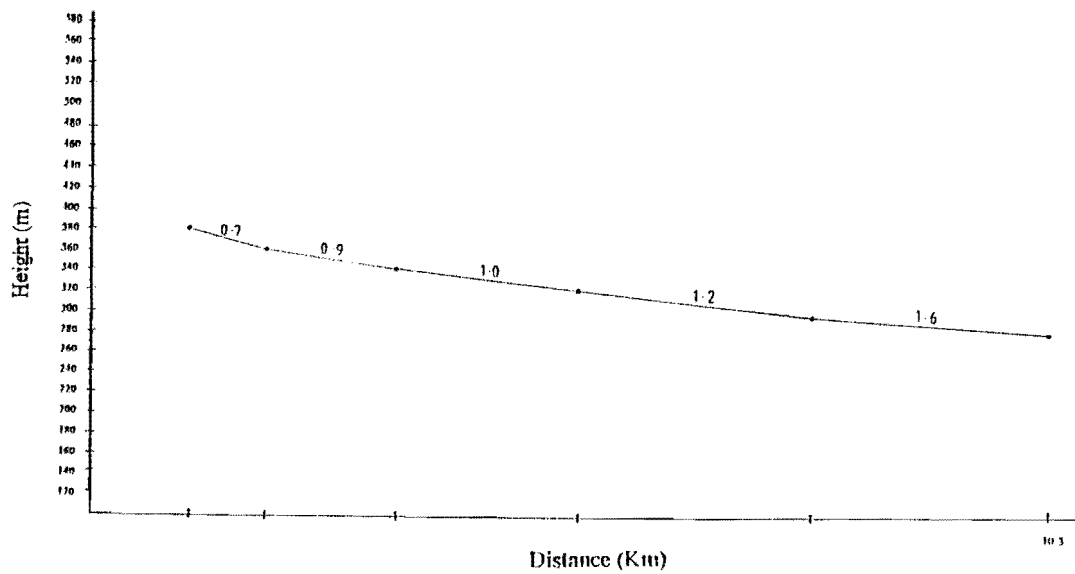


Figure 6.10cntd Stream gradient index results for the major streams.



Catchment: 9 River: 12 Waikari Stream B



Waikari River

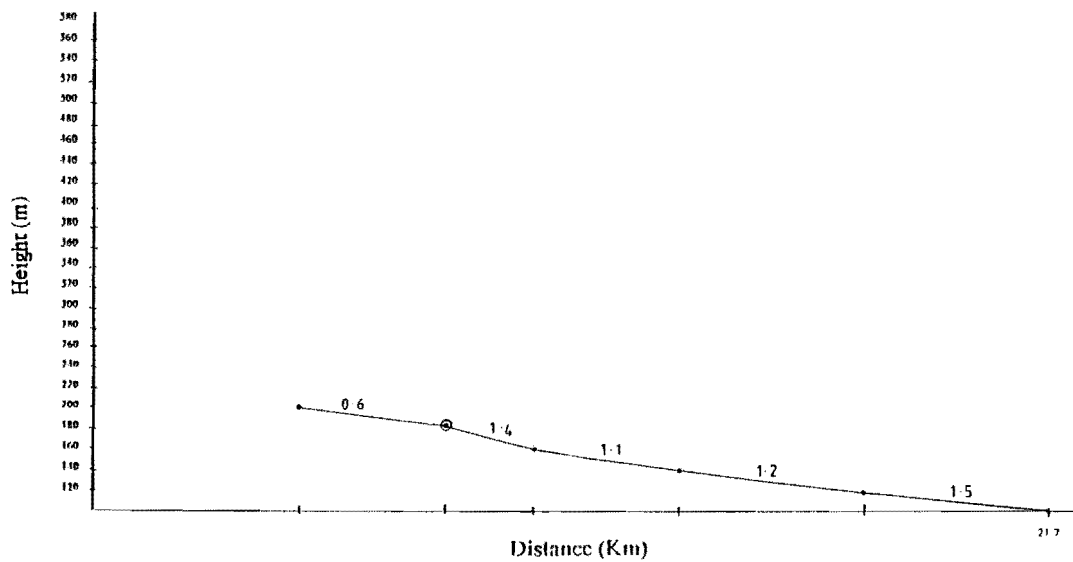


Figure 6.10cntd Stream gradient index results for the major streams.

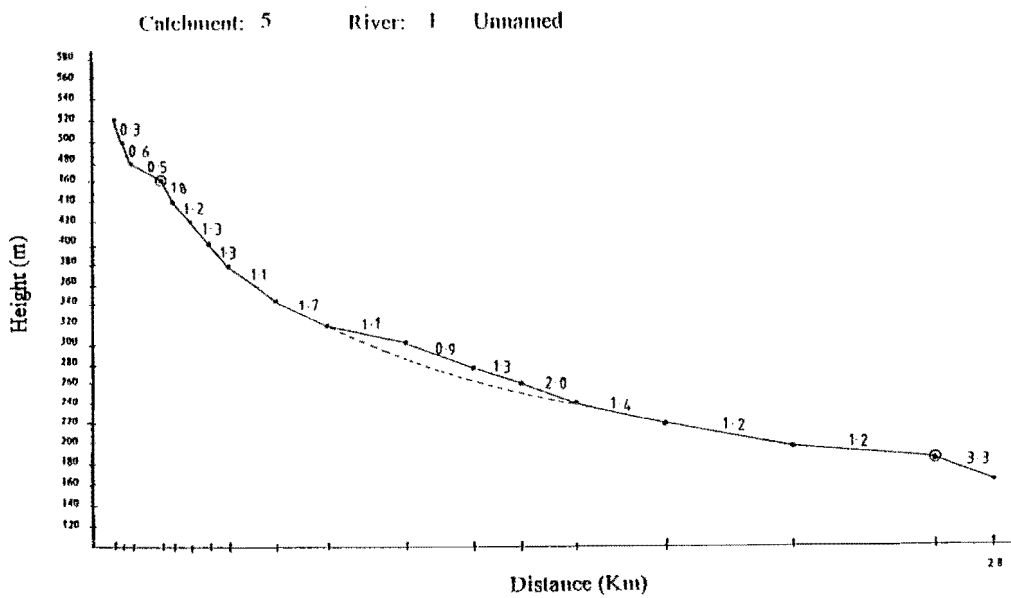
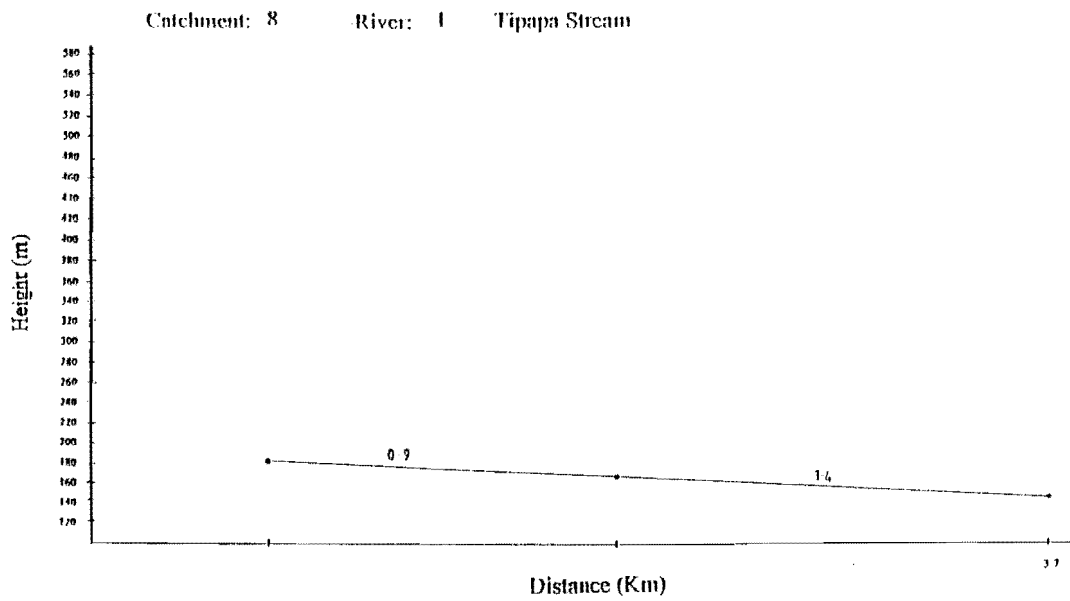
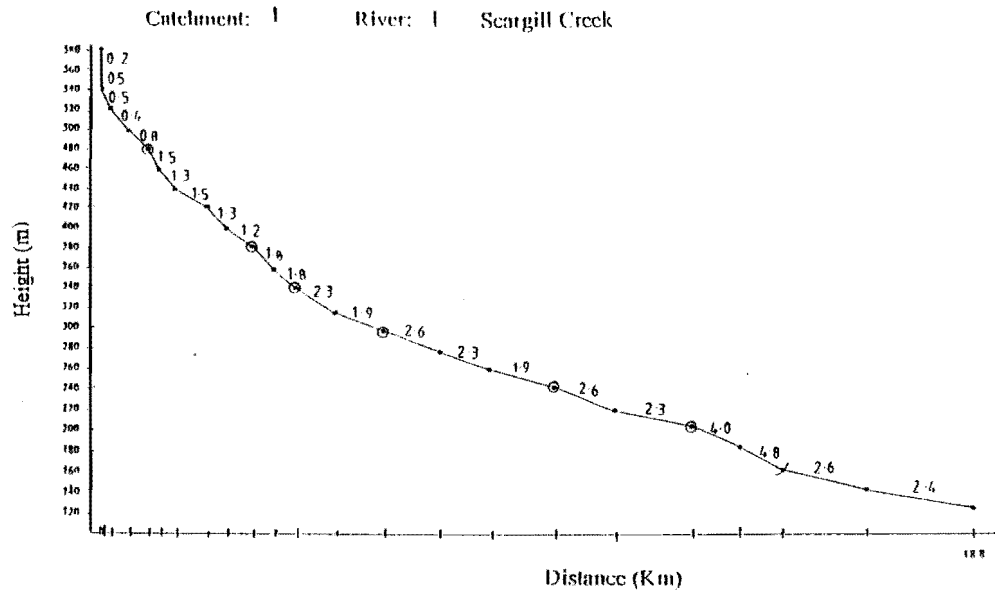


Figure 6.10cntd Stream gradient index results for the major streams.

#### 6.4.5.1 Isolating the effects of Bedrock

It is clear from map 4C that there are a considerable number of correlations between all types of anomalies and bedrock, and furthermore, that there is a great difference in the frequency of anomalies between the three major rock units (basement rocks, cover rocks and Quaternary deposits). These are discussed below.

There are very few effects at all shown in the gravel units, but this is likely to be largely a function of the very low range in relief that the gravels occupy. Two major convex breaks in slope are the most obvious effects in this unit, one immediately NE of Pyramid Valley, the other south of Foxdown Homestead. The latter can clearly be attributed to the presence of a major fan system over which the stream flows somewhat obliquely. The convexity NE of Pyramid Valley is interesting in that it crosses the highly faulted Pyramid Valley Anticline. Therefore, it may provide evidence for some activity there, although the presence of resistant Weka Pass Stone Member on either side may mean that the thin gravels there are reflecting the resistance of the underlying bedrock.

Effects in the cover rocks can largely be related to the presence of resistant lithologies. A number of convex profile segments occur in Scargill Hills Outlier, SE of Roto-iti homestead and along the northeastern boundary of Scargill Valley, generally reflecting drainage off the dip-slope of both Weka Pass Stone Member and Mt Brown Formation resistant beds. Conversely, a number of “cusp”-type knick-points appear to correlate well with drainage through the resistant beds. It is interesting to note that there are very few “step”-type knick-points in the cover rocks, the few that are present can either be related to drainage through the resistant beds as above, or as migrated knick-points from other units as discussed below.

The effects of resistant beds in the basement rocks are slightly more difficult to assess. The relatively wide spacing of the inferred trends compared to the size of individual beds appears to suggest that individual beds do not assert a direct control on the trends shown on the maps, although this is partly a function of the spacing of the topographic contours. Instead the trends of “packets” of beds were compared to the trends drawn from the knick-points. In a very broad sense it appears that there is a very good correlation between the beds and the trends at the very western and eastern end of the southern slopes of the Mt Alexander Range, but in most other places, the beds and the

trends are oblique. Therefore, it is interpreted that the major control on the gradient index anomalies in the basement rocks are faulting, as discussed below.

#### 6.4.5.2 The effects of faulting

##### *Moore's Hill - Greta Peaks Range*

Two major trends can be observed, paralleling, but slightly above the range-front along both the Moore's Hill and Greta Peaks Ranges. The lower of these is defined by both types of distinct knick-points, and these are interpreted to represent the upstream-migrated knick-points defining the original fault-trace. (The contours in these localities clearly trace a v-shape up the gullies for a short distance, suggesting that they originally occurred right at the range-front and furthermore these are only accurate to the nearest contour.) It is interesting to note that the knick-points are slightly closer to the range-front in the Moore's Hill Range than in the Greta Peaks Range, which may suggest that the last faulting event of Moore's Hill Fault is slightly younger than Greta Peaks Fault.

The second trend could either represent a secondary imbricate thrust fault immediately above the major fault, or a faulting and folding "event" (see below) at least one event prior to the event that produced by the lower trend; the study of drainage patterns along the range-front did not reveal the presence of any secondary faults there, and so the second interpretation is preferred. It is important to note that the level of resolution of the study (ie. using 20m contour intervals) means that each knick-point is not likely to represent a single thrust fault rupture, but likely the culmination of faulting, and more importantly, folding events over a period of time. Furthermore, the effects of folding are likely to accentuate the height of such steps, so that they do not represent the actual throw of a faulting event.

##### *Mt Alexander Range*

A similar set of trends can be observed on the northern side of Mt Alexander Range, although there they are considerably less continuous. The sets of anomalies immediately west of the major bend in the fault described in Chapter 4 are interpreted to represent



the now-migrated knick points of Mt Alexander Fault. The trend at the western end of Mt Alexander Range is interesting in that it appears to suggest that the fault continues further west than where mapped, a conclusion supported by the drainage pattern analysis.

On the southern slopes of Mt Alexander Range, particularly south and SW of Mt Alexander, a significant number of trends of anomalies can be observed to cut obliquely across bedding. These form parallel sets and the fact that at least two correspond well to the back-thrusts implied by the drainage study and the structure contouring suggests that these may represent a number of W-E to WSW-ENE trending back-thrusts splaying off Mt Alexander Fault. The close alignment of the anomalies with the anomalous drainage patterns suggest that these have not migrated any significance distance upstream, and therefore may be very young.

### *Lowry Peaks Range*

The northern side of the Lowry Peaks Range is characterised by a significant number of parallel trends that swing sympathetically with the mapped trace of Hurunui Bluff Fault. The northernmost trend is again interpreted to represent the slightly migrated last faulting event, the apparently large distance of this trend to the fault in eastern portions can be attributed to the presence of the now-uplifted, high altitude river terrace that has trimmed back the range-front in that region. Like the other faults, higher trends may simply represent the migrated evidence for earlier events, but the great number of these, and correlation with fractures suggested by the drainage pattern analysis, suggests that it is likely that at least some represent higher imbricate thrust splays faulting the Lowry Peaks Anticline, particularly the sets marked with an \* (map 4B).

The southern side of the Lowry Peaks Range possesses a number of trends very similar to that on the southern side of the Mt Alexander Range. Again, a close correlation with the fractures inferred from the drainage pattern analysis and a definite obliquity to bedding suggests that these represent back-thrusts. At the western end these, like those characterising Mt Alexander Range, trend W-E, and therefore may be directly reflecting the W-E trend of faulting of the Trig C Faults to the west, which show the same sense of movement.

#### **6.4.6 Conclusions: *Gradient index analysis***

Three sets of structures have been interpreted from the study of gradient indexes. The first appears to delineate the major fault traces as mapped on map 1, the majority of the knick-point determined trends are now situated some metres back from the mapped trace, logically interpreted as a function of upstream migration. It is also likely to be a function of the sensitivity of the method (definition of the position of the knick-points only to the nearest position of a 20 m topographic contour).

Significantly higher and wider spaced trends on the northern side of the Lowry Peaks Range however, are considered to represent true imbricate splays of the major thrust faults, the faulting of which may partly account for the lack of asymmetry of the Lowry Peaks Anticline, as shown on the cross sections. A trace on the northern side of the Mt Alexander Range suggests that Mt Alexander Fault may continue some distance further west than that mapped.

A number of back-thrusts are interpreted to characterise the southern slopes of both the Lowry Peaks and Mt Alexander Ranges. These trend W-E in western portions, where they are interpreted to reflect the apparently recent switch in facing direction of movement on the Lowry Peaks Fault System, to the southward verging Trig C Faults.

### **6.5 SINUOSITY INDEX ANALYSIS : *WAIKARI RIVER***

#### **6.5.1 Introduction**

Recent experimental work performed on the sinuosity of a river has suggested that in the absence of other features controlling the degree of sinuosity (such as changes in sediment load, sediment size, flow velocity and stream power), a change in sinuosity can often be used to infer subtle adjustments of bedform to disturbances of the stream bed (eg. Adams, 1980, Ouchi, 1985, Burnett and Schumm, 1983, Campbell and Yousif, 1985, Gomez and Marron, 1991). Campbell and Yousif (1985) proposed a model particularly applicable to New Zealand rivers, (ie. that characteristically flow on a relatively steep background gradient) whereby a distinct increase in sinuosity occurs on

the upstream side of an anticlinal axis (ie. where a decrease in gradient occurs), followed by a distinct decrease on the downstream side (ie. where an increase in gradient occurs) (figure 6.11). Therefore, it was hoped that similar relationships, when applied to the Waikari River, may reflect the presence or absence of structures beneath Waikari River, particularly considering the trimming of the ends of a number of major structures in the Moores Hill Region as noted in Chapter 3.

### 6.5.2 Methodology

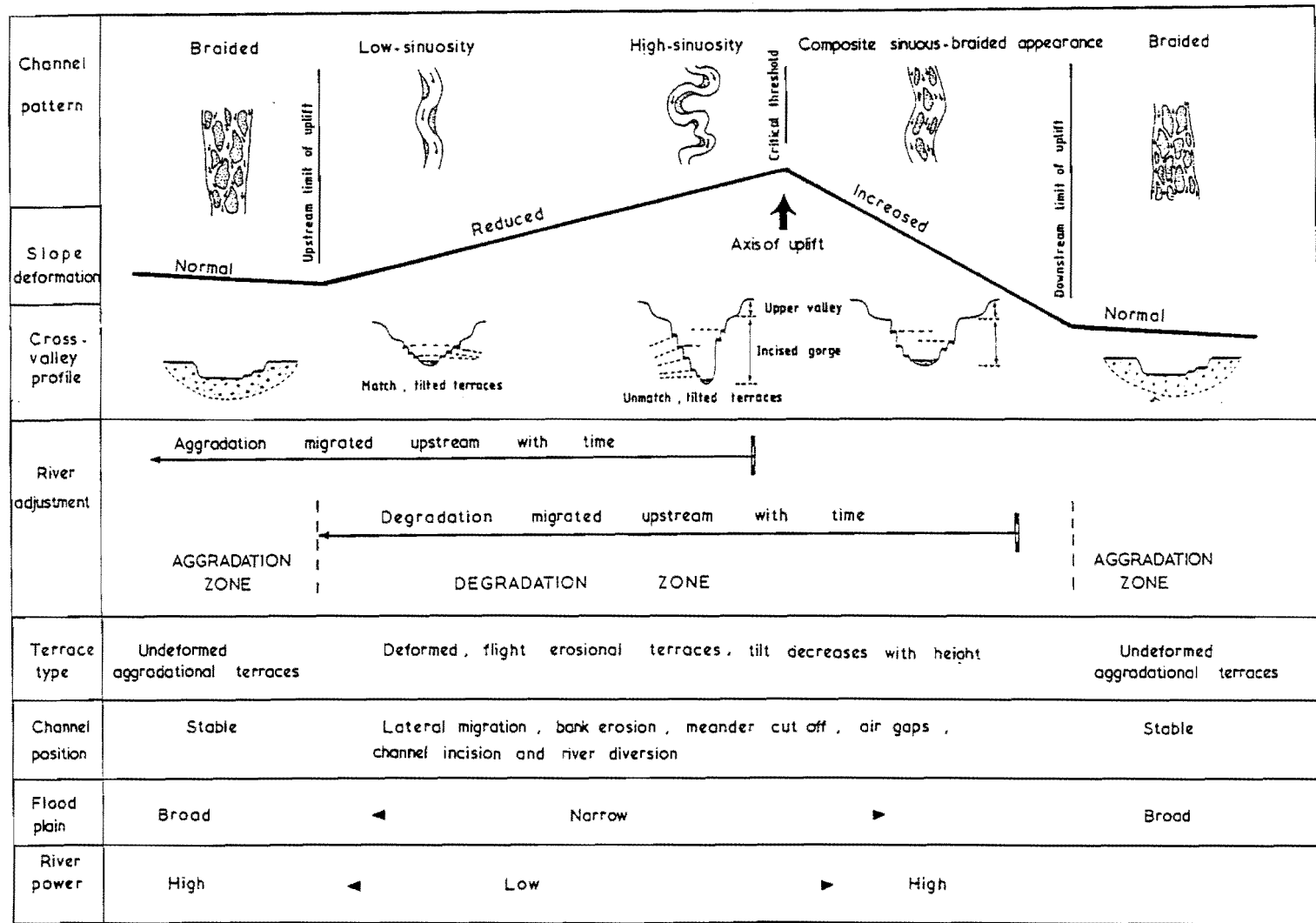
The sinuosity index (SI) is defined as:

$$SI = \frac{\text{the length of a river between two points (here i and j)}}{\text{the straight line distance between the same two points}} = \frac{RL_{ij}}{SL_{ij}}$$

(the abbreviations SI, RL and SL defined here).

Therefore, to measure the sinuosity of a river, the usual method employed is to take a segment of fixed straight line length (SL) and to superimpose it along the length of a stream a number of times. To calculate the sinuosity index value of the river (SI), the thalweg length (RL) must be measured between the endpoints of straight line segments and compared to SL. Besides the actual difficulties of accurately measuring the length of the curved line RL (either by hand, using a planimeter or a piece of cotton and a ruler, or by computer in which the stream has to be broken into segments between the two points and the length of that segment listed by the computer, which can be tedious), the positioning of the endpoint of the line can be somewhat arbitrary, particularly for highly sinuous streams. Consequently, a slightly “inverted” measure of sinuosity index was employed here, whereby the stream length itself was divided into a number of equal-length segments (easily achieved on AutoCAD) and the straight-line distance measured between them. Values of SI will therefore differ from those evaluated by other studies and areas of increased sinuosity will be characterised by a greater number of intervals measured, but they will still show areas of increased and decreased sinuosity relative to this stream.

**Figure 6.11** The effects on a braided river as it crosses a growing anticlinal structure. (From Yousif, 1987)



Two other major problems exist with a study of sinuosity index in terms of fixed intervals, namely:

- i) the choice of an appropriate interval length
- and ii) the choice of a starting position for the first segment.

Therefore, as part of this analysis, values of sinuosity index were measured for Waikari River 15 times, using three different interval sizes and five different starting points for each interval size, to test the relative effects that each have upon the results. These effects are described in full in Appendix 3, the results described below being those that were concluded to be the most representative for Waikari River, as shown on map 5.

The results are shown both directly in relation to the stream trace on maps 5A, 5B and 5C, (values of SI plotted beside their appropriate interval) and as a plot of SI versus distance (although it should be noted that distance here refers to the distance along the stream trace, not the straight line distance along the ground).

### **6.5.3 Results**

The graphs of sinuosity index versus distance, using the 4km interval possess three major areas of sudden increased sinuosity (and followed by a corresponding decrease to the base level sinuosity for the river; 1.5 and 1.7 as described in Appendix 3). Two extra “increases” are shown on the graph using the 2 km interval, but as described in Appendix 3, these may only be interpreted with caution. The positions of these anomalies are replotted on the trace of the river in figure 6.12 and are discussed from west to east in turn below.

The first, and smallest sudden increase in sinuosity can largely be related to a lithological control. The increase in sinuosity occurs due to the forcing of the river into a sharp meander around the western end of the strike-ridge of Weka Pass Stone Member on the southern limb of Mt Alexander Anticline. West of this point erosion of the ridge (which can be traced between gullies, see map 1) is likely to be a function of the end of the Late Quaternary drainage implied for the floor of Waikari Flat and that off the large alluvial fans there. Nevertheless, once the river crosses the ridge, it flows along the back of the dip-slope, hence possessing a very straight trace. However, it is notable that this is the area where Waikari Valley suddenly tightens, and is characterised by a fracture-

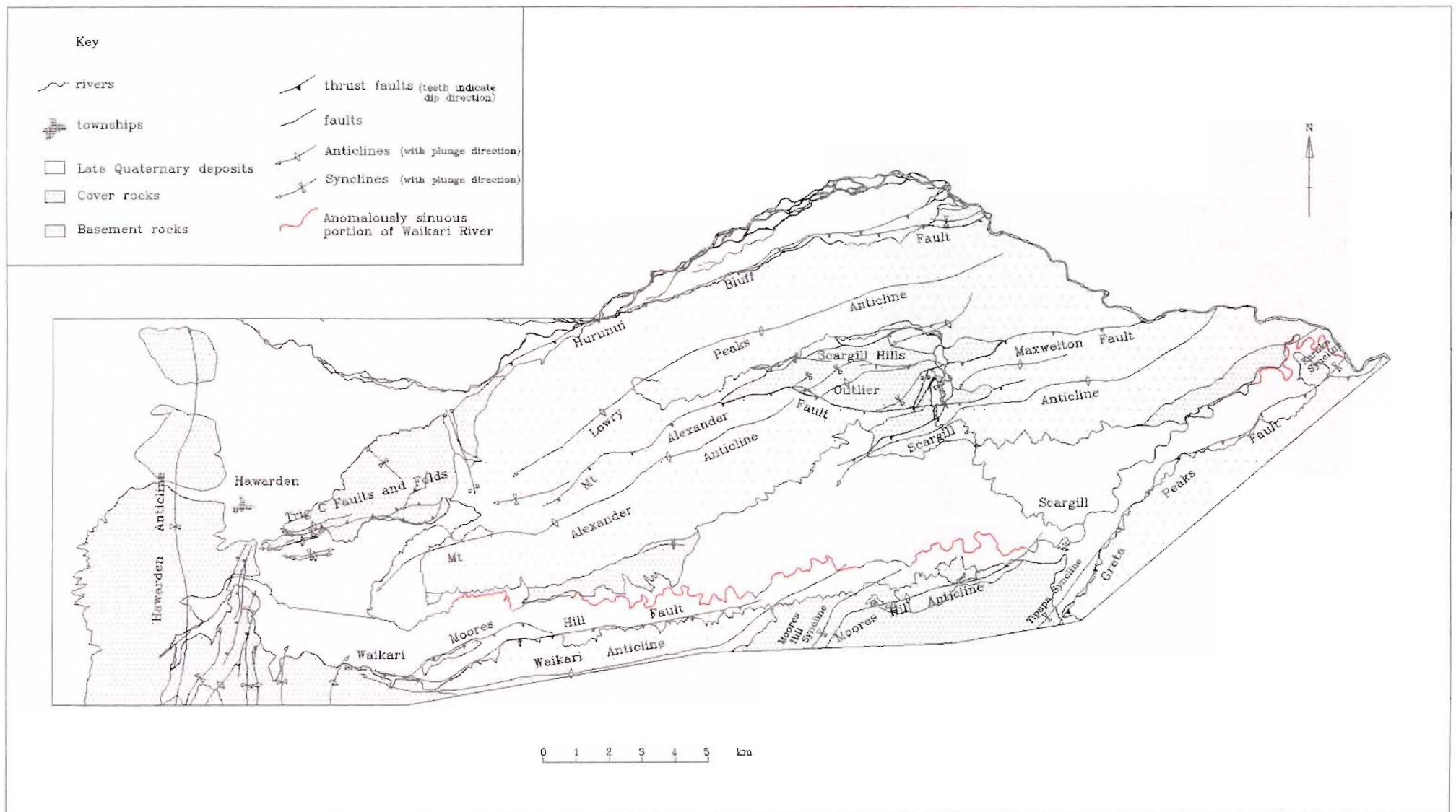


**Figure 6.12** The results of the sinuosity index study in relation to mapped structures.

controlled hummocky topography. Therefore, it may also be possible that some of the sinuosity may be uplift-controlled, particularly along the northern splay of Moores Hill Fault.

The next major increase in sinuosity occurs immediately at the end of the above-mentioned straight segment of the river. The increase is somewhat more gradual than that of the first segment, and appears to terminate at approximately the position of the last mapped trace of Moores Hill Fault. Therefore, if other factors such as sediment load and size, flow velocity and stream power have not suddenly decreased (for which there seems little evidence, given that the river has largely flowed over gravels for almost its entire length, and that no major tributaries have entered the river to this point), an increase in gradient due to faulting (or more likely, synclinal folding associated with faulting), may be implied. It is also interesting to note that the degree of curvature of the major terraces bounding the river (eg. map 1) there has apparently mimicked the changes in sinuosity of the river, suggesting prolonged downcutting of a meandering portion of the river. (Comparably, portions to the east show little effects of terracing, the small terraces that are preserved possess rather straight edges.)

The next, small anomaly could be interpreted as denoting the position of the plunging end of Waikari Anticline, but it should be noted that Laverock Stream flows into Waikari River immediately west of this anomaly. This together with the cautions concerning this anomaly, discussed of Appendix 5, make such an interpretation highly tentative.

The next major increase in sinuosity, is thought to reflect a true change in gradient, denoting the position of Moores Hill Anticline. The change appears to be large enough not to have been affected by the entrance of either Eastcott Stream to the west, or Foxdown Stream (the latter flows into Waikari River without affecting the central portions of the highly sinuous segment). In accordance with the model of Campbell and Yousif (1985), a dramatic increase in sinuosity occurs on the upstream side of the extrapolated trace of the anticline, followed by a comparatively straight segment on the downstream side, which fits well with the sinuosity patterns noted here. Like the last major sinuosity anomaly, similar effects can be noted in the degree of curvature of the terrace risers formed, particularly on northern sides of that segment, where a dramatic increase is followed by a decrease in curvature.

The sinuosity of Waikari River for the majority of Scargill Valley is very regular, the only exceptions being the dramatic increase at the very eastern end. The steady sinuosity throughout the majority of the valley is suggested to be largely a function of both: i) the increase in stream power gained by entrance of two large tributaries at Scargill (Scargill Creek and Tipapa Stream) and ii) the flow over cover rocks for at least the second half of the valley, where the added presence of resistant, dipping beds of Mt Brown Limestone have restricted the path of the river. In contrast to the valley upstream of the Scargill Creek junction, the major terraces bounding the river have very straight edges, which suggests a prolonged period of downcutting into the valley fill when base level was relatively static. There has been time for downward migration of meanders of regular amplitude to trim the terrace edge and establish an inner strath before renewed incision into the present meander thalweg.

The sudden and dramatic increase in sinuosity at the eastern end may reflect the sudden down-cutting into the softer cover rocks in the lower part of the sequence, but also it is notable in that it cuts into an abandoned surface of the Hurunui River, and hence may represent incision of an originally meandering pattern created by sudden flow onto a former river flat surface controlled by the changing base level of the Hurunui River.

#### **6.5.4 Conclusions: *Sinuosity index analysis***

In portions of the Waikari River where the effects of changes in sediment load and size, flow velocity and stream power can be dismissed, sudden increases in sinuosity may be attributed to subtle changes in bedform in response to the maintenance of grade on a deforming surface. In particular, it appears that Moores Hill Fault (and possibly Waikari Anticline) and Moores Hill Anticline have propagated into Waikari Valley, which suggests both:

- i) that these structures are active
- ii) that this evidence supports the highly sinuous, sigmoidal trace discussed in Chapter 5.



## 6.6 TIMING OF EVENTS

The influence of active tectonics in preceding chapters has thus far only been described in relative terms. The purpose of this discussion is to attempt to place some constraints on the timing of such events.

There are four major geomorphological features that constrain the timing of the diversion of the Waitohi and Hurunui Rivers proposed here. The first is the age of the major alluvial fans of Waikari Valley. These do not rest on major glacial-related aggradation surfaces that characterise large parts of north Canterbury (eg. Gregg, 1964). Furthermore, they possess a loess covering. Lastly, they are relatively thin. Together, these suggest that the fans were predominantly built during the Late Pleistocene, with very little addition during the Holocene. Therefore, any drainage that may have either flowed along Waikari Valley, or more likely, across Scargill Hills Outlier, must pre-date the last Pleistocene glaciation event. The fact that these fans have not been built extensively in the Holocene suggests that the major uplift along the range-bounding faults may have been relatively quiet in this time.

The second major geomorphological feature of concern is the alluvial aggradation surface that makes up the floor of Waikari Flat and the immediately adjacent portion of the Culverden Basin. This surface is overlain by a number of alluvial fan deposits around its margins, which at the eastern end of Waikari Flat appear to be continuous with those described above for Waikari Valley. Uplifted gravels of the floor of Waikari Flat on the plunging end of Mt Alexander Anticline possess a loess covering that is slightly thicker than that of the alluvial fans of Waikari Valley, but apparently still only one sheet (P. Tonkin, pers. comm., 1995). Therefore, this surface must have been formed during the later glaciation events of the Late Pleistocene. Consequently, the age of the structures considered to be the most active in this area (the Trig C Structures) is Late Pleistocene. The uplifted gravels now lying above the watershed between Hawarden township and Waikari Flat, through which it is suggested the Waitohi River may have once flowed, have a loess capping exposed in the old railway cuttings. This would indicate that the latest time of which the river could have crossed the Trig C Structures predated the last Otiran aggradation phase.

The section of gravels of the eastern entrance to Weka Pass that contains reworked greensand provides the third geomorphological feature that can constrain the timing of proposed major recent tectonic events. These gravels form the lower part of the major alluvial fans that have formed on the northwestern side of the Omihi Valley. The gravels are exposed in a gully in the main road at an elevation which is comparable to the up-warped aggradation surface which predates the last, Late Otiran aggradation event forming the Omihi (Canterbury) surfaces (Nicol et al, 1994). This surface is thought to be a correlative of the Teviotdale Surface (Yousif, 1987) stratigraphically bracketed on the coast as post-dating the high sea-level stands of the last Interstadial. It is cut by a later marine terrace predating the final low stand of the last glaciation. It is thought to relate to Glaciation isotope stage 5, (approximately 60 000 years b.p., Yousif, 1987). The fan gravels in the road cutting have been trimmed by a late degradation terrace so that the height of the original surface and any indications of age such as loess and soil cover have now been removed.

The final geomorphological feature is the major degradational surface along the Lowry Peaks Range-front. This surface contains pockets of gravels of both fluvial and alluvial fan origin, but has largely been cut into basement bedrock. The lack of a loess capping on this surface, suggests that a Holocene age for its abandonment by the Hurunui River, which is likely to represent the last uplift event along the Hurunui Bluff Fault. This also confirms that the most active system of the Lowry Peaks Range - Waikari Valley district is the Lowry Peaks System.

## **6.7 HISTORICAL SEISMICITY**

The seismicity of the region, as recorded by the (relatively widely spaced) National Seismograph Unit (figure 6.13), over three periods, namely 1965-1975 (Hatherton, 1980), 1964-1987 (Reyners, 1989) and 1990-1993 (Anderson and Webb, 1994) is shown in figure 6.14 and 6.15. All three indicate that activity in the upper crust of this study area currently represents a seismically quiet portion of north Canterbury, most motion either concentrated on the Porters Pass - Amberley Fault Zone to the south or the Hope Fault to the north. The more closely spaced, temporary network established for a 10 week study on a north Canterbury (figure 6.16) by Cowan (1992), which

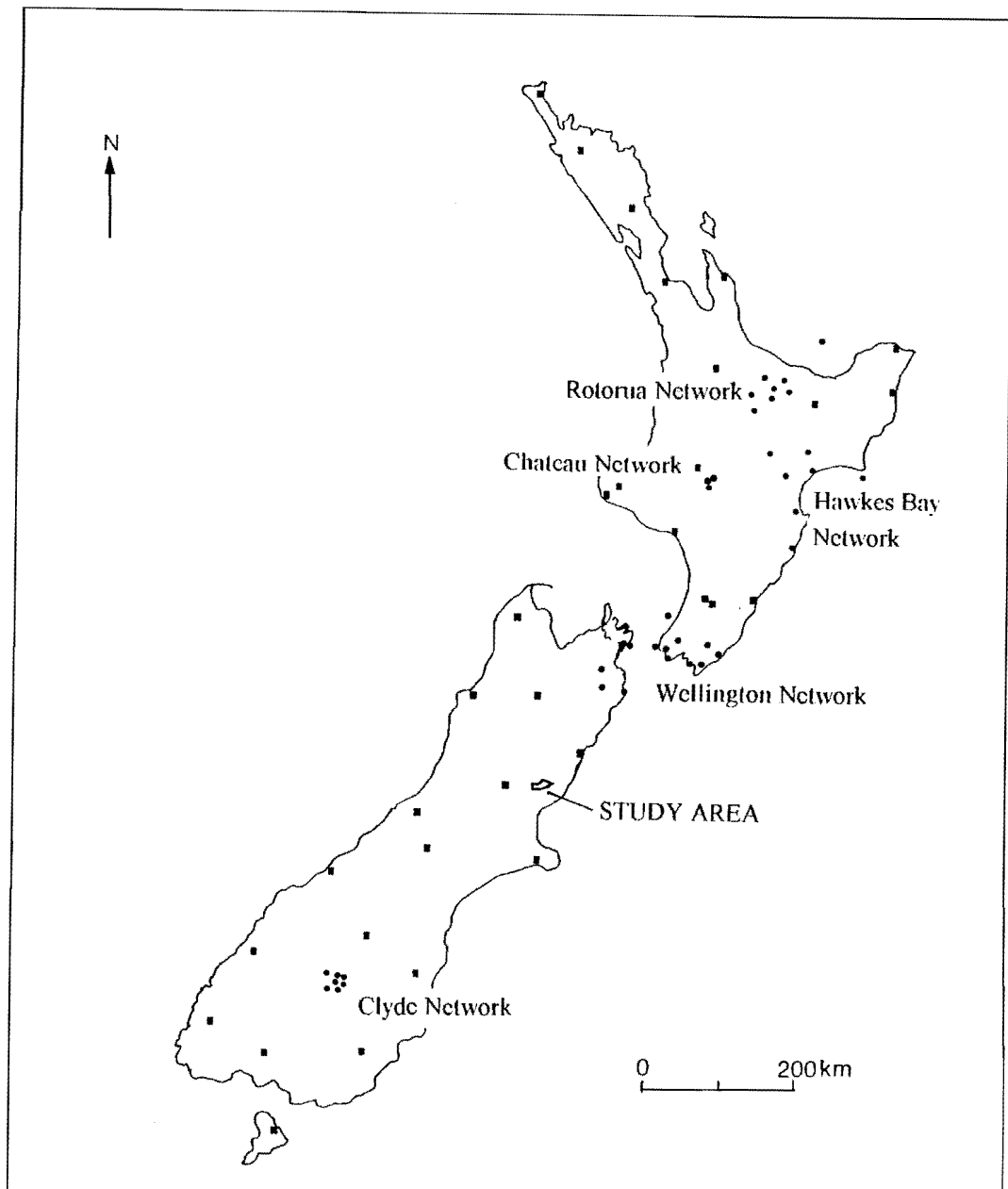


**Figure 6.13** Location of stations of the National Digital Seismograph Network. Circles represent telemetered stations, squares represent EARSS stations (stand-alone, gain-ranging stations). (Redrafted from Anderson and Webb, 1994).

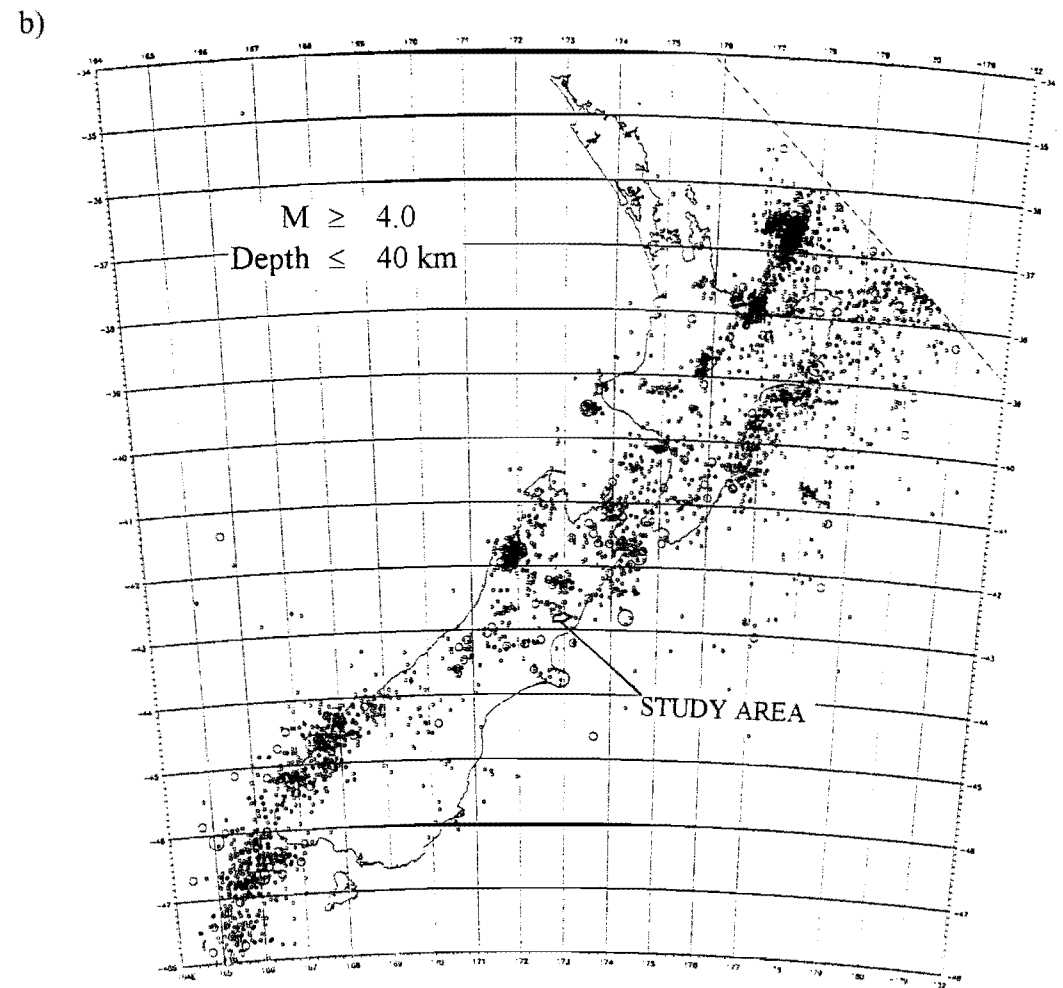
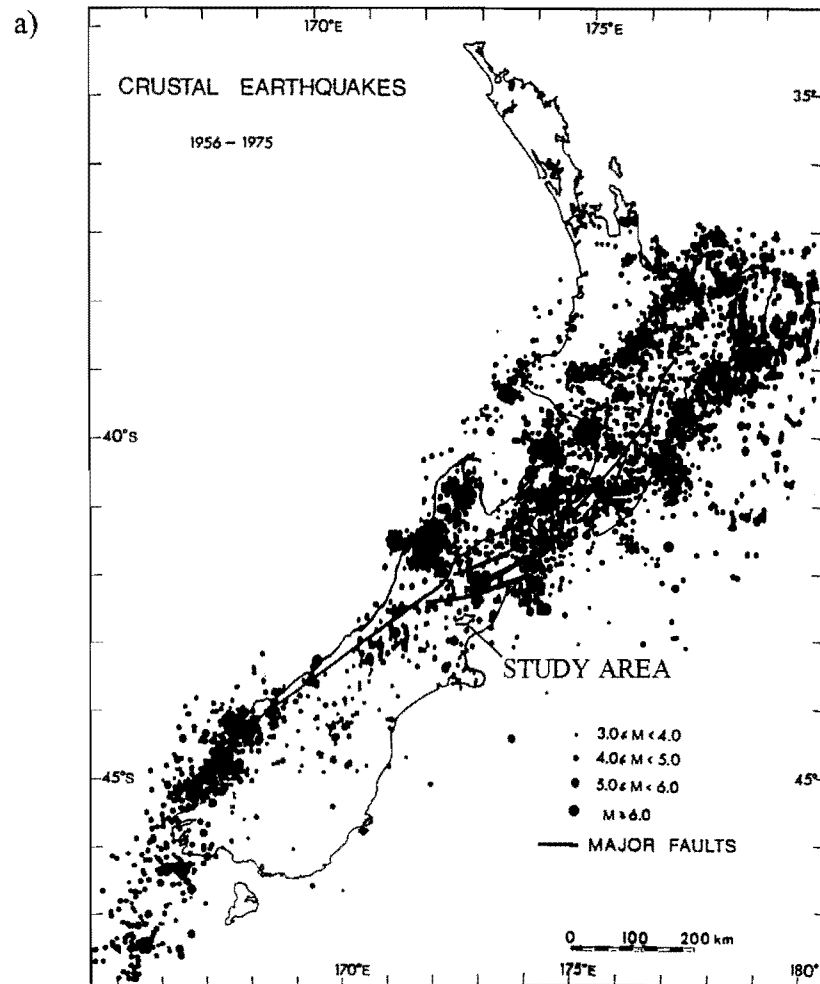


**Figure 6.14** Seismicity within New Zealand for the periods: a) 1965-1975 (Hatherton, 1980) and b) 1964-1987 (Reyners, 1989).

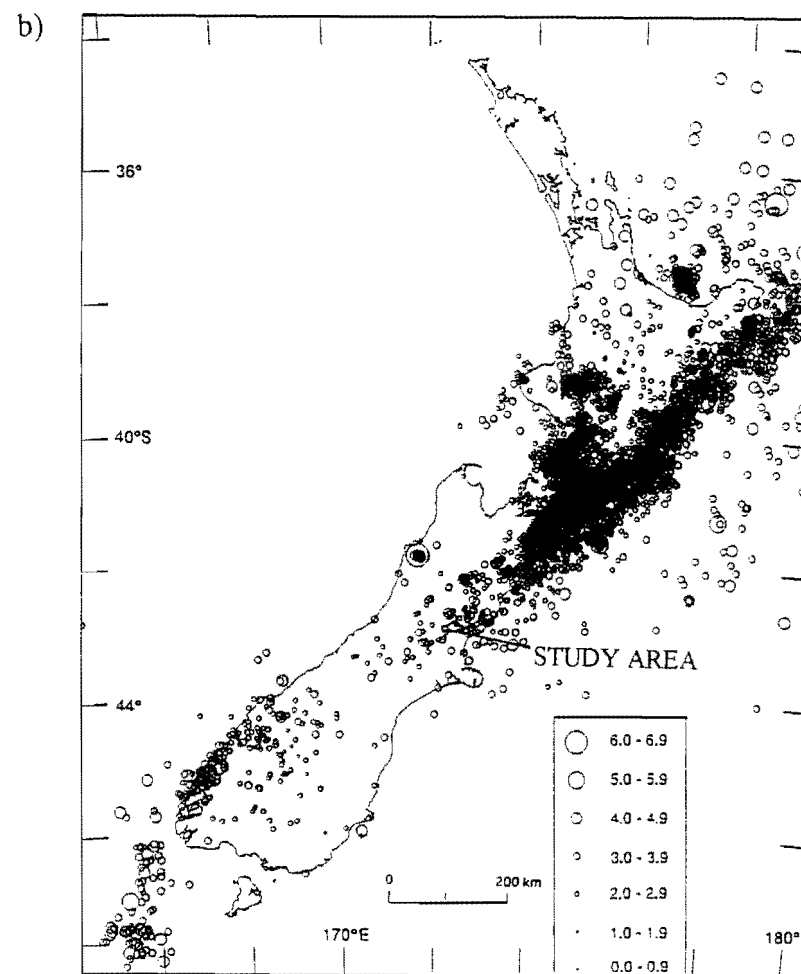
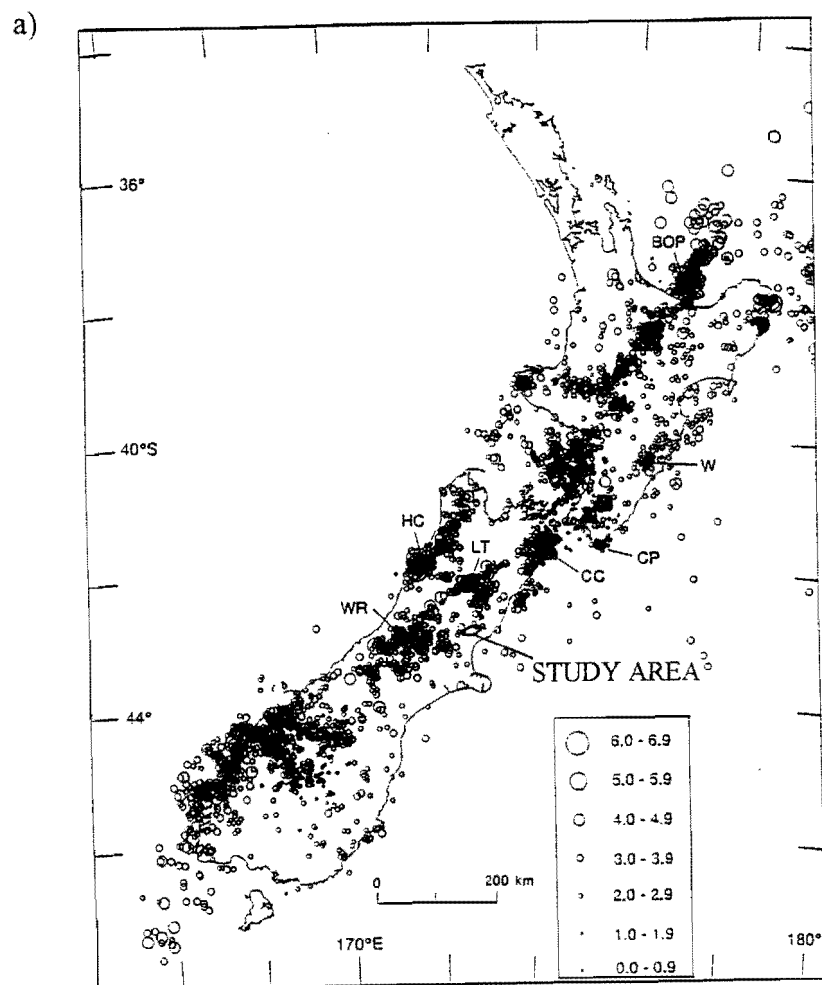


**Figure 6.15** Seismicity within New Zealand for the period 1990-1993 (Anderson and Webb, 1994), with focal depths: a) < 15km and b) < 40km.

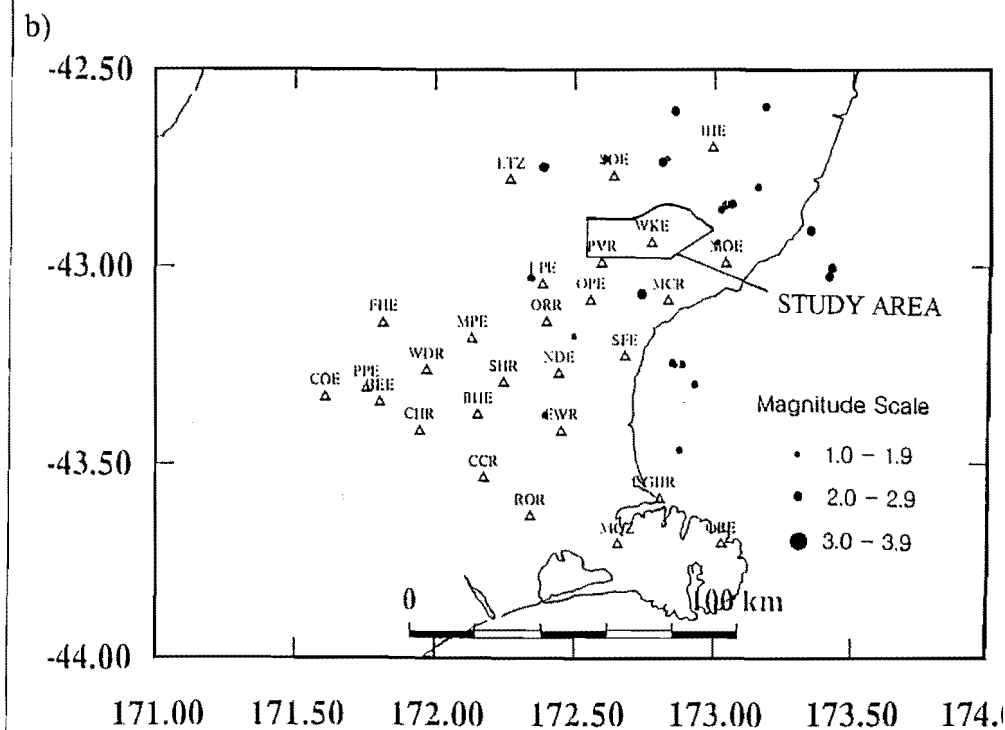
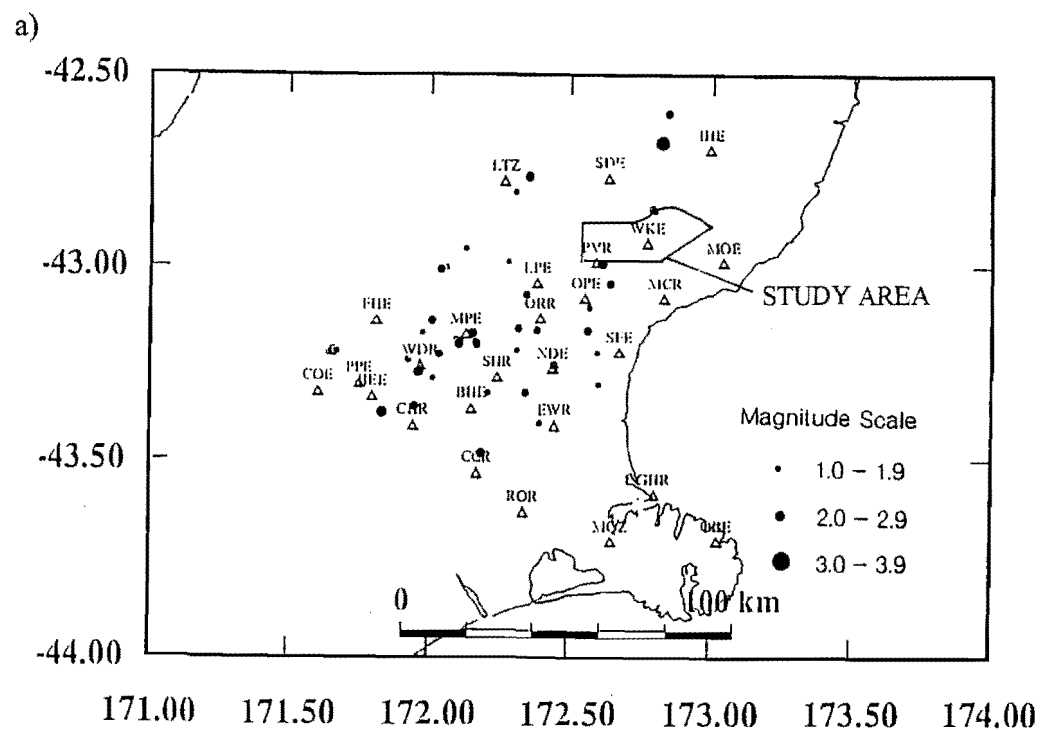


**Figure 6.16** Seismicity of the north Canterbury region for the 10 week survey (September 1 - November 15, 1990) by Cowan (1992), with focal depths: a) < 12 km and b) > 17 km.

included stations at Pyramid Valley and near Laverock Homestead, also suggests that this area is currently seismically quiet compared to other portions of north Canterbury, although a notable exception does exist with two shallow level events occurring in approximately the position of Hurunui Bluff Fault. These data support the general conclusion that the majority of this area is either currently inactive, or strain rates are very low, and may support the suggestion that the latest motion is concentrated on the Lowry Peaks Fault.

Interestingly however, there is some evidence to suggest that a major earthquake may have been centered on the study area in 1922. The Christmas Day Earthquake of 1922 was felt from Napier in the North Island to Dunedin in the South Island. Damage was not extensive, but was intensive in the Hawarden to Cheviot Region, where widespread toppling of chimneys occurred, and an “extension slip” occurred on the north bank of the Waikari River “two miles below Scargill”, which temporarily dammed the river there (Skey, 1925, Jobberns, 1925). The magnitude of the earthquake was 6.4 Ms and of crustal depth (Dowrick and Smith, 1990), and the information from the Seismological Survey suggested an epicentre of 43 S 173 E, approximately the Motonau Region, as shown on figure 6.17a (Gutenberg and Richter, 1949, Eiby, 1968, Dowrick and Smith, 1990, Dowrick, 1991). However, a different set of isoseismals were produced by Skey (1925), considered by G. Downs (pers. comm. to J.K. Campbell, 1994) to be based on a “different and more extensive set of information from that which was available to the Seismological Observatory in 1922 and Eiby” and are shown in figure 6.17b. These are principally centered on the Waikari - Scargill Valley area, suggesting movement on the Kaiwara Fault System, or perhaps on southern portions of the Mt Alexander - Maxwellton Fault System, particularly given the possibility for evidence of an active scarp on Scargill Creek Fault. Given the nature of the data however, any such suggestions remain purely speculative. It may be important to note that the data from Cowan’s (1992) survey predicted mainly strike-slip motion on ENE to NE - striking focal planes in the north Canterbury Region, which may favour movement on faults such as Moores Hill Fault.

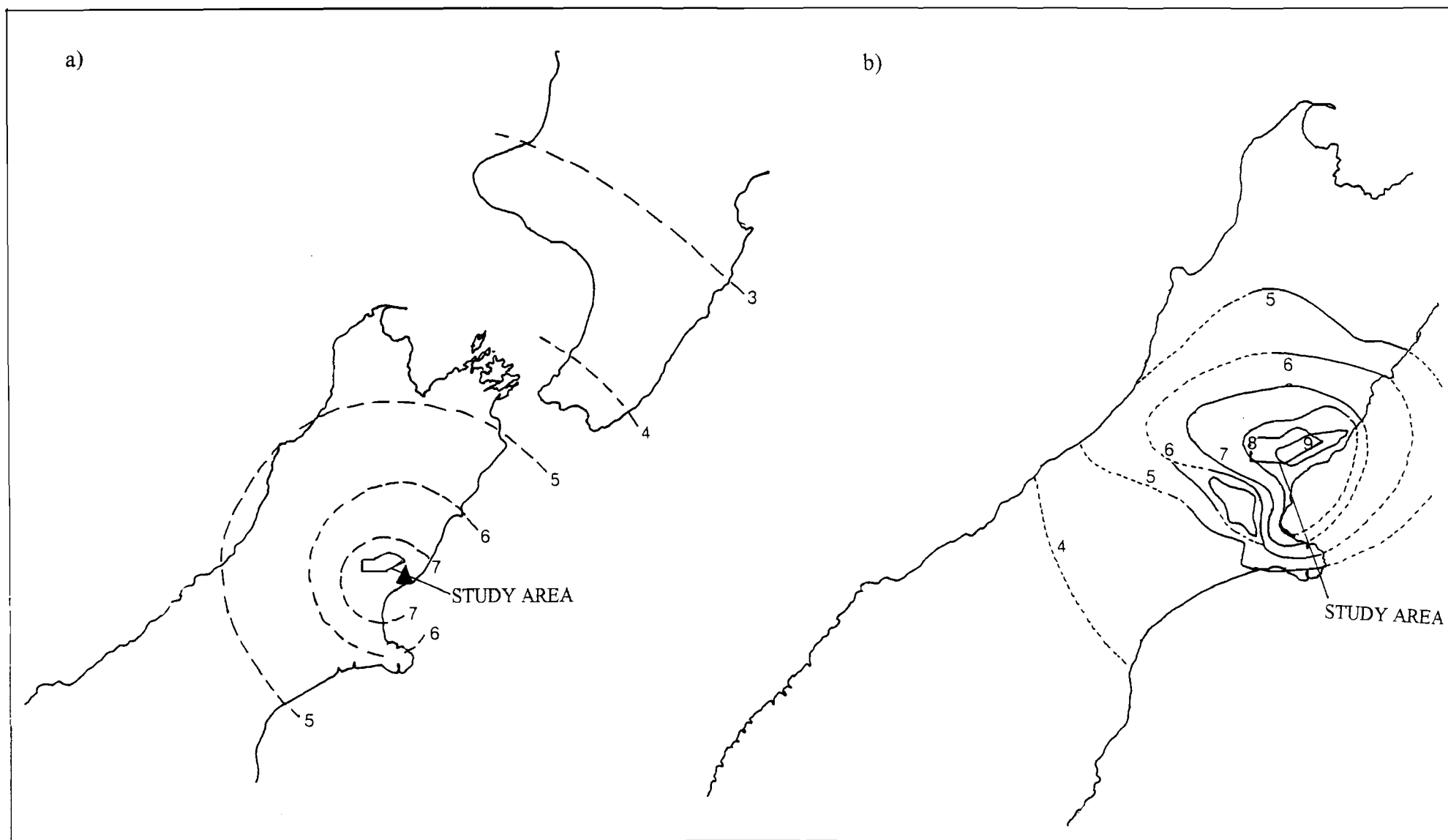


**Figure 6.17** Isoseismal maps of the Magnitude 6.4 earthquake of 25th December, 1922, produced by: a) Eiby (reference supplied by G.Downs, 1994) and b) Skey (1925).



## 6.8 CONCLUSIONS AND NEOTECTONIC GEOMORPHIC MAP

The combination of the historic seismicity data, the observations of active fault scarps and the influence of tectonics on drainage suggests that movement on the major faults (and associated folding) has largely ceased in this area, or at least continuing at a much slower rate than that of other faults in north Canterbury (such as the Hope Fault and members of the Porters Pass Amberley Fault Zone). The majority of recent motion appears to have occurred during late Pleistocene times. The nature of that motion, and the likely relative ages have been summarised on a generalised neotectonic geomorphic map (Map 6), based loosely on that of Yousif (1987). The major features on the map are:

- i) The majority of the most recent motion in the study area is situated on the Lowry Peaks Fault System (to which a number of splays have now been added), with the possible exception of dextral strike-slip motion on Moores Hill Fault and some indications of Holocene rupture on Scargill Creek Fault.
- ii) A large component of the motion on the Lowry Peaks Fault System, and portions of the Mt Alexander - Maxwelton Fault System has now been transferred to southward-verging motion on the Trig C Faults (and associated folds), and a number of back-thrusts on the south-western sides of Lowry Peaks and Mt Alexander Anticlines, which are oriented W-E due to partitioning of SW-directed thrusting between these and N-S trending, eastwards verging structures that combine to over-thrust the plunging ends of the major WSW-ENE trending imbricate thrust system.
- iii) Within Mt Alexander and Lowry Peaks Ranges, partitioning of strain has locally produced complementing sets of N-S trending cross-fractures
- iv) Evidence for some continued oblique thrust-type motion on the major faults is supplied however by the along-strike propagation of folds such as Moores Hill, Mt Alexander and possibly Waikari Anticlines, the trends of which adhere to the observed sinuous trend of a number of the major folds in the area, again reflecting the oblique angle of a number of the faults to the major compression direction.

## CONCLUSIONS

### 7.1 SYNTHESIS

The purpose of this thesis was to determine the geometry and kinematics of deformation in the Lowry Peaks - Waikari Valley district, where two fundamental sets of structures in north Canterbury locally meet. The following discussion summarises the results of this study in the context of the likely deformation history of the district during the major Late Pliocene-Recent deformation events.

Stress tensor analysis results for Mt Alexander Fault can be resolved in a number of ways. One is that an early period of localised NE-SW to N-S sub-horizontal compression has been overprinted by later NW-SE horizontal compression, which has been found to be the predominant tensor configuration for the rest of the area. Geomorphology suggests that the majority of motion on Mt Alexander Fault is currently situated at the western end. Therefore, the NE-SW to N-S horizontal compression recorded at the eastern end must be older, and is likely to be locked. That the fault is currently locked fits well with the sinistral motion recorded by the fault at Scargill Hills Quarry, which is opposite in sense to the recent dextral motion of other W-E trending faults in north Canterbury. Therefore, the first fault to be formed in the study area is the eastern end (or ramp area) of Mt Alexander Fault, in response to likely localised NE-SW to N-S sub-horizontal compression.

The major deformation event now affecting all but possibly the eastern end of Mt Alexander Fault appears to have formed in response to NW-SE oriented sub-horizontal compression. Earliest deformation of this event occurred along the Kaiwara Fault System, initially as both faulting and associated fault-propagation folding of the true NE-SW trending Greta Peaks Fault and associated folds. Faulting on Moores Hill Fault (and associated folding) may have also been early, forming with a distinct WSW-ENE trend, which may represent reactivation of pre-existing Late Cretaceous basement faults relating to the Hurunui High. It is notable that Moores Hill Fault represents the apparent northern boundary of the distribution of Waipara Greensand Formation in the area, and therefore is likely to be close to the original edge of the structural high. The result of the

obliquity between the fault and NE-SW trends predicted by NW-SE oriented compression is the development of sigmoidal-shaped, angular fault-propagation folds (Waikari Anticline, Moores hill Syncline and Moores Hill Anticline), whereby the central axial trace parallels the fault and the ends are oriented normal to the compression direction. The other manifestation of oblique compression is the development of NNW-SSE trending cross-folds, which create the low topography on the central portions of the system and complementary high points such as Mt Alexander, Castle Hill and Ben Lomond.

Structures of the Mt Alexander - Maxwellton Fault System and associated structures are the next youngest, likely to have incorporated the now locked portions of Mt Alexander Fault during early stages of deformation, and causing the displacement transfer between this fault (and the associated fault-propagation fold, Mt Alexander Anticline) and the Maxwellton Fault - Scargill Anticline structures. The entire system, particularly at the eastern end is again largely oblique to the NE-SW trend predicted by NW-SE compression and the result is the development of NNW-SSE trending cross-folds, some of which can be correlated across to those of the Moores Range area. Cross folding also can be noted on a small scale in Scargill Hills Outlier, the complex set of cover rocks preserved within the centre of Mt Alexander Range due to a combination of down-warping on a large synclinal cross-fold and displacement transfer between the two major members, and results in a conical interference fold shape.

Continued NW-SE compression is then likely to have resulted in folding, and more recently faulting on new structures at the leading edge of the imbricate thrust system, the Lowry Peaks Fault System and associated structures. Folding occurs on a single fault-propagation anticline (Lowry Peaks Anticline) and faulting on two splays, Hurunui Bluff Fault and Hurunui Gorge Fault. The displacement transfer between these two faults has resulted in the creation of an intermediate-size anticline-syncline pair between them. NNW-SSE trending cross folding also characterises this system, but is not as well developed as for the other two systems.

Deformation on the three members of the large imbricate thrust system appears to have continued into at least Late Pleistocene times. Folding has continued to propagate into Waikari Valley in central portions of the Kaiwara Fault System, with Late Pleistocene uplift occurring on a WSW-ENE trending splay at the western end of Moores Hill Fault.

The along-strike propagation of Mt Alexander Anticline has lead to the uplift of gravels in the Waikari Flat area during the Late Pleistocene, the orientation of which suggests that it is likely to link with synchronous faulting and folding on eastwards-verging, N-S trending structures to the south of the area. Pleistocene, eastward motion on the N-S trending structures is likely to have caused the truncation of the western end of Moores Hill Fault by thrust faulting at depth reflected in the tilting and squared off end of E-W trending folds such as the Timpendean Syncline. Uplift along the frontal edge of the Lowry Peaks Fault System and associated structures has continued right into the Holocene.

Following Late Pleistocene uplift along the Kaiwara Fault System, Moores Hill Fault has been reactivated as a dextral strike-slip fault. This has bearings on the origin of the sigmoidal fold shapes. Sigmoidal fold shapes can be generated by fundamental strike-slip motion on a sub-vertical fault at depth (eg. Jamison, 1991) for which this fault now clearly has evidence. However, the reactivation of this fault as a predominantly dextral strike-slip fault is proposed to be late stage, after the main faulting event in which the fault was acting as the western end of the southern member of the major imbricate thrust system. The result is that the highly curled ends of the sigmoidal folds are oriented largely normal to the motion direction, and are now in fact acting as new fault-propagation folds in their own right. The reactivation can largely be attributed to its nearly W-E trend. Widening of the plate boundary transfer zone in north Canterbury due to rotation of the Hikurangi Margin with time means that W-E trending faults are now more optimally oriented to accommodate strike-slip motion, the result being the development of a number of new oblique dextral strike-slip faults in north Canterbury (eg. Boby's Creek Fault, Pyramid Valley Fault, Nicol, 1991).

The result of the collision of the WSW-ENE trending structures (propagating along-strike to the west) and the eastward-verging, N-S trending structures related to major imbricate thrusting on the western margin of the Culverden Basin (interpreted recently as back-thrusts off the listric east-dipping Alpine Fault, Pettinga et al, 1995) is the development of superficial over-thrusting of the plunging western end of the WSW-ENE trending system. Out-of-sequence faulting, or roof-thrusting off the plunging, western end of Hurunui Bluff Fault has developed on a W-E trend (Trig C Structures), the trend likely to be the result of strain-partitioning of SE-verging motion on these and the

associated N-S trending structures to which they appear south of Hawarden to just beginning to link.

The result of this over-thrusting is to force the major members of the imbricate thrust system down beneath Waikari Flat, so that the N-S trending set of structures is being largely stacked on top of the WSW-ENE trending thrust belt. An exception does exist in that the major N-S trending thrust fault forming the boundary between the two sets of structures at Waikari is forming beneath Old Weka Pass Anticline, which appears to link with Mt Alexander Anticline to the north. Therefore in that region, the WSW-ENE trending belt of structures is over-riding the N-S set. The analogy to this interaction of the two sets is an interfingering or interleaving relationship, achieved on largely shallow-dipping, and currently rather superficial thrust faults.

Associated with the change in facing direction of the western end of the Lowry Peaks Fault System, is the recent development of a number of back-thrusts on the southwestern limbs of Mt Alexander and Lowry Peaks Anticlines. Internal shortening due to continued oblique motion may also be accompanying these structures as both cross-faulting and folding. It has been noted that the influence of N-S cross-folds becomes increasingly prominent from east to west.

In conclusion, the deformation of the Lowry Peaks Range - Waikari Valley district from the Late Pliocene to Recent has been complex. Apart from some early effects of NE-SW to N-S sub-horizontal compression, NW-SE sub-horizontal compression has been partitioned between a number of orientations, producing complex oblique structures and interactions analogous to interleaving between sets of structures on all scales.

## **7.2 REGIONAL CONTEXT**

The major WSW-ENE trending imbricate thrust system described above forms the northern portions of the western end of a major belt of SW-NE trending structures that characterise the east coast of north Canterbury and the area immediately offshore (figure 1.1).

The continuation of a number of the structures mapped here to the NE has been suggested throughout this study, although it is clear that such structures are likely not to continue indefinitely on the same strand. In particular, both the Lowry Peaks and Kaiwara “Faults” have now been recognised as systems of overlapping faults. The former undergoes at least one set of displacement transfer at the mouth of the Hurunui Gorge and the shape of the latter suggests that it may also splay in the Hurunui Gorge region, another strand continuing the major range-bounding activity on the eastern side of the Kaiwara Valley. Further NE again, the recognition of the importance of splaying may facilitate the apparent change in facing direction of the Kaiwara Fault System to bound the western margin of the Cheviot Basin.

To the west, the imbricate thrust system is clearly beginning to “collide” with structures of the N-S trending Mt Grey to Island Hills system, which has its origins in the Porters Pass Amberley Fault Zone, and the associated set of clearly orthogonal structures of the Waipara - Weka Pass region to the south. The collision is just starting to be “felt” in the Waikari Flat region, where two sets of structures at right angles appear to be moving synchronously as the apparently superficial over-thrusting of the plunging ends of the WSW-ENE trending imbricate thrust system as described above.

Structures in the Amberley to Motunau region to the south have been considered in recent years to represent surface expressions of the eastern end of strike-slip faulting on the Porters Pass Amberley Fault Zone at depth (Yousif, 1987, Cowan, 1992). Folds were interpreted as en-echelon folds resulting from deep-seated dextral motion on rigid blocks at depth, later affected by faulting on high angle reverse faults. However, this study shows that highly sinuous folds may also be created within a thrust faulting regime, if motion has been largely conducted on faults at an oblique angle to the original normal compression imposed on the strike of the thrust front. The observations of the clear presence of a major thrust system and associated folds directly along strike and offshore of the structures of the Amberley to Motunau Region by Barnes (1993) suggests that these structures may need to be re-examined in that context (particularly given the very clear W-E trend of the centre of two of the clearest sigmoidal folds, the Kate Anticline and Teviotdale Syncline).

In Chapter 1 it was noted that the W-E or WSW-ENE trend of the structures in this region could also be observed in many other parts of north Canterbury. In particular,

they appear to be forming with a regular spacing. Evidence from the Waipara - Weka Pass Region to the south and this study suggests that the likely control on these trends is inherited from Late Cretaceous basement structures, of which this area appears to have been characterised by a horst structure. Logically then, the regularity of these structures is likely to be reflecting the original spacing of Late Cretaceous, extensional horst and graben structures.

Drainage of the Lowry Peaks Range - Waikari Valley area appears to have been highly affected by tectonics. In particular, the Waitohi and Hurunui Rivers may have once followed more direct paths to the sea from their exit out of the high topography domain (Southern Alps region) in the NW. Structural lows such as that west of the Trig C Structures and then west of the Timpendean Syncline, and that currently occupied by Scargill Hills Outlier and the western end of Moores Hill range may have been utilised as alternatives to the current path traversing the major WSW-ENE trending structures towards the sea. The abandonment of the latter is likely to be due to continued uplift of the relatively continuous Lowry Peaks Anticline along Hurunui Bluff Fault. Once this reached a level too high for breaching, the river would have been forced along strike until cover rocks preserved in the displacement transfer zone between Hurunui Bluff Fault and Hurunui Gorge Fault were encountered, combined with the buffer of basement rocks associated with the step-over, and the river forced to traverse the basement rocks of the major anticlines there. The abandonment of the former, is clearly attributable to the uplift by the Trig C Structures.

### **7.3 FUTURE WORK**

This study has highlighted a number of new insights into the geology of north Canterbury. From the above discussions of regional tectonics, it is clear that this study has only just begun to examine the structures of a very major portion of north Canterbury, namely the NE-SW trending belt of thrust faults and folds, both onshore and offshore (particularly at depth) of eastern north Canterbury. Many of the structures to the NE and the south now need to be re-examined in the light of new knowledge of the plate boundary zone kinematics there.

A major problem with structural mapping in north Canterbury, is the very poor definition of the uppermost units of the cover rock sequence. The Greta Formation and the Kowai Formation include a very wide variety of rock-types and ages (the latter both marine and non-marine), with poor definition of the boundaries between them. Problems were highlighted by the apparent lack of junction between the two units, which should have been contained within this study area. However, mapping in the Moores Hill Range area suggests that they are likely to meet directly to the south, where studies should likely focus. Furthermore, the ages of the Kowai Formation gravels have been largely based on height above current river level and have been distinguished from the Kowai Formation by the degree of tilting, but the indications of continued activity over much of north Canterbury, with variable rates of deformation, suggest that this is not necessarily valid, and therefore, dating of all of these units should use some independent criteria.

The approach of the morphotectonic study of geomorphology was found to be very useful in terms of determining active deformation. In particular, new structures in areas of either no exposure (ie. valleys and alluvial plains) or complex deformation (ie. the basement rock ranges) were able to be added to structures evaluated by geological mapping. This thesis restricted such studies to their broadest sense, but it is clear that more detail could be evaluated when combined with detailed surveying of stream gradient profiles, dating of geomorphologic features such as fault scarps and offset features such as terrace surfaces, and detailed geomorphological mapping of some of the more subtle features described, such as surface warping and tilting.



## ACKNOWLEDGMENTS

Many people have lent invaluable assistance towards the preparation of this thesis. Funding was gratefully received from the Mason Trust and the North Canterbury Active Tectonics Group; the latter is also thanked for the use of the Hilux 4WD vehicle. My supervisors, Jarg Pettinga and Jocelyn Campbell are very gratefully acknowledged for suggesting the project, and then patiently seeing it through all stages; in particular, Jocelyn is thanked for her many discussions on nearly all aspects of the project, including a great deal of assistance towards computing. Dr A. Nicol is also thanked for his input into many aspects of this project.

Field-work was performed with the assistance of a great number of people. Field assistance is acknowledged to my sisters, Jacqui and Cheryl, friends and classmates Matthew, Michelle, Kathryn, James, Carl and Mark. Mark is also acknowledged for a number of discussions on the geology of the Culverden Basin portion of the study area and for the frontispeice photograph. Dr P.Tonkin is also acknowledged for his help in the field with aspects of Quaternary geology. The large number of land-owners in the study area allowed me to visit their properties without hesitation, and are also thanked, particularly Messers A. Fox, B. Murray and T. Maxwellton.

Technical staff of the Geology Department are acknowledged for their assistance, particularly Michael Finnemore, for his patient assistance with computing.

Fellow classmates, friends and relatives are gratefully acknowledged for their assistance in many ways to their thesis. Classmates, Kathryn, Kay, Ange, Nic, Gregg, Pete, Tim, Phil, Paul (H) and Paul (W) are thanked for their many tea breaks and discussions of "what shall we do when we finish?", which were very instrumental in keeping things rolling, particularly in the later stages. Fellow students, particularly of the following year are also thanked for restoring sanity throughout the later stages. Friends Kellie, Michelle, Ang, Pip, Kirsty, Lauree, Chris, Mark are also thanked for their support throughout in a great deal of ways.

Finally, I would like to say a big thank-you to my parents, whose continued and unfailing support throughout all stages of this project provided perhaps the major ingredient towards the final completion.

## REFERENCES

- Adams, J., 1980. Active tilting of the United States midcontinent: Geodetic and geomorphic evidence. *Geology* 8: 442-446
- Aleksandrowski, P., 1985. Graphical determination of principle stress directions for slickenside lineation populations: an attempt to modify Arthaud's method. *J.Struct. Geol.* 7: 73-82
- Allen, C.R., A.R. Gillespie, H. Yuan, K.E., Sieh, Z. Buchin and Z. Chengnan, 1984. Red River and associated faults, Yunnan Province, China: Quaternary geology, slip rates, and seismic hazard. *Geol.Soc.Am.Bull.* 95: 686-700
- Anderson, H. and T. Webb, 1994. New Zealand seismicity: patterns revealed by the upgraded National Seismograph Network. *N.Z.J.Geol.Geophys.* 37: 477-493
- Andrews, P.B., 1960. Sedimentary history of the Lowermost Otaian horizon in North Canterbury, New Zealand. Unpubl. MSc Thesis. University of Canterbury Library, 129 pp.
- 1963. Stratigraphic nomenclature of the Omihi and Waikari Formations, North Canterbury. *N.Z.J.Geol.Geophys.* 6: 228-256.
- 1968. Patterns of sedimentation during Early Otaian (Early Miocene) time. *N.Z.J.Geol.Geophys.* 11: 711-52.
- Angelier, J., 1979. Determination of the mean principle stresses for a given fault population. *Tectonophysics* 56: T17--T26
- 1984. Tectonic analysis of fault data sets. *J.Geophys.Res.* 89: 5953-5848
- 1989. From orientation to magnitudes in paleostress determinations using fault slip data. *J.Struct.Geol.* 11: 37-50
- Angelier, J. and P. Mechler, 1977. Sur une methode graphique de recherche des contraintes principales egalement utilisable en tectonique et en seismologie: la methode des diedres droits. *Bull.Soc.Geol.Fr.* 19: 1309-1318
- Angelier, J., A. Tarantola, B. Valette and S. Manoussis, 1982. Inversio of field data in fault tectonics to obtain the regional stress. I. Single phase fault populations: a new method of computation the stress tensor. *Geophys.J.R.Astr.Soc.* 69: 607-621
- Arabasz, W.J. and R.Robinson, 1976. Microseismicity and geologic structure in the northern South Island, New Zealand. *N.Z.J.Geol.Geophys.* 19: 569-601
- Armijo, R. and A. Cisternas, 1978. Un probleme inverse en microtectonique cassante. *Cr.Acad.-Sci.Paris D287: 595-598*

- Arthaud, F., 1969. Methode de determination graphique des directions da raccourcissement d'allongement et intermediaire d'une population failles. *Bull.Soc.Geol.Fr.* 11: 729-737
- Avouac, J.P., 1993. Analysis of scarp profiles: evaluation of errors in morphologic dating. *J.Geophys.Res.* 98: 6745-6754
- Barnes, P.M., 1993. Structural Styles and sedimentation at the southern termination of the Hikurangi Subduction Zone, offshore North Canterbury, New Zealand. Unpubl. Ph.D. Thesis, University of Canterbury Library, 211 pp.
- Barrell, D., 1989. Geomorphic evolution and engineering geology studies at coastal Motunau, North Canterbury. Unpubl. Msc Thesis, University of Canterbury Library, 221 pp.
- Beck, A.C., 1968. Gravity Faulting as a mechanism of topographic adjustment. *N.Z.J.Geol.Geophys.* 11: 191-199
- Bibby, H.M., 1975. Crustal strain from triangulation in Marlborough, New Zealand. *Tectonophysics* 29: 529-540
- 1976. Crustal strain across the Marlborough Faults, New Zealand. *N.Z.J.Geol.Geophys.* 19: 407-425
- 1981. Geodetically determined strain across the southern end of the Tonga-Kermadec-Hikurangi Subduction Zone. *Geophys.J.R.Astr.Soc.* 66: 513-533
- Bishop, D.G., J.D. Bradshaw and C.A. Landis, 1985. Provisional Terrane map of the South Island, New Zealand. in: Tectonostratigraphic Terranes in the Circum-Pacific Region p 515-521 D.G. Howell (ed) Circum-Pacific Council for Minerals and Energy, Houston, Texas.
- Bott, M.H.P., 1959. The mechanics of oblique slip faulting. *Geol.Mag.* 96: 109-117
- Bradshaw, J.D., 1972. Stratigraphy and structure of the Torlesse Supergroup (Triassic to Jurassic) in the foothills of the Southern Alps near Hawarden (S60-61), Canterbury. *N.Z.J.Geol.Geophys.* 15: 71-87
- 1989. Cretaceous geotectonic patterns in the New Zealand Region. *Tectonics* 8: 803-820
- Bradshaw, J.D., P.B. Andrews and C.J. Adams, 1980. Carboniferous to Cretaceous on the Pacific margin of Gondwana: The Rangitata Phase of New Zealand. in: *Gondwana Five*, 1981: 217-222. M.M Cresswell and P. Vella (eds), Balkema, Rotterdam
- Brown, S.P. and J.H. Spang, 1978. Geometry and mechanical relationships of folds to thrust propogation using a minor thrust in the Front Ranges of the Canadian Rocky Mountains. *Bull.Can.Petr.Geol.* 26: 551-571
- Browne, G.H., 1985. Diapiric Sandstones from North Canterbury. *Geol.Soc.N.Z.Misc. Publ.* 32a, p26

- Browne, G.H. and B.D. Field, 1985. The Lithostratigraphy of Late Cretaceous to Early Pleistocene rocks of Northern Canterbury, New Zealand. *N.Z. Geol. Surv. Rec.* 6, 63 pp.
- 1988. A review of Cretaceous - Cenozoic sedimentation and tectonics, East Coast, South Island, New Zealand. in: Sequences, stratigraphy, sedimentology: surface and subsurface. D.P. James and D.A. Leckie (eds). *Can. Soc. Petrol. Geol. Mem.* 15: 37-48
- Buchanan, J., 1868. Marlborough and Eastern Nelson. *Report on Geological Explorations, 1866-1867* 4:17, 34-41
- Buchner, F., 1981. Rhinegraben: horizontal stylolites indicating stress regimes of earlier stages of rifting. *Tectonophysics* 73: 113-118
- Bucknam, R.C. and R.E. Anderson, 1979. Estimation of fault-scarp ages from a scarp-height-slope-angle relationship. *Geology* 7: 11-14
- Bull, W.B., 1984. Tectonic geomorphology. *J. Geol. Educ.* 32: 310-324
- Bull, W.B. and P.L.K. Knuepfer, 1987. Adjustments by the Charwell River, New Zealand, to uplift and climatic changes. *Geomorphology* 1: 15-32
- Burnett, A.W. and S.A. Schumm, 1983. Alluvial-River response to Neotectonic deformation in Louisiana and Mississippi. *Science* 222: 49-50
- Butler, W.H., 1982. The terminology of structure in thrust belts. *J. Struct. Geol.* 4: 239-245
- Campbell, J.K. and H.S. Yousif, 1985. Tectonic geomorphology of the Lower Waipara Gorge, North Canterbury. *Geol. Soc. Misc. Publ.* 32b: 53-65
- Campbell, J.K., H.A. Cowan, A. Nicol, and J.R. Pettinga, 1994. Interpreting paleoseismic data in areas of structural complexity. *I.A.S.P.E.I. conference abstracts, Wellington, 1994, W99.4*
- Campbell, M.R., 1896. Drainage modifications and their interpretation. *J. Geol.* 4: 567-581
- Carey, E and B. Brunier, 1974. Analyse theoretique et numerique d'un modele mecanique elementaire applique a l'etude d'une population de failles. *Cr. Acad. Sci. Paris* d179: 891-894
- Carlson, J.R., J.A. Grant-Mackie and K.A. Rodgers, 1980. Stratigraphy and sedimentology of the Coalgate area, Canterbury, New Zealand. *N.Z. J. Geol. Geophys.* 23: 179-192
- Celerier, B., 1988. How much does the slip on a reactivated fault plane constrain the stress tensor? *Tectonics* 7: 1257-1278
- Chase, C.G., 1978. Plate kinematics: the Americas, East Africa and the rest of the world. *Earth and Planetary Science Letters* 31: 85-94

- Cotton, C.A., 1913. The physiography of the Middle Clarence Valley, New Zealand. *Geogr.Jour.* 42: 225-245
- 1938. Some peneplanations in Otago, Canterbury and the North Island of New Zealand. *N.Z.Sci.Tech.* 20b: 1-8
- Cook, D.G., 1988. Balancing basement-cored folds of the Rocky Mountain foreland. *Geol.Soc.Am.Mem.* 171: 53-64
- Couzens, B.A. and W.M. Dunne, 1994. Displacement transfer at thrust terminations: the Saltville thrust and Sinking Creek anticline, Virginia, U.S.A. *J.Struct.Geol.* 16: 781-793
- Cowan, H.A., 1989. An evaluation of the Late Quaternary displacements and seismic hazard associated with the Hope and Kakapo Faults, Amuri District, North Canterbury, New Zealand. Unpubl. Msc. Thesis, University of Canterbury Library, 213 pp.
- 1992. Structure, seismicity and tectonics of the Porters Pass-Amberley Fault Zone, North Canterbury. Unpubl. Ph.D. Thesis, University of Canterbury Library, 181 pp.
- Dahlstrom, C.D.A., 1970. Structural geology in the eastern margin of the Canadian Rocky Mountains. *Bull.Can.Petr.Geol.* 18: 332-406
- Dean, A.A., 1993. Analysis and correlation of Igneous clast geochemistry and petrography from four Mesozoic conglomerates. Unpubl. MSc. Thesis. University of Canterbury Library, 263 pp.
- Deffontaines, B. and J. Chorowitz, 1991. Principles of drainage analysis from multisource data: Application to the structural analysis of the Zaire Basin. *Tectonophysics* 194: 237-263
- Deffontaines, B., P.Chotin, L.Ait Brahim and M. Rozanov, 1992. Investigation of active faults in Morrocco using morphometric methods and drainage pattern analysis. *Geologische Rundschau* 81: 199-210
- De Lamotte, D.F. and J.C. Guezou, 1995. Distinguishing lateral folds in thrust systems; examples from Corbieres (SW France) and Betic Cordilleras (SE Spain). *J.Struct.Geol.* 17: 233-244
- de Mets, C., R.G. Gordon, D.F. Argus and S. Stein, 1990. Current plate motions. *Geophys.J.Int.* 101: 425-428
- Dibble, R.R., unpublished: Gravity data, with map and cross sections, from the Culverden Basin Area, North Canterbury
- Dixon, J.M. and S. Liu, 1992. Centrifuge modelling of the propagation of thrust faults. in: *Thrust Tectonics*. K.R. McClay (ed), Chapman and Hall, London. 447 pp.
- Dixon, J.M. and R. Tirrul, 1991. Centrifuge modelling of fold-thrust structures in a tripartite stratigraphic succession. *J.Struct.Geol.* 13: 3-20

- Douglas, R.J.W., 1950. Callum Creek, Langford Creek and Gap map areas, Alberta. *Geol.Surv.Can.Mem.* 255, 124 pp.
- Dowrick, D.J., 1991. A revision of attenuation relationships for Modified Mercalli Intensity in New Zealand earthquakes. *Bull.N.Z.Nat.Soc.Earthq.Eng* 24: 210-224
- Dowrick, D.J. and E.G.C. Smith, 1990. Surface wave magnitudes of some New Zealand Earthquakes 1901-1988. *Bull.N.Z.Nat.Soc.Earthq.Eng.* 23: 198-210
- Dupin, J.M., W. Sassi and J. Angelier, 1993. Homogeneous stress hypothesis and actual fault slip: a distinct element analysis. *J.Struct.Geol.* 15: 1033-1043
- Eiby, G.A., 1968. A descriptive catalogue of New Zealand Earthquakes. *N.Z.J.Geol.Geophys.* 11: 16-40
- Elliot, D., 1976. The energy balance and deformation mechanisms of thrust sheets. *Phil.Trans.Roy.Soc.Lond.* A283: 289-312
- Engeldier, T. and P. Geiser, 1980. On the use of regional joints sets as trajectories of paleostress fields during the development of the Appalachian Plateau. *J.Geophys.Res.* 85: 6319-6341
- Erslev, E.A., 1988. Normalised center-to-center strain analysis of packed aggregates. *J.Struct.Geol.* 10: 201-209
- Erslev, E.A. and H. Ge., 1990. Least-squares center-to-center and mean object ellipse fabric analysis. *J.Struct.Geol.* 8: 1047-1059
- Etchecopar, A., G. Vasseur and M. Daignieres, 1981. An inverse problem in microtectonics for the determination of stress tensors from striation analysis. *J.Struct.Geol.* 3: 51-65
- Falloon, A.S., 1954. Geology of the Culverden Basin, North Canterbury, New Zealand. Unpubl. MSc Thesis, University of Canterbury Library
- Field, B.D. and G.H. Browne, 1989. Cretaceous and Cenozoic sedimentary basins and geological evolution of the Canterbury Region, South Island, New Zealand. *N.Z.Geol. Surv. Basin Studies* 2. N.Z. Geological Survey, Lower Hutt. 94 pp.
- Fisher, D.M. and Anastasio, 1994. Kinematic analysis of a large-scale leading edge folds, Lost River Range, Idaho. *J.Struct.Geol.* 16: 781-793
- Fischer, M.P., N.B. Woodward and M.M. Mitchell, 1992. The kinematics of break-thrust folds. *J.Struct.Geol.* 14: 451-460
- Friederking, R.L., 1989. Experiments with directional statistics for analysing stream channel pattern. *Geol.Soc.Am.Prog. Abstr.* pA61
- Fry, N., 1979. Random point distributions and strain measurements in rocks. *Tectonophysics* 60: 89-105

- 1992. Stress ratio determinations from striated faults: a spherical plot for cases of near-vertical principal stress. *J.Struct.Geol.* 10: 1121-1131
- Gardner, D.A.C. and J.H. Spang, 1973. Model studies of the displacement transfer associated with overthrust faulting. *Bull.Can.Petr.Geol.* 21: 534-552
- Garlick, R.D., 1992. Lees Valley Fault, North Canterbury. BSc (Hons) project, 86 pp.
- Gephart, J.W. and D.W. Forsyth, 1984. An important method for determining the regional stress tensor using earthquake focal mechanism data: application to the San Fernando earthquake sequence. *J.Geophys.Res.* 89: 9305-9320
- Gomez, B. and D.C. Marron, 1991. Neotectonic effects on sinuosity and channel migration, Belle Fourche River, Western South Dakota. *Earth surface processes and landforms* 16: 227-235
- Gregg, D.R., 1964. Sheet 18 Hurunui. Geological map of New Zealand 1:250 000. Wellington. New Zealand Department of Scientific and Industrial Research.
- Gutenberg, B. and C.F. Richter, 1949. Seismicity of the Earth and associated phenomena, pp 45-47, 159-160. Princeton University Press, New Jersey, 273 pp.
- Haast, J. von, 1871a. On the geology of the Amuri District, in the Provinces of Nelson and Marlborough. *Report on Geolgocial Explorations 1870-1871* 6: 5-19.
- 1871b. On the geology of the Waipara District, Canterbury, with geological map and sections. *Report on Geological Explorations 1870-1871* 6: 25-46
- Hack, J.T., 1957. Studies of lonigitudinal stream profiles in Virginia and Maryland. *U.S.Geol.Surv.Prof.Pap.* 294B: 45-97
- 1973. Stream profile analysis and stream gradient indexes. *J.Res.Geol.Surv.* 1: 421-429
- Hamilton, D., 1950. The Geology of the Waikari Valley and its northern ridges, North Canterbury, New Zealand. Unpubl. MSc Thesis, University of Canterbury Library, 202pp.
- Hancock, P.L., 1985. Brittle microtectonics: principles and practise. *J.Struct.Geol.* 7: 437-459
- Hardcastle, K.C and L.S. Hills, 1991. Brute3 and Select: Quickbasic 4 programs for determination of stress tensor configurations and seperation of heterogenous populations of fault-slip data. *Comp.and Geosc.* 17: 23-43
- Harvey, A.M. and S.G. Wells, 1987. Response of Quaternary fluvial systems to differential epeirogenic uplift: Aguas and Feos river systesms, southeast Spain. *Geology* 15: 689-693
- Hatherton, T., 1980. Shallow seismicity in New Zealand 1956-1975. *J.Roy.Soc.N.Z.* 10: 19-25

- Hobbs, W.H., 1901. The river system of Connecticut. *J.Geol.* 9: 469-485
- 1911. Repeating patterns in the relief and in the structure of the land. *Geol.Soc.Am.Bull.* 22: 123-176
- House, W.M. and R.D. Gray, 1982. Displacement transfer at thrust terminations in Southern Appalachians - Saltville Thrust as example. *A.A.P.G.Bull.* 830-842
- Howard, A.D., 1967. Drainage analysis in geologic interpretation: a summation. *A.A.P.G. Bull.* 51: 2246-2259
- Howard, A.D. and A.T. Hemberger, 1991. Multivariate characterisation of meandering. *Geomorphology* 4: 161-186
- Hutton, F.W., 1874. Report on the geology of the North-East Portion of the South Island, from Cook Straits to the Rakaia. *Report on Geological Explorations 1873-1874 8b*: 27-58
- 1885. On the geological position of the Weka Pass Stone of New Zealand. *Quat.J.Geol.Soc.Lond.* 41: 266-278
- 1888. On some railway cuttings in the Weka Pass. *Trans.N.Z.Inst.* 20: 257-263
- Jamison, W.R., 1987. Geometric analysis of fold development in overthrust terranes. *J.Struct.Geol.* 9: 207-219
- 1991. Kinematics of compressional fold development in convergent wrench terranes. *Tectonophysics* 190: 209-232
- 1993. Mechanical stability of the triangle zone:the backthrust wedge. *J.Geophys.Res.* B98: 20015-20030
- Jobberns, G., 1925. Report on the Motonau earthquake phenomena. 25th December, 1922. *Dept. Lands and Survey. Rec.Surv.N.Z.* 1: 70
- Lamb, S.H., 1988. Tectonic rotations about vertical axes during the last 4 Ma in part of the New Zealand plate-boundary zone. *J.Struct.Geol.* 11: 473-492
- Lewis, D.W., 1992. Anatomy of an unconformity on Mid-Oligocene Amuri Limestone, Canterbury, New Zealand. *N.Z.J.Geol.Geophys.* 35: 463-475.
- Lewis, D.W., D. Smale and G. van der Lingen, 1979. A sandstone diapir cutting the Amuri Limestone, North Canterbury, New Zealand. *N.Z.Geol.Geophys.* 22: 295-305.
- Lisle, R.J., 1979. Strain analysis using deformed pebbles: the influence of initial pebble shape. *Tectonophysics* 53: T21-T27
- Liu, S. and J.M. Dixon, 1990. Centrifuge modelling of thrust faulting: strain partitioning and sequence of thrusting in duplex structures. in: *Deformation Mechanisms, Rheology and Tectonics*, *Geol.Soc.Spec.Publ.* 54: 431-444



- 1991. Centrifuge modelling of thrust faulting: structural variation along strike in fold-thrust belts. *Tectonophysics* 188: 39-62
- Mason, B.H., 1941. The Geology of the Mount Grey District, North Canterbury. *Trans.Roy.Soc.N.Z.* 71: 103-127
- Maxwell, P.A., 1964. Structural Geology and Pre-Quaternary stratigraphy of the Kaiwara District. Unpubl. MSc. Thesis University of Canterbury Library. 223pp + map volume
- Mayer, L., 1984. Dating Quaternary fault scarps formed in alluvium using Morphologic parameters. *Quat.Res.* 22: 300-313
- 1986. Tectonic geomorphology of escarpments and mountain fronts. in: Active Tectonics: studies in geophysics. R.E. Wallace (panel chairman). National Academy Press, Washington D.C., pp 125-324
- McMorran, T., 1992. Hope Fault at Hossack Station east of Hanmer Basin. Unpubl. MSc. Thesis, University of Canterbury Library, 207 pp.
- McPherson, E.O. 1947. Stratigraphy of Chalk Hill, Oxford survey district, with notes on grading the Chalk. *N.Z.J.Sci.Tech.* 28(B): 164-172
- Merritts, D. and K.R. Vincent, 1989. Geomorphic response of coastal streams to low, intermediate, and high rates of uplift, Mendocino triple junction region, northern California. *Geol.Soc.Am.Bull.* 101: 1373-1388
- Michael, A., 1984. Determination of stress from slip data: faults and folds. *J.Geophys. Res.* B89: 11517-11526
- Mitra, S., 1990. Fault-propagation folds: geometry, kinematic evolution and hydrocarbon traps. *A.A.P.G.Bull.* 74: 921-945
- Mould, R.J., 1992. Structure and kinematics of Late Cenozoic deformation along the western margin of the Culverden Basin, North Canterbury, New Zealand. Unpubl. MSc. Thesis, University of Canterbury Library, 174 pp.
- Nash, D.B., 1984. Morphologic dating of fluvial terrace scarps and fault scarps near West Yellowstone, Montana. *Geol.Soc.Am.Bull.* 95: 1413-1424
- Nicol, A., 1991. Structural Styles and Kinematics of Deformation on the edge of the New Zealand Plate Boundary Zone, Mid Waipara Region, North Canterbury. Unpubl. Ph.D. Thesis, University of Canterbury Library. 171 pp.
- 1992. Tectonic structures developed in Oligocene Limestones: implications for the New Zealand plate boundary deformation in North Canterbury. *N.Z.J.Geol.Geophys.* 35: 353-362
- 1993a. Haumarian (c.66-80 Ma) half-graben development and deformation, mid-Waipara, North Canterbury. *N.Z.J.Geol.Geophys.* 36: 127-130

- 1993b. Conical folds produced by dome and basin fold interference and their application to determining strain: examples from North Canterbury, New Zealand. *J.Struct.Geol.* 15: 785-792
- Nicol, A., B. Alloway and P. Tonkin, 1994. Rates of deformation, uplift and landscape development with active folding in the Waipara area of North Canterbury, New Zealand. *Tectonics* 13: 1327-1344
- Nicol, A. and J.K. Campbell, 1990. Late Cenozoic Thrust Tectonics, Picton, New Zealand. *N.Z.J.Geol.Geophys.* 33: 485-494
- Nicol, A., H. Cowan, J.K. Campbell and J.R.Pettinger, 1995. Folding and the development of small sedimentary basins along the New Zealand Plate Boundary. *Tectonophysics* 241: 47-54
- Nicol, A. and D.U. Wise, 1992. Paleostress adjacent to the Alpine Fault of New Zealand: Fault, Vein and Stylolite Data from the Doctors Dome Area. *J.Geophys.Res.* 97: 17685-17692
- Nicol, A., D.U. Wise and J.D. Bradshaw, 1990. The Torlesse, New Zealand's largest beanbag. *Geol.Soc.N.Z.Misc.Publ.* 50A: p 104
- Norris, R.J., P.O. Koons and A.F. Cooper, 1990. The obliquely-convergent plate boundary in the South Island of New Zealand: implications for ancient collision zones. *J.Struct.Geol.* 12: 715-725
- O'Keefe, F.Z. and D.W. Stearns, 1982. Characteristics of displacement transfer zones associated with thrust faults. in: *Geologic Studies of the Cordilleran Thrust Belt* 1:219-233. Rocky Mountains Association of Geologists, Denver, Colorado
- Ouchi, S., 1985. Response of alluvial rivers to slow tectonic movement. *Geol.Soc.Am. Bull.* 96: 504-515
- Pettinga, J.R. and D.U. Wise, 1994. Paleostress adjacent to the Alpine Fault: Broader implications from fault analysis near Nelson, South Island, New Zealand. *J.Geophys.Res.* 99: 2767-2736
- Pollard, D.D., S.D. Saltzer and A.M. Rubin, 1993. Stress inversion methods: are they based on faulty assumptions? *J.Struct.Geol.* 15: 1045-1054
- Pope, J.G., 1994. Secondary structures, Holocene displacements and paleoseismicity of the Conway Segment of the Hope Fault, Greenburn Stream to Sawyers Creek. Unpubl. Bsc (Hons) project, 109pp.
- Powers, W.E., 1962. Terraces of the Hurunui River, New Zealand. *N.Z.J.Geol. Geophys.* 5: 114-129
- Pubellier, M., B. Deffontaines, R. Quebral and C.Rangin, 1994. Drainage network analysis and tectonics of Mindanao, southern Phillipines. *Geomorphology* 9: 325-342
- Ramsay, J.G., 1967. *Folding and Fracturing of Rocks*. McGraw Hill Inc., New York.

- Ramsay, J.G. and M.I. Huber, 1987a. The techniques of modern structural geology volume 1: Strain analysis. Academic Press Inc., London. 307pp.
- 1987b. The techniques of modern structural geology volume 2: folds and fractures. Academic Press Inc., London. 293pp.
- Reches, Z., 1978. Development of monoclines: Part I. Structure of the Palisades Creek branch of the East Kaibab monocline, Grand Canyon, Arizona. *Geol.Soc.Am. Mem. 151: 235-271*
- 1987. Determination of the tectonic stress tensor from slip faults that obey the coulomb yield condition. *Tectonics 6: 849-861*
- Reches, Z. and A.M. Johnson, 1978. Development of monoclines: Part II. Theoretical analysis of monoclines. *Geol.Soc.Am.Mem. 151: 273-311*
- Reyners, M., 1989. New Zealand Seismicity 1964-1987: an interpretation. *N.Z.J.Geol. Geophys. 32: 307-315*
- Reyners, M. and H. Cowan, 1993. The transition from subduction to continental collision: crustal structure in the North Canterbury region, New Zealand. *Geophys.J.Int. 115: 1124-1136*
- Rhea, S., 1993. Geomorphic observations of rivers in the Oregon Coast Range from a regional reconnaissance perspective. *Geomorphology 6: 135-150*
- Rich, R.L., 1934. Mechanics of low-angle overthrust faulting as illustrated by Cumberland thrust block, Virginia, Kentucky and Tennessee. *A.A.P.G.Bull. 18: 1584-1596*
- Ritz, J.F., 1994. Determining the slip vector by graphical construction: use of a simplified representation of the stress vector. *J.Struct.Geol. 737-742*
- Rogers, W.B. and H.D. Rogers, 1894. On the physical structure of the Appalachian Chain, as exemplifying the laws which have regulated the elevation of great mountain chains generally. *Ass.Amer.Geol.Nat.Rep. 474-531*
- Rynn, J.M.W. and C.H. Scholz, 1978. Seismotectonics of the Arthurs Pass Region, South Island, New Zealand. *Geol.Soc.Am.Bull. 89: 1373-1388*
- Schofield, J.C., 1949. The geology of the McDonald Downs and Waikari Districts, North Canterbury. Unpubl. MSc Thesis, University of Canterbury Library.
- Schumm, S.A., 1963. Sinuosity of Alluvial Rivers on the Great Plains. *Geol.Soc.Am. Bull. 74:1089-1100*
- 1981. Evolution and response of the fluvial system, sedimentologic implications. *Soc.Econ.Paleo.Min.Spec.Publ. 31: 19-29*
- Seeber, L. and V. Gornitz, 1983. River profiles along the Himalayan Arc as indicators of Active Tectonics. *Tectonophysics 92: 333-387*

- Segall, P. and D.D. Pollard, 1983. Joint formation in granitic rock of the Sierra Nevada. *Geol.Soc.Am.Bull.* 94: 563-575
- Shepherd, R.G., 1985. Regression analysis of river profiles. *Jour.Geol.* 93: 377-384
- Skey, H.F., 1925. Report on the North Canterbury earthquake of 25th December, 1922. *Dept. Lands and Survey. Rec.Surv.N.Z.* 1: 69-70
- Smale, D., 1978. The composition of a Torlesse Conglomerate - Ethelton, North Canterbury. *N.Z.J.Geol.Geophys.* 21: 699-711.
- Snow, R.S. and R.L. Singerland, 1987. Mathematical modelling of graded profiles. *Jour. Geol.* 95: 15-33
- Speight, R., 1915a. The Intermontaine Basins of Canterbury. *Trans.Proc.N.Z.Inst.* 47: 336-353
- 1915b. The orientation of the River Valleys of Canterbury. *Trans.Proc. N.Z. Inst.* 48: 137-144
- 1918. Structural and Glacial features of the Hurunui Valley. *Trans.Proc.N.Z. Inst.*50: 93-105
- 1919. The older gravels of North Canterbury. *Trans.N.Z.Inst.* 51: 269-281
- Speight, R. and L.J. Wild, 1918. The stratigraphical relationship of the Weka Pass Stone and the Amuri Limestone. *Trans.Proc.N.Z.Inst.* 50: 65-93
- Stauffer, M.R., 1988. Fold interference structures and coaptation folds. *Tectonophysics* 149: 339-343
- Stearns, D.W., 1978. Faulting and forced folding in the Rocky Mountains foreland. *Geol.Soc.Am.Mem.* 151: 1-37
- Strahler, A.N., 1957. Quantitative analysis of watershed geomorphology. *Am.Geophys. Un.Trans.* 38: 913-920
- Suppe, J., 1983. Geometry and kinematics of fault-bend folding. *Am.J.Sci.* 283: 684-721
- 1985. Principles of Structural Geology. Prentice-Hill, New Jersey
- Suppe, J., G.T. Chou and S.C. Hook, 1991. Rates of folding and faulting from growth strata. in: Thrust Tectonics, pp 105-121, K.R. McClay (ed), Chapman and Hall, London
- Suppe, J. and D.A. Medwedeff, 1984. Fault-propagation folding. *Geol.Soc.Am.Abstr. Progr.* p60
- Syme, A.R., 1991. Structural analysis of the deformation of the Marble Point Outlier, Waiau River, North Canterbury. Unpubl. BSc (Hons) project, 95 pp.

- Thomson, J.A., 1920. The Notocene Geology of the Middle Waipara and Weka Pass District, North Canterbury, New Zealand. *Trans.Proc.N.Z.Inst.* 52:322-415
- Walcott, R.I., 1978. Present tectonics and Late Cenozoic evolution of New Zealand. *J.Geophys.Res.* 52: 137-164
- Wallace, R.E., 1951. Geometry of shearing stress and relation to faulting. *Jour.Geol.* 59: 118-130
- 1977. Profiles and ages of young scarps, north-central Nevada. *Geol.Soc. Am.Bull.* 88:1267-1281
- 1978. Geometry and rates of change of fault-generated Range-fronts, north-Central Nevada. *Jour.Res.U.S.Geol.Surv.* 6: 637-650
- Warren, G., 1967. Sheet 17 Hokitika. Geological map of New Zealand 1:250 000. Wellington. New Zealand Department of Scientific and Industrial Research
- Warren, G and I.G. Speden, 1978. The Piripauan and Haumurian stratotypes (Mata Series, Upper Cretaceous) and correlative sequences in the Haumuri Bluff district, South Marlborough (S56). *N.Z.Geol.Surv.Bull.* 92. 60 pp.
- Wells, S.G., T.F. Bullard, C.M. Menges, P.G. Drake, P.A. Kelson, J.B. Ritter and J.R. Wesling, 1988. Regional variations in tectonic geomorphology along a segmented convergent plate boundary, Pacific Coast of Costa Rica. *Geomorphology* 1: 239-265
- Wilkerson, M.S., 1992. Differential transport and continuity of thrust sheets. *J.Struct.Geol.* 14: 749-751
- Will, T.M. and R. Powell, 1991. A robust approach to the calculation of paleostress fields from fault plane data. *J.Struct.Geol.* 13: 813-821
- Willis, B., 1894. The mechanics of Appalachian structure. *U.S.Geol.Surv.Ann.Rep.* Part II: 211-282
- Wilson, D.D., 1963. Geology of the Waipara Subdivision. *N.Z.Geol.Surv.Bull.* 64, 122 pp.
- Woodward, A.D., 1951. Stream gradients and Moterey sea valley. *Geol.Soc.Am.Bull.* 92:189-169
- Yousif, H.M.S., 1987. The applications of remote sensing to geomorphological mapping in North Canterbury. unpubl. PhD. Thesis, University of Canterbury Library, 410pp.
- Zernitz, E.R., 1932. Drainage patterns and their significance. *J.Geol.* 40: 498-521
- Zhao, G. and A.M. Johnson, 1992. Sequence of deformation recorded in joints and faults, Arches National Park, Utah. *J.Struct.Geol.* 14: 939-951

## STRESS TENSOR ANALYSIS

### Stress tensor analysis using BRUTE10

The BRUTE10 computer program, combined with the file manipulation programs FLTWRTIE, FLTMERGE, FLTREAD and SIGSELEC is capable of calculating a reduced stress tensor (Angelier, 1979) for a measured set of fault planes. A reduced stress tensor can be defined by four variables  $\sigma_1$ ,  $\sigma_2$ ,  $\sigma_3$  (where  $\sigma_1 \geq \sigma_2 \geq \sigma_3$ ) and  $\phi$  (where  $\phi = \frac{\sigma_1 - \sigma_2}{\sigma_2 - \sigma_3}$ ), hence an indication of the relative amount and orientation of that stress can

be given, but no indication of the actual stress magnitudes.

To calculate the stress tensor configurations for a given data set, the program performs a grid search of all possible tensor configurations for each given fault plane, by rotating  $\sigma_2$  and  $\sigma_3$  in  $10^\circ$  intervals about  $\sigma_1$ , while in turn moving  $\sigma_1$  about  $10^\circ$  intervals on the stereonet (hence involving up to 20 000 calculations for each). For configurations in which fault motion is possible (taking into account coefficients of friction and fluid pressures), the slip vector is calculated and if it falls within a user-defined angle (suggested angle =  $20^\circ$ ) to the slip direction measured in the field it is stored. If more than a given percentage of faults are recorded for each tensor configuration (suggested percent = 25%), the calculated stress tensor is stored for later plotting.

The plots of  $\sigma_1$ ,  $\sigma_2$  and  $\sigma_3$  are contoured, the resulting contours then surround areas in which a stress axis could have been located for the given percentage of the fault population to have moved. Erratic members of the population should occur as small separate clusters, or as fringes on the main plots.

### Steps in performing a stress tensor analysis

1. The raw data is loaded into the program FLTWRTIE.EXE in the following format:

- i) strike of the fault plane (using the right hand rule)
- ii) dip of the fault plane
- iii) trend of the slickensides } It was found that it was easier to measure
- iv) plunge of the slickensides } these as a rake to the horizontal on the
- fault plane in the field and then to convert
- them to a trend and plunge either on a
- stereonet or using the following formulas:

$$\sin(\text{plunge angle}) = \sin(\text{rake}) \cdot \sin(\text{dip angle of the fault})$$

$$\sin(\text{strike of fault} \wedge \text{plunge of net slip direction}) = \frac{\tan(\text{plunge angle of net slip})}{\tan(\text{true dip angle of fault})}$$

- v) rotation sense of the motion indicators (based on the down-plunge view of an imaginary line on the fault plane drawn perpendicular to the motion indicators, ie. CW or CCW)
- vi) level of reliability of the motion sense indicators (1 = good, 3 = poor)

2. The file saved in FLTWRITE.EXE can then be loaded directly into BRUTE10 to calculate the stress tensor configurations. Six user-defined parameters need to be provided when performing a grid search:

- i) Whether a total search is to be performed (usually “yes” (1) as “no” (2) creates very large files when they are merged)
- ii) The increment for the rotation of  $\sigma_1$  during the search (if 1 was chosen above then the suggestion is  $10^\circ$ )
- iii) The minimum percent of the faults on which slip is possible for each tested stress orientation (needs to be varied according to the data set and is discussed below)
- iv) The maximum angular divergence of the calculated slip direction from the measured slip direction in order for it to be stored (also need to be varied according to the data set and is discussed below)
- v) Minimum values for cohesion and the coefficient of friction for the rock (here 0 cohesion was assumed due to the likely presence of pre-existing disconformities and a coefficient of friction of 0.364 for the basement and 0.532 for the Amuri Limestone)
- vi) The minimum confidence interval to be tested (the level of reliability of the motion indicators that wishes to be tested, ie., 1,2 or 3 and is discussed below)

3. The resulting tensor file contains 9 columns of information

- i) number of faults fit
- ii) trend of  $\sigma_1$
- iii) plunge of  $\sigma_1$
- iv) trend of  $\sigma_2$
- v) plunge of  $\sigma_2$
- vi) trend of  $\sigma_3$
- vii) plunge of  $\sigma_3$
- viii)  $\phi$
- ix) Average angular divergence

(and when first displayed contains a record of the parameters used, so it is often worth printing the first few rows of data). The files can be divided into three, two column ascii files containing ii) and iii); iv) and v); vi) and vii) respectively using the program SIGSELEC.EXE, and can then be plotted using any standard stereonet contour program. The following steps apply to plotting of the files in STEREO for ROCKWARE.

4. The data may be converted easily into the required ascii-file standard for STEREO by Microsoft EXCEL5 (particularly if the files are rather large), by opening each file as a fixed-width file and then changing the column width of the two columns to 3. The file is then saved as an ascii file (a “Text (OS/2 or MS-DOS)” file).

5. The files can then be appropriately labeled for plotting in STEREO and plotted as density plots. A discussion of the methods used for constructing the density plots follows.

## Further discussion of the choice of parameters for step 2

When the BRUTE10 computer program is running the screen scrolls through:

- i) the  $\sigma_1$  trend and plunge that it is testing
- ii) the corresponding percent of tensors tried
- iii) the number of "good" tensors found for the tensors tested
- and iv) the cumulative totals of iii)

The program will cease running either when iii) reaches 100% or when iv) reaches 2500. If iv) reaches 2500 first all of the faults have not been used in the data search, and hence the search is not complete. Two suggestions are made in the program to reconcile this for a particular data set, either:

- i) record the % of tensors tried when the program stopped and start the program running again as a partial search (parameter i) under step 2 above) from that point. This is a rather messy approach, particularly if the process has to be repeated several times, and will create very large data sets for plotting, as mentioned under step 2 above
- ii) Vary parameters iii), iv) and possibly vi) above

To test the relative effects of ii) above, a series of tests, changing one variable at a time, were run for two of the basement localities (described in section 4.2.1.2), the results of which are shown in table 8.1. Plots of those in which 100% of the data from both localities were able to be calculated are shown in figure 8.1.

From the plots it is clear that the most accurate plots are those that contain a relatively large number of data points (~2000-2500), ie. compare figures 8.1a and 8.1c for the Scargill Hills Quarry locality. This clearly will only occur for the minimum % of faults and the maximum divergence angle that allows 100% of the data to be collected for the desired confidence interval. In this case, at intervals of 5% and 5° for the minimum % of faults and maximum divergence angle respectively, the most accurate plot is that of 30% and 30° at a confidence interval of 3, and 30 % and 25° for a confidence interval of 2. Because of the relatively small difference in the number of faults here between confidence interval 2 and 3 it was considered that a confidence interval of 3 was acceptable and therefore, figure 8.1c was considered to be the most reliable.

Lastly, the tests also show that the % of faults is the most sensitive to change, particularly in terms of the 5 % intervals that were used here, and therefore, the angular divergence should preferably be changed first.

## Discussion of the construction of density plots in STEREO

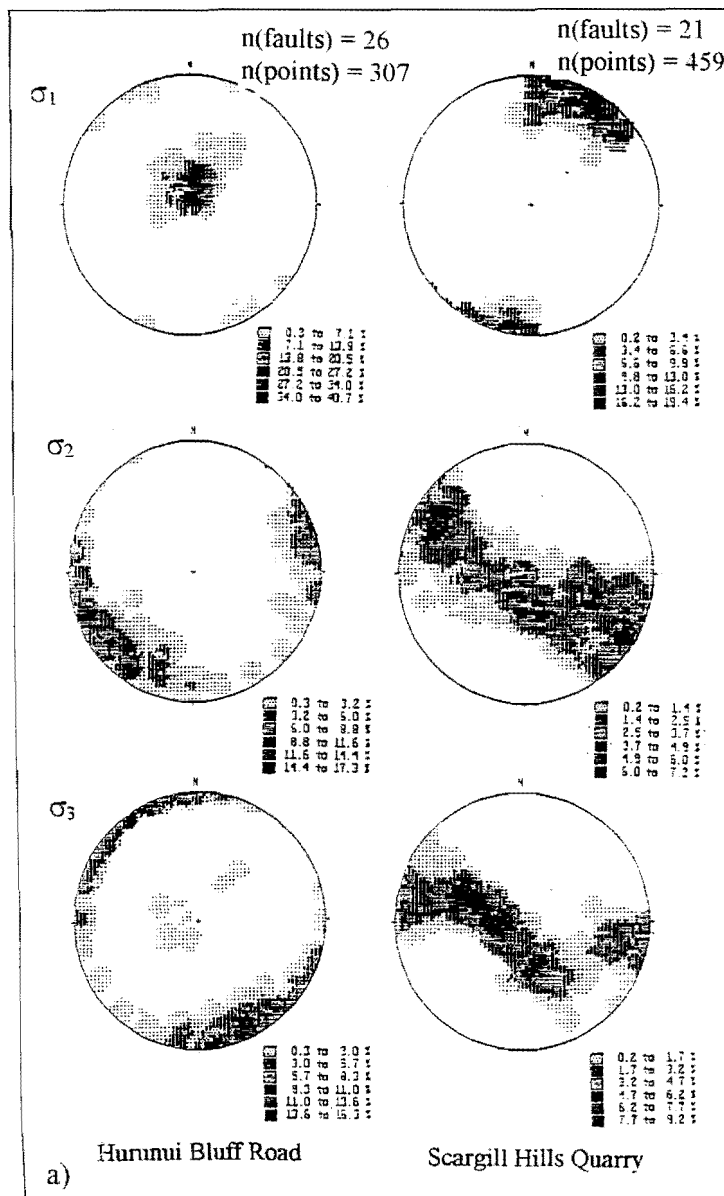
The method of construction of the density plots used in this thesis was the "Step Function Method", mainly due to its relatively rapid calculation in STEREO, compared to any other method. However, when the "Spherical Gaussian Method" was applied to the  $\sigma_1$  plots for the Hurunui Bluff Road locality, the difference in quality was considerable (see figure 8.2). The spherical gaussian contoured plot is perhaps more readily interpretable for this kind of interpretation, where the centre of the plot is the desired feature. However, attempts to vary the size of the "counting circle" using the Kamb Method failed on the current version of STEREO, which limited the study to the pre-set variable. As stated above however, the major reason that this method was not utilised was, its very slow application on the 486 computer used.



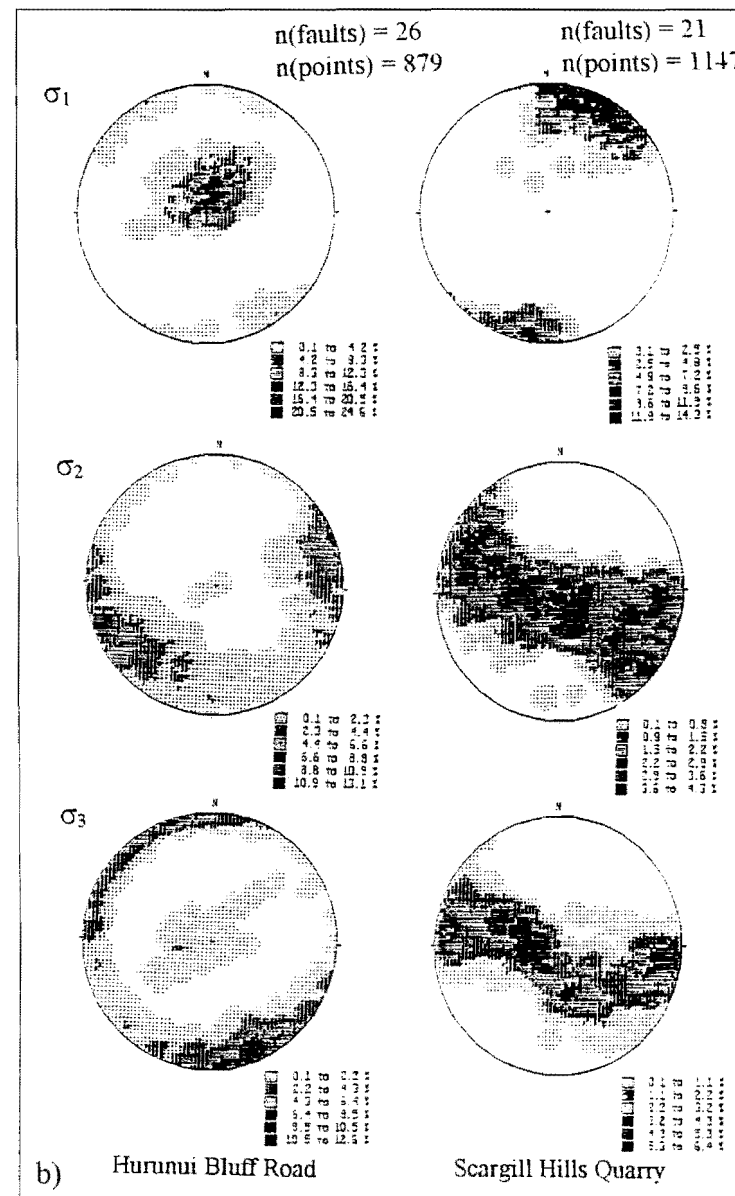
CONFIDENCE INTERVAL	% OF FAULTS	ANGULAR DIVERGENCE	RESULTS: Hurunui Bluff Rd	Scargill Hills Quarry	PLOT
3	30	30	100%	100%	*
		25	100%	100%	*
		20	100%	100%	*
	25	30	19%	68%	
		25	54%	100%	
		20	100%	100%	*
	20	30	-	-	
		25	18%	60%	
		20	-	-	
2	30	30	100%	92%	
		25	100%	100%	*
		20	100%	100%	*
	25	30	19%	60%	
		25	54%	74%	
		20	100%	92%	
	20	30	-	-	
		25	18%	37.00%	
		20	-	-	
1	30	25	86%	68%	
	25	25	28%	68%	

**Table 8.1** Full set of stress tensor analysis results for Hurunui Bluff Road and Scargill Hills Quarry at different values of confidence interval, % of faults that a tensor must fit to be considered, and accepted angular divergence of the orientation of the stress tensor from the faults measured. The results are listed in terms of the percentage of the faults that were used in the analysis.

CI = 3  
% = 20  
AD = 25

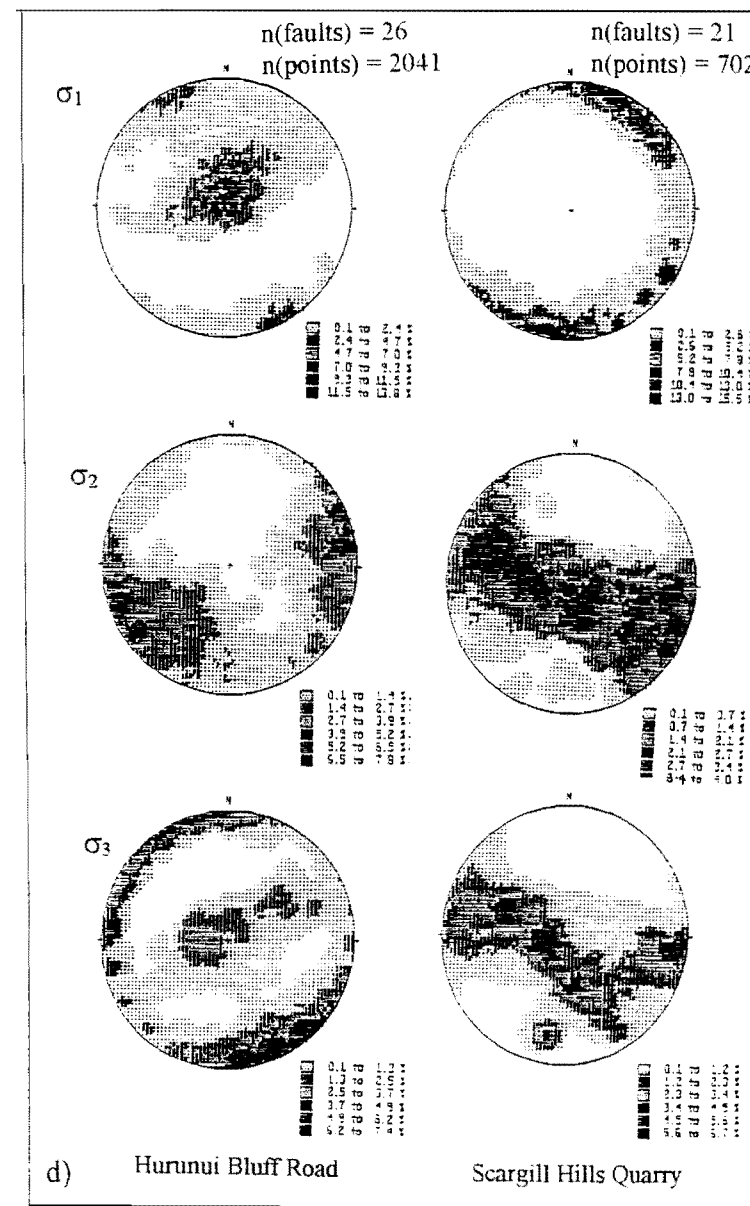
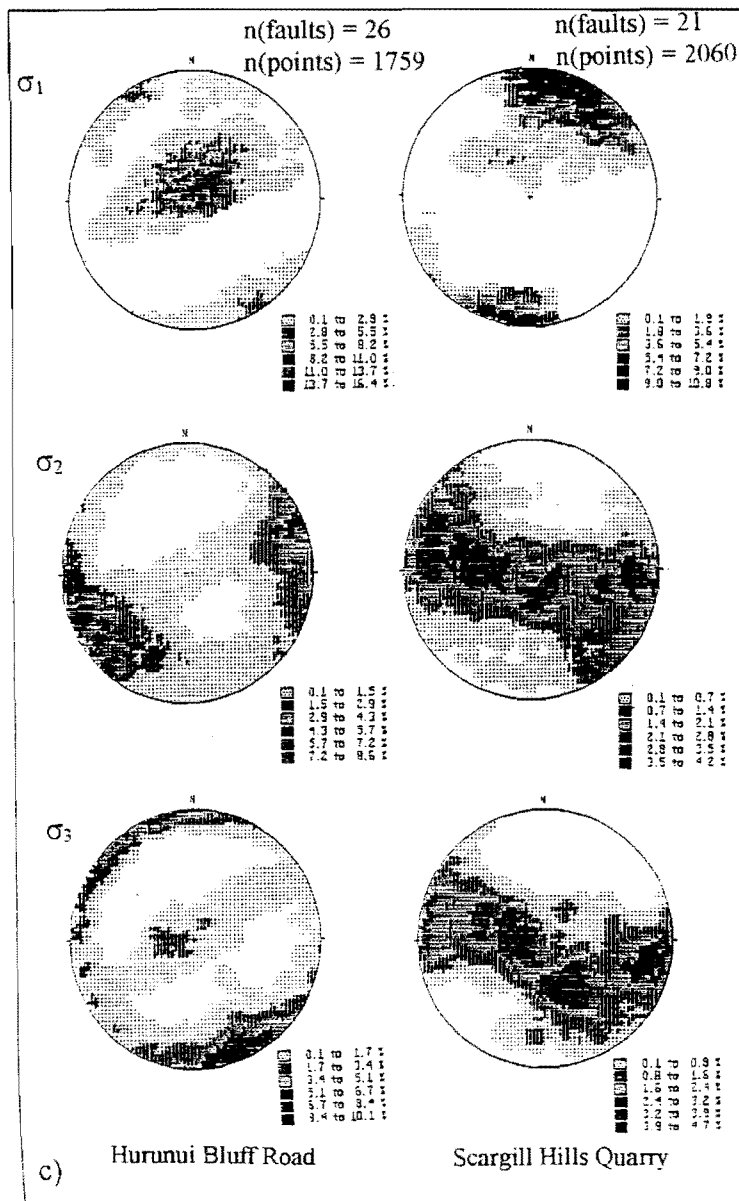


CI = 3  
% = 30  
AD = 25



**Figure 8.1** Stress tensor analysis results of Hurunui Bluff Road and Scargill Hills Quarry at different values of confidence interval (CI), percentage of faults that a tensor must fit to be considered (%) and accepted angular divergence (AD) of the stress tensor to the faults recorded. Values are listed beside each data set.

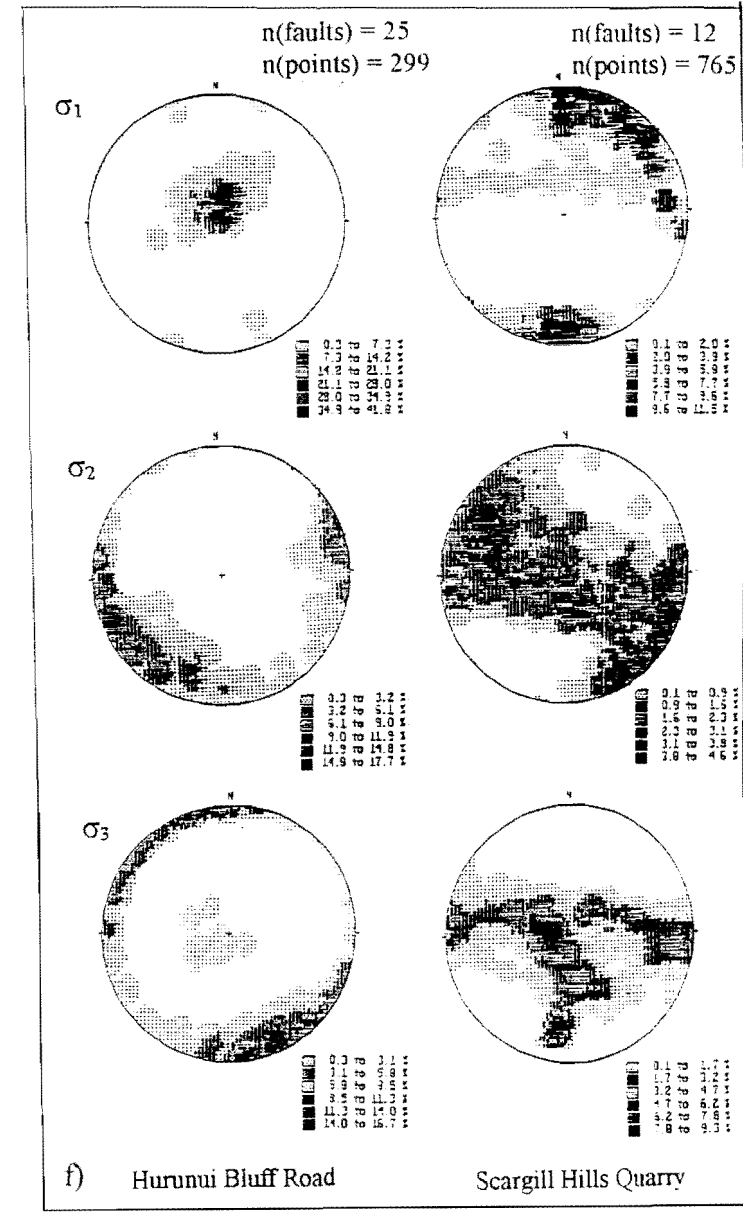
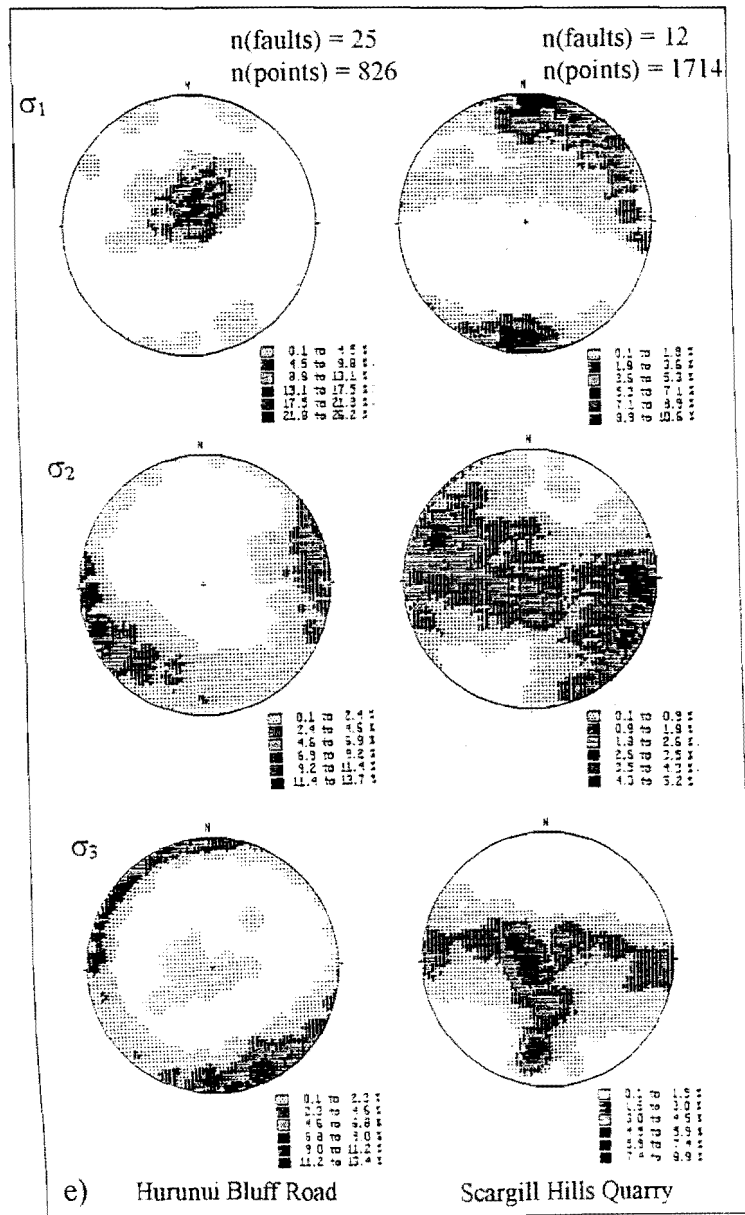
CI = 3  
% = 30  
AD = 30



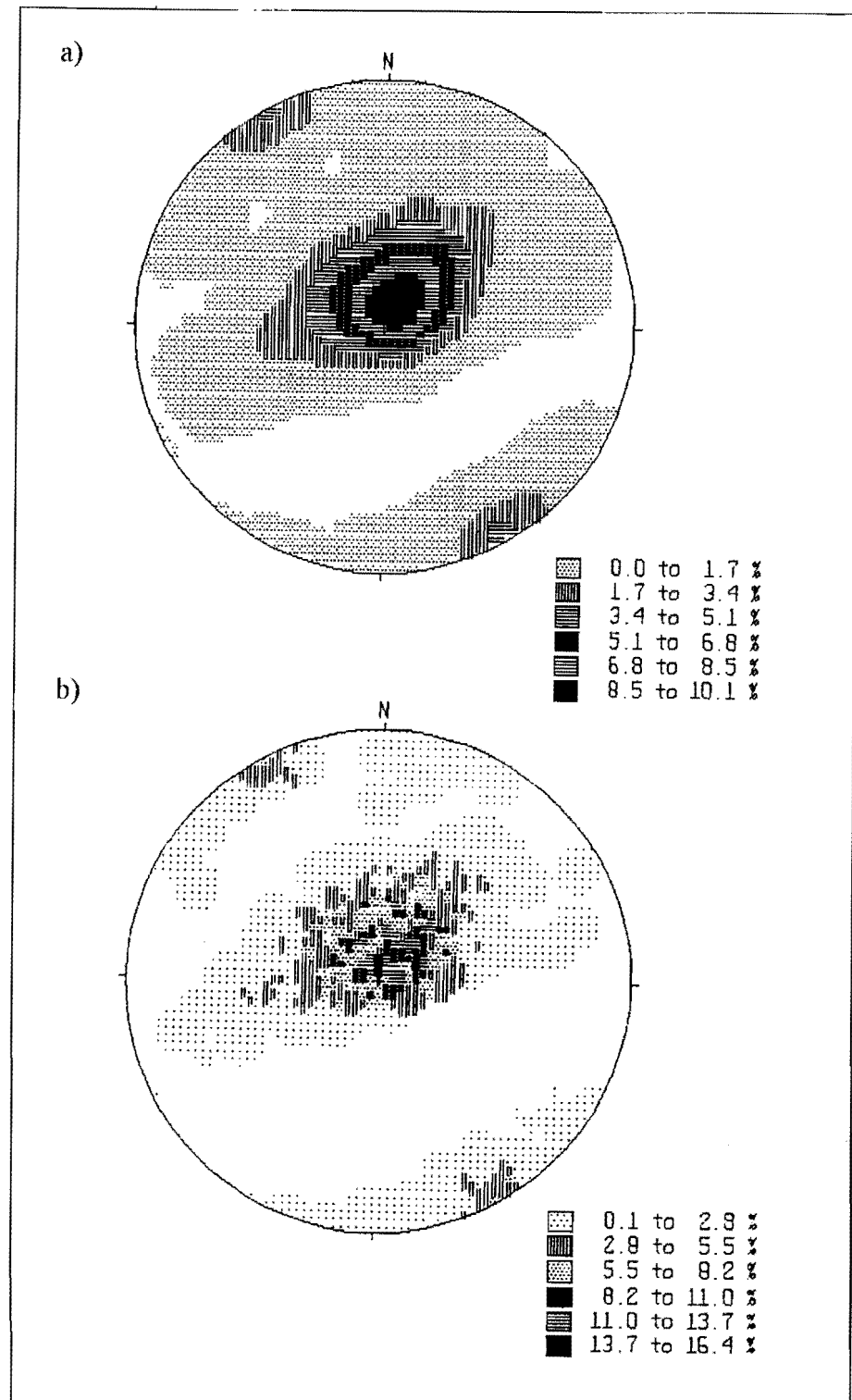
CI = 3  
% = 25  
AD = 20

Figure 8.1 cntd See figure 8.1a) and b) for caption

CI = 2  
% = 30  
AD = 25



CI = 2  
% = 30  
AD = 20



**Figure 8.2** Comparison of contouring by the spherical gaussian method (a) and the step function method (b) for the  $\sigma_1$  plot of Hurunui Bluff Road.

## STRAIN ANALYSIS

### The Fry Method

The Fry Method is very simple in its application, merely involving the placement of a marked central point of a piece of paper over each object to be measured (here glauconite grains) on a face in turn, while tracing the relative positions of the centres of the remaining objects (grains) (figure 8.3). Once this has been repeated for every point, the pattern of an unstrained distribution will be characterised by a central cavity that is circular in shape, directly proportional in size to the closest distance between any grain and its neighbour, while a strained aggregate will produce an ellipse-shaped cavity, stretched in the direction of maximum strain, directly reflecting the orientation of the strain ellipse (figure 8.3).

The computer package INSTRAIN 2.5 (Erslev, 1988 and Erslev and Ge, 1990), used in conjunction with a A3-sized digitiser, greatly speeds the above process, the points only need be digitised once, the computer program then rapidly calculating the rest of the plot. Other features of INSTRAIN 2.5 are discussed below.

### Tests to set up the parameters of the measurements

A control test on a strained ironstone oolite (page 79 Ramsay and Huber, 1987a), was used to ascertain the optimum size and number of grains needed to interpret the resulting strain ellipse. Three plots were produced to test the optimum paper size (shown in figure 8.4). From these plots it was concluded that approximately 100 points on an A4 sheet of paper produced the best plot. The variable shape of the rocks measured meant that many of the faces were in fact enlarged by photocopying onto an A3 sheet of paper, the actual area measured often not larger than A4 size.

Only the 100 largest grains were measured on a face, hence the choosing of these introduces an element of subjectivity, but it was hoped that this would minimise distortions of the grains due to photocopying (as was observed when the face was enlarged to the point where all of the grains could be measured), and hopefully avoid the measurement of small sections of larger grains not containing their true centre-point, due to the cutting of a 2-d slice.

### Further features of INSTRAIN 2.5

INSTRAIN 2.5 has a number of other features which serve to enhance the definition of the strain ellipse produced and are briefly explained here (even the authors suggest that the ellipses produced by the standard Fry Method are not always easy to interpret). These are restricted to aggregates in which the grain shape can also be measured, particularly those that can be entered in one of the following forms:

- i) centre and radius end-point coordinates of objects
- ii) three points on the margin of inscribed circles

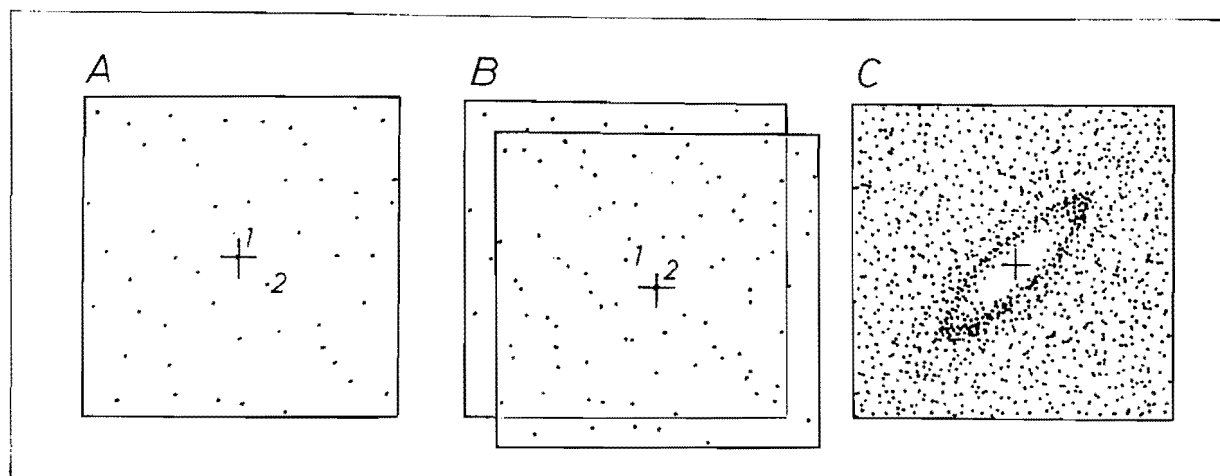


**Figure 8.3** The construction of a strain ellipse using the Fry Method. (From Ramsay and Huber, 1987a).

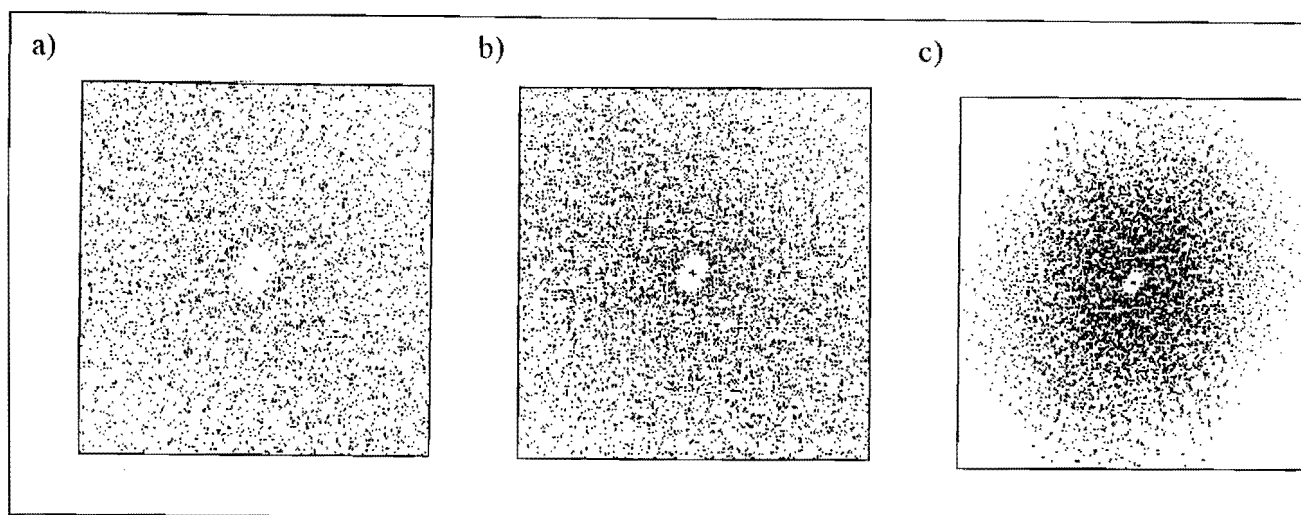


**Figure 8.4** Comparison of strain analyses of a strained aggregate of ooids (Ramsay and Huber, 1987a), at A3 (a), A4 (b) and B4 size (c). Plots a) and b) used 110 objects and c) used 100 objects.

- iii) four points at the end points of major and minor ellipses
- iv) five spaced points on the margin of ellipses

These data entry options allow calculation of a “normalised” centre-to-centre plot which takes into account grains that have not been cut through their centre in a 2-d slice (and hence the actual centre of the grains not measured). Furthermore, these plots can be "enhanced" by removing all of those points that don't contribute to the rim of maximum point intensity (so-called enhanced Normalised Fry plots) and a least-squares best-fit ellipse fitted to the remaining data. Data options iii) and iv) also allow an  $R/\phi$  diagram to be plotted.



### appendix three:

## STREAM SINUOSITY INDEX STUDY

### Discussion of the choice of appropriate interval length

As discussed in chapter six, the major problem with measuring significant values of stream sinuosity is the choice of the appropriate interval length. Some of the studies in the literature have approached this either by strictly measuring:

- i) total sinuosity (eg. Schumm, 1963)
- or ii) sinuosity between wavelengths or half-wavelengths (eg. Howard and Hemberger, 1991)

However, for most studies (as here), these intervals are not appropriate and an intermediate interval must be chosen. This interval is dependent on the following factors:

- i) the total length of the river
- ii) the degree of detail needed to evaluate the data appropriate to the study
- iii) the range of sinuosity for the river

As mentioned in chapter six, the relative ease of the method used here allowed the sinuosity index of Waikari River to be calculated a number of times, and hence the effects of different size of interval length can be noted directly. Accordingly, the sinuosity was measured in terms of three different size intervals, 4, 2 and 1 km respectively, the results of which are shown as both values against the trace of the river and as graphs of sinuosity index verses distance (along the river) on maps 4A, 4B and 4C and are discussed below.

The three graphs of sinuosity against distance clearly show that the level of detail in the plot increases with decrease in interval size to the point where the graphs undergo a number of sharp increases and decreases. This is a function of the range of sinuosities that a stream possesses; on the largest meanders of Waikari River (eg. those marked with an \*), an interval of 1km will sometimes span less than half a wavelength and therefore, the straight line distance measured will depend entirely on the shape of the meander. Therefore, it is proposed that unless some control on the shape of the meander can be introduced, the interval should be at least larger than the half-wavelength of the largest meander. (This will not apply to streams containing meanders at significantly different scales however, ie. where small meanders have developed on larger meanders, there the scale of meander to be measured will have to be carefully chosen first).

In terms of this study then, only the measurements using intervals of 2 and 4 km were considered to be significant. It is difficult to determine further which of the two plots is the most representative, apart from the fact that the expected wavelength of any warping expected to be affecting the floor of Waikari Valley is only on the order of a few km (particularly given that they were not detected by the gradient index analysis), and therefore the plot at an interval of 2 km may be favoured.

### **Discussion of the use of a running window**

The other problem with calculation of sinuosity in segments lies with the starting point for the first segment. The position of any sudden change along the stream will only be measured to the closest endpoint of the segment for which it has been measured, which in turn is dependent on where the first interval was started. The solution is, again due to the ease of the proposed method, to perform a type of “running window test”, whereby the stream is measured a number of times, starting at different points within the length of the first interval and accordingly as mentioned in Chapter 6, each of the above tests was run with five different starting points to determine the relative effects.

It is apparent from each of the graphs that the relative effects of the positions of the starting points for each set of measurements, increases with the decreasing interval size. The effects are at a minimum for the interval of 4 km, despite the fact that, due to the fact only five runs were made each time, the distance between successive start points is greater there.

Therefore, again, the tests show that an interval of 1 km is too small; here each run shows significantly different peaks and troughs to the others and therefore cannot be interpreted accurately. Each run, using an interval of 4km however, shows exactly the same pattern of peaks and troughs and therefore is considered to be completely reliable. The runs at 2 km are slightly more ambiguous, but it is proposed that they could be used, after an inspection of the results for the 4 km interval, to cautiously evaluate some more detail, which is exactly the approach used in Chapter 6.